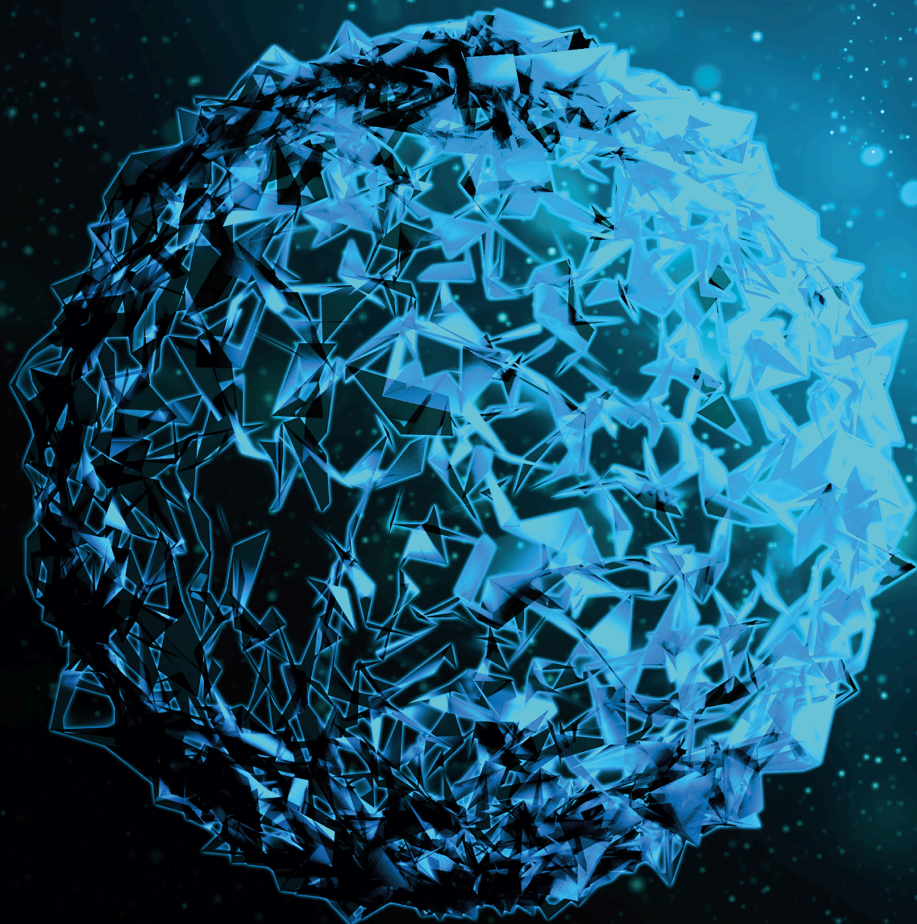


Biomedical Application of Functional Substances and Associated Molecular Mechanisms

Lead Guest Editor: Abdul-Rehman Phull

Guest Editors: Akhtar Ali and Madiha Ahmed





Biomedical Application of Functional Substances and Associated Molecular Mechanisms

BioMed Research International

**Biomedical Application of Functional
Substances and Associated Molecular
Mechanisms**

Lead Guest Editor: Abdul-Rehman Phull


Guest Editors: Akhtar Ali and Madiha Ahmed



Copyright © 2022 Hindawi Limited. All rights reserved.

This is a special issue published in "BioMed Research International." All articles are open access articles distributed under the Creative Commons Attribution License, which permits unrestricted use, distribution, and reproduction in any medium, provided the original work is properly cited.

Section Editors




Penny A. Asbell, USA
David Bernardo , Spain
Gerald Brandacher, USA
Kim Bridle , Australia
Laura Chronopoulou , Italy
Gerald A. Colvin , USA
Aaron S. Dumont, USA
Pierfrancesco Franco , Italy
Raj P. Kandpal , USA
Fabrizio Montecucco , Italy
Mangesh S. Pednekar , India
Letterio S. Politi , USA
Jinsong Ren , China
William B. Rodgers, USA
Harry W. Schroeder , USA
Andrea Scribante , Italy
Germán Vicente-Rodríguez , Spain
Momiao Xiong , USA
Hui Zhang , China

Academic Editors

Molecular Biology




Contents

Investigation into Antiepileptic Effect of Ganoderic Acid A and Its Mechanism in Seizure Rats Induced by Pentylentetrazole

Wei Pang, Shuqing Lu, Rong Zheng, Xin Li, Shunbo Yang, Yuxia Feng, Shuqiu Wang , Jin Guo , and Shaobo Zhou 

Research Article (14 pages), Article ID 5940372, Volume 2022 (2022)

Targeted Inhibition of Protein Tyrosine Phosphatase 1B by Viscosol Ameliorates Type 2 Diabetes Pathophysiology and Histology in Diabetic Mouse Model

Aamir Sohail, Hajra Fayyaz, Hamza Muneer, Idrees Raza, Muhammad Ikram , Zia Uddin, Sarah Gul , Hailah M. Almohaimeed, Ifat Alsharif, Fatima S. Alaryani, and Imran Ullah 


Research Article (12 pages), Article ID 2323078, Volume 2022 (2022)

Qizhi Kebutong Formula Ameliorates Streptozocin-Induced Diabetic Osteoporosis through Regulating the PI3K/Akt/NF- κ B Pathway

Lulu Tian, Lu Ding , Guoqiang Wang, Yu Guo, Yunyun Zhao , Yuchi Wei, Xingquan Li, Wei Zhang, Jia Mi , Xiangyan Li , Zeyu Wang , and Xiuge Wang 




Research Article (16 pages), Article ID 4469766, Volume 2022 (2022)

Alpha-Amylase Inhibits Cell Proliferation and Glucose Uptake in Human Neuroblastoma Cell Lines

Kateryna Pierzynowska , Sofia Thomasson, and Stina Oredsson 






Research Article (11 pages), Article ID 4271358, Volume 2022 (2022)

Nutraceuticals: Pharmacologically Active Potent Dietary Supplements

Subhash Chandra , Sarla Saklani, Pramod Kumar, Bonglee Kim , and Henrique D. M. Coutinho 

Review Article (10 pages), Article ID 2051017, Volume 2022 (2022)

The Leaf Extract of *Mitrephora chulabhorniana* Suppresses Migration and Invasion and Induces Human Cervical Cancer Cell Apoptosis through Caspase-Dependent Pathway

Wutigri Nimlamool , Sunee Chansakaow , Saranyapin Potikanond , Nitwara Wikan , Phateep Hankittichai , Jirapak Ruttanapattanakul , and Phatarawat Thaklaewphan 






Research Article (13 pages), Article ID 2028082, Volume 2022 (2022)

Looking for Responders among Women with Chronic Pelvic Pain Treated with a Comiconized Formulation of Micronized Palmitoylethanolamide and Polydatin

Ugo Indraccolo , Alessandro Favilli, Arianna Dell'Anna, Antonio Di Francesco, Barbara Dionisi, Emilio Giugliano, Filippo Murina, and Erica Stocco



Review Article (10 pages), Article ID 8620077, Volume 2022 (2022)

Oridonin Attenuates Cisplatin-Induced Acute Kidney Injury via Inhibiting Oxidative Stress, Apoptosis, and Inflammation in Mice

Hyemin Gu , Mi-Gyeong Gwon , Jong Hyun Kim , Jaechan Leem , and Sun-Jae Lee 



Research Article (10 pages), Article ID 3002962, Volume 2022 (2022)

***Datura stramonium* Leaf Extract Exhibits Anti-inflammatory Activity in CCL₄-Induced Hepatic Injury Model by Modulating Oxidative Stress Markers and iNOS/Nrf2 Expression**

Bakht Nasir, Ashraf Ullah Khan, Muhammad Waleed Baig, Yusuf S. Althobaiti , Muhammad Faheem, and Ihsan-Ul Haq 




Research Article (20 pages), Article ID 1382878, Volume 2022 (2022)

Effects and Mechanism of *Ganoderma lucidum* Polysaccharides in the Treatment of Diabetic Nephropathy in Streptozotocin-Induced Diabetic Rats

Yu Hu, Shu-Xiang Wang , Fu-Yu Wu, Ke-Jia Wu, Rui-Ping Shi, Li-Hong Qin, Chun-Feng Lu, Shu-Qiu Wang, Fang-Fang Wang, and Shaobo Zhou 

Research Article (13 pages), Article ID 4314415, Volume 2022 (2022)

Preparation of Spice Extracts: Evaluation of Their Phytochemical, Antioxidant, Antityrosinase, and Anti- α -Glucosidase Properties Exploring Their Mechanism of Enzyme Inhibition with Antibrowning and Antidiabetic Studies *In Vivo*

Yahya S. Alqahtani, Mater H. Mahnashi , Bandar A. Alyami, Ali O. Alqarni, Mohammed A. Huneif, Mohammed H. Nahari , Anser Ali, Qamar Javed, Hina Ilyas, and Muhammad Rafiq 

Research Article (10 pages), Article ID 9983124, Volume 2022 (2022)

Research Article

Investigation into Antiepileptic Effect of Ganoderic Acid A and Its Mechanism in Seizure Rats Induced by Pentylenetetrazole

Wei Pang,^{1,2} Shuqing Lu,³ Rong Zheng,⁴ Xin Li,² Shunbo Yang,² Yuxia Feng,² Shuqiu Wang^①,¹ Jin Guo^②,² and Shaobo Zhou^③^{5,6}

¹College of Basic Medicine, Jiamusi University, Jiamusi, Heilongjiang 154007, China

²College of Rehabilitation Medicine, Jiamusi University, Jiamusi, Heilongjiang 154007, China

³Department of Physical Medicine and Rehabilitation, Qilu Hospital, Cheeloo College of Medicine, Shandong University, Jinan, Shandong 250012, China

⁴College of Stomatology, Jiamusi University, Jiamusi, Heilongjiang 154007, China

⁵School of Science, Faculty of Engineering and Science, University of Greenwich, Central Avenue, Chatham ME4 4TB, UK

⁶School of Life Sciences, Institute of Biomedical and Environmental Science and Technology, University of Bedfordshire, Luton LU1 3JU, UK

Correspondence should be addressed to Shuqiu Wang; wang_shuq@163.com, Jin Guo; guojin8002@163.com, and Shaobo Zhou; sbzhou@yahoo.com

Received 7 March 2022; Revised 7 June 2022; Accepted 14 June 2022; Published 1 September 2022

Academic Editor: Abdul Rehman Phull

Copyright © 2022 Wei Pang et al. This is an open access article distributed under the Creative Commons Attribution License, which permits unrestricted use, distribution, and reproduction in any medium, provided the original work is properly cited.

Ganoderic acid A (GAA) exhibited neuron protection in *in vitro* epilepsy study, but no study has been done *in vivo*. Rats were administered (i.p.) pentylenetetrazole daily for 28 days to induce seizure. Rats with grade II or above of epileptic score were divided into three groups and given placebo, sodium valproate, or GAA treatment, respectively, for 7 days. The electrical signals of brain were monitored with electroencephalography (EGG); epileptic behavior was assessed using the Racine scale; morphological changes and apoptosis rate of cortical neurons were assessed with H&E staining and TUNEL staining, respectively. Protein expression of calcium-sensing receptor, p-ERK, p-JNK, and p-p38 in hippocampal tissue and Bcl-2, cleaved caspase-3, and Bax in cortical tissues was observed by Western blot and immunohistochemistry assay, respectively. After GAA treatment, apparent seizure-like EEG with significant arrhythmic disorder and spike waves was reduced or disappeared, and wave amplitude of EEG was reduced significantly. GAA showed similar effect with sodium valproate treatments on epilepsy. There were an apparent improvement of the epileptic behavior and a significant increase in the epileptic latency and shortening of the epileptic duration in the treatment group compared to control. GAA treatment ameliorated the nuclear pyknosis of neurons which appeared seriously in the epilepsy group. GAA treatment significantly reduced the cortical neuron apoptosis of epilepsy and the expression of calcium-sensing receptor, p-P38, p-JNK, cleaved caspase-3, and Bax but increased the expression of both p-ERK and Bcl-2. In conclusion, GAA treatment showed strong antiepileptic effect by decreasing apoptosis in cortical neuron and the expression of calcium-sensing receptor and stimulating the MAPK pathway.

1. Introduction

There are approximately 70 million people suffering from epilepsy in the world which can be caused by the abnormal discharge of brain neurons due to brain injuries, such as trauma, stroke, intracranial infection, and medical, personal, genetic, and social factors [1, 2]. Up to 90% of patients with

epilepsy are living in low income and poor medical conditions [3]. Epilepsy generally cannot be cured and sometimes cannot be controlled by common drugs, e.g., sodium valproate; thus, it seriously affects patients' health and quality of life [4]. Therefore, finding new therapeutic agents is urgently needed.

Ganoderma lucidum, a kind of fungus, belongs to the Basidiomycete, Polyporaceae. *Ganoderma lucidum* is widely

used to promote health, and it contains compounds such as triterpenoids (ganoderic acids), polysaccharides, sterols, and alkaloids with pharmacological activities. These components can regulate the nervous system and immune system, improve hypoxia tolerance and scavenge free radical, and protect liver function [5]. We have demonstrated the antiepileptic effects of *G. lucidum* in *in vitro* and *in vivo* studies [6–8]. We also found that ganoderic acid A (GAA) reduced the apoptosis in primary hippocampal neurons cultured in medium without magnesium, an *in vitro* epileptic model, but no study on neuroprotection has been done *in vivo* [9]. Thus, this study tested the antiepileptic effect of GAA in an epileptic rat model.

GAA is one of the 140 triterpenoids isolated from *G. lucidum* [10, 11]. GAA has been shown to inhibit cancers of the liver, lung, and kidney, improve insulin resistance, and exhibit anti-HIV activities [12–18]. For instance, after 5 weeks of treatment with GAA (10 mg/kg), the volume of anaplastic meningioma was significantly reduced, and the overall survival rate of mice was improved [12]. GAA can significantly inhibit the invasion and migration of U251 glioblastoma multiforme cells with dose- and time-dependent effects [19]. GAA significantly inhibits the PI3K/AKT pathway by reducing the phosphorylation of AKT, mTOR, and cyclin [19].

The activation of calcium-sensing receptor (CaSR) has been linked to neuron damage in epilepsy and has attracted research interest recently [20–22]. CaSR is distributed in the digestive system, cardiovascular system, etc. and exhibits the ability to regulate gastrointestinal motility, bone metabolism, and kidney function. It is also found in the central nervous system but with limited information on its role in epilepsy [23–30]. CaSR participates in the maintenance of Ca^{2+} homeostasis, as well as the regulation of brain growth and development, cell proliferation, and differentiation, maintenance of membrane potential, and ion channel switching [31–33]. CaSR has also been highly expressed in the hippocampus of epileptic rats [26], and its genetic mutation is related to idiopathic epileptic syndrome [34–37]. Also, there is a positive link between CaSR and the mitogen-activated protein kinase (MAPK) pathway; for example, the overexpression of CaSR can cause epilepsy by affecting the expression of proteins linked to the MAPK pathway.

The effect of GAA on epilepsy and the underlying molecular mechanism *in vivo* have not yet been reported. Therefore, in this pilot study, the effect of GAA on electroencephalography (EEG), epileptic behavior, histological changes, and apoptosis of brain tissues was investigated in an epileptic rat model induced by pentylenetetrazole. The workflow of the study is listed in Figure 1. The aim is to test antiepileptic effect of GAA and provide a theoretical target of GAA on the calcium-sensing receptor and MAPK pathway in order to pave the way for its use in epilepsy treatment.

2. Methods

2.1. Chemicals. Sodium valproate and pentylenetetrazole (PTZ) were bought from Sigma-Aldrich (MO, USA). GAA

(purity was $\geq 95\%$) was bought from Dalian Meilun Biotechnology Co., Ltd. (Dalian, China). Antibodies against CaSR, Bcl-2, and Bax were obtained from Proteintech Group, Inc. (Wuhan, China). Caspase-3, p-JNK, p-ERK, and p-P38 were purchased from Cell Signaling Technology, Inc. (Danvers, MA, USA). The TUNEL apoptosis kit was bought from Boster Biological Technology Co., Ltd. (Wuhan, China).

2.2. Animal Experimental Design. The Research Ethics Committee of Jiamusi University approved this study (no. jmsukf-2020006). Animals were cared and handled by a specially trained technician on rats in accordance with the guideline of laboratory animal's study by the Chinese Ministry of Science and Technology. A total of 48 healthy male Sprague-Dawley (SD) rats, weighing 180 ± 20 g, were bought from the Liaoning Changsheng Biotechnology Co., Ltd. (Benxi, China), and three rats were raised in each cage away from strong light and noise in the lab of Animal Center of Jiamusi University. The lab has a controlled temperature of $21 \pm 2^\circ\text{C}$, relative humidity of 30–70%, and day-night period of 12/12 h. They had free access to food and water. After one-week adaptation, rats were randomly divided into four groups: control group, epilepsy group, valproate group, and GAA group, with 12 rats in each group. The rats in the epilepsy group, sodium valproate group, and GAA group were administered PTZ injection intraperitoneally (i.p.), with a subconvulsive dose of 35 mg/kg (100 mg of PTZ dissolved in 10 mL saline) at 8–10 am once a day for 28 days according to previous [26] and our studies [38]. The rats in the control group were given the same volume of saline (i.p.). EEG was assessed (see Section 2.3); together with the EEG changes, rats also appeared as grade II for more than 5 consecutive days during this period and were used for the study. From day 29 to day 35, the rats in the control group, epilepsy group, sodium valproate group, and GAA group were given placebo (saline+5% DMSO), sodium valproate (200 mg/kg, dissolved in saline), and GAA (10 mg/kg, dissolved in 5% of DMSO with a concentration of 30 mg/mL) by intragastric administration at 8–10 am once a day, respectively [39]. On day 36, except the control group, the other three groups were administered PTZ (35 mg/kg) again to induce the kindling epilepsy, and their behavior was observed. Then, rats were euthanized with pentobarbital sodium (i.p. 300 mg/kg body weight, dissolving to concentration of 3% in phosphate-buffered saline). Until the signs of ataxia (stumbling, falling, and crossing feet) appeared following injection, the rats were given transcardiac perfusion and the cerebral hemispheres were removed. Half of them (6) were fixed in 4% paraformaldehyde solution, and the others were stored in liquid nitrogen.

2.3. Electroencephalography (EEG) Assessment. Rats were given with isoflurane with 5% for induction and 1%–2% for maintenance their general anesthesia. Then, three stainless-steel screw electrodes, with a diameter of 1.2 mm, were individually implanted into the rat's bilateral temporal lobe and the right frontal lobe which are used as a reference electrode. EEG was recorded for up to 90 min using Mfile

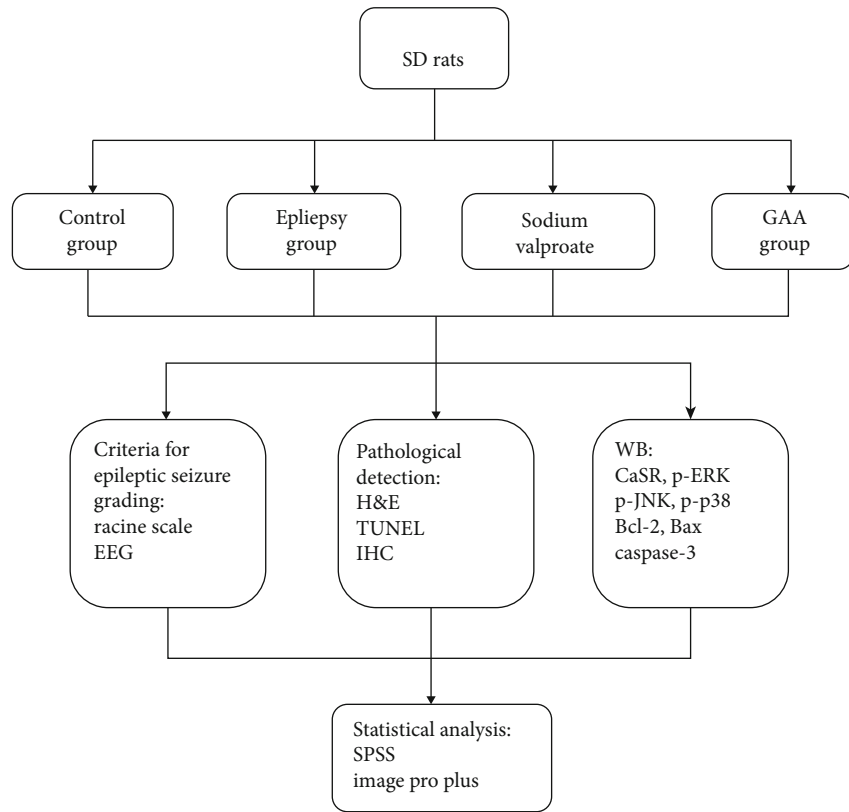


FIGURE 1: Workflow of the study. Rats were divided into 4 groups; three of them were administered (i.p.) to induce seizure; then, they were given treatment with placebo (normal group), placebo (epilepsy group), sodium valproate (epilepsy treated group), or GAA (epilepsy treated group), respectively. Electroencephalography (EEG); epileptic behavior was assessed, and morphological changes and apoptosis were tested. Protein expression of calcium-sensing receptor, p-ERK, p-JNK, p-p38, Bcl-2, cleaved caspase-3, and Bax in brain tissues was observed by Western blot and immunohistochemistry (IHC) assay, respectively.

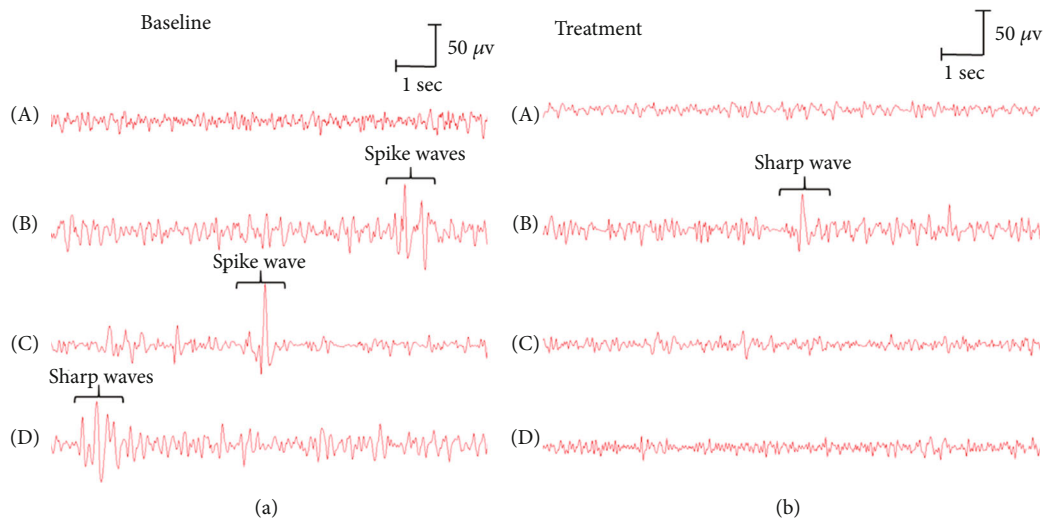


FIGURE 2: Representative EEG of a group of rats at baseline (a) and treatment (b). A–D represent groups of control, epileptic model, sodium valproate, and GAA, respectively.

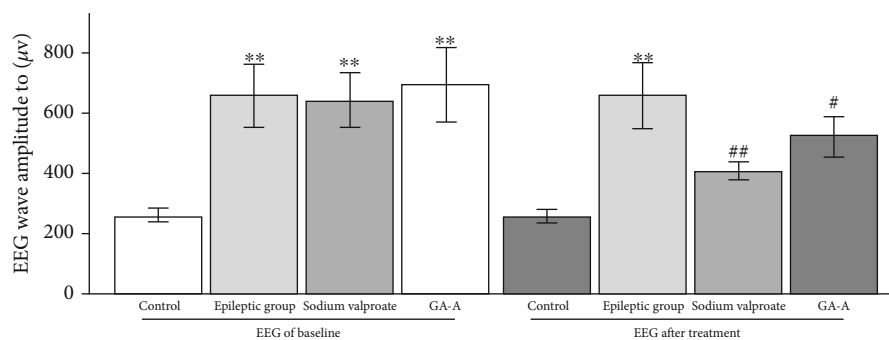


FIGURE 3: The wave amplitude of EEG in each group before and after treatment. ** $p < 0.01$ vs. control group, ## $p < 0.01$ vs. epilepsy group, and # $p < 0.05$ vs. epilepsy group.

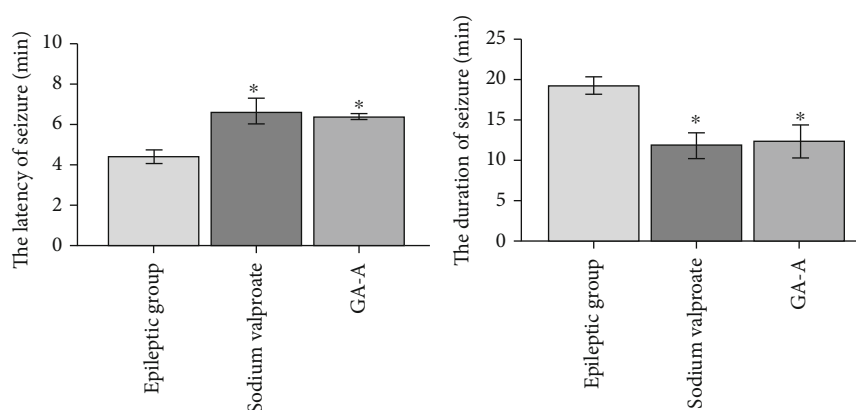


FIGURE 4: The latency of seizure (min) and the duration of seizure (min) of rats from three groups. They are epilepsy, sodium valproate, and GAA treatment groups. The seizure latency is the time difference from the completion of the last seizure to the start of the next one; seizure duration is the time from reaching the Racine score of grade 1 to the end of the seizures. Values represent mean \pm SE; $n = 6$ in each group. * $p < 0.05$ vs. epilepsy group.

software. All successful modeling rats were monitored at baseline and after treatment.

2.4. Criteria for Epileptic Seizure Grading. Detailed grading of convulsion was based on the Racine scale [40]. It was scaled as in the following: 0: no response; 1: immobilization; 2: partial myoclonus, e.g., nodding head; 3: whole body myoclonus; 4: rearing tonic seizure and multilimb twitches; and 5: generalized persistent tonic-clonic seizures, wild rushing, and jumping [41]. Only rat with five consecutive seizure scores of grade II or above was considered a successful chronic epileptic model [40]. The seizure latency (time difference from the completion of the last seizure to the start of the next one) and seizure duration (from reaching the Racine score of grade 1 to end of the seizure) were analysed.

2.5. Hematoxylin-Eosin (H&E) Staining. The rat brain tissues fixed with 4% paraformaldehyde were cut into $4\mu\text{m}$ sections and stained with H&E as described previously [42], and the histological structure was observed using a 400x microscope (Nikon ECLIPSE Ni, Japan). Damaged neurons from 6 observed optical fields per rat were counted and used for the statistical analysis among groups.

2.6. TdT-mediated dUTP Nick-End Labeling (TUNEL) Assay. The TUNEL apoptosis assay was based on its commercial company manual and our previous study [38]. The results were observed with a fluorescence microscope (OLYMPUS BX51, Japan), and images of a bright-field microscope were taken. The apoptosis rate was calculated by using the number of positive cells to total cells in the same area (%).

2.7. Immunohistochemistry (IHC) Staining. The method was based on our previous study with some modification [5]. Paraffin sections of rat cortical tissue were routinely dewaxed and hydrated. The endogenous peroxidase inhibitor was added and incubated for 10 min and then rinsed with distilled water. The sections were put into citrate antigen retrieval solution and heated for 2 min in a microwave oven. Then, blocking buffer with 5% BSA was used. Drops of primary antibody (Bax, 1:100; caspase-3, 1:1000; or Bcl-2, 1:300) were added and stored at 4°C overnight. The following day, the sections were incubated at 37°C for 30 min first and then washed with PBS. The biotin-labeled goat anti-rabbit IgG (second antibody) was added and incubated for 30 min at 37°C . After washing, drops of DAB chromogen were dripped on the sections (the degree of staining

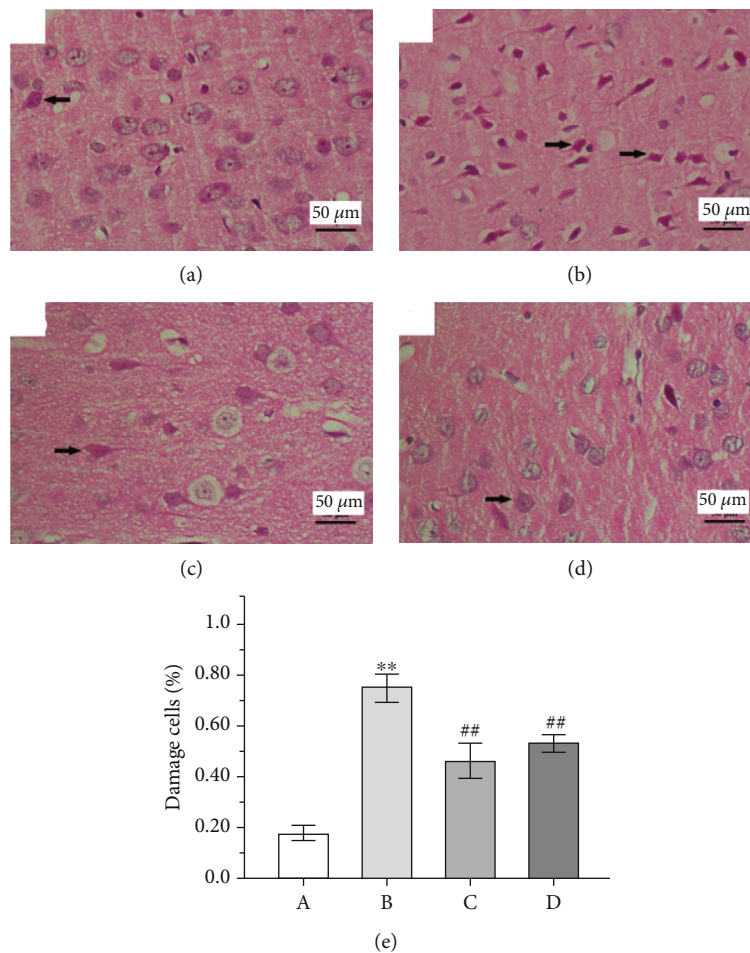


FIGURE 5: Representative images showing pathological changes in cortex tissue of the rat brain in different groups ($\times 400$, arrows indicate the damaged cells). (a) Control group. (b) Epilepsy group. (c) Sodium valproate group. (d) GAA group. (e) The quantitative analysis of neurons' damaged rate based on the damaged nerve cells to total nerve cells in six observed fields per rat from each group. Values represent mean \pm SE; $n = 6$ in each group.

was monitored with regular microscopy). Sections were then stained with hematoxylin.

2.8. Western Blot Analysis. The Western blot method was based on our previous study with some modification [5]. It was used to test the expression of CaSR, p-ERK, p-JNK, p-p38, Bcl-2, Bax, and caspase-3 in rat brain cerebral cortex or hippocampal tissue. Briefly, the tissue was homogenized, and the supernatant was collected (12,000 rpm, 10 min, at 4°C). The protein concentration was measured by a BCA assay. A 10 mg of protein sample was loaded and separated by SDS gel electrophoresis. The proteins separated from the gel were transferred onto PVDF membranes which were then blocked at 37°C in a TBS solution for 1.5 h. The concentrations of the primary antibody used for the incubation were 1:1000 for CaSR, p-ERK, p-JNK, p-p38, Bcl-2, Bax, and caspase-3 and 1:5000 for GAPDH. After they were incubated overnight at 4°C , the membrane was washed 3 times with a solution with TBST. Then, alkaline phosphatase-conjugated IgG (secondary antibody) was added and then washed 3 times with a TBST solution. When the protein bands appeared, then the images were taken.

GAPDH was used as an endogenous protein for normalization.

2.9. Statistical Analysis. SPSS software (version 23; IBM Corp., Armonk, NY, USA) was used for statistical analysis. Values are expressed as the mean \pm SE. Student's *t*-test or one-way ANOVA followed by a post hoc analysis (Tukey test) was used for group comparisons. Significant statistical differences were considered when $p < 0.05$ and $p < 0.01$.

3. Results

3.1. Effect of GAA on the EEG. There were no significant waves and pattern difference in the control group at baseline and treatment. However, significant arrhythmic disorder and spike waves were observed in the epilepsy group (Figure 2), and the appearance of burst suppression episodes was observed in the GAA group. For EEG of baseline, seizure-like EEG in PTZ-induced seizure model was observed in the B, C, and D group. After treatment, significant arrhythmic disorder and spike waves were still observed in the B group, but they were dramatically reduced in C and

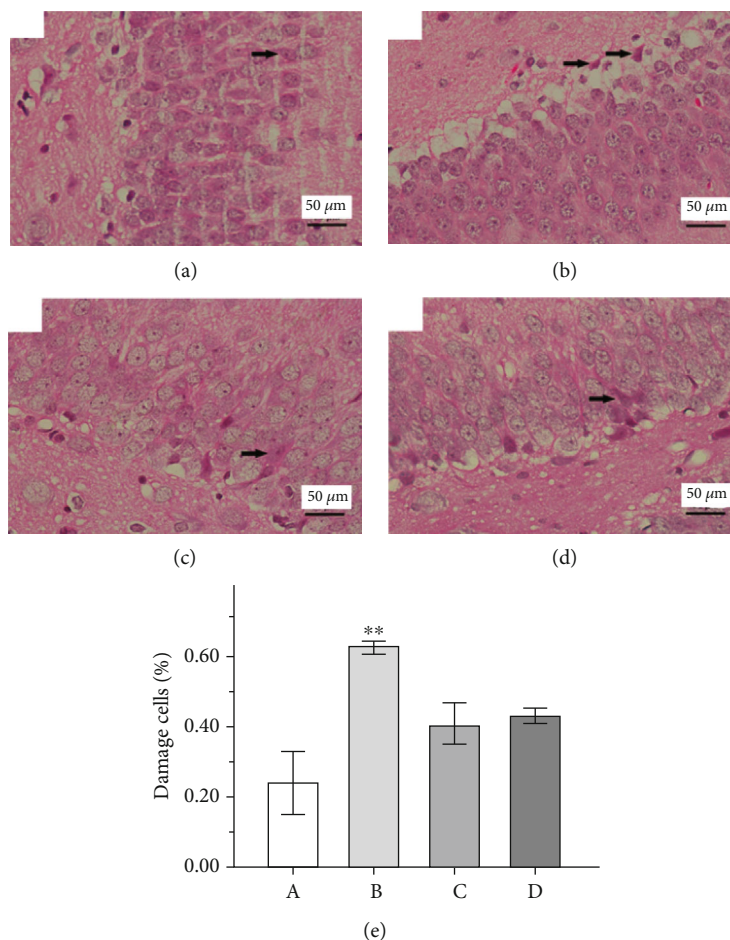


FIGURE 6: Representative images showing pathological changes in hippocampal tissue of the rat brain in different groups ($\times 400$, arrows indicate the damaged cells). (a) Control. (b) Epilepsy. (c) Sodium valproate. (d) GAA. (e) The quantitative analysis of neurons' damaged rate based on the damaged nerve cells to the total nerve cells in six observed fields per rat from each group. Values represent mean \pm SE; $n = 6$ in each group.

D groups (Figure 2), and their wave amplitude of EEG in the GAA treatment group was reduced significantly compared to that in the epilepsy group (Figure 3).

3.2. Effect of GAA on the Rat's Epileptic Scores. After rats were given PTZ injection intraperitoneally, they started frequent blinking, staring, rhythmic nodding, tail flick, and clonic convulsion of forelimbs within 10-30 min of the injection. After 30 min, the forelimbs of rats were rigid and left the ground. In grade V epileptic seizure, the rats showed limb and body rigidity, jumping, and falling. Rats with 5 consecutive times of grade II or above seizures met the standard of epileptic kindling. There was no seizure in the control group. The successful epileptic kindling model was also confirmed by the EEG monitoring (see Figure 2). During the 7-day treatment with GAA or sodium valproate, the epileptic behavior at day 35, in both the GAA and sodium valproate groups, was much reduced on the rat's epileptic scores, but there were no statistically differences compared to the epileptic model group. However, the seizure latency of the rats in both sodium valproate and GAA groups was significantly increased, but the duration of sei-

zure symptoms was significantly lower than that in the epilepsy group ($p < 0.05$) (Figure 4).

3.3. Effect of GAA on Histopathological Changes. Figure 5 shows the morphology of cortical tissues. In the control group, the neurons of the cerebral cortex were normal in shape with good order and good structure with the full cytoplasm. In the epilepsy group, nucleus pyknosis or lysis occurred, the cell structure was destroyed, and the shape was changed. Compared with the epilepsy group, the degree of damage of cells in both the GAA group and sodium valproate group was less severe, and the cell structure was well improved. Results show that the GAA treatments significantly reduced the damaged neurons compared with the epilepsy group without given treatment (Figure 5(e)).

Morphology of hippocampal tissues is shown in Figure 6. The neurons of the hippocampus in the control group were arranged in good order without abnormal morphological changes observed. However, in the epilepsy group, a large number of neurons in necrosis and dissolution appeared, neurons were not arranged in good order, and severely damaged cells were observed. In both the GAA

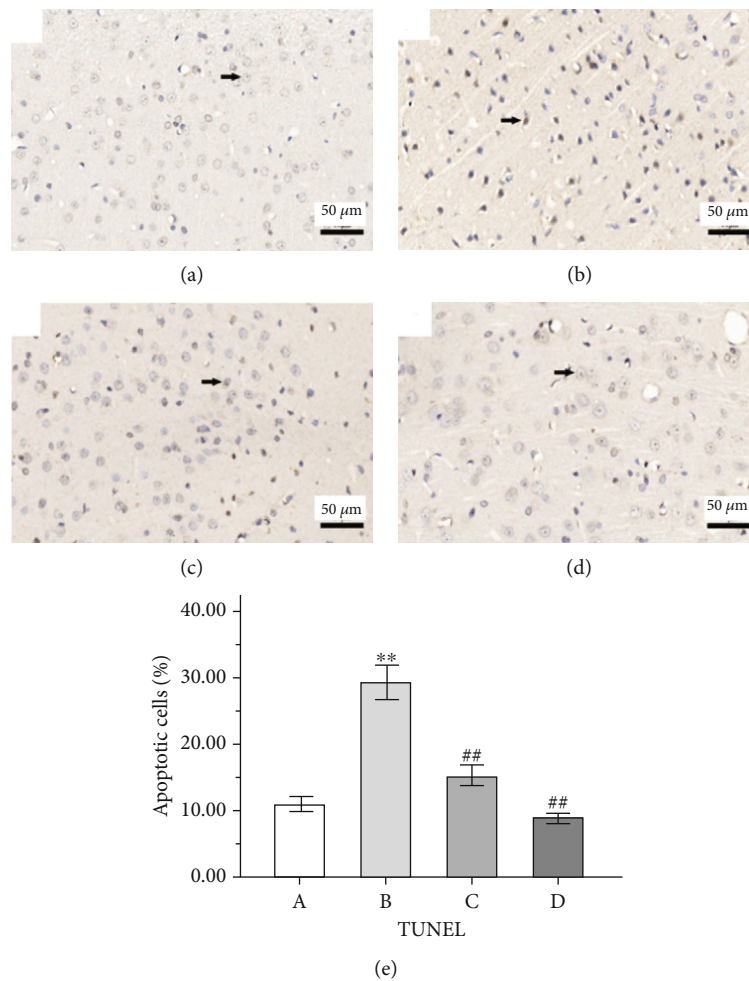


FIGURE 7: Representative immunohistochemistry micrographs of the TUNEL assay on apoptosis in cortical tissue of the rat brain (magnification $\times 400$). Arrow indicates the apoptosis neuron. (a) Control. (b) Epilepsy. (c) Sodium valproate. (d) GAA. (e) The quantitative analysis from these images for apoptosis rate. Values represent mean \pm SE; $n = 6$ in each group. In the x -axis of (e), A indicates control, B indicates epilepsy, C indicates sodium valproate, and D indicates GAA. ** $p < 0.01$ vs. control group, ## $p < 0.01$ vs. epilepsy group.

group and sodium valproate group, hippocampal neurons are arranged more orderly than those in the epilepsy group. There is a significant increase in damage neurons in the epilepsy group compared to the normal group, but both the GAA group and sodium valproate group did not statistically reduce the damaged neuron rate, even though there is an apparent reduction.

3.4. Effect of GAA on the Apoptosis and the Proteins' Expressions Related to the Mitochondrial Apoptosis Pathway. The apoptosis in rat cerebral cortex tissue stained by the TUNEL technique is shown in Figure 7, where the brown-stained nuclei are apoptotic cells. The apoptosis rate was calculated as the total apoptotic neurons to total neurons in six observed fields. The apoptosis rate in the epilepsy group was significantly highest compared to that in other groups, while treatment with both sodium valproate and GAA significantly reduced the apoptosis rate significantly

($p < 0.01$). The expression of Bcl-2 in the IHC assay is presented in the IHC micrograph (Figures 8(a)–8(d)), and its level of the Western blot assay was decreased significantly in the epilepsy group compared with the control group ($p < 0.01$, Figure 8). However, compared with the epilepsy group, the expression level of Bcl-2 protein was significantly increased in both sodium valproate and GAA groups ($p < 0.05$, respectively).

The expression of Bax protein of cortical tissue is shown in the IHC micrograph (Figures 9(a)–9(d)), and its expression level in hippocampus tissue was increased significantly in the epilepsy group compared with the control group ($p < 0.05$, Figure 9(e)) in the Western blot assay. Compared with the epilepsy group, the expression level of Bax protein in the Western blot assay was significantly decreased in both the GAA group and sodium valproate group ($p < 0.05$, respectively). The expression level of caspase-3 appeared at 17 kDa which is cleaved caspase-3, and it was significantly

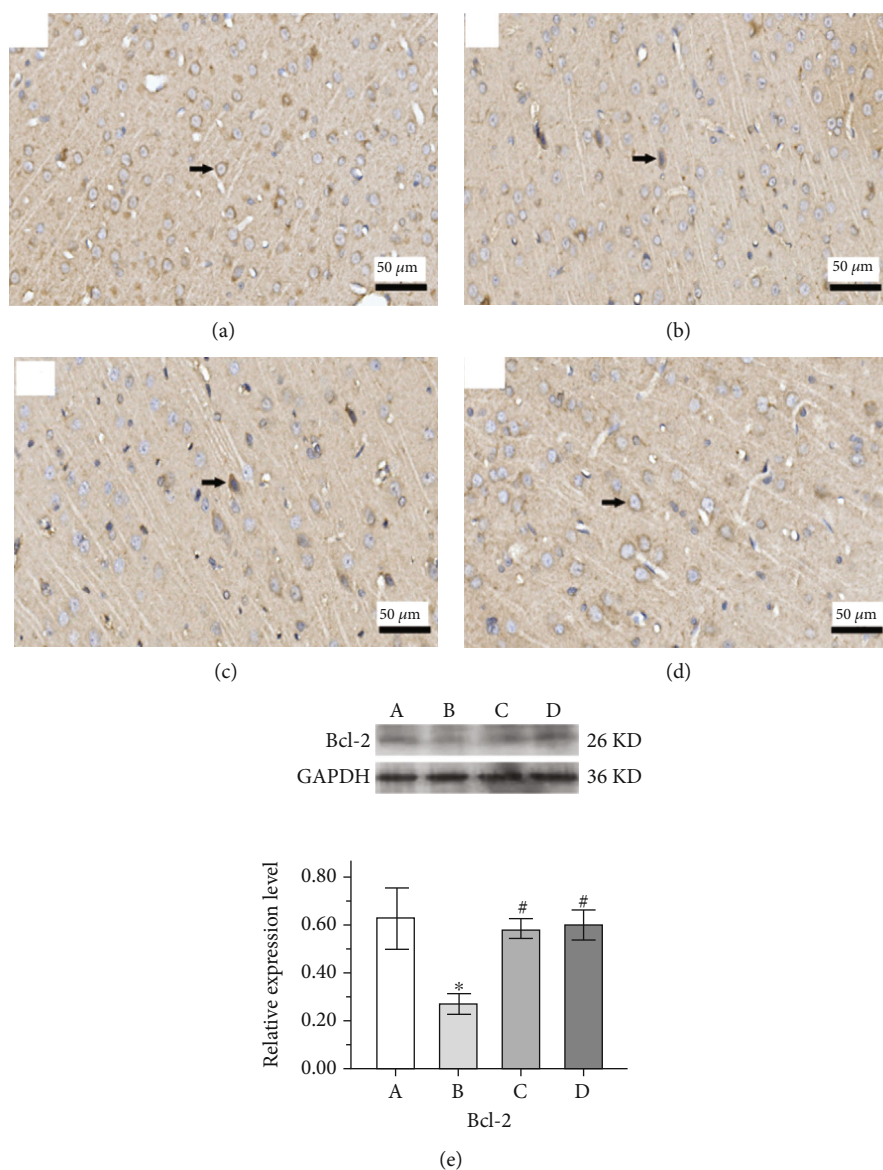


FIGURE 8: Representative immunohistochemistry micrographs of cortical tissues from different groups (arrow indicates the changes, original magnification $\times 400$). (a) Control. (b) Epilepsy. (c) Sodium valproate. (d) GAA. Representative analysis of expression of Bcl-2 protein in hippocampus tissue of the Western blot assay (e). Values represent mean \pm SE; $n = 6$ in each group. * $p < 0.05$ vs. control group, # $p < 0.05$ vs. epilepsy group.

elevated in the epilepsy group compared with the control group but decreased significantly after both sodium valproate and GAA treatments ($p < 0.05$, respectively, Figure 10).

The expression level of CaSR in hippocampus tissue was increased in the epilepsy group compared to the control group ($p < 0.05$), but its expression was decreased in both the sodium valproate group and GAA group compared with the epilepsy group ($p < 0.05$, Figure 11(a)). The expression level of p-ERK in hippocampus tissue was decreased in the epilepsy group compared to the control group ($p < 0.01$, Figure 11(b)), and its expression was increased in both the sodium valproate group and GAA group compared with the epilepsy group ($p < 0.01$). The expression level of both p-JNK and p-P38 in hippocampus tissue was elevated in the epilepsy group compared to the control group ($p < 0.05$

and $p < 0.01$, respectively); however, their expressions were decreased in both the sodium valproate group and GAA group compared with the epilepsy group ($p < 0.05$ and $p < 0.01$, respectively, Figures 11(c) and 8(d)).

4. Discussion

This study established an epilepsy rat model by administration of PTZ daily for continuous 28 days, and those with successfully induced grade II or above of Racine scale were selected and EEG monitored. Then, they were given GAA treatment or placebo treatment for 7 days, and the antiepileptic effect of GAA was monitored by behavior improvement and histological changes. Finally, the molecular biomarkers were assessed by the expression of CaSR, as well

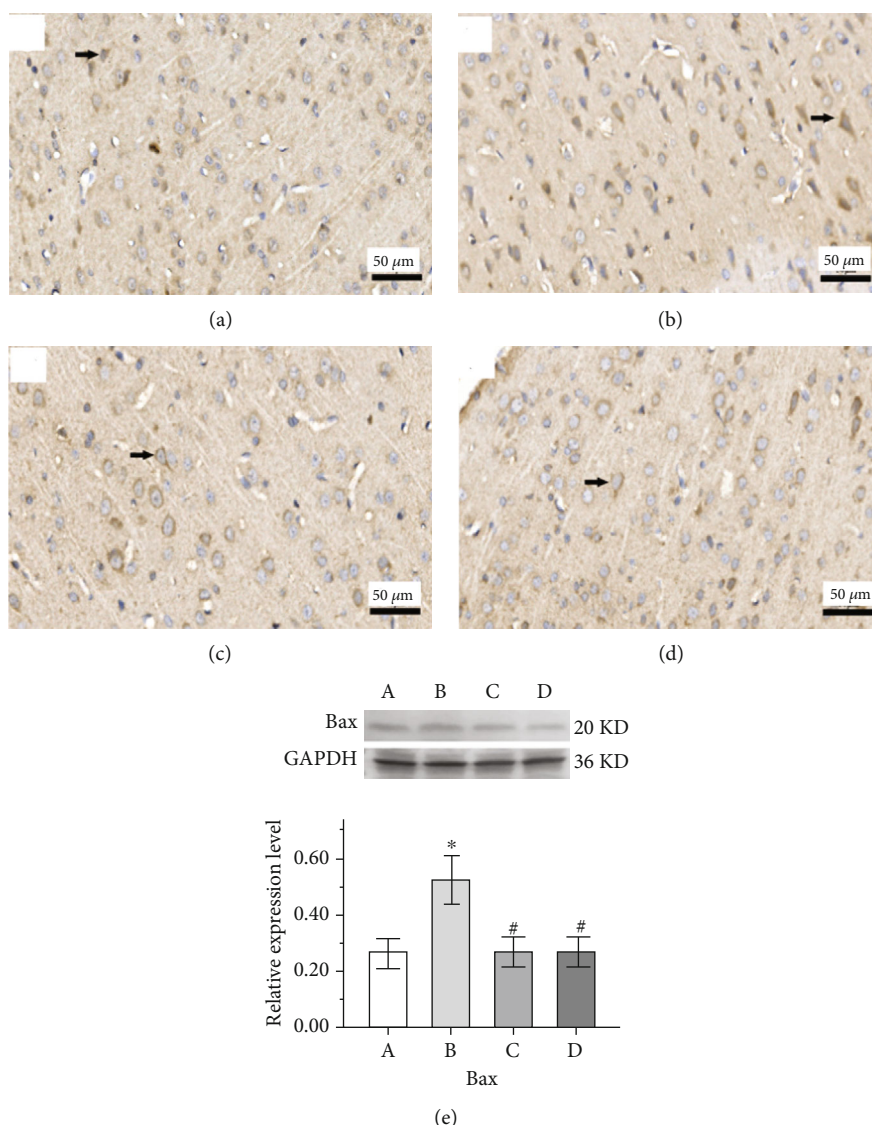


FIGURE 9: Representative immunohistochemistry micrographs of Bax protein in cortical tissues from different groups (arrow indicates the changes, original magnification $\times 400$). (a) Control. (b) Epilepsy. (c) Sodium valproate. (d) GAA. (e) Representative analysis of expression of Bax protein in hippocampus tissue of the Western blot assay; values represent mean \pm SE; $n = 6$ in each group. * $p < 0.05$ vs. control group, # $p < 0.05$ vs. epilepsy group.

as the proteins in the MAPK pathway, e.g., p-JNK, p-P38, p-ERK, Bcl-2, Bax, and cleaved caspase-3 in brain tissue.

PTZ, a GABA-A receptor antagonist, can induce generalized seizure. It can be a mild seizure without convulsion, a tonic-clonic seizure, or an acute severe seizure based on the dosage and frequency given. This model has been widely used in epilepsy research, for screening antiepileptic drugs or anticonvulsant candidates and investigation of neuronal damage after seizure, as the histological changes observed in this model are similar to the brain changes of patients with epilepsy [41]. The epilepsy model was successfully established by administration of PTZ daily for 28 days. Seven-day treatment with GAA and extra PTZ challenge at day 36 both showed the dramatic amelioration of epileptic behavior by GAA treatment to a similar extent as sodium valproate treatment, even though neither showed statistically

significant differences compared to the epileptic control group. This indicates that the treatment time should be increased further. However, the latency was increased dramatically, and duration of seizure was decreased significantly; both showed the efficacy of the GAA treatment.

The hippocampus is the key damaged area for chronic epilepsy. The most common damage is the hippocampal angle sclerosis which can originate from vascular disease or hypoxia, loss of nerve cells at the lesion, and proliferation of glial cells and fibers. Another damage area is the cortex where abnormal cells and gliosis appeared at the edge of the cerebral cortex. The degree of cell damage varies. In severe cases, dead cells are replaced by scar tissue and gliosis. In mild cases, only local blood supply disorders or tissue structure disorders are present. Our results showed that neurons in the cortex and hippocampus of the epilepsy group

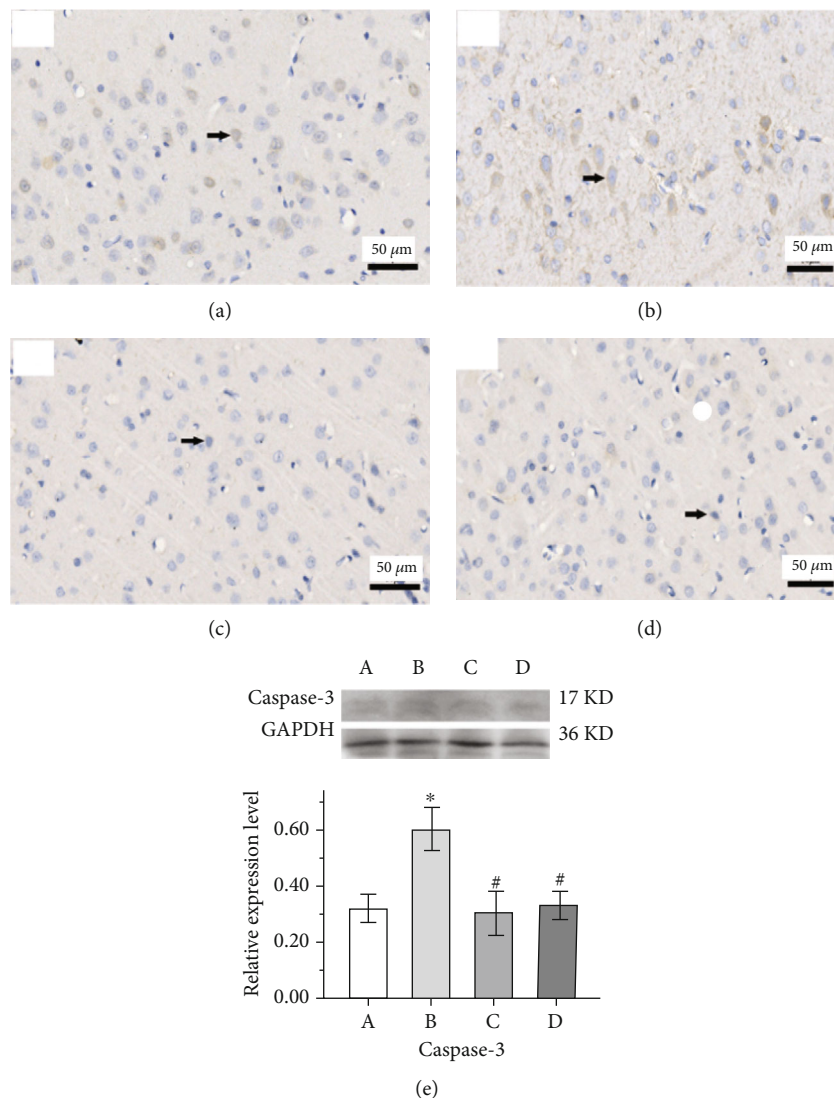


FIGURE 10: Representative immunohistochemistry micrographs of cortical tissues from different groups (arrow indicates the changes, original magnification $\times 400$). (a) Control. (b) Epilepsy. (c) Sodium valproate. (d) GAA. (e) Representative analysis of expression of caspase-3 protein in hippocampus tissue of the Western blot assay; values represent mean \pm SE; $n = 6$ in each group. * $p < 0.05$ vs. control group, # $p < 0.05$ vs. epilepsy group.

were most seriously damaged by PTZ treatment. In the epilepsy group, the damage was more serious, but GAA and sodium valproate could alleviate the damage by pathological assessment. GAA treatment clearly reduced nucleus pyknosis and lysis occurring in the epilepsy group and restored the neuron histology structure both in cortex and hippocampal tissues. The intervention effect of GAA was comparable to that of the first-line antiepileptic drug, sodium valproate.

Moreover, TUNEL results showed that the apoptosis of neurons in the epilepsy group was the most serious in the cerebral cortex of rats. However, after GAA treatment, the neuron apoptosis rate was reduced significantly, even more than that of the sodium valproate group. The detection of cleaved caspase-3 indicates cell death induction, while its decrease indicates reduction in apoptosis in both cancer and Alzheimer's disease [43]. In this study, GAA treatment decreased the level of cleaved caspase-3 which is consistent

with TUNEL results and our previous results of an *in vitro* study [9]. GAA has also shown protective effects via its anti-apoptotic role in kidney cyst, intestinal epithelial injury, colitis, and other diseases by inhibiting the MAPK pathway or promoting the apoptosis of cancer cells by enhancing the expression of the MAPK pathway [44, 45].

The expression of CaSR in brain tissue of epileptic rats was increased, accompanied by cell injury and apoptosis [21, 22]. The overexpression of CaSR induces the activation of JNK and p38 in the MAPK signal transduction pathway and promotes cell apoptosis in myocardial and brain tissues; meanwhile, the activation of the p-ERK in the ERK pathway has exhibited protective effect on myocardial and brain tissue cells [20, 22, 26, 46]. Our results showed that protein expression of p-JNK and p-p38 in the hippocampus tissue of epileptic rats increased significantly, and there was a significant increase in CaSR expression in the epilepsy group

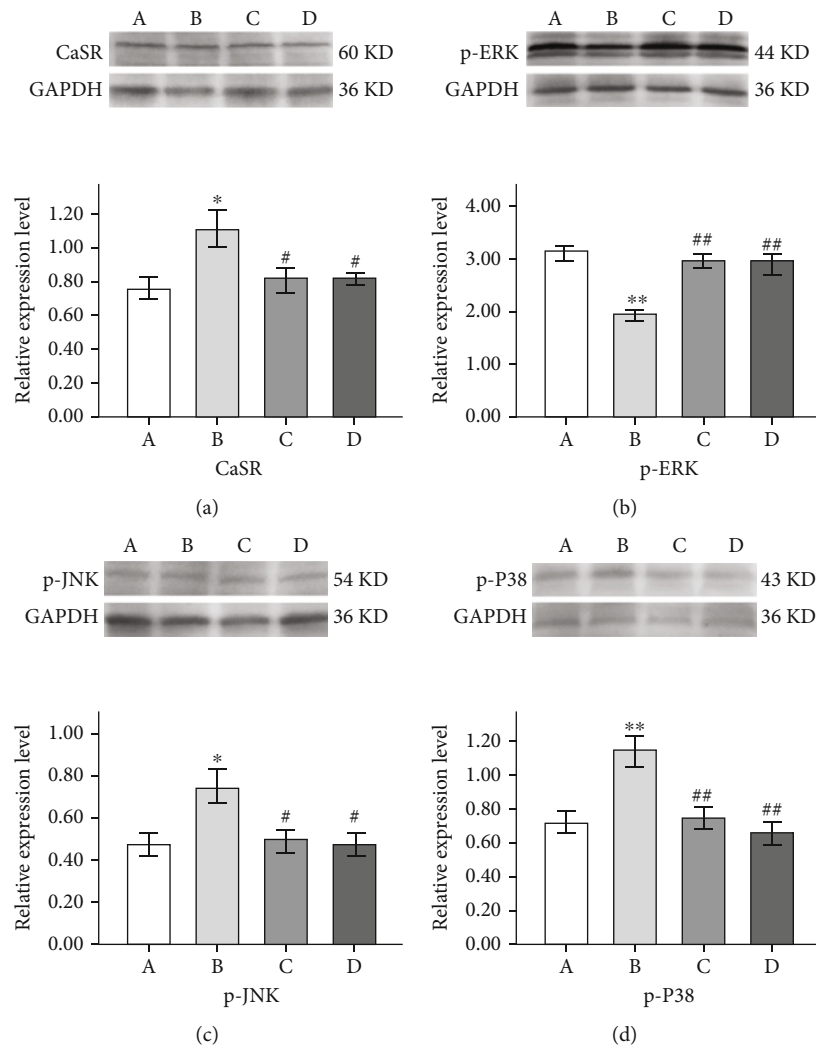


FIGURE 11: Effect of GAA treatment on the expression of CaSR (a), p-ERK (b), p-JNK (c), and p-P38 (d) in hippocampus tissue of the Western blot assay. Values in bottom figures represent mean \pm SE; $n = 6$ in each group. In top figures and the x -axis of bottom figures, A indicates control, B indicates epilepsy, C indicates sodium valproate, and D indicates GAA. ** $p < 0.01$ vs. control group, * $p < 0.05$ vs. control group, ## $p < 0.01$ vs. epilepsy group, and # $p < 0.05$ vs. epilepsy group.

compared with the control group, while the expression of p-ERK was decreased. GAA treatments reduced the expression of CaSR in the hippocampus, downregulated the expression of p-JNK and p-p38 in the MAPK pathway, and upregulated the expression of p-ERK. There was no significant difference between the GAA group and sodium valproate group. These results indicate that GAA can change the expression of related proteins in the MAPK signal transduction pathway, inhibit nerve cell apoptosis, and protect brain tissue by decreasing the expression of CaSR protein in brain tissue of epileptic rats. Moreover, GAA showed significant effect comparable with sodium valproate, the first-line antiepileptic drug.

Calcium overload can speed up the apoptosis and cause mitochondrial damage [47–49]. Previously, we found calcium overload in cultured epileptic neurons, while *G. lucidum* polysaccharides can inhibit the intracellular calcium accumulation by stimulating the expression of CaMKII to inhibit epileptic effect [50]. The activation of CaSR leads to

intracellular calcium overload and causes mitochondrial damage via changing the mitochondrial membrane permeability and disintegration [47]. It has been confirmed that the expression of CaSR is increased in the apoptosis process of the cardiomyocytes of epileptic rats [20].

The expression levels of Bax, cleaved caspase-3, and CaSR are higher in spontaneously epileptic rats while the trend of Bcl-2 expression was opposite with Bax and cleaved caspase-3 [51]. Activation of CaSR can upregulate the expression of the proapoptotic protein Bax but downregulate the expression of the antiapoptotic protein Bcl-2 on the mitochondrial outer membrane, then promote the mitochondrial disruption and cytochrome C release, and further activate caspase-9 and caspase-3 [52, 53]. This is involved in the activation of the JNK/p38 factor in the MAPK signaling pathway, regulating MAPK cascade reaction, thus causing cell damage and apoptosis [54–56]. Both Western blot analysis and IHC analysis found that in the brain tissue of rats, the expression of Bax and cleaved caspase-3 in the epilepsy

group was higher than that in the control group, and the expression of Bcl-2 protein which inhibited apoptosis was decreased, which was consistent with the study of Wang [20]. In the GAA group and valproate group, the expression of Bax and cleaved caspase-3 was decreased, and the expression of Bcl-2 protein was increased. This suggests that GAA could decrease the protein content of both proapoptotic proteins Bax and cleaved caspase-3 and increase the content of the antiapoptotic protein Bcl-2 by decreasing the expression of CaSR. While the pathophysiological mechanism of cell damage and apoptosis induced by epilepsy has not been fully elucidated, this and other studies have shown that the activation of CaSR is indeed involved in epilepsy-induced cell damage and apoptosis. Both Kapoor et al. and Delgado-Escueta et al. have shown that genetic error mutations in CaSR are associated with idiopathic epilepsy syndrome [34, 35]. Gene mutation of CaSR can change the abundance of receptors in the plasma membrane, strengthen the activation of related signaling pathways, and alter the regulation of the central nervous system to induce epilepsy [36, 37].

The antiepileptic effect of GAA may be related to the intervention time and dosage [57]. In the treatment of epilepsy, patients often need long-term antiepileptic drug treatment with adjusted dosage based on the degree and frequency of seizures. In this study, a medium dose of GAA intragastric intervention for 7 days due to the cost of GAA exhibited antiepileptic effect similar to sodium valproate, even though there was no statistically significant reduction in the epileptic scores in either treatment group. A follow-up study can prolong the treatment time of GAA to observe the effect of administration time on its antiepileptic effect.

This study did not examine the toxicity and side effects of GAA and sodium valproate, but it was reported that sodium valproate had hepatotoxicity with higher vacuolar degeneration on PZT-induced chronic epileptic rats. However, 10 mg/kg GAA did not cause any hepatotoxicity in mice with meningioma for 5 weeks [12]. In addition, this study did not detect the blood concentration of GAA in epileptic rats and could not adjust the dosage according to the blood concentration of GAA; the study did not compare the different intervention doses of GAA. Future studies of the antiepileptic effect of GAA will focus on the above problems in order to determine the optimal intervention dose and further clarify the antiepileptic effect and mechanism of GAA.

5. Conclusions

In conclusion, this pilot study explored the antiepileptic effect of GAA and its molecular mechanism. GAA showed antiepileptic effect by ameliorating epileptic behavior and brain tissue damage by epilepsy. The neuroprotective effects may be via decreasing apoptosis and CaSR expression as well as through the MAPK pathway by decreasing the expression of p-JNK, p-p38, Bax, and cleaved caspase-3 and increasing the expression of p-ERK and Bcl-2. This pilot study paved the way for the further study of its use in antiepileptic treatment.

Data Availability

Data are available upon request to the corresponding author.

Conflicts of Interest

The authors declare that they have no conflicts of interest.

References




- [1] R. S. Fisher, W. V. E. Boas, W. Blume et al., "Epileptic seizures and epilepsy: definitions proposed by the International League Against Epilepsy (ILAE) and the International Bureau for Epilepsy (IBE)," *Epilepsia*, vol. 46, no. 4, pp. 470–472, 2005.
- [2] S. D. Shorvon, "Drug treatment of epilepsy in the century of the ILAE: the second 50 years, 1959-2009," *Epilepsia*, vol. 50, Suppl. 3, pp. 93–130, 2009.
- [3] A. K. Ngugi, C. Bottomley, I. Kleinschmidt, J. W. Sander, and C. R. Newton, "Estimation of the burden of active and life-time epilepsy: a meta-analytic approach," *Epilepsia*, vol. 51, no. 5, pp. 883–890, 2010.
- [4] F. Tang, A. M. S. Hartz, and B. Bauer, "Drug-resistant epilepsy: multiple hypotheses, few answers," *Frontiers in Neurology*, vol. 8, article 301, 2017.
- [5] F. Shaher, H. Qiu, S. Wang et al., "Associated targets of the antioxidant cardioprotection of Ganoderma lucidum in diabetic cardiomyopathy by using open targets platform: a systematic review," *BioMed Research International*, vol. 2020, Article ID 7136075, 20 pages, 2020.
- [6] S. Q. Wang, X. J. Li, S. Zhou et al., "Intervention effects of Ganoderma lucidum spores on epileptiform discharge hippocampal neurons and expression of neurotrophin-4 and N-cadherin," *Plos One*, vol. 8, no. 4, article e1687, 2013.
- [7] F. Wang, F. Tan, Y. Jiang et al., "Changes of N-cadherins and NT-4 in the brain of pentylenetetrazol induced epileptic rats and the intervention effect of Ganoderma acid," *Heilongjiang Medicine and Pharmacy*, vol. 38, no. 4, pp. 133–136, 2015.
- [8] F. F. Wang, F. L. Tan, D. L. Chen et al., "The protective effect of Ganoderma lucidum acid on the brain of epilepsy rats induced by lithium-pilocarpine," *Chinese Journal of Microecology*, vol. 27, no. 7, pp. 757–760, 2015.
- [9] Z. M. Jiang, H. B. Qiu, S. Q. Wang, J. Guo, Z. W. Yang, and S. B. Zhou, "Ganoderic acid A potentiates the antioxidant effect and protection of mitochondrial membranes and reduces the apoptosis rate in primary hippocampal neurons in magnesium free medium," *Die Pharmazie*, vol. 73, no. 2, pp. 87–91, 2018.
- [10] J. Lu, J. Z. Qin, P. Chen, X. Chen, Y. Z. Zhang, and S. J. Zhao, "Quality difference study of six varieties of Ganoderma lucidum with different origins," *Frontiers in Pharmacology*, vol. 3, article 57, 2012.
- [11] T. Nakagawa, Q. Zhu, S. Tamrakar et al., "Changes in content of triterpenoids and polysaccharides in Ganoderma lingzhi at different growth stages," *Journal of Natural Medicines*, vol. 72, no. 3, pp. 734–744, 2018.
- [12] A. Das, M. Alshareef, F. Henderson Jr. et al., "Ganoderic acid A/DM-induced NDRG2 over-expression suppresses high-grade meningioma growth," *Clinical & Translational Oncology*, vol. 22, no. 7, pp. 1138–1145, 2020.
- [13] M. Zhu, Q. Chang, L. K. Wong, F. S. Chong, and R. C. Li, "Triterpene antioxidants from Ganoderma lucidum," *Phytotherapy Research*, vol. 13, no. 6, pp. 529–531, 1999.

- [14] L. Xu, L. Yan, and S. Huang, "Ganoderic acid A against cyclophosphamide-induced hepatic toxicity in mice," *Journal of Biochemical and Molecular Toxicology*, vol. 33, no. 4, article e22271, 2019.
- [15] B. Wan, Y. Li, S. Sun et al., "Ganoderic acid A attenuates lipopolysaccharide-induced lung injury in mice," *Bioscience Reports*, vol. 39, no. 5, article BSR20190301, 2019.
- [16] J. Meng, S. Z. Wang, J. Z. He et al., "Ganoderic acid A is the effective ingredient of Ganoderma triterpenes in retarding renal cyst development in polycystic kidney disease," *Acta Pharmacologica Sinica*, vol. 41, no. 6, pp. 782–790, 2020.
- [17] J. Zhu, J. Jin, J. Ding et al., "Ganoderic acid A improves high fat diet-induced obesity, lipid accumulation and insulin sensitivity through regulating SREBP pathway," *Chemico-Biological Interactions*, vol. 290, pp. 77–87, 2018.
- [18] B. S. Min, N. Nakamura, H. Miyashiro, K. W. Bae, and M. Hattori, "Triterpenes from the spores of Ganoderma lucidum and their inhibitory activity against HIV-1 protease," *Chemical & Pharmaceutical Bulletin*, vol. 46, no. 10, pp. 1607–1612, 1998.
- [19] Y. Cheng and P. Xie, "Ganoderic acid A holds promising cytotoxicity on human glioblastoma mediated by incurring apoptosis and autophagy and inactivating PI3K/AKT signaling pathway," *Journal of Biochemical and Molecular Toxicology*, vol. 33, no. 11, article e22392, 2019.
- [20] C. Wang, "Expression and mechanism of calcium-sensing receptor in cardiomyocytes of pentylenetetrazol kindled chronic epilepsy rat model," *Jiamusi University*, pp. 33–35, 2015.
- [21] L. M. Wang, X. W. Han, C. Wang et al., "Expression of calcium-sensing receptor and P13k/Akt pathway regulate the cardiac myocyte apoptosis of epilepsy rats," *Chinese Journal of Child Health Care*, vol. 24, no. 5, pp. 479–482, 2016.
- [22] Y. W. Zhang, J. Guo, M. Yan et al., "Expression of CaSR in neurins and cardiomyocytes incubated with magnesium-free extracellular fluid and its relationship with the MAPK pathway," *Journal of Medical Postgraduates*, vol. 31, no. 8, pp. 795–799, 2018.
- [23] A. L. Magno, B. K. Ward, and T. Ratajczak, "The calcium-sensing receptor: a molecular perspective," *Endocrine Reviews*, vol. 32, no. 1, pp. 3–30, 2011.
- [24] R. Pais, F. M. Gribble, and F. Reimann, "Signalling pathways involved in the detection of peptones by murine small intestinal enteroendocrine L-cells," *Peptides*, vol. 77, pp. 9–15, 2016.
- [25] S. Smajilovic and J. Tfeh-Hansen, "Calcium acts as a first messenger through the calcium-sensing receptor in the cardiovascular system," *Cardiovascular Research*, vol. 75, no. 3, pp. 457–467, 2007.
- [26] J. Guo, X. J. Li, Z. M. Jiang et al., "Expression of calcium sensing receptor and apoptosis pathway changes in epilepsy rat," *Journal of Apoplexy and Nervous Diseases*, vol. 30, no. 11, pp. 981–984, 2013.
- [27] T. Yamnguchi and T. Sugimoyo, "Impaired bone mineralization in calcium-sensing receptor (CaSR) knockout mice: the physiological action of CaSR in bone microenvironments," *Clinical Calcium*, vol. 17, no. 10, pp. 1567–1573, 2007.
- [28] E. M. Brown and R. J. Macleod, "Extracellular calcium sensing and extracellular calcium signaling," *Physiological Reviews*, vol. 81, no. 1, pp. 239–297, 2001.
- [29] K. I. Lin, N. Chattopadhyay, M. Bai et al., "Elevated extracellular calcium can prevent apoptosis via the calcium-sensing receptor," *Archives of Biochemistry and Biophysics*, vol. 249, no. 2, pp. 325–331, 1998.
- [30] J. Ba and P. A. Friedman, "Calcium-sensing receptor regulation of renal mineral ion transport," *Cell Calcium*, vol. 35, no. 3, pp. 229–237, 2004.
- [31] X. L. Liu, Y. S. Lu, J. Y. Gao et al., "Calcium sensing receptor absence delays postnatal brain development via direct and indirect mechanisms," *Molecular Neurobiology*, vol. 48, no. 3, pp. 590–600, 2013.
- [32] M. Ruat and E. Traiffort, "Roles of the calcium sensing receptor in the central nervous system," *Best Practice & Research. Clinical Endocrinology & Metabolism*, vol. 27, no. 3, pp. 429–442, 2013.
- [33] R. C. Ziegelstein, Y. Xiong, C. He, and Q. Hu, "Expression of a functional extracellular calcium-sensing receptor in human aortic endothelial cells," *Biochemical and Biophysical Research Communications*, vol. 342, no. 1, pp. 153–163, 2006.
- [34] A. Kapoor, P. Satishchandra, R. Ratnapriya et al., "An idiopathic epilepsy syndrome linked to 3q13.3-q21 and missense mutations in the extracellular calcium sensing receptor gene," *Annals of Neurology*, vol. 64, no. 2, pp. 158–167, 2008.
- [35] A. V. Delgado-Escueta, B. P. Koeleman, J. N. Bailey, M. T. Medina, and R. M. Durón, "The quest for juvenile myoclonic epilepsy genes," *Epilepsy & Behavior: E&B*, vol. 28, pp. S52–S57, 2013.
- [36] A. Stepanchick, J. McKenna, O. McGovern, Y. Huang, and G. E. Breitwieser, "Calcium sensing receptor mutations implicated in pancreatitis and idiopathic epilepsy syndrome disrupt an arginine-rich retention motif," *Cellular Physiology and Biochemistry: International Journal of Experimental Cellular Physiology, Biochemistry, and Pharmacology*, vol. 26, no. 3, pp. 363–374, 2010.
- [37] T. N. Vizard, G. W. O'Keeffe, H. Gutierrez, C. H. Kos, D. Riccardi, and A. M. Davies, "Regulation of axonal and dendritic growth by the extracellular calcium-sensing receptor," *Nature Neuroscience*, vol. 11, no. 3, pp. 285–291, 2008.
- [38] S. H. Zhang, D. Liu, Q. Hu, J. Zhu, S. Wang, and S. Zhou, "Ferulic acid ameliorates pentylenetetrazol-induced seizures by reducing neuron cell death," *Epilepsy Research*, vol. 156, article 106183, 2019.
- [39] L. Wang, L. Liu, and J. Liu, "Protective effect of Ganoderma acid on hippocampal neurons in rats with lithium pilocarpine induced epilepsy," *Chinese Journal of Geriatrics*, vol. 35, no. 7, pp. 1907–1909, 2015.
- [40] R. J. Racine, "Modification of seizure activity by electrical stimulation: II. Motor seizure," *Electroencephalography and Clinical Neurophysiology*, vol. 32, no. 3, pp. 281–294, 1972.
- [41] T. Shimada and K. Yamagata, "Pentylenetetrazole-induced kindling mouse model," *Journal of Visualized Experiments: JoVE*, vol. 136, article e56573, 2018.
- [42] S. Zhou, S. Q. Wang, C. Y. Sun et al., "Investigation into anti-epileptic effect and mechanisms of Ganoderma lucidum polysaccharides in vivo and in vitro models," *Proceedings of the Nutrition Society*, vol. 74, article E65, 2015.
- [43] I. Dolka, M. Król, and R. Sapierzyński, "Evaluation of apoptosis-associated protein (Bcl-2, Bax, cleaved caspase-3 and p53) expression in canine mammary tumors: an immunohistochemical and prognostic study," *Research in Veterinary Science*, vol. 105, pp. 124–133, 2016.
- [44] M. S. Kim, W. S. Lee, J. Jeong, S. J. Kim, and W. Jin, "Induction of metastatic potential by TrkB via activation of IL6/JAK2/

- STAT3 and PI3K/AKT signaling in breast cancer,” *Oncotarget*, vol. 6, no. 37, pp. 40158–40171, 2015.
- [45] H. Zhao, Y. Guo, S. Li et al., “A novel anti-cancer agent Icaritin suppresses hepatocellular carcinoma initiation and malignant growth through the IL-6/Jak2/Stat3 pathway,” *Oncotarget*, vol. 6, no. 31, pp. 31927–31943, 2015.
- [46] J. Guo, Y. Liu, C. Wang et al., “The expression of calcium sensing receptor (CaSR) and MAPK pathway changes in myocardial cells of epilepsy rats,” *Chinese Journal of Applied Physiology*, vol. 32, no. 5, pp. 454–458, 2016.
- [47] F. del Monte, D. Lebeche, J. L. Guerrero et al., “Abrogation of ventricular arrhythmias in a model of ischemia and reperfusion by targeting myocardial calcium cycling,” *Proceedings of the National Academy of Sciences of the United States of America*, vol. 101, no. 15, pp. 5622–5627, 2004.
- [48] Y. Matsumoto, S. Yamamoto, Y. Suzuki et al., “Na⁺/H⁺ exchanger inhibitor, SM-20220, is protective against excitotoxicity in cultured cortical neurons,” *Stroke*, vol. 35, no. 1, pp. 185–190, 2004.
- [49] A. P. Halestrap, S. J. Clarke, and S. A. Javadov, “Mitochondrial permeability transition pore opening during myocardial reperfusion—a target for cardioprotection,” *Cardiovascular Research*, vol. 61, no. 3, pp. 372–385, 2004.
- [50] S. Q. Wang, X. J. Li, H. B. Qiu et al., “Anti-epileptic effect of Ganoderma lucidum polysaccharides by inhibition of intracellular calcium accumulation and stimulation of expression of CaMKII α in epileptic hippocampal neurons,” *PLoS One*, vol. 9, no. 7, article e102161, 2014.
- [51] L. Li, F. Chen, Y. G. Cao et al., “Role of calcium-sensing receptor in cardiac injury of hereditary epileptic rats,” *Pharmacology*, vol. 95, no. 1-2, pp. 10–21, 2015.
- [52] J. F. Ferri and G. Kroemer, “Organelle-specific initiation of cell death pathways,” *Nature Cell Biology*, vol. 3, no. 11, pp. E255–E263, 2001.
- [53] M. Degli Esposti and C. Dive, “Mitochondrial membrane permeabilisation by Bax/Bak,” *Biochemical and Biophysical Research Communications*, vol. 304, no. 3, pp. 455–461, 2003.
- [54] Y. Zhen, C. Ding, J. Sun, Y. Wang, S. Li, and L. Dong, “Activation of the calcium-sensing receptor promotes apoptosis by modulating the JNK/p38 MAPK pathway in focal cerebral ischemia-reperfusion in mice,” *American Journal of Translational Research*, vol. 8, no. 2, pp. 911–921, 2016.
- [55] A. Cuenda, J. M. Lizcano, and J. Lozano, “Editorial: mitogen activated protein kinases,” *Frontiers in Cell and Developmental Biology*, vol. 5, article 80, 2017.
- [56] Y. Son, Y. K. Cheong, N. H. Kim, H. T. Chung, D. J. Kang, and H. O. Pae, “Mitogen-activated protein kinases and reactive oxygen species: how can ROS activate MAPK pathways?,” *Journal of Signal Transduction*, vol. 2011, Article ID e792639, 6 pages, 2011.
- [57] X. Q. Geng, A. Ma, J. Z. He et al., “Ganoderic acid hinders renal fibrosis via suppressing the TGF- β /Smad and MAPK signaling pathways,” *Acta Pharmacologica Sinica*, vol. 41, no. 5, pp. 670–677, 2020.

Research Article

Targeted Inhibition of Protein Tyrosine Phosphatase 1B by Viscosol Ameliorates Type 2 Diabetes Pathophysiology and Histology in Diabetic Mouse Model

Aamir Sohail,¹ Hajra Fayyaz,¹ Hamza Muneer,¹ Idrees Raza,¹ Muhammad Ikram ,² Zia Uddin,² Sarah Gul ,³ Hailah M. Almohaimed,⁴ Ifat Alsharif,⁵ Fatima S. Alaryani,⁶ and Imran Ullah ¹

¹Department of Biochemistry, Faculty of Biological Sciences, Quaid-i-Azam University, Islamabad 45320, Pakistan

²Department of Pharmacy, COMSATS University Islamabad, Abbottabad Campus, Abbottabad, 22060 KP, Pakistan

³Department of Biological Sciences, FBAS, International Islamic University, Islamabad, Pakistan

⁴Department of Basic Science, College of Medicine, Princess Nourah Bint Abdulrahman University, P.O.Box 84428, Riyadh 11671, Saudi Arabia

⁵Department of Biology, Jamoum University College, Umm Al-Qura University, 21955 Makkah, Saudi Arabia

⁶College of Science, Department of Biology, University of Jeddah, Jeddah, Saudi Arabia

Correspondence should be addressed to Imran Ullah; imranullah@qau.edu.pk

Received 3 February 2022; Accepted 11 July 2022; Published 22 August 2022

Academic Editor: Abdul Rehman Phull

Copyright © 2022 Aamir Sohail et al. This is an open access article distributed under the Creative Commons Attribution License, which permits unrestricted use, distribution, and reproduction in any medium, provided the original work is properly cited.

Type 2 diabetes mellitus (T2DM) is one of the most common forms of diabetes. We are living in the middle of a global diabetes epidemic. Emerging pieces of evidence are suggesting the increased expression of protein tyrosine phosphatase 1B (PTP1B) in the pancreas and adipose tissues during T2DM. The negative regulation of the insulin signaling pathway by PTP1B helps the researchers to consider it as a potential therapeutic target for the treatment of insulin resistance and its associated complications. From the literature, we found that compound 5,7-dihydroxy-3,6-dimethoxy-2-(4-methoxy-3-(3-methyl-2-enyl)phenyl)-4H-chromen-4-one (Viscosol) extracted from *Dodonaea viscosa* can inhibit PTP1B in vitro. Therefore, in this study, we aimed to evaluate the antidiabetic effect of this compound in a high-fat diet (HFD) and low-dose streptozotocin (STZ-) induced T2DM mouse model. For this purpose, T2DM was induced in C57BL/6 male mice by using an already established protocol with minor modification. The compound-treated T2DM mice showed improvements in biochemical parameters, i.e., decrease in the fasting blood glucose level, increased body weight, improved liver profile, and reduction in oxidative stress. Furthermore, to elucidate the inhibition of PTP1B, the expression level of PTP1B was also measured at mRNA and protein levels by real-time PCR and western blot, respectively. Additionally, downstream targets (INSR, IRS1, PI3K, and GLUT4) were examined for confirming the inhibitory effect of PTP1B. Our results suggest that the compound can specifically inhibit PTP1B in vivo and might have the ability to improve insulin resistance and insulin secretion. Based on our experiment, we can confidently state that this compound can be a new PTP1B drug candidate for the treatment of T2DM in the coming future.

1. Introduction

T2DM is a disorder characterized by chronic hyperglycemic condition and appears as one of the defining medical challenges of the 21st century. According to the International Diabetes Federation (IDF) Atlas of Diabetes (2021), currently, 537 million individuals are living with diabetes. Paki-

stan has 33 million reported cases of diabetes and has a comparative prevalence of 30.8%, and an increase up to 33.6% in 2045 is expected, while a 46% increase is expected to occur globally [1]. About 90-95% of diabetes cases are T2DM [2]. It is a complex metabolic disorder, described with the increase in blood glucose level caused by the dysfunction in pancreatic β cells which leads to defective insulin

TABLE 1: List of primers used in RT-qP.

No.	Primer name	Sequence (5' → 3')	Tm	Amplicon size
1	mPdx1-F	ACTTGAGCGTTCCAATACGG	60.1	85 bp
	mPdx1-R	CTTAGCTTGCTCAGCCGTTC	60.3	
2	mIrs1-F	AAGCACTGTGACACCGGAA	60.3	72 bp
	mIrs1-R	CTTCGTGACCAGCTGTCCTT	60.4	
3	mGlut4-F	ACATACCTGACAGGGCAAGG	60	110 bp
	mGlut4-R	TGGAGGGGAACAAGAAAGTG	60.1	
4	mPi3k-F	GAGACAGGATGGGTCAAGGA	60	132 bp
	mPi3k-R	CAAAGCAACACAGGAGAGCA	60.2	
5	mPtpn1-F	GCATAGGACAGTGGTAATGCG	60.5	123 bp
	mPtpn1-R	AACTCACAGGGAAAGCAGAGG	60.8	
6	mInsr-F	CCTGTGGAGGGCTAACTGTG	60.7	76 bp
	mInsr-R	GGTTTGATACGGTGGAGGC	60.3	
7	mInsulin-F	GCCAAACAGCAAAGTCCAG	59.4	85 bp
	mInsulin-R	CACTAAGGGCTGGGGGTTA	59.9	
8	m β -actin-F	GATCATTGCTCCTCTGAGC	60	83 bp
	m β -actin-R	ACATCTGCTGGAAGGTGGAC	60	

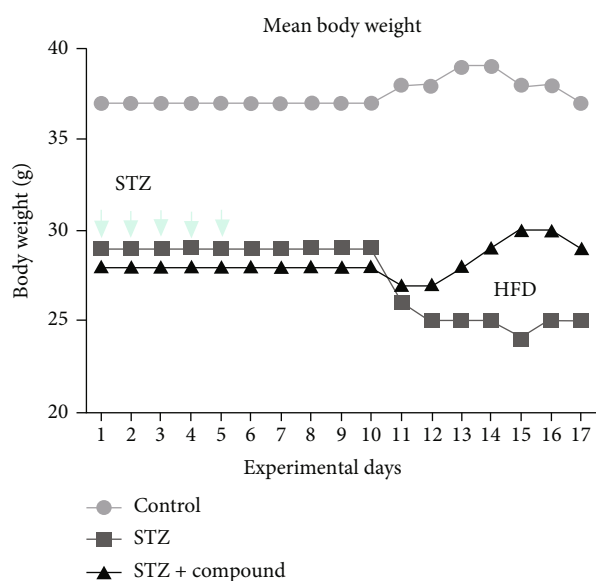


FIGURE 1: Mean body weight (g) of all groups of mice versus experimental days. The normal group was only given a standard diet, while STZ-HDF induced and STZ-HDF compound treated were given 5 I.P. STZ injections. Ordinary two-way ANOVA was performed, and results were found significant, **** $p < 0.0001$.

signaling and secretion [3]. This type of diabetes is also known as non-insulin-dependent diabetes mellitus and is described as the combination of hyperglycemia, insulin deficiency, and insulin resistance [4], and this combinatory condition causes impairment to a number of the systems in the human body, i.e., immune, musculoskeletal, neurological, and vascular. Numerous drugs are available for the treatment of T2DM but have several side effects and implications such as weight gain, cardiovascular problems, hypoglycemia,

and gastrointestinal problems. Therefore, there is a need to find a solution for T2DM which would have fewer side effects [5]. The insulin signaling pathway starts as the insulin (INS) binds with the insulin receptors (IR). The autophosphorylation of IR leads to the recruitment of insulin receptor substrate (IRS); further downstream phosphorylation of IRS1/2 results in the activation of the combinatorial possibility of the pathway IR-IRS1/2-PI3K-Akt. Akt is also called Protein Kinase B (PKB). The activation of Akt leads to the translocation of GLUT-4 [6], while the translocation of GLUT4 from the cytoplasm to the plasma membrane handles transferring more glucose inside the cell to minimize the glucose level in blood [7]. Insulin signaling is regulated at several steps as cellular phosphatases are involved in attenuating the insulin signaling by dephosphorylating the insulin receptor which is activated by autophosphorylation [8]. PTP1B, a member of the PTP superfamily, is a major nontransmembrane PTP, encoded by the Ptpn1 gene and ubiquitously expressed in all tissues [9]. PTP1B has a C-terminal hydrophobic region which anchors the protein to the cytoplasmic face of the endoplasmic reticulum and facilitates its ability to substrates. PTP1B inhibits insulin signaling by dephosphorylating the tyrosine residues of IRS-1 and IR- β [10]. The PTP1B is highly expressed in tissues that regulate glucose metabolism, i.e., the heart, skeletal muscles, pancreatic β cells, and liver [11]. In recent years, PTP1B has been the center of focus because of its ability to attenuate the insulin signaling pathway and is currently considered a therapeutic target against diabetes. The negative regulation of insulin metabolism via PTP1B is already demonstrated by using tissue-specific (liver) and whole-body PTP1B knock-out mice. It is well-known that inhibition of PTP1B can reduce insulin insensitivity hence increasing glucose uptake [12, 13]. Dephosphorylation of insulin receptors by PTP1B is reported both in vitro as well as in vivo. Furthermore, an increase in the expression of PTP1B causes insulin resistance

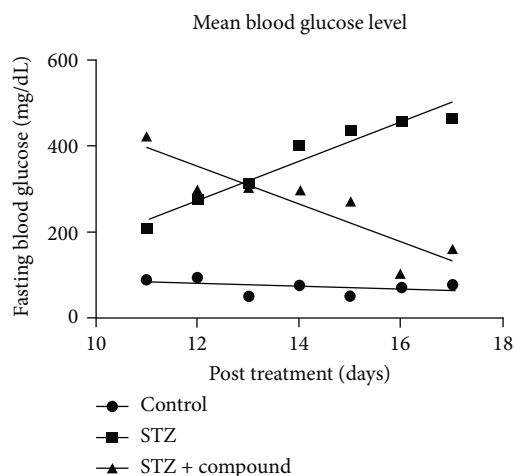


FIGURE 2: Mean blood glucose level (BGL). The bar graph showing increased BGL in the STZ-HFD-induced group as compared to the control group. While a significant reduction was observed in the compound-treated group as compared to diabetic, two-way ANOVA was used for calculating the statistical significance; ** $p < 0.001$.

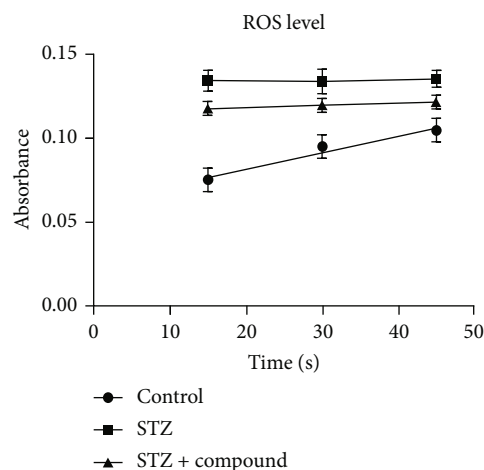


FIGURE 4: Serum ROS level. ROS level was elevated in the STZ-HFD-induced group as compared to the control and treated groups. Two-way ANOVA was used for calculating the statistical significance; *** $p < 0.0531$.

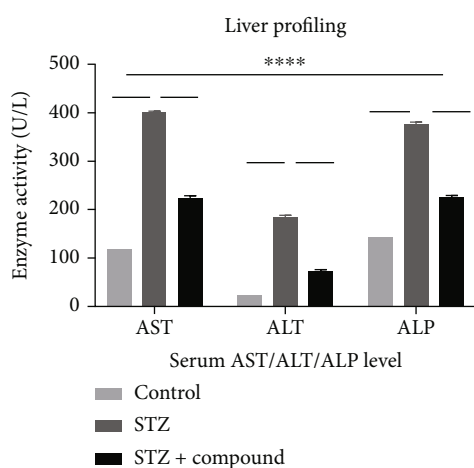


FIGURE 3: Serum enzymatic activities (U/L) of liver function (AST, ALT, and ALP) in mice. The bar graph showing the levels of AST, ALT, and ALP which was elevated in the STZ-HFD-induced group as compared to the control group. And significant reduction was observed in the compound-treated group as compared to diabetic. Two-way ANOVA was used for calculating the statistical significance; **** $p < 0.0001$.

in the liver, adipose, and muscle tissues [14–16]. *Dodonaea viscosa* (L). Jacq, a member of the family Sapindaceae grows on rocky and poor soils, is an evergreen shrub. *Dodonaea viscosa* is centrally originated in Australia and is also distributed in Mexico, Africa, New Zealand, India, Northern Mariana Islands, Virginia Islands, Florida, Arizona, South America, and Pakistan [17]. Extracts from the *Dodonaea viscosa* showed antidiabetic effects in alloxan and streptozotocin-induced diabetes in animal models [18, 19]. In 2010, Veerapur et al. reported the antidiabetic, antioxidant, and hypolipidemic activity of the aerial parts of *Dodo-*

naea viscosa in the streptozotocin-induced diabetes rat model [20]. Several studies have confirmed the antimicrobial, anti-inflammatory, antiulcer, smooth muscle relaxant, and wound healing activity of this plant [21]. Rojas et al. screened 294 plants and identified the hypoglycemic activity of *Dodonaea viscosa* [22]. *Dodonaea viscosa* is a major source of PTP inhibitors, as revealed by Ziauddin et al. in 2018. They were able to identify a purified polyphenolic compound from aerial parts of the plant which was showing an antidiabetic effect. This potent bioactive compound was isolated as a pale-yellow solid (molecular formula $C_{23}H_{24}O_7$), with a molecular weight of 412.1522. Overall, they have isolated 9 compounds and all compounds have an IC_{50} value of 13.5–57.9 μM . However, the compound 4, (5,7-dihydroxy-3,6-dimethoxy-2-(4-methoxy-3-(3-methyl but-2-enyl)phenyl)-4H-chromen-4-one), a potent inhibitor of PTP1B has an IC_{50} value of 13.5 μM and exhibits more fold inhibitory activity than other isolated compounds [23]. It was also inferred from the analysis that this compound works by the mechanism of mixed type 1 inhibition in vitro. In the current study, diabetes was induced by feeding mice with a high-fat diet and carbohydrates resulting in increased plasma insulin levels causing glucose intolerance and insulin resistance. The mice were further followed by a streptozotocin injection causing β cell death and a decrease in β cell mass [24]. Furthermore, we have designed our study to explore the insulin signaling pathway in the presence of compound 4, and the obtained results suggested that the compound was able to block PTP1B. This inhibition also enhances the secretion of insulin and glucose metabolism by increasing the GLUT4 translocation.

2. Materials and Methods

2.1. Animals and Grouping. C57BL/6 mice (25–40 g, 8–12 weeks old), purchased from the National Institute of Health

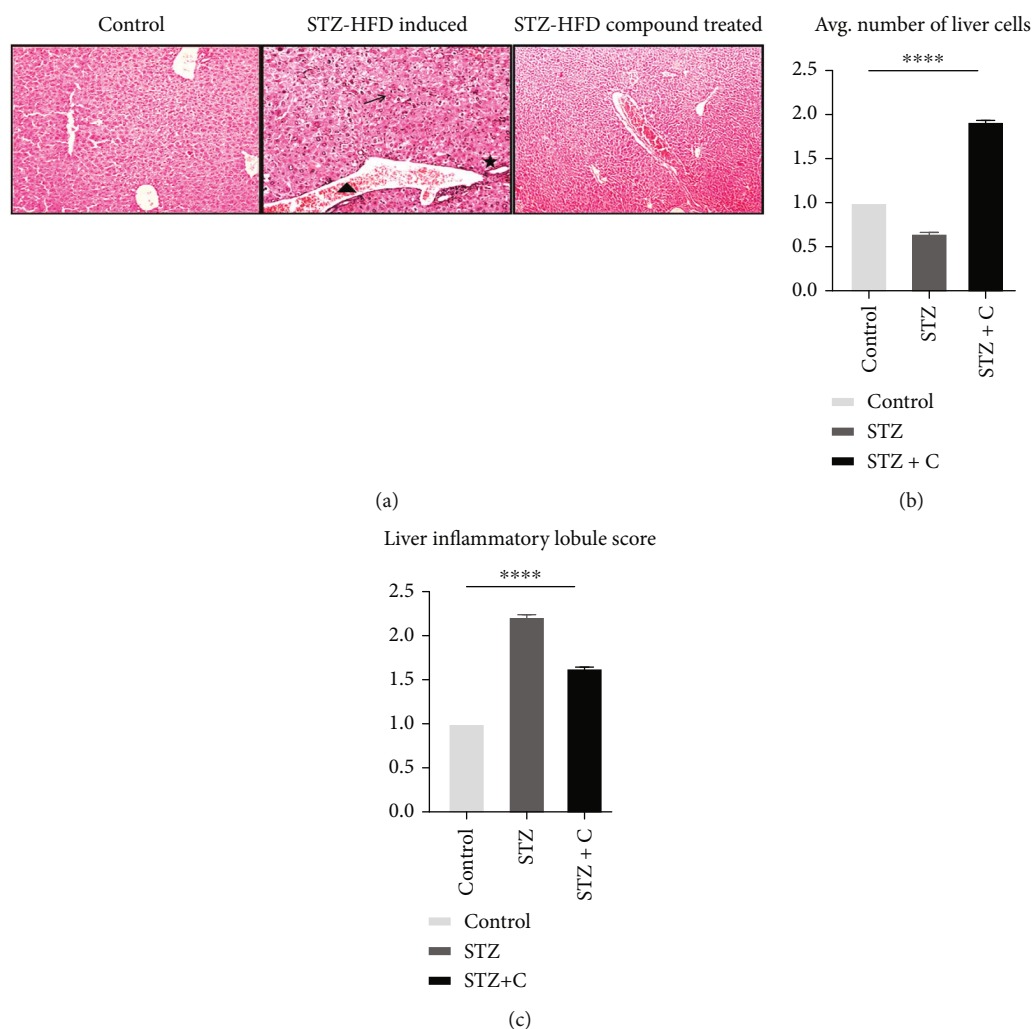


FIGURE 5: (a) H&E staining of liver tissue at 10x. Normal control, no significant change was seen in the morphology of the liver. STZ-HFD-induced diabetic mice, representing tissue damage, necrosis at many spots, and lymphocyte infiltration. STZ-HFD compound treated, the image was comparable to the normal with slight inflammatory invasion and tissue regeneration. Here, arrow represents lobular inflammation and cell invasion, star represents hyperaemia, and triangle represents cellular degeneration. (b) The area was selected by using ImageJ, and cells were analyzed. The number of the normal cell was represented in the form of a bar graph. Significant results were found with one-way ANOVA, as $***p=0.5483$. (c) The inflammatory lobules were represented in the form of a bar graph. Significant results were found with one-way ANOVA, as $***p=0.3272$.

(Islamabad, Pakistan), were used in the current study. Animals were maintained in the animal facility of Quaid-i-Azam University according to the guidelines of the National Institute of Health (USA) and the bioethics committee of our university. All protocols for animal handling and experimentation were approved by the Institutional Review Board. The mice were divided into three separate groups ($n=3$ in each group): group 1, control as a positive control; group 2, STZ-HFD-induced diabetic; and group 3, STZ-HFD compound-treated group.

2.2. Induction of Diabetes and Compound Treatment. The control group was fed the standard diet (4.1% fat, 22.2% protein, and 12.1% carbohydrates, as a percentage of total kcal) and injected with a single 500 μ L injection of saline. For dia-

betes induction, all the mice fasted for 4-6 hours before the injection of STZ, and blood glucose level (BGL) was estimated by a glucometer (ACCU-CHEK Instant S, Roche Diagnostic, Mannheim, Germany). Diabetes was induced by intraperitoneal injection of streptozotocin (Bio plus Fine Research Chemical, CAT # 41910012-3, Bioworld) for 5 consecutive days at a dose of 40 mg/kg in 500 μ L saline. The STZ injected mice were fed on a high-fat diet (HFD, 58% fat, 25% protein, and 17% carbohydrate, as a percentage of total kcal) with 10% glucose solution. On the sixth day, mice were given, and it took around 9-10 days for mice to develop diabetes. Mice with fasting blood glucose levels of >250 mg/dL (>11.1 mM) were considered diabetic. The BGL was continuously checked by a glucometer until euthanized. In group 3, after the induction of diabetes, HFD was

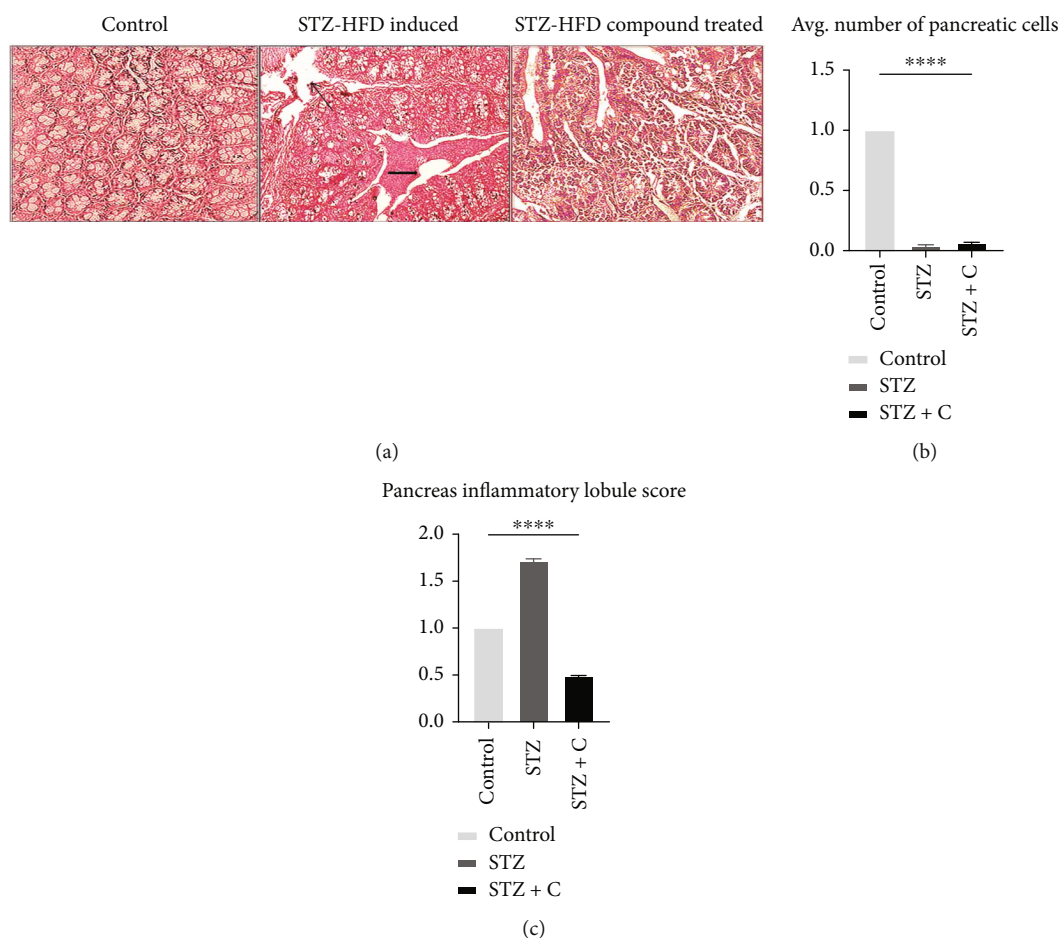


FIGURE 6: (a) H&E staining of pancreatic tissues. The images are obtained from a bright field microscope at 40x. Normal control with normal pancreatic structure. STZ-HFD-induced diabetic with damaged pancreatic tissue reduced β cell mass and inflammatory cell invasion. STZ-HFD compound treated having a structure comparable to the normal group. Here, upper arrow represents inflammatory lobules and cells, and arrow represents a reduction in β cell mass. (b) The area was selected by using ImageJ, and cells were analyzed. The number of normal cell was represented in the form of a bar graph. Significant results were found with one-way ANOVA, as $***p = 0.2058$. (c) The inflammatory lobules were represented in the form of a bar graph. Significant results were found with one-way ANOVA, as $***p = 0.1526$.

removed. On the 11th day, the compound (5,7-dihydroxy-3,6-dimethoxy-2-(4-methoxy-3-(3-methyl but-2-enyl)phenyl)-4H-chromen-4-one) was dissolved in 1% dimethyl sulfoxide (DMSO), and a single intraperitoneal injection (500 μ L) was given to mice (33 mg/kg). After the treatment with the compound, the BGL of the mice was continuously checked for 7 days. On the 17th day after BGL estimation, mice were euthanized for further analysis.

2.3. Serum Blood Glucose Analysis. The fasted mice for 4-6 hours were used to check the blood glucose level during the whole study. For output, blood was obtained through the tail vein, and glucose level was checked using a glucometer (ACCU-CHEK Instant S).

2.4. Blood Collection and Serum Separation. At the end of the study, mice were anesthetized, and blood was collected by cardiac puncture with the help of a 23G needle. Serum was

separated in 4 mL gel and clot activator vacutainer (Xinle) by centrifuging the tubes at 6000 rpm for 10 min. The supernatant was collected, and sera were stored at -20°C until further use.

2.5. Biochemical Parameters. The antidiabetic effects of the compound in HFD-STZ-induced diabetes in mice were seen. Different biochemical parameters were analyzed. These assays were performed by using enzymatic kits bought from AMP diagnostics. All the procedures and methods performed were according to the given protocol of kits.

2.5.1. Liver Profiling. Liver function biomarkers, including alanine aminotransferase (ALT), aspartate aminotransferase (AST), and alkaline phosphatase (ALP), were assayed by using a commercially available liver profiling kit (AMP Diagnostics, Austria).

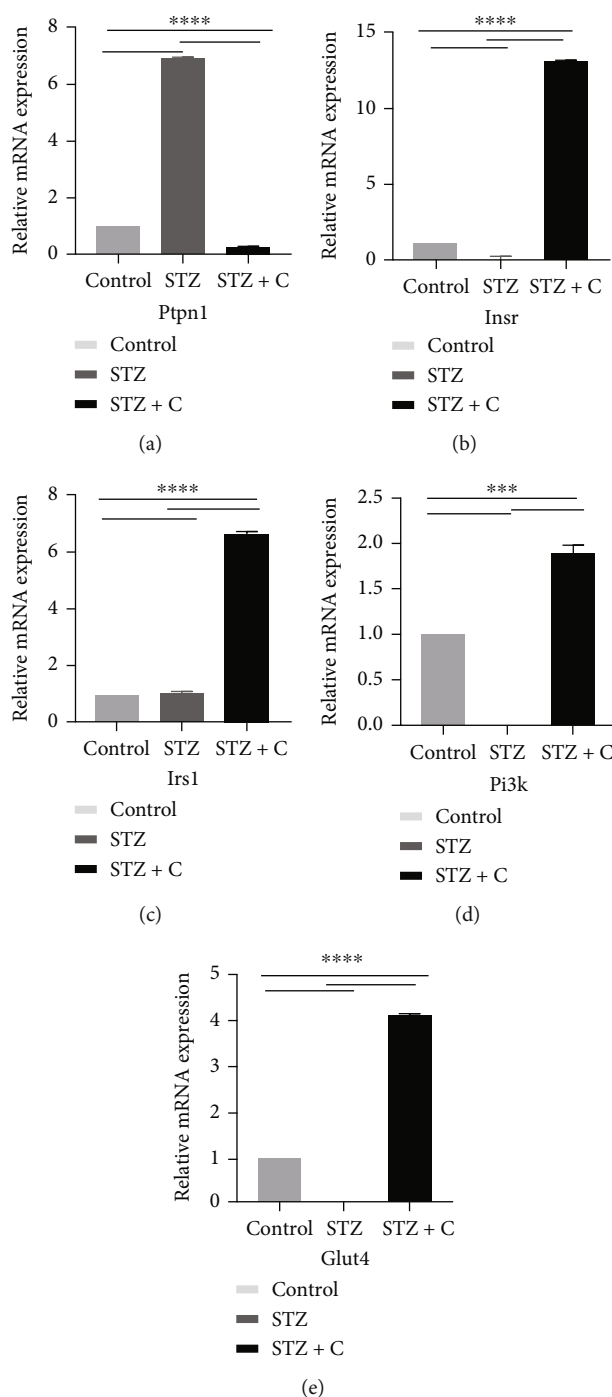


FIGURE 7: Expression profile of PTPN1 and downstream component of insulin signaling in mouse adipose tissue reveal significant difference. (a–e) The bar graphs show relative abundance of PTPN1, INSR, IRS1, PI3K, and GLUT4 mRNAs presented as fold change using control group as a reference sample. $n = 3$ mice. Two-way ANOVA test was used for calculating the statistical significance; **** $p < 0.05$.

2.5.2. *ROS Assay*. For ROS assay, according to Hayashi et al., protocol was followed for estimating the ROS levels in the serum of mice. Hydrogen peroxide was used as the standard solution and incubated at 37°C after 5 min. The working buffer was prepared according to the protocol by adding

100 μ L of R1 and R2 buffers. The working buffer was added at a ratio of 1:25 and incubated at 37°C for 1 min. Afterward, absorbance was measured by a multiskan GO, spectrophotometric plate reader (Thermo Fisher Scientific, USA) spectrophotometer at 505 nm. Three readings were recorded

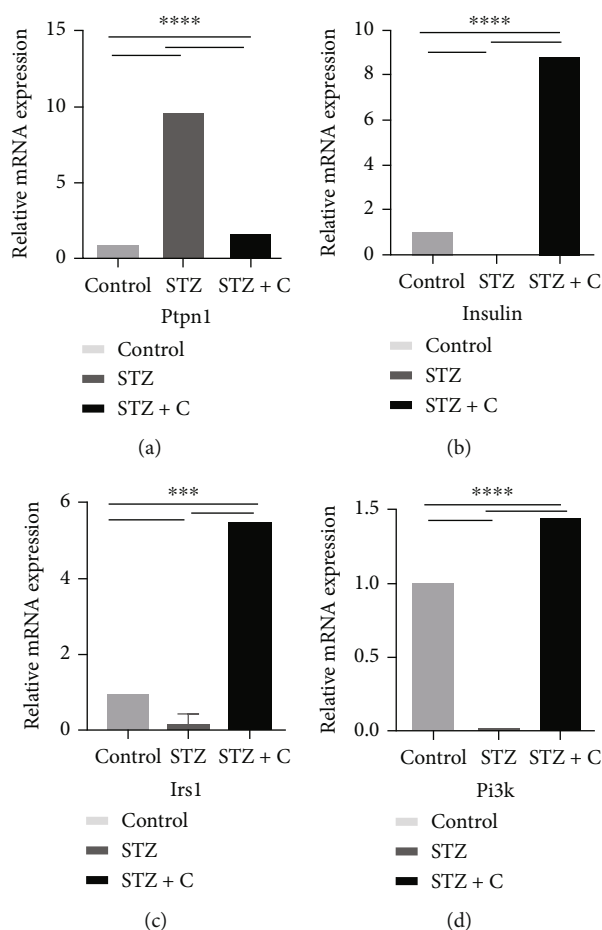


FIGURE 8: Expression profile of PTPN1 and downstream component of insulin signaling in mouse pancreatic tissue reveal significant difference. (a–d) The bar graphs show relative abundance of PTPN1, INS, IRS1, and PI3K mRNAs presented as fold change using control group as a reference sample. $n = 3$ mice. Two-way ANOVA test was used for calculating the statistical significance; $***p < 0.05$.

at 505 nm at an interval of 15 seconds. A calibration curve was constructed by using the concentration of hydrogen peroxide, and, respectively, samples were analyzed according to that [25].

2.6. Histological Analysis by H&E Staining. The liver and pancreas were removed and flushed with PBS and distilled water. The organs were fixed in 10% formalin and kept at room temperature. For histological studies, these organs were then removed, dehydrated, and embedded in the paraffin wax. The fixed tissues were sectioned ($4\ \mu\text{m}$) using a microtome (KD202, China). The tissue sections were stained with hematoxylin and eosin stains. The stained slides were then examined under the bright field microscope (CX41, Olympus Microscope, Japan). ImageJ was used for image analysis and graphical representation of H&E staining.

2.7. RNA Isolation, cDNA Synthesis, and Real-Time qPCR. RNA was extracted from the respective tissues by using the RNA Extraction Kit (PureLink™, RNA Minikit, Invitrogen by Thermo Fisher Scientific, Cat No # 1218301 8A). Approximately, 30–40 mg of tissue was used for the isolation

of total RNA. Isolated RNA ($1\ \mu\text{g}$) was reverse transcribed to cDNA using a high-capacity cDNA synthesis kit (Thermo Fischer Scientific, RevertAid First Strand cDNA Synthesis Kit, USA). The relative abundance of mRNA levels was measured by SYBER Green-based RT-PCR chemistry (Maxima SYBR Green/ROX qPCR Master Mix (2X), Thermo Scientific, USA) using the MyGo Pro PCR system (MyGo PCR systems, IT-IS Life Sciences). Specific primers were used for RT-PCR (Table 1). Each sample was run in triplicates, and β -actin was used as a housekeeping gene. The data were analyzed by the $\Delta\Delta\text{Ct}$ method, and mRNA fold change was calculated.

2.8. Western Blotting. For western blotting, whole-cell lysate was prepared by using radioimmunoprecipitation assay (RIPA) buffer (10 mM Tris pH 8, 140 mM NaCl, 1% Triton X-100, 0.1% SDS, 0.01% sodium deoxycholate, 1 mM EDTA, 1 mM DTT, 1% protease inhibitor, 1% phosphate inhibitor). Depending upon the size of the tissue (20–30 mg), the 200–300 μL buffer was added to a tube having tissue and was minced. The samples were incubated on ice for 15 minutes

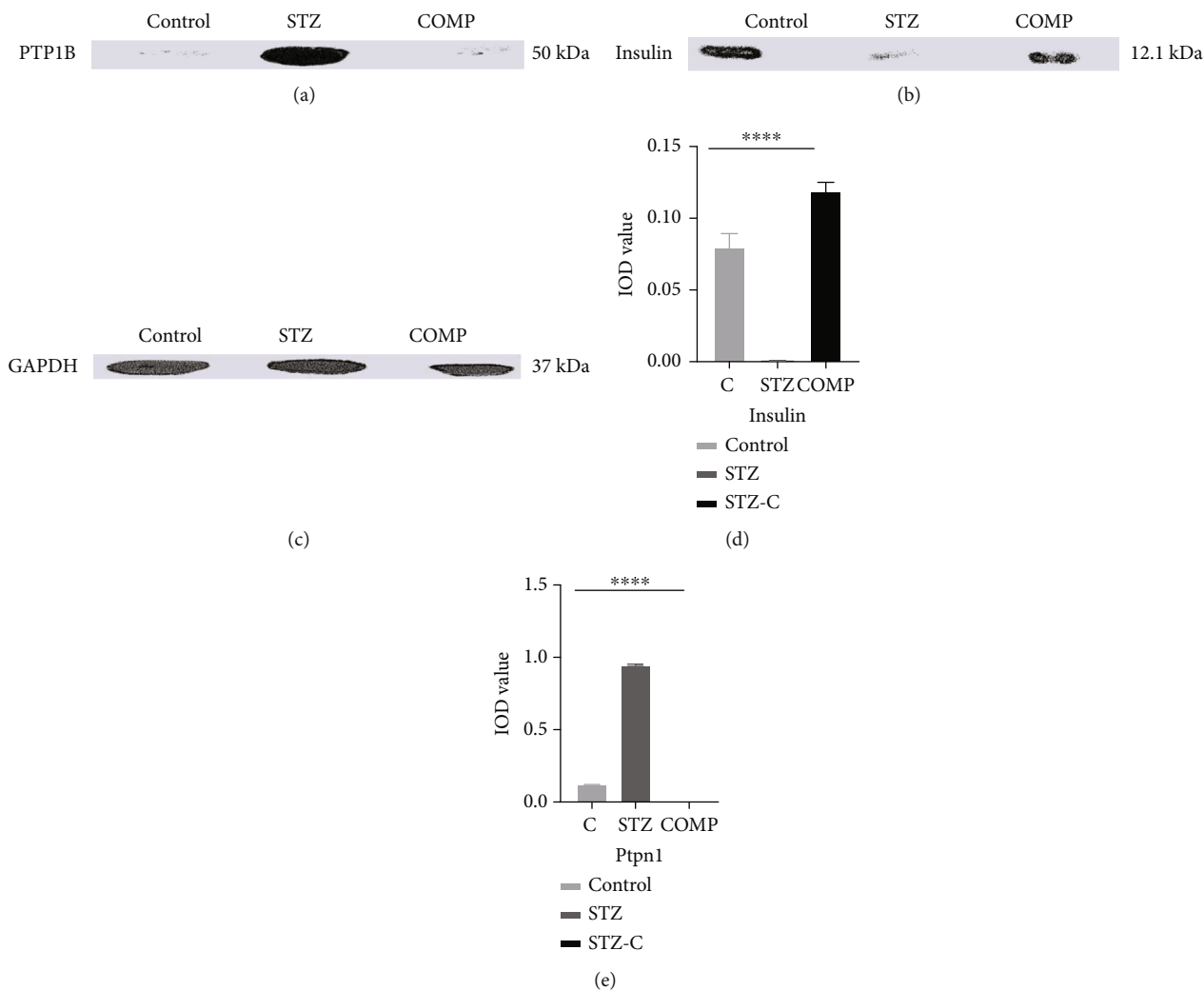


FIGURE 9: Immunoblotting reveals the expression of PTP1B and insulin in adipose tissue. The immunoblot (a, b) shows the expression of PTP1B and insulin. GAPDH was used as a loading control (c). The bar graph is plotted by calculating integrated optical density (IOD) value (d, e). It shows an increase in the expression of insulin and a decrease in PTP1B. We found significant results with one-way ANOVA, $***p = 0.0008$.

and vortexed at intermittent intervals of 15 seconds. The samples were additionally incubated on ice for 15 minutes. The whole-cell lysate was centrifuged at 4°C at maximum speed (13000 rpm) for 10 minutes. The supernatant was pipetted out and stored at -20°C for future use. The isolated protein was quantified by Bradford assay using BSA. The concentration of unknown protein samples was figured out from the standard curve by applying the trendline formula of MS Excel. GAPDH was used as a loading control. The data of immunoblotting was analyzed by software (Alpha-View SA version 3.4.4.0), and integrated optical density was calculated.

2.9. Statistical Analysis. For statistical analysis, data from at least three replicates were used and analyzed with a one-way, two-way ANOVA, and post hoc Tukey or LSD test using GraphPad Prism (version 9). Microsoft Excel was used

for $\Delta\Delta Ct$ calculation. A p value of < 0.05 was considered statistically significant. All experiments were performed in triplicates.

3. Results

3.1. Mean Body Weight and Fasting Blood Glucose Level. Bodyweight and blood glucose levels (BGL) were monitored during the experimental period in all three groups. STZ-HFZ compound-treated group showed improvements in body weight as compared to the STZ-HFD-induced diabetic group (diabetic) (Figure 1). In STZ-HFD compound-treated group, a gradual decrease in the BGL was seen after the treatment with a single injection of the compound (Figure 2), while BGL levels in STZ-HFD-induced group remained constantly high.

3.2. Biochemical Parameters. Biochemical testing was performed using the serum. In diabetes, liver damage and alteration in liver enzymes were seen. Hence, liver profiling was performed by analyzing the level of AST, ALT, and ALP enzymes. The level of AST, ALT, and ALP was significantly higher in the STZ-HFD-induced group as compared to normal and STZ-HFD compound treated (Figure 3). Moreover, the compound showed a liver protective effect as the level of AST, ALT, and ALP was comparable to the control group. The absorbance was measured at 340 nm, and analyzed data were represented in the form of a bar graph. Furthermore, ROS level was analyzed in the serum which was found significantly low in the STZ-HFD compound-treated group compared to STZ-HFD-induced group (Figure 4).

3.3. Histological Analysis by H&E Staining. The liver of the STZ-HFD-induced group showed abnormal patterns with lymphocyte infiltration, lobular inflammation, hyperammonemia, and various spots of cytoplasmic degeneration. However, the morphology of the STZ-HFD compound-treated group was like the control group with slight lymphocyte infiltration and liver regeneration (Figure 5(a)). In the case of the liver, the area was selected by using ImageJ, and cells were analyzed. The obtained value was exported to excel for analysis. The selected area obtained from the STZ-HFD-induced and STZ-HFD compound-treated groups was normalized by the control group. The relative number of the normal cell in the liver (Figure 5(b)) and inflammatory lobules in the liver (Figure 5(c)) was represented in the form of a bar graph. Significant results were found with one-way ANOVA, with a p value < 0.0001 .

In the pancreas, the control and STZ-HFD compound-treated groups showed similar morphology as compared to STZ-HFD-induced group; as the pancreatic morphology was distorted, inflammatory cell invasion and reduction in the β cell mass were seen (Figure 6(a)). In the case of the pancreas, the area was selected by using ImageJ, and cells were analyzed. The obtained value was exported to Excel for analysis. The selected area obtained from the STZ-HFD-induced and STZ-HFD compound-treated groups was normalized by the control group. The relative number of the normal cell in the pancreas (Figure 6(b)) and inflammatory lobules in the pancreas (Figure 6(c)) was represented in the form of a bar graph. Significant results were found with one-way ANOVA, with a p value < 0.0001 .

3.4. Correlation of Inhibition of PTP1B in Adipose and Pancreas with the Expression of Downstream Regulators. PTP1B is widely expressed in insulin-sensitive tissues and plays a role as an important negative regulator of insulin signaling. Many studies have reported that inhibition of PTP1B can be considered a therapeutic target in T2DM. Therefore, we further investigated the expression of different downstream components in both tissue (adipose and pancreas) as possibly the inhibition of PTP1B is a contributing factor to insulin signaling. Each cDNA sample was run in triplicates, and GAPDH was used as a housekeeping gene. The data from three independent experiments were analyzed by a $\Delta\Delta C_t$ method to calculate the mRNA fold change using

normal as a control. The data were represented as means \pm SD. The differences between groups were analyzed by two-way ANOVA using Bonferroni post hoc test. A p value of 0.05 was considered statistically significant. Our data showed that the relative abundance of PTPN1 mRNA, the main unit of our study, was decreased in the treated group in both tissues (Figures 7(a) and 8(a)). Moreover, it is known that PTPN1 inhibits the phosphorylation of IR and IRS1. Therefore, inhibition of PTPN1 results in increased expression of INSR, IRS1, PI3K, and GLUT4 in adipose (Figures 7(b)–7(e)) and INS, IRS1, and PI3K in the pancreas (Figures 8(b)–8(d)) in the compound-treated group as compared to the STZ-HFD diabetic group. Hence, we can conclude that inhibition of PTP1B results in the reduction of mRNA level of PTPN1 which increased downstream regulatory components of insulin signaling. These results show that the compound used during the study can block the activity of PTPN1 at the mRNA level which affects the components of insulin signaling.

3.5. Immunoblotting Showing the Expression of PTP1B and Insulin in Adipose Tissue. To further substantiate the RT-qPCR results, the expression of PTP1B and insulin at the protein level was analyzed by immunoblotting in adipose tissue. The results showed that PTP1B was increased in the adipose tissue of the STZ-HFD-induced group while the reduction in the expression was seen in the compound-treated group (Figure 9(a)). Furthermore, lower expression of insulin was found in the STZ-HFD-induced group, while in the control and compound-treated groups, significant insulin secretion was detected (Figure 9(b)). The immunoblot was analyzed by software (AlphaView SA version 3.4.4.0), and the bar graph is plotted by calculating the integrated optical density (IOD) value by ImageJ. IOD of targets was normalized with GAPDH as an internal control (Figures 9(c)–9(e)). Significant results were found with one-way ANOVA, as $*** p = 0.0008$.

4. Discussion

Type 2 diabetes mellitus is regarded as resistance to insulin hormone which occurs because of attenuated signaling from the insulin receptors. The global occurrence of T2DM is increasing at an alarming rate. Protein tyrosine phosphatase 1B (PTP1B), a member of PTPase, has been getting intensive attention in research as it takes part in the insulin signaling cascade. The compelling experiments have revealed that PTP1B plays a significant regulatory role in modulating insulin sensitivity, hence, signifying PTP1B as a potential therapeutic target. PTP1B is not only involved in T2DM but also involved in several other diseases, including autoimmune disorders, cardiovascular diseases, cancer, and liver diseases.

Several pieces of evidence from cellular, biochemical, and chemical inhibitor studies have found that PTP1B is a major negative regulator of insulin signaling. Additionally, many studies suggest that the action of insulin can be enhanced by the inhibition of PTP1B. Subsequently, PTP1B has been considered an attractive target for the treatment of

T2DM. In the present study, we tried to analyze the PTP1B inhibitory role of our specific compound extract from *Dodonaea viscosa* in *in vivo*. Our findings highlight the intriguing fact that inhibition of PTP1B might help to improve insulin resistance and insulin secretion in adipose and pancreatic tissue. Improvements in biochemical parameters such as the decrease in the fasting blood glucose level, increased body weight, and improved liver profile were also seen in our experiment which is consistent with the previously published reports [26]. Histopathological analysis by H&E staining of the liver and pancreas showed comparable results of the STZ-HFD compound-treated and normal groups, while the morphology of liver and pancreas was distorted in the STZ-HFD diabetic group as lymphocyte infiltration, reduced β cell mass, and apoptotic cells were seen. In recent years, *in vitro* analysis has shown that PTP1B expression can be induced by high glucose, palmitate, fatty acids, and cytokines such as TNF- α and IL-6 [11, 27–29]. The increased level of PTP1B is reported in insulin-sensitive tissues in STZ-induced diabetic mice and rats [30]. In 2012, Vakili et al. reported that inhibiting PTP1B by using shRNA in STZ-induced diabetic mice resulted in a decrease in plasma glucose level [31]. Furthermore, our study also shows a significant reduction in oxidative stress. The elevated level of reactive oxygen species (ROS) in obesity and diabetic individuals has been previously reported [32]. Likewise, in the current study, the level of ROS in the STZ-HFD-induced group was significantly high than in the STZ-HFD compound-treated group which confirms the protective effect of our compound.

It has been previously reported that PTP1B inhibitors increased the IR and IRS1 phosphorylation which results in the increased GLUT4 translocation and glucose uptake in insulin target tissues [33]. Several studies also showed that PTP1B deficient animals enhanced insulin sensitivity, prevented them from weight gain, and increased phosphorylation of IR even if they are fed with an HFD [34]. Likewise, our study also shows that there would be an increased translocation of glucose via GLUT4 which ultimately upregulate the insulin signaling pathway. This phenomenon was confirmed by analyzing the relative mRNA expression of *INS*, *INSR*, *IRS1*, *PI3K*, *GLUT4*, and *PTPN1*. In adipose tissue, we found that the relative mRNA expression of *INSR*, *IRS1*, *PI3K*, and *GLUT4* was downregulated in the STZ-HFD diabetic group while upregulated in the STZ-HFD compound-treated group. Furthermore, expression of *PTPN1* was significantly decreased in the compound-treated group. Similarly, we have seen an increased expression of *INS* and *IRS1* in the compound-treated group, while downregulation of *PTPN1* in pancreatic tissues which were found consistent with the previously reported studies [10].

To substantiate our results, we have confirmed the expression of PTP1B and insulin at the protein level in adipose tissue. We found increased expression of PTP1B in the STZ-HFD-induced group, while it was inhibited in the compound-treated group. The antidiabetic activity of *Dodonaea viscosa* (plant extract) is well-known and observed for many years, but a lead compound that can inhibit the PTP1B enzyme was yet not explored. Hence, this assures

us that the compound used in the current study can be considered a specific inhibitor of PTP1B.

5. Conclusion

Concluding, we have targeted PTP1B and its downstream targets in the STZ-HFD-induced type II diabetic model via the help of a compound, 5,7-dihydroxy-3,6-dimethoxy-2-(4-methoxy-3-(3-methyl-2-enyl)phenyl)-4H-chromen-4-one, extracted from the *Dodonaea viscosa*. The antidiabetic and inhibitory potential of this compound on PTP1B has been evaluated in the current study. Collectively, we have investigated the effect of our compound on body weight, histological, and biochemical parameters. Additionally, the study was supported by transcriptomic and proteomic analyses. The data shows a decrease in the level of PTP1B at the mRNA level, and complete inhibition was seen in the compound-treated group. Conclusively, this study will help to develop a new pharmacological drug for the treatment of T2DM specifically by targeting PTP1B.

Abbreviations

IRS:	Insulin receptor substrate
STZ:	Streptozotocin
PTP1B:	Protein-tyrosine phosphatase 1B
TCPTP45:	T cell protein tyrosine phosphatase 45
Akt:	Ak strain transforming
T2DM:	Type 2 diabetes mellitus
AST:	Serum aspartate aminotransferase
ALT:	Serum alanine aminotransferase
ALP:	Serum alkaline phosphatase
ROS:	Reactive oxygen specie
b.w:	Bodyweight
HFD:	High-fat diet
PKB:	Protein kinase B
IR:	Insulin receptor
DMSO:	Dimethyl sulfoxide.

Data Availability

Our data will be available upon the publication of this manuscript.

Ethical Approval

All the requirements for this study were fulfilled, and the experiment was done with standard protocols. The study was approved by the Institutional Bioethics Committee of Quaid-i-Azam University, Islamabad.

Conflicts of Interest

The authors declare no competing interests.

Acknowledgments

This work was supported by the University Research Funding (URF 2019-20) of the Quaid-I-Azam University, Islamabad, Pakistan, and the Princess Nourah Bint Abdulrahman

University Researcher Supporting Project Number PNURSP2022R213, Riyadh, Saudi Arabia.

References

- [1] International Diabetes Federation, *IDF Diabetes Atlas*, Brussels, Belgium, 2021.
- [2] American Diabetes Association, "Classification and diagnosis of diabetes: standards of medical care in diabetes—2020," *Diabetes Care*, vol. 43, Supplement_1, pp. S14–S31, 2020.
- [3] R. A. DeFronzo, E. Ferrannini, L. Groop et al., "Type 2 diabetes mellitus," *Nature Reviews Disease Primers*, vol. 1, no. 1, pp. 1–22, 2015.
- [4] A. B. Olokoba, O. A. Obateru, and L. B. Olokoba, "Type 2 diabetes mellitus: a review of current trends," *Oman Medical Journal*, vol. 27, no. 4, pp. 269–273, 2012.
- [5] A. Chaudhury, C. Duvoor, V. S. Reddy Dendi et al., "Clinical review of antidiabetic drugs: implications for type 2 diabetes mellitus management," *Frontiers in Endocrinology*, vol. 8, p. 6, 2017.
- [6] J. M. Lizcano and D. R. Alessi, "The insulin signalling pathway," *Current Biology*, vol. 12, no. 7, pp. R236–R238, 2002.
- [7] B. SarathKumar and B. S. Lakshmi, "In silico investigations on the binding efficacy and allosteric mechanism of six different natural product compounds towards PTP1B inhibition through docking and molecular dynamics simulations," *Journal of Molecular Modeling*, vol. 25, no. 9, pp. 1–17, 2019.
- [8] E. L. White, Y. Amitai, and M. J. Gutnick, "A comparison of synapses onto the somata of intrinsically bursting and regular spiking neurons in layer V of rat SmI cortex," *Journal of Comparative Neurology*, vol. 342, no. 1, pp. 1–14, 1994.
- [9] J. V. Frangioni, P. H. Beahm, V. Shifrin, C. A. Jost, and B. G. Neel, "The nontransmembrane tyrosine phosphatase PTP-1B localizes to the endoplasmic reticulum via its 35 amino acid C-terminal sequence," *Cell*, vol. 68, no. 3, pp. 545–560, 1992.
- [10] F. Gu, D. T. Nguyễn, M. Stuiblé et al., "Protein-tyrosine phosphatase 1B potentiates IRE1 signaling during endoplasmic reticulum stress," *Journal of Biological Chemistry*, vol. 279, no. 48, pp. 49689–49693, 2004.
- [11] J. M. Zabolotny, Y.-B. Kim, L. A. Welsh, E. E. Kershaw, B. G. Neel, and B. B. Kahn, "Protein-tyrosine phosphatase 1B expression is induced by inflammation in vivo," *Journal of Biological Chemistry*, vol. 283, no. 21, pp. 14230–14241, 2008.
- [12] M. J. Quon, A. J. Butte, and S. I. Taylor, "Insulin signal transduction pathways," *Trends in Endocrinology & Metabolism*, vol. 5, no. 9, pp. 369–376, 1994.
- [13] J. Montalibet and B. P. Kennedy, "Therapeutic strategies for targeting PTP1B in diabetes," *Drug Discovery Today: Therapeutic Strategies*, vol. 2, no. 2, pp. 129–135, 2005.
- [14] S. S. Dadke, H. C. Li, A. B. Kusari, N. Begum, and J. Kusari, "Elevated expression and activity of protein-tyrosine phosphatase 1B in skeletal muscle of insulin-resistant type II diabetic Goto-Kakizaki rats," *Biochemical and Biophysical Research Communications*, vol. 274, no. 3, pp. 583–589, 2000.
- [15] M. Elchebly, P. Payette, E. Michaliszyn et al., "Increased insulin sensitivity and obesity resistance in mice lacking the protein tyrosine phosphatase-1B gene," *Science*, vol. 283, no. 5407, pp. 1544–1548, 1999.
- [16] J. M. Zabolotny, F. G. Haj, Y.-B. Kim et al., "Transgenic overexpression of protein-tyrosine phosphatase 1B in muscle causes insulin resistance, but overexpression with leukocyte antigen-related phosphatase does not additively impair insulin action," *Journal of Biological Chemistry*, vol. 279, no. 23, pp. 24844–24851, 2004.
- [17] D. Lawal and I. Yunusa, "Dodoniaea viscosa Linn: it's medicinal, pharmacological and phytochemical properties," *International Journal of Innovation and Applied Studies*, vol. 2, no. 4, pp. 476–482, 2013.
- [18] P. Muthukumran, V. Hazeena Begumand, and P. Kalaiarasan, "Anti-diabetic activity of Dodoniaea viscosa (L) leaf extracts," *International Journal of PharmTech Research*, vol. 3, pp. 136–139, 2011.
- [19] World Health Organization, *WHO Traditional Medicine Strategy: 2014-2023*, World Health Organization, 2013.
- [20] V. P. Veerapur, K. R. Prabhakar, V. K. Parihar et al., "Antidiabetic, hypolipidaemic and antioxidant activity of Dodoniaea viscosa aerial parts in streptozotocin-induced diabetic rats," *International Journal of Phytomedicine*, vol. 2, no. 1, 2010.
- [21] M. Getie, T. Gebre-Mariam, R. Rietz et al., "Evaluation of the anti-microbial and anti-inflammatory activities of the medicinal plants Dodoniaea viscosa, Rumex nervosus and Rumex abyssinicus," *Fitoterapia*, vol. 74, no. 1-2, pp. 139–143, 2003.
- [22] A. Rojas, S. Cruz, H. Ponce-Monter, and R. Mata, "Smooth muscle relaxing compounds from Dodoniaea viscosa5," *Planta Medica*, vol. 62, no. 2, pp. 154–159, 1996.
- [23] Z. Uddin, Y. H. Song, M. Ullah, Z. Li, J. Y. Kim, and K. H. Park, "Isolation and characterization of protein tyrosine phosphatase 1B (PTP1B) inhibitory polyphenolic compounds from Dodoniaea viscosa and their kinetic analysis," *Chemistry*, vol. 6, p. 40, 2018.
- [24] S. Lenzen, "The mechanisms of alloxan-and streptozotocin-induced diabetes," *Diabetologia*, vol. 51, no. 2, pp. 216–226, 2008.
- [25] I. Hayashi, Y. Morishita, K. Imai, M. Nakamura, K. Nakachi, and T. Hayashi, "High-throughput spectrophotometric assay of reactive oxygen species in serum," *Mutation Research/ Genetic Toxicology and Environmental Mutagenesis*, vol. 631, no. 1, pp. 55–61, 2007.
- [26] D. H. Kim, S. Lee, Y. W. Chung et al., "Antiobesity and antidiabetes effects of a Cudrania tricuspidata hydrophilic extract presenting PTP1B inhibitory potential," *BioMed Research International*, vol. 2016, Article ID 8432759, 11 pages, 2016.
- [27] M. Delibegovic, D. Zimmer, C. Kauffman et al., "Liver-specific deletion of protein-tyrosine phosphatase 1B (PTP1B) improves metabolic syndrome and attenuates diet-induced endoplasmic reticulum stress," *Diabetes*, vol. 58, no. 3, pp. 590–599, 2009.
- [28] J. Wu, L.-J. Yang, and D.-J. Zou, "Rosiglitazone attenuates tumor necrosis factor- α -induced protein-tyrosine phosphatase-1B production in HepG2 cells," *Journal of Endocrinological Investigation*, vol. 35, no. 1, pp. 28–34, 2012.
- [29] L. Parvaneh, R. Meshkani, S. Bakhtiyari et al., "Palmitate and inflammatory state additively induce the expression of PTP1B in muscle cells," *Biochemical and Biophysical Research Communications*, vol. 396, no. 2, pp. 467–471, 2010.
- [30] K. Adeli, J. Macri, A. Mohammadi, M. Kito, R. Urade, and D. Cavallo, "Apolipoprotein B is intracellularly associated with an ER-60 protease homologue in HepG2 cells," *Journal of Biological Chemistry*, vol. 272, no. 36, pp. 22489–22494, 1997.
- [31] S. Vakili, S. S. S. Ebrahimi, A. Sadeghi et al., "Hydrodynamic-based delivery of PTP1B shRNA reduces plasma glucose levels

- in diabetic mice,” *Molecular Medicine Reports*, vol. 7, no. 1, pp. 211–216, 2013.
- [32] X.-H. Wang, K.-X. Zhu, J.-Y. Li, C. Lei, and A.-J. Hou, “Vistriterpenoids A and B, two new 24-nor-oleanane triterpenoids from *Dodonaea viscosa*,” *Chemistry & Biodiversity*, vol. 15, no. 11, article e1800426, 2018.
- [33] K. Egawa, H. Maegawa, S. Shimizu et al., “Protein-tyrosine phosphatase-1B negatively regulates insulin signaling in I6 myocytes and Fao hepatoma cells,” *Journal of Biological Chemistry*, vol. 276, no. 13, pp. 10207–10211, 2001.
- [34] S. Koren and I. George Fantus, “Inhibition of the protein tyrosine phosphatase PTP1B: potential therapy for obesity, insulin resistance and type-2 diabetes mellitus,” *Best Practice & Research Clinical Endocrinology & Metabolism*, vol. 21, no. 4, pp. 621–640, 2007.

Research Article

Qizhi Kebutong Formula Ameliorates Streptozocin-Induced Diabetic Osteoporosis through Regulating the PI3K/Akt/NF- κ B Pathway

Lulu Tian,¹ Lu Ding ,² Guoqiang Wang,³ Yu Guo,¹ Yunyun Zhao ,¹ Yuchi Wei,¹ Xingquan Li,¹ Wei Zhang,² Jia Mi ,³ Xiangyan Li ,² Zeyu Wang ,⁴ and Xiuge Wang ³

¹College of Chinese Medicine, Changchun University of Chinese Medicine, 130117, China

²Jilin Ginseng Academy, Key Laboratory of Active Substances and Biological Mechanisms of Ginseng Efficacy, Ministry of Education, Jilin Provincial Key Laboratory of Bio-Macromolecules of Chinese Medicine, Changchun University of Chinese Medicine, Changchun, 130117 Jilin, China

³Department of Endocrinology, The Affiliated Hospital to Changchun University of Chinese Medicine, Changchun 130021, China

⁴Department of Scientific Research, Changchun University of Chinese Medicine, Changchun, China

Correspondence should be addressed to Zeyu Wang; zeyu781022@163.com and Xiuge Wang; xiuge_w@163.com

Lulu Tian and Lu Ding contributed equally to this work.

Received 5 March 2022; Revised 22 June 2022; Accepted 15 July 2022; Published 21 August 2022

Academic Editor: Madiha Ahmed

Copyright © 2022 Lulu Tian et al. This is an open access article distributed under the Creative Commons Attribution License, which permits unrestricted use, distribution, and reproduction in any medium, provided the original work is properly cited.

Background. Diabetic osteoporosis (DOP) is a progressive osteoblast dysfunction induced by high glucose, which has negative impacts on bone homeostasis. Qizhi Kebutong formula (QKF) is a traditional Chinese medicine (TCM) formula for treating DOP. However, its role in the protection of DOP has not been clarified yet. Here, we aimed to explore the potential mechanisms of QKF on DOP development via *in vivo* experiment. **Methods.** Network pharmacology was used to detect the key targets and signaling pathways of QKF on DOP. The effects of QKF on DOP were examined by the phenotypic characteristics, micro-CT, and hematoxylin-eosin (H&E) staining. The predicted targets and pathways were validated by a streptozocin- (STZ-) induced mouse model. Subsequently, the levels of the selected genes and proteins were analyzed using qRT-PCR and Western blot. Finally, AutoDock and PyMOL were used for molecular docking. **Results.** In this study, 90 active compounds and 2970 related disease targets have been found through network pharmacology. And QKF could improve the microstructures of femur bone mass, reduce inflammatory cell infiltration, and downregulate the levels of TNF- α , IKBKB, IL-6, and IL-1 β . Moreover, the underlying effect of PI3K/Akt/NF- κ B pathways was also recommended in the treatment. **Conclusion.** Altogether, our findings suggested that QKF could markedly alleviate osteoblast dysfunction by modulating the key targets and PI3K/Akt/NF- κ B signaling pathway.

1. Introduction

Diabetic osteoporosis (DOP) is a common complication of diabetes, which primarily affects bone metabolism, joints, and kidney [1, 2]. DOP is a skeletal disorder characterized by a chronic high glucose, decreased bone mass, and damaged bone tissue [3–5]. With the increasing incidence of diabetes, DOP has become a systemic bone disease to increase bone brittleness, fracture risk, and impaired bone healing

[6]. However, the pathogenesis of DOP has not been fully clarified. Notably, studies have shown that high glucose is a crucial determinant of DOP [7], especially increased diabetes-related pathological factors [8, 9]. Interestingly, inflammation is defined as one of the major pathological factors of DOP, which leads to bone loss [10], destroys the bone microenvironment, and inhibits bone formation [11, 12]. However, a series of DM-induced inflammation is often overlooked or underestimated, seriously affecting the quality

TABLE 1: The compositions of QKF.

Chinese pinyin name	Taxonomy name	Abbr.	Family	Weight (g)	Part used
Huang-qi	<i>Astragalus mongholicus</i> Bunge	HQ	Fabaceae	30	Root
Ji-xue-teng	<i>Spatholobus suberectus</i> Dunn	JXT	Fabaceae	15	Dry rattan stem
Huai-niu-xi	<i>Achyranthes bidentata</i> Blume	HNX	Amaranthaceae	10	Root
Sang-zhi	<i>Morus alba</i> L.	SZ	Moraceae	20	Twig
Wei-ling-xian	<i>Clematis chinensis</i> Osbeck	WLX	Ranunculaceae	15	Root
Xi-xian-cao	<i>Sigesbeckia orientalis</i> L.	XXC	Asteraceae	20	Aboveground part
Quan-xie	Scorpion	QX	<i>Buthus martensi</i> Karsch	5	Dry body

TABLE 2: Primer sequences of qRT-PCR in mouse.

Target	Forward (5' to 3')	Reverse (5' to 3')
IKK	GGCAGAAGAGCGAAGTGGACATC	CCAGCCGTTTCAGCCAAGACAC
IL-1 β	GAAATGCCACCTTTTGACAGTG	TGGATGCTCTCATCAGGACAG
IL-6	CCAAGAGGTGAGTGCTTCCC	CTGTTGTTTCAGACTCTCTCCCT
TNF- α	TGAGCACAGAAAGCATGATCC	GCCATTTGGGAACCTTCTCATC
GAPDH	AGGTCGGTGTGAACGGATTTG	TGTAGACCATGTAGTTGAGGTC

of people's life in the later period [13]. Therefore, it is an urgent strategy to prevent the development of inflammation and find effective therapies for DOP.

Traditional Chinese medicine (TCM) has a long history in treating DOP and accumulated rich experience [14]. Qizhi Kebutong formula (QKF) is a classical TCM formula composed of seven TCMS, including Huang-qi (*Astragalus mongholicus* Bunge, Fabaceae, root), Ji-xue-teng (*Spatholobus suberectus* Dunn, Fabaceae, dry rattan stem), Huai-niu-xi (*Achyranthes bidentata* Blume, Amaranthaceae, root), Sang-zhi (*Morus alba* L., Moraceae, twig), Wei-ling-xian (*Clematis chinensis* Osbeck, Ranunculaceae, root), Xi-xian-cao (*Sigesbeckia orientalis* L., Asteraceae, aboveground part), and Quan-xie (scorpion, *Buthus martensi* Karsch, whole animal) in Table 1. Accumulating evidence demonstrates that QKF has beneficial effects on clinical observation, and the indispensable role of QKF has been widely accepted. But the mechanisms remain unknown.

In this study, the potential targets and protective pathways of QKF on DOP were screened *via* network pharmacology, and the results were verified in the mouse model. Then, we provided some insights with the possible molecular mechanisms of QKF on the clinical application for delaying DOP progression.

2. Materials and Methods

2.1. Preparation of QKF and Reagents. Herbal compounds of QKF were provided by a pharmacy of Jilin Provincial Hospital of Traditional Chinese Medicine (Changchun, China). All of the crude drugs (98 g, two-thirds are used clinically) were extracted in 1000 ml of distilled water three times (100°C, 1 h each time) to obtain the aqueous extract. The extracts were centrifuged at 3,500 rpm for 15 min, and the supernatant was freeze-dried to obtain the powdery extract of QKF, with a yield of 20% (13 g) for further experiments. According to dose translation of animal studies, the medium

treatment concentration of a mouse is approximately equal to 3 g/kg/day; the low and high treatment concentrations are approximately equal to 1.5 g/kg/day and 6 g/kg/day, respectively. Streptozotocin (STZ) was purchased from Sigma-Aldrich (Shanghai, China). Antibodies against p-PI3K (AF3241, Affinity Biosciences, China), PI3K (ab227204, Abcam, USA), p-Akt (4058, Cell Signaling Technology, USA), Akt (ab179463, Abcam, USA), p-NF- κ B (3033, Cell Signaling Technology, USA), NF- κ B (ab16502, Abcam, USA), IL-6 (ab208113, Abcam, USA), IL-1 β (ab254360, Abcam, USA), TNF- α (8184, Cell Signaling Technology, USA), IKK β (15649-1AP, Proteintech, China), and GAPDH (60004-1-Ig, Proteintech, China) were used in this study.

2.2. Network Construction and Analysis. According to the pinyin form, "Huang-qi", "Sang-zhi", "Ji-xue-teng", "Xi-xian-cao", "Wei-ling-xian", "Quan-xie", and "Huai-niu-xi" were used as the keywords to search the active ingredients of XBC via the TCMSP (<http://tcmsp.com/tcmsp.php>) database. Meanwhile, DOP-associated targets were acquired from GeneCards (<http://www.swisstargetprediction.ch/>), OMIM, (<https://OMIM.org/>), PharmGKB, (<https://www.pharmgkb.org/>), and DrugBank (<https://www.drugbank.ca/>). The protein-protein interaction (PPI) network was obtained from STRING (<http://string-db.org/>, v.11) with parameter conditions filtered by "Homo sapiens" (confidence score > 0.9) and visualized using Cytoscape 3.8.0. And Gene Ontology (GO) and Kyoto Encyclopedia of Genes and Genomes (KEGG) enrichment analyses were performed for the above targets.

2.3. Animals and Treatments. In this study, 48 male C57 BL/6 mice were used for animal experiments. They were purchased from Changchun Yisi Experimental Animal Co., Ltd. (license number SCXK (Beijing) 2016-0006) with the weight in 18~22 g. Meanwhile, all mice were approved for ethical use by the Experimental Animal Ethics Committee

TABLE 3: The 90 active components of QKF were screened from the TCMSP database.

Drug	MOL_ID	Molecule name	OB (%)	DL
	MOL000211	Mairin	55.38	0.78
	MOL000239	Jaranol	50.83	0.29
	MOL000295	Alexandrin	20.63	0.63
	MOL000296	Hederagenin	36.91	0.75
	MOL000033	(3S,8S,9S,10R,13R,14S,17R)-10,13-Dimethyl-17-[(2R,5S)-5-propan-2-yloctan-2-yl]-2,3,4,7,8,9,11,12,14,15,16,17-dodecahydro-1H-cyclopenta[a]phenanthren-3-ol	36.23	0.78
	MOL000354	Isorhamnetin	49.6	0.31
	MOL000371	3,9-Di-O-methylnissolin	53.74	0.48
	MOL000374	5'-Hydroxyiso-muronulatol-2',5'-di-O-glucoside	41.72	0.69
	MOL000378	7-O-Methylisomucronulatol	74.69	0.3
	MOL000379	9,10-Dimethoxypterocarpan-3-O- β -D-glucoside	36.74	0.92
<i>Astragalus mongholicus</i> Bunge (Huang-qi)	MOL000380	(6aR,11aR)-9,10-Dimethoxy-6a,11a-dihydro-6H-benzofurano[3,2-]chromen-3-ol	64.26	0.42
	MOL000387	Bifendate	31.1	0.67
	MOL000392	Formononetin	69.67	0.21
	MOL000398	Isoflavanone	109.99	0.3
	MOL000417	Calycosin	47.75	0.24
	MOL000422	Kaempferol	41.88	0.24
	MOL000433	FA	68.96	0.71
	MOL000438	(3R)-3-(2-Hydroxy-3,4-dimethoxyphenyl)chroman-7-ol	67.67	0.26
	MOL000439	Isomucronulatol-7,2'-di-O-glucosiole	49.28	0.62
	MOL000440	Isomucronulatol-7,2'-di-O-glucosiole_qt	23.42	0.79
	MOL000442	1,7-Dihydroxy-3,9-dimethoxy pterocarpene	39.05	0.48
	MOL000098	Quercetin	46.43	0.28
	MOL000422	Kaempferol	41.88	0.24
<i>Morus alba</i> L. (Sang-zhi)	MOL000729	Oxysanguinarine	46.97	0.87
	MOL000737	Morin	46.23	0.27
	MOL000392	Formononetin	69.67	0.21
	MOL000471	Aloe-emodin	83.38	0.24
	MOL000492	(+)-Catechin	54.83	0.24
	MOL000417	Calycosin	47.75	0.24
	MOL000006	Luteolin	36.16	0.25
	MOL000461	3,7-Dihydroxy-6-methoxy-dihydroflavonol	43.8	0.26
	MOL000483	(Z)-3-(4-Hydroxy-3-methoxy-phenyl)-N-[2-(4-hydroxyphenyl)ethyl]acrylamide	118.35	0.26
	MOL000468	8-o-Methylreyusi	70.32	0.27
	MOL000501	Consume close grain	68.12	0.27
	MOL000502	Cajinin	68.8	0.27
<i>Spatholobus suberectus</i> Dunn (Ji-xue-teng)	MOL000497	Licochalcone A	40.79	0.29
	MOL000490	Petunidin	30.05	0.31
	MOL000507	Psi-baptigenin	70.12	0.31
	MOL000503	Medicagol	57.49	0.6
	MOL000491	Angelicin	37.5	0.66
	MOL000470	8-C- α -L-Arabinosylluteolin	35.54	0.66
	MOL000493	Campesterol	37.58	0.71
	MOL000296	Hederagenin	36.91	0.75
	MOL000358	Beta-sitosterol	36.91	0.75
	MOL000449	Stigmasterol	43.83	0.76
	MOL000033	(3S,8S,9S,10R,13R,14S,17R)-10,13-Dimethyl-17-[(2R,5S)-5-propan-2-yloctan-2-yl]-2,3,4,7,8,9,11,12,14,15,16,17-dodecahydro-1H-cyclopenta[a]phenanthren-3-ol	36.23	0.78

TABLE 3: Continued.

Drug	MOL_ID	Molecule name	OB (%)	DL
<i>Sigesbeckia orientalis</i> L. (Xi-xian-cao)	MOL000469	3-Hydroxystigmast-5-en-7-one	40.93	0.78
	MOL004180	Coronaridine	34.97	0.68
	MOL000296	Hederagenin	36.91	0.75
	MOL000358	Beta-sitosterol	36.91	0.75
	MOL004179	Vernolic acid	37.63	0.19
	MOL000449	Stigmasterol	43.83	0.76
	MOL004172	(1R)-1-[(2S,4aR,4bS,7R,8aS)-7-Hydroxy-2,4b,8,8-tetramethyl-4,4a,5,6,7,8a,9,10-octahydro-3H-phenanthren-2-yl]ethane-1,2-diol	46.7	0.31
	MOL004184	Siegesesteric acid II	51.98	0.48
	MOL004177	15alpha-Hydroxy-ent-kaur-16-en-19-oic acid	58.73	0.38
	MOL004185	Siegesmethyletheric acid	60.72	0.43
<i>Clematis chinensis</i> Osbeck (Wei-ling-xian)	MOL001663	(4aS,6aR,6aS,6bR,8aR,10R,12aR,14bS)-10-Hydroxy-2,2,6a,6b,9,9,12a-heptamethyl-1,3,4,5,6,6a,7,8,8a,10,11,12,13,14b-tetradecahydronicene-4a-carboxylic acid	32.03	0.76
	MOL002372	(6Z,10E,14E,18E)-2,6,10,15,19,23-Hexamethyltetracos-2,6,10,14,18,22-hexaene	33.55	0.42
	MOL005598	Embinin	33.91	0.73
	MOL000358	Beta-sitosterol	36.91	0.75
	MOL005594	ClematosideA'qt	37.51	0.76
	MOL005603	Heptyl phthalate	42.26	0.31
	MOL000449	Stigmasterol	43.83	0.76
	MOL001006	Poriferasta-7,22E-dien-3beta-ol	42.98	0.76
	MOL012461	28-Norolean-17-en-3-ol	35.93	0.78
	MOL012505	Bidentatoside,iiqt	31.76	0.59
<i>Achyranthes bidentata</i> Blume (Huai-niu-xi)	MOL012537	Spinoside A	41.75	0.4
	MOL012542	β -Ecdysterone	44.23	0.82
	MOL001454	Berberine	36.86	0.78
	MOL001458	Coptisine	30.67	0.86
	MOL000173	Wogonin	30.68	0.23
	MOL002643	Delta 7-stigmastanol	37.42	0.75
	MOL002714	Baicalein	33.52	0.21
	MOL002776	Baicalin	40.12	0.75
	MOL002897	Epiberberine	43.09	0.78
	MOL000358	Beta-sitosterol	36.91	0.75
<i>Scorpion</i> (Quan-xie)	MOL003847	Inophyllum E	38.81	0.85
	MOL000422	Kaempferol	41.88	0.24
	MOL004355	Spinasterol	42.98	0.76
	MOL000449	Stigmasterol	43.83	0.76
	MOL000785	Palmatine	64.6	0.65
	MOL000085	Beta-daucosterolqt	36.91	0.75
	MOL000098	Quercetin	46.43	0.28
	MOL011455	20-Hexadecanoylingenol	32.7	0.65
	MOL000953	Cholesterol	37.87	0.68
	MOL002223	Taurine	24.37	0.21
MOL002156	Trimethylamine	59.98	0.18	
MOL000860	Stearic acid	17.83	0.14	
MOL002223	Taurine	24.37	0.01	
MOL000069	Palmitic acid	19.3	0.1	

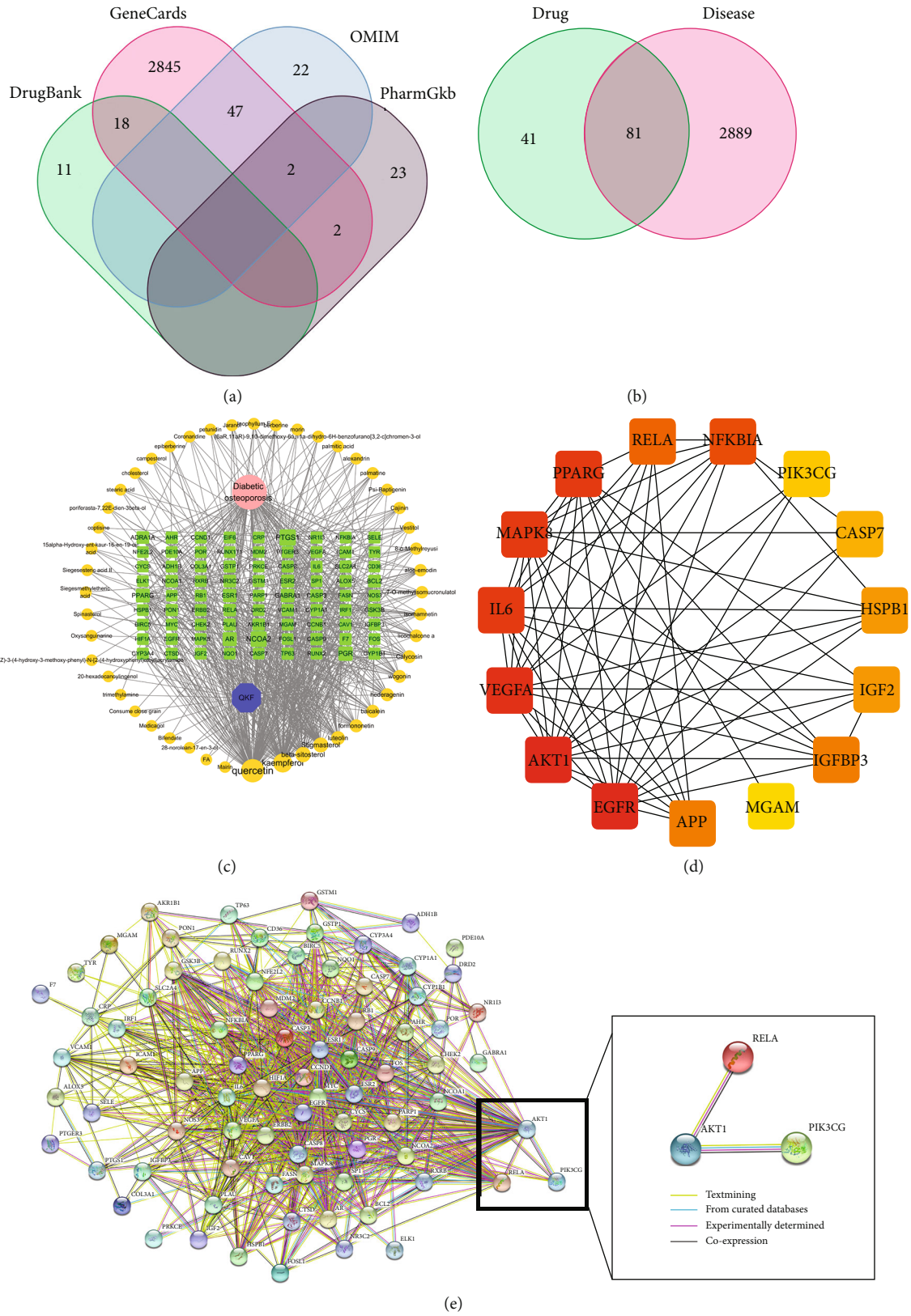
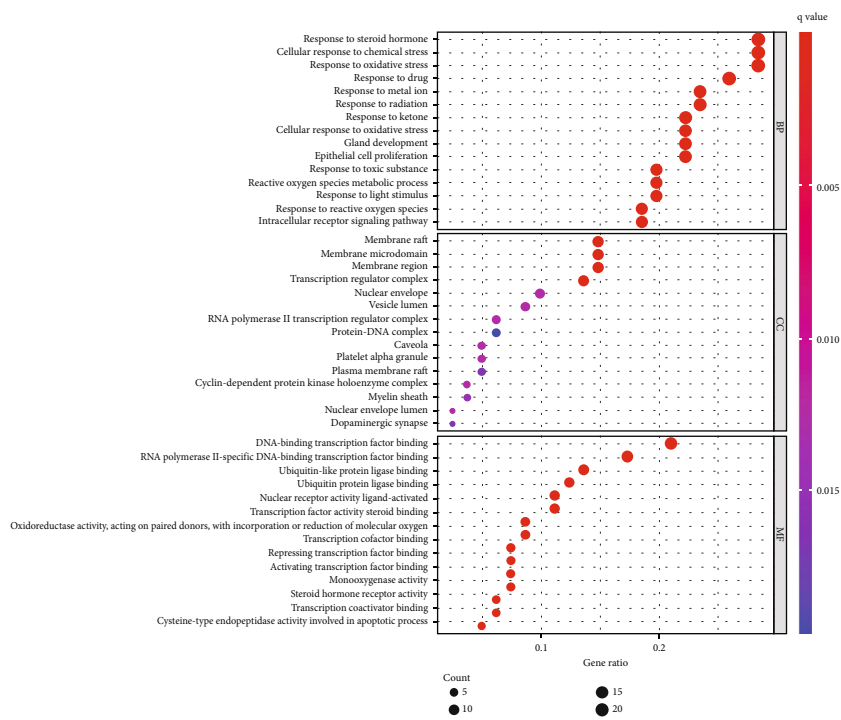
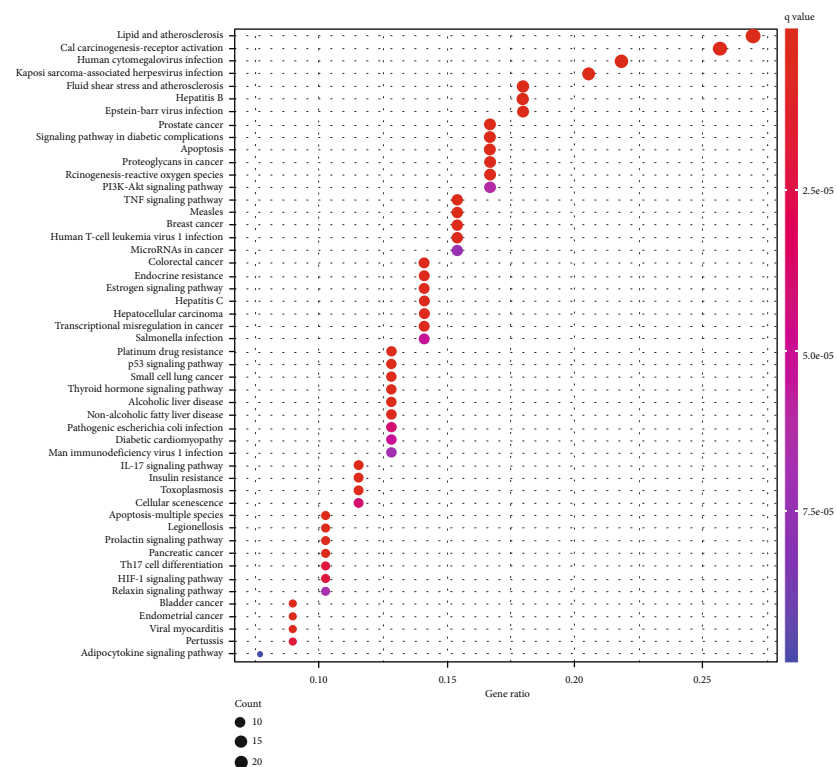


FIGURE 1: Construction and analysis of the network pharmacology. (a) Disease-related targets. (b) The interactive targets of QKF and DOP. (c) The drug-compound-target-disease network. (d) PPI network and cluster analysis of the potential targets. (e) PPI network of significant genes was extracted.



(a)



(b)

FIGURE 2: Continued.

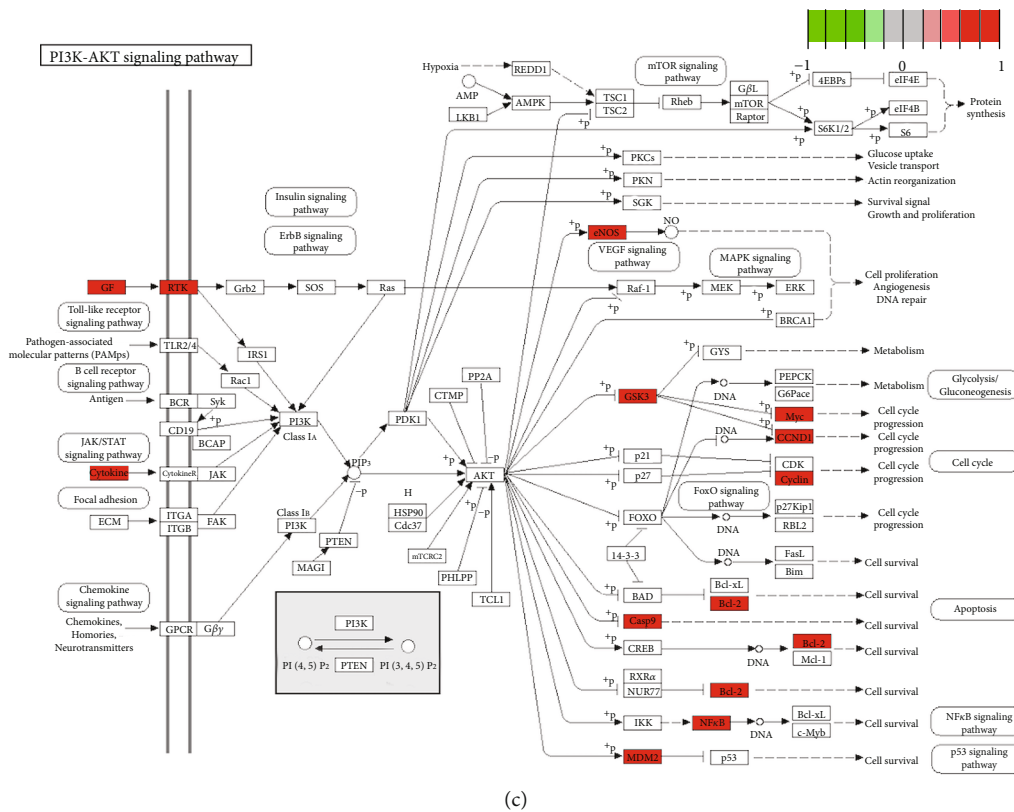


FIGURE 2: (a) GO enrichment analysis. The top 15 BP terms, CC terms, and MF terms are shown as a bubble chart according to the $-\log p$ value. The colors represent the different adjusted p value < 0.05 , and the abscissa represents the number of target genes. The smaller p value represents higher significance. (b) The top 50 entries of KEGG pathway analysis are ordered according to the $-\lg p$ value. The redder color represents more obvious enrichment. (c) The PI3K/Akt signaling pathway modified from hsa04151. Red represents the targets of QKF.

of Changchun University of Traditional Chinese Medicine (batch number 20190134). They were kept in the Animal Experimental Center of Changchun University of Traditional Chinese Medicine (Changchun, China). The ambient temperature is $18\sim 22^{\circ}\text{C}$, and the humidity is $50\sim 60\%$. Then, the mice were randomly divided into 5 groups ($n = 8$): control (Ctrl), STZ, QKF (1.5 g/kg), QKF (3 g/kg), and QKF (6 g/kg) groups. Except for the Ctrl group, all other mice were intraperitoneally injected with STZ 130 mg/kg. After 7 days, the tail of the mice was cut short to test the random blood glucose levels ≥ 300 mg/dl (16.7 mmol/l) which were considered to be diabetic.

2.4. Micro-Computed Tomography (Micro-CT) Scanning. The femurs were scanned with a high-resolution Quantum FX Micro-CT (PerkinElmer, Inc. Waltham, MA, USA), using the following settings: $80\ \mu\text{A}$ current, 90 kV voltage, 360° gantry rotation, 4 min scanning time, and 36 mm reconstructed visual field. The images were recombined via micro-CT, and the following parameters were recorded: bone mineral density (BMD), specific bone surface (BS/BV), trabecular separation (Tb.Sp), trabecular thickness (Tb.Th), bone volume over total volume (BV/TV), and connectivity density (Conn.D).

2.5. The Hematoxylin/Eosin (H&E) Staining. The exfoliated femurs were fixed using 4% formaldehyde, decalcified in

EDTA glycerol solution, and embedded in paraffin. Paraffin sections were cut into the slices at $4\ \mu\text{m}$ thickness and stained with H&E. Images of the sections were captured using light microscopy (Olympus BX51, Japan) at 200x and 400x ratios, respectively.

2.6. Quantitative Real-Time PCR (qRT-PCR) Analysis. Total RNA was extracted from the femur tissues with a total RNA extraction kit (TIANGEN BIOTECH, China). Subsequently, the reverse transcription of $1\ \mu\text{g}$ total RNA into cDNA was conducted with the iScript cDNA synthesis kit (TIANGEN BIOTECH, China). The qRT-PCR assay was performed with a Bio-Rad CFX96 system, and the gene expressions of IKK, IL- 1β , IL-6, and TNF- α were normalized to GAPDH. Relative mRNA levels were quantified using the $2^{-\Delta\Delta\text{Ct}}$ method. The mouse primer sequences are shown in Table 2.

2.7. Western Blotting Assay. Proteins were extracted from the femurs using RIPA lysis buffer (Beyotime, China) with phosphatase inhibitors and protease inhibitors. Protein quantification was measured using a BCA protein assay kit (Beyotime, China). The equivalent amount of protein was separated by 8%, 10%, or 12% SDS-PAGE and transferred to a PVDF membrane. The membrane was blocked with 5% BSA 1~2 h at room temperature. The antibodies against PI3K (1:1000), p-PI3K (1:1000), Akt (1:10000), p-Akt (1:1000), NF- κB (1:2000), p-NF- κB (1:1000), IKKB

TABLE 4: GO enrichment analysis of QKF.

Ontology	ID	Description	<i>p</i> value	<i>p</i> .adjust	GeneID	Count
Biological process (BP)	GO:0048545	Response to steroid hormone	$2.00E-21$	$6.65E-18$	PGR/AR/ESR2/NCOA2/NR3C2/NCOA1/ESR1/RELA/RXR/BCL2/CASP3/ICAM1/GSTP1/EGFR/CCND1/FOS/CASP9/IL6/TP63/CAV1/PARP1/MDM2/FOSL1	23
	GO:0062197	Cellular response to chemical stress	$4.92E-21$	$8.18E-18$	PPARG/AKR1B1/RELA/BCL2/CASP3/MAPK8/CYP1B1/ALOX5/GSTP1/SLC2A4/EGFR/FOS/IL6/HIF1A/CAV1/NOS3/HSPB1/NFE2L2/NQO1/PARP1/MDM2/CYCS/CD36	23
	GO:1901654	Response to ketone	$3.35E-19$	$3.71E-16$	AR/NCOA2/NCOA1/PPARG/AKR1B1/F7/RELA/ICAM1/AHR/EGFR/CCND1/FOS/CASP9/ELK1/CAV1/PARP1/PRKCE/FOSL1	18
	GO:0006979	Response to oxidative stress	$1.09E-18$	$9.05E-16$	PTGS1/RELA/BCL2/CASP3/MAPK8/CYP1B1/ALOX5/GSTP1/EGFR/FOS/IL6/HIF1A/NOS3/HSPB1/NFE2L2/NQO1/PARP1/MDM2/APP/FOSL1/CYCS/SP1/CD36	23
	GO:0042493	Response to drug	$1.55E-17$	$1.03E-14$	NCOA1/PPARG/F7/RELA/ADRA1A/BCL2/CASP3/CYP3A4/CYP1A1/ICAM1/EGFR/CCND1/FOS/POR/MYC/CCNB1/NFE2L2/CHEK2/MDM2/FOSL1/DRD2	21
	GO:0034599	Cellular response to oxidative stress	$8.36E-16$	$4.44E-13$	RELA/BCL2/MAPK8/CYP1B1/ALOX5/GSTP1/EGFR/FOS/IL6/HIF1A/NOS3/HSPB1/NFE2L2/NQO1/PARP1/MDM2/CYCS/CD36	18
	GO:0010038	Response to metal ion	$9.35E-16$	$4.44E-13$	BCL2/CASP3/MAPK8/CYP1A1/ICAM1/EGFR/CCND1/FOS/CASP9/CASP8/HIF1A/CAV1/CCNB1/NFE2L2/NQO1/PARP1/MDM2/APP/DRD2	19
	GO:0009636	Response to toxic substance	$8.72E-15$	$3.62E-12$	PTGS1/BCL2/CYP1A1/CYP1B1/GSTP1/AHR/GSTM1/FOS/NOS3/CCNB1/NFE2L2/NQO1/PON1/MDM2/CD36/DRD2	16
	GO:0009314	Response to radiation	$3.52E-14$	$1.30E-11$	RELA/BCL2/CASP3/MAPK8/ICAM1/EGFR/CCND1/FOS/CASP9/ELK1/HIF1A/MYC/PARP1/COL3A1/CHEK2/MDM2/APP/TYR/DRD2	19
	GO:0000302	Response to reactive oxygen species	$6.77E-14$	$2.25E-11$	RELA/BCL2/CASP3/MAPK8/CYP1B1/GSTP1/EGFR/FOS/IL6/NOS3/NFE2L2/NQO1/MDM2/FOSL1/CD36	15
	GO:0045121	Membrane raft	$1.05E-08$	$1.31E-06$	ADRA1A/CASP3/ICAM1/SELE/SLC2A4/EGFR/CASP8/CAV1/NOS3/CTSD/APP/CD36	12
	GO:0098857	Membrane microdomain	$1.09E-08$	$1.31E-06$	ADRA1A/CASP3/ICAM1/SELE/SLC2A4/EGFR/CASP8/CAV1/NOS3/CTSD/APP/CD36	12
	GO:0098589	Membrane region	$1.67E-08$	$1.34E-06$	ADRA1A/CASP3/ICAM1/SELE/SLC2A4/EGFR/CASP8/CAV1/NOS3/CTSD/APP/CD36	12
	GO:0005667	Transcription regulator complex	$1.05E-06$	$6.29E-05$	PPARG/RELA/RXR/B/AHR/CCND1/FOS/RB1/HIF1A/PARP1/RUNX2/SP1	11
	Cell component (CC)	GO:0005901	Caveola	0.000373551	0.016511501	ADRA1A/SELE/CAV1/NOS3
GO:0031983		Vesicle lumen	0.000420556	0.016511501	ALOX5/GSTP1/EGFR/VEGFA/CTSD/IGF2/APP	7
GO:0090575		RNA polymerase II transcription regulator complex	0.000549681	0.016511501	PPARG/RXR/B/FOS/RB1/HIF1A	5
GO:0031091		Platelet alpha granule	0.000554949	0.016511501	VEGFA/IGF2/APP/CD36	4
GO:0005641		Nuclear envelope lumen	0.000746032	0.016511501	ALOX5/APP	2
GO:0000307	Cyclin-dependent protein kinase holoenzyme complex	0.000749375	0.016511501	CCND1/RB1/CCNB1	3	

TABLE 4: Continued.

Ontology	ID	Description	<i>p</i> value	<i>p</i> .adjust	GeneID	Count
Molecular functions (mf)	GO:0140297	DNA-binding transcription factor binding	1.46E-13	5.42E-11	NCOA2/NCOA1/ESR1/PPARG/GSK3B/RELA/BCL2/FOS/RB1/NFKBIA/HIF1A/MYC/HSPB1/NFE2L2/PARP1/RUNX2/SP1	17
	GO:0004879	Nuclear receptor activity	1.27E-12	1.57E-10	PGR/AR/ESR2/NR3C2/ESR1/PPARG/RXR/ AHR/NR1I3	9
	GO:0098531	Ligand-activated transcription factor activity	1.27E-12	1.57E-10	PGR/AR/ESR2/NR3C2/ESR1/PPARG/RXR/ AHR/NR1I3	9
	GO:0061629	RNA polymerase II-specific DNA-binding transcription factor binding	1.04E-11	9.58E-10	NCOA2/NCOA1/ESR1/PPARG/GSK3B/RELA/FOS/RB1/NFKBIA/HIF1A/HSPB1/ NFE2L2/PARP1/SP1	14
	GO:0003707	Steroid hormone receptor activity	9.04E-08	5.81E-06	PGR/ESR2/NR3C2/ESR1/RXR	5
	GO:0001221	Transcription cofactor binding	9.41E-08	5.81E-06	PGR/AR/ESR1/RELA/AHR/NFE2L2	6
	GO:0044389	Ubiquitin-like protein ligase binding	1.38E-07	7.27E-06	GSK3B/RELA/BCL2/EGFR/RB1/NFKBIA/ CASP8/HIF1A/CCNB1/CHEK2/MDM2	11
	GO:0001223	Transcription coactivator binding	1.62E-07	7.47E-06	PGR/AR/ESR1/RELA/AHR	5
	GO:0005496	Steroid binding	4.30E-07	1.71E-05	PGR/AR/ESR2/NR3C2/ESR1/CYP3A4/CAV1	7
GO:0097153	Cysteine-type endopeptidase activity involved in apoptotic process	4.63E-07	1.71E-05	CASP3/CASP9/CASP8/CASP7	4	

(1 : 1000), TNF- α (1 : 1000), IL-1 β (1 : 1000), IL-6 (1 : 1000), and GAPDH (1 : 5000) were added at 4°C overnight. After washing with 1× TBST, the membranes were further probed with the corresponding secondary antibody (1 : 5000) for 2 h at 18-25°C; the labeled protein bands were visualized using a BeyoECL Plus Kit (Beyotime, China). Image Lab software was used for semiquantitative analysis.

2.8. Molecular Docking. AutoDock software, version 4.2, was used for molecular docking. The composite targets were verified using the Lamarckian genetic algorithm; proteins and ligands were prepared using the AutoDock tool. The three-dimensional structure of the proteins was downloaded from the RCSB-PDB database (<http://www.pdb.org>), and the hydrogen atoms were added. We calculated the docking binding energy using the Auto tool. The docking diagrams of target proteins and molecules were performed by the PyMOL visualization software.

2.9. Statistical Analysis. All data were analyzed using Graph-Pad Prism 9.0. These data were compared with several groups by one-way ANOVA. For all statistical analysis, $p < 0.05$ was considered statistically significant.

3. Results

3.1. Screening of the Intersection Targets and Constructing a Series of Network. With OB $\geq 30\%$ and DL ≥ 0.18 as screening parameters, 90 candidate compounds of QKF were

found for further analysis (Table 3). Besides, 2970 potential targets of DOP were obtained from the four authoritative databases (Figure 1(a)). Through taking the intersection of 122 QKF targets and 2,970 DOP targets, 81 potential targets were obtained (Figure 1(b)). Subsequently, the intersection targets were inputted to Cytoscape software to build the network diagram with multicomponent and multitarget (Figure 1(c)). In addition, 81 potential targets were uploaded to the STRING database to construct the PPI network (Figure 1(d)). Among these nodes, PIK3CG, Akt1, and RELA were screened out with more relevance and biological functions in the PPI network (Figure 1(e)), suggesting that PIK3CG, Akt1, and RELA were the key genes, probably exhibiting therapeutic effect in DOP.

3.2. Functional Enrichment Analysis. To investigate the potential mechanisms, the 1660 biological processes (BP), 24 cellular components (CC), and 104 molecular functions (MF) were performed using the DAVID database. Moreover, the top 15 results were selected with the p value from small to large (Figure 2(a) and Table 4). KEGG enrichment analysis obtained 128 results. Subsequently, we selected the top 50 according to the p value for further analysis (Figure 2(b)). Notably, previous studies indicated the osteogenic differentiation through activating the PI3K/Akt pathway, connected with the multitarget and multicomponent. Among these enriched pathways, PI3K/Akt played an important role in DOP; the predictive targets are shown in Figure 2(c).

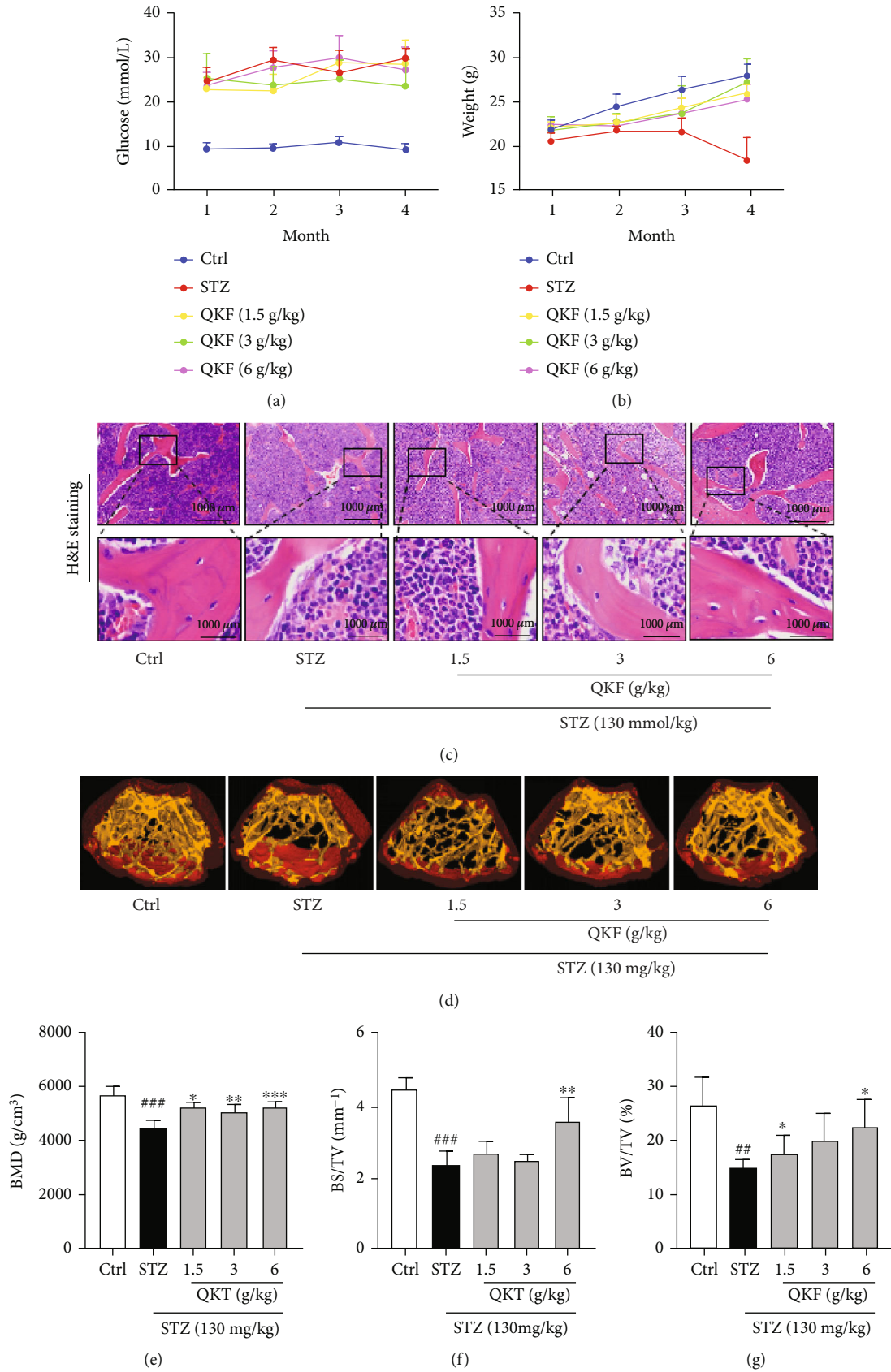


FIGURE 3: Continued.

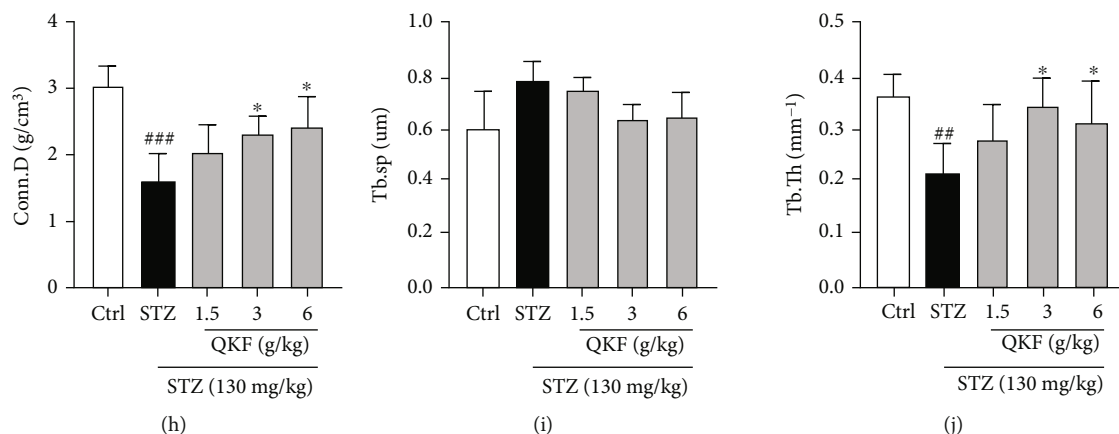


FIGURE 3: Effect of QKF on the general features of STZ-induced mice. (a) Blood glucose. (b) Body weight. (c) Representative HE staining images of the trabecular bone. (d) Three-dimensional (3D) micro-CT images of femur. Trabecular bone biological parameters: (e) BMD, (f) BS/TV, (g) BV/TV, (h) Conn.D, (i) Tb.Sp, and (j) Tb.Th. The results are triplicates from a representative experiment. * $p < 0.05$, ** $p < 0.01$, and *** $p < 0.001$ vs. STZ group. ## $p < 0.01$ and ### $p < 0.001$ vs. Ctrl group.

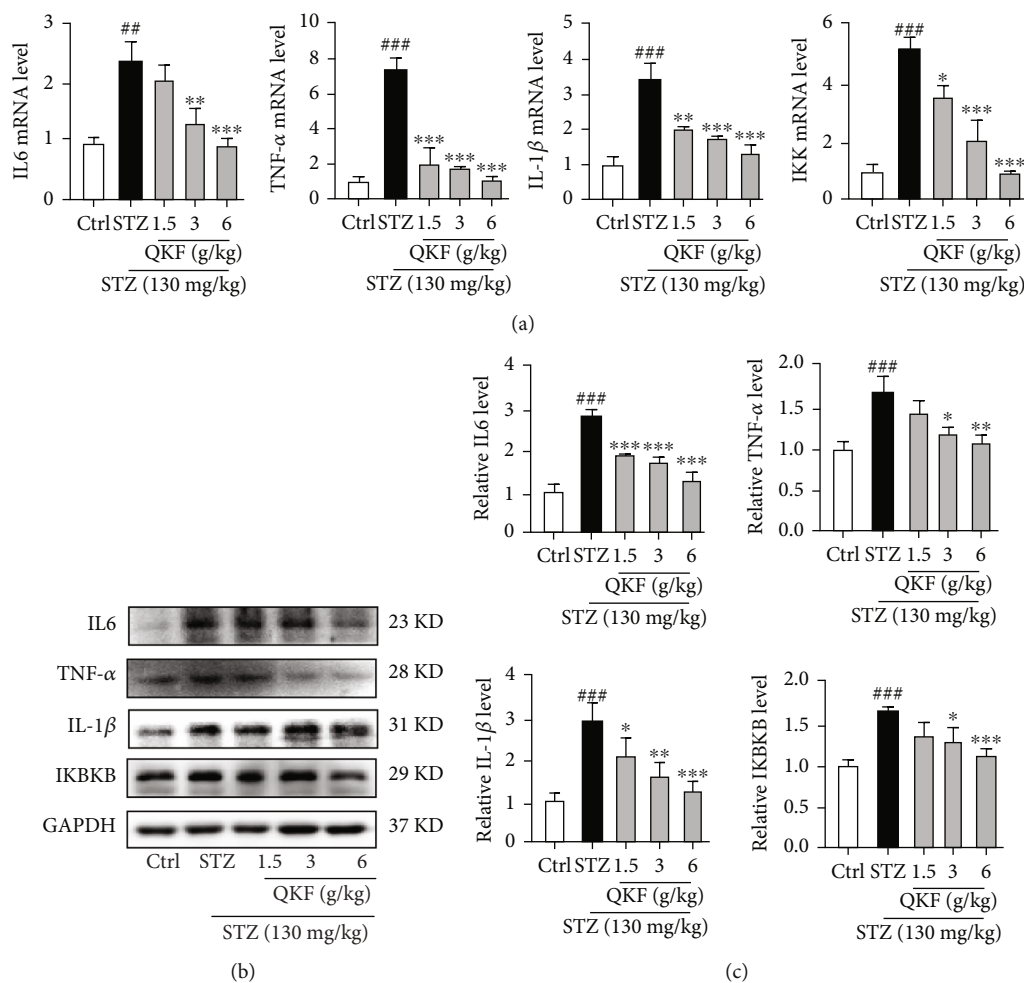


FIGURE 4: QKF improves STZ-induced mouse inflammation. (a) qRT-PCR method was used to detect the mRNA levels of TNF-α, IKK, IL-6, and IL-1β. (b, c) Western blot method was used to detect the protein levels of TNF-α, IKKB, IL-6, and IL-1β. Data were expressed as mean ± SD (n = 8). * $p < 0.05$, ** $p < 0.01$, and *** $p < 0.001$ vs. STZ group. # $p < 0.05$, ## $p < 0.01$, and ### $p < 0.001$ vs. Ctrl group.

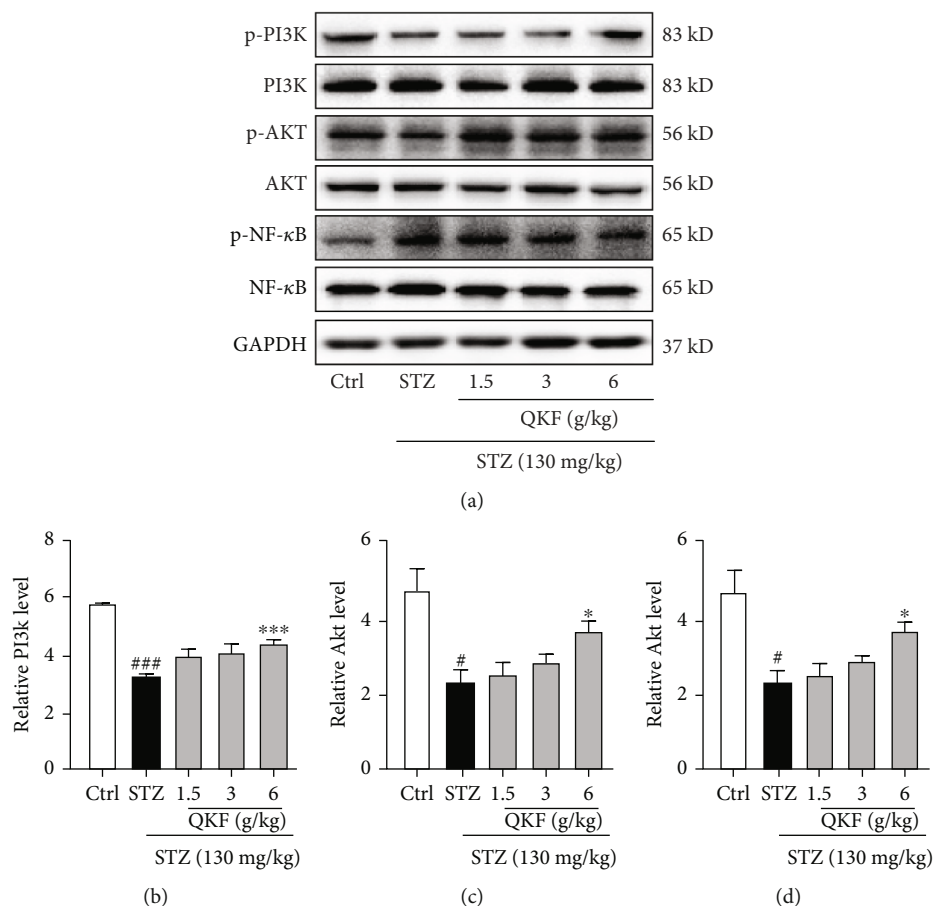


FIGURE 5: QKF mediated inflammation through the PI3K/Akt/NF-κB pathway. Western blot method was used to detect the protein levels of (b) p-PI3K/PI3K, (c) p-Akt/Akt, and (d) p-NF-κB/NF-κB. * $p < 0.05$ and *** $p < 0.001$ vs. STZ group. # $p < 0.05$ and ### $p < 0.001$ vs. Ctrl group.

3.3. Effect of QKF on the General Features of STZ-Induced Mice. In order to determine the effect of QKF on DOP, we established a STZ-induced mouse model and compared disease evolution in groups (Figure 3). After administration of QKF for 4 months, blood glucose levels of STZ-induced mice were significantly higher (Figure 3(a)), while body weight was significantly lower (Figure 3(b)). The results demonstrated that the blood glucose of mice increased sharply, which consumed a lot of fat in the body. And compared to the Ctrl group, the weight of mice in STZ and QKF groups was decreased significantly. Meanwhile, the trabecular bone at distal femoral metaphysis was assessed by HE staining (Figure 3(c)); obvious bone loss was observed in STZ-induced mice compared with the Ctrl group, which was gradually mitigated with the increasing dose of QKF. The femurs of normal mice scattered pink trabecular bones, and the number of trabecular bones was reduced in STZ-induced mice. Furthermore, the profiles of 3D images (Figure 3(d)) clearly exhibited the breakage of cancellous bone of diabetic mice, and the 3D bone biological parameters (Figures 3(e)–3(j)) quantitatively reflected the significant reduction in Conn.D ($p < 0.001$), BMD ($p < 0.001$), BV/TV ($p < 0.01$), BS/TV ($p < 0.001$), and Tb.Th ($p < 0.01$) in the STZ group, while Tb.Sp was significantly increased. However, after the treatment of QKF for 4 months,

improved bone mass of trabecular bone and reversed changes of biological parameters indicated the potential therapeutic efficacy of QKF on DOP.

3.4. QKF Improves STZ-Induced Mouse Inflammation. DOP is an inflammatory response caused by high blood glucose [15]. To validate that QKF could reduce the inflammatory expression of STZ-induced mice, we used qRT-PCR and Western blot to determine changes in mRNA and protein levels (Figure 4). The qRT-PCR results indicated that the mRNA levels of TNF- α , IKK, IL-6, and IL-1 β were significantly downregulated after administration (Figure 4(a)). Meanwhile, Western blot results demonstrated that QKF had a similar inhibitory effect at the protein levels (Figures 4(b) and 4(c)). Above all, these results indicate that QKF could attenuate inflammation in STZ-induced mice.

3.5. QKF Mediated Inflammation through the PI3K/Akt/NF-κB Pathway. Based on the network pharmacological analysis, the PI3K/Akt signaling pathway may be predicted as a potential mechanism of QKF for DOP protection. Meanwhile, NF-κB was a key downstream factor of the PI3K/Akt pathway, which was closely related to the regulation of glucose and lipid metabolism [16]. Therefore, we explored the PI3K/Akt/NF-κB signaling pathway as

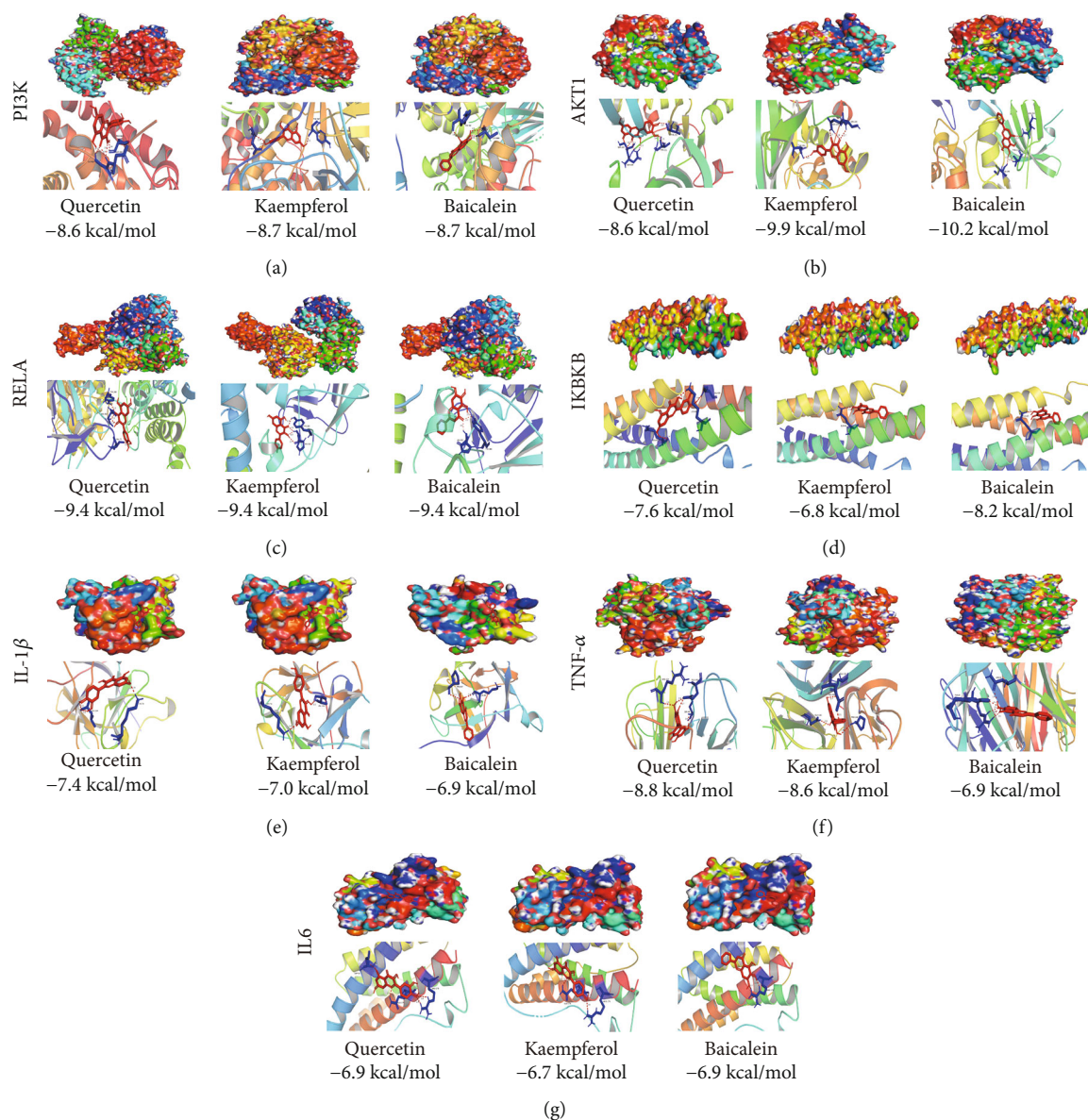


FIGURE 6: The protein-ligand of the docking simulation. Simulated molecular docking of (a) PI3K with quercetin, kaempferol, and baicalein. (b) Akt1 with quercetin, kaempferol, and baicalein. (c) RELA with quercetin, kaempferol, and baicalein. (d) IKKB with quercetin, kaempferol, and baicalein. (e) IL-1 β with quercetin, kaempferol, and baicalein. (f) TNF- α with quercetin, kaempferol, and baicalein. (g) IL-6 with quercetin, kaempferol, and baicalein.

the potential mechanism of QKF for experimental verification. After administration of QKF, the protein levels of p-PI3K/PI3K and p-Akt/Akt were further upregulated compared with the STZ group, while p-NF- κ B/NF- κ B was downregulated (Figure 5). The results indicated that PI3K/Akt/NF- κ B signaling could regulate the protective effects of QKF on DOP.

3.6. Molecular Docking Analysis. To further explore the effect of the 3 major compounds of QKF on the 7 potential targets, including PI3K, Akt1, RELA, IKKB, IL-1 β , TNF- α , and IL-6, the binding energies were determined by molecular docking (Figure 6). Firstly, kaempferol and baicalein had a strong binding ability with PI3K, so they would be a

potential bioactive compound of QKF on DOP (Figure 6(a)). Akt1 had a stronger binding energy with all compounds (Figure 6(b)). The strongest binding energy was as high as -10.2 kcal/mol. Interestingly, quercetin, kaempferol, and baicalein had the same binding power with RELA and IL-6 (Figures 6(c) and 6(g)). It means that RELA and IL-6 have the best binding force with the above components. Meanwhile, IKKB and baicalein, IL-1 β and quercetin, and TNF- α and quercetin have a stronger binding force (Figures 6(d)–6(f)). Above, quercetin, kaempferol, and baicalein played an important role in QKF. Although they have higher binding force with inflammatory factors, the pharmacological effects of these active compounds in regulating key targets needed to be further verified.

4. Discussion

In this study, we performed network pharmacology, animal experiments, and molecular docking to explore the active compositions and molecular mechanisms of QKF in the treatment of DOP. The potential targets and enrichment pathways were predicted by network pharmacology. Histo-pathological staining and micro-CT imaging confirmed the therapeutic effect of QKF on the STZ-induced mouse model. qRT-PCR and Western Blot confirmed that QKF could mediate inflammation through the PI3K/Akt/NF- κ B pathway. In summary, this study demonstrated for the first time that QKF mediated inflammation through the PI3K/Akt/NF- κ B pathway, thereby improving bone mass of trabecular bone and reversing the changes of biological parameters in the STZ-induced mouse model.

Based on the TCM theory, seven drugs of QKF were formed for clinical application of DOP-related diseases [17]. Among these drugs, HQ (qi-tonifying), JXT (blood-activating), HNX (kidney-invigorating), and WLX, SZ, and XXC (dredging collateral) were used for the treatment of DOP [18–20]. A large number of reports have focused on bones and kidneys [21]; kidney weakness and blood stasis were the main causes of DOP [22]. Therefore, the kidney-nourishing herbs used for the treatment of DOP have aroused concerns [23]. HNX and WLX could tonify the kidney [24], which was deemed as one of the effective methods to alleviate DOP [25]. Furthermore, SZ and XXC had the ability to tonify the kidney and strengthen muscle and bone [26]. Above all, TCM has a series of effects on DOP [27], and it could improve the clinical symptoms of patients, which was worthy of clinical promotion [28]. At the same time, a previous study suggested that quercetin not only promoted the differentiation activity of osteoblasts but also inhibited the absorption activity of osteoclasts, thereby increasing the expression of osteogenic markers [29]. Kaempferol has a significant anti-inflammatory benefits, including promoting osteoblast proliferation, differentiation, and bone formation [30]. Previous studies suggested that baicalin could promote osteogenic differentiation by regulating protein kinases and transcription factors [31]. In sum, the compounds of QKF could provide an alternative strategy to prevent bone loss.

According to reports, trabecular bone loss was one of the common pathological processes occurring in DOP mice. To evaluate the effects of QKF for the treatment of DOP, we assessed trabecular architectural parameters using 3D micro-CT images. The results suggested that QKF could prevent the loss of bone mass induced by DOP and restore the trabecular connectivity by increasing BMD and Conn.D. Moreover, compared with the STZ group, the parameters of Tb.Th, BS/BV, and BV/TV in the QKF group increased significantly, while that of Tb.Sp was inhibited. Treatment of STZ-induced mice with QKF markedly increased trabecular BMD and improved trabecular bone and enhanced trabecular bone area.

In the present study, QKF treatment significantly decreased the mRNA and protein levels of a series of inflammatory factors, including IL-6, TNF- α , IKBKB, and IL-1 β in the STZ-induced mouse model, which contributed to the

improvement of DOP. However, QKF mediated inflammation through the PI3K/Akt/NF- κ B pathway; the relevant key targets were also proven to induce antioxidation, anti-inflammation, and immune regulation. Among them, Akt was identified as a unique signaling intermediate in bone homeostasis that controlled the differentiation of osteoblasts and osteoclasts, which was a direct downstream target of PI3K to inhibit the release of inflammatory factors [32–36]. Moreover, NF- κ B was also a key downstream factor of the PI3K/Akt pathway, which enhanced the degree of inflammatory response and promoted the differentiation of osteoclast precursors [37, 38]. Meanwhile, the PI3K/Akt signaling pathway not only affects inflammatory factors such as NF- κ B and TNF- α but also induced the inflammatory reaction in the internal environment of the body. Furthermore, the differentiation of osteoblasts was regulated by TNF- α , which was the earliest inflammatory mediator produced in response to oxidative stress and promoted the production of inflammatory cytokines to promote osteoblast apoptosis [39, 40]. In addition, accumulating studies have revealed that the expressions of core targets, including Akt1, TNF- α , IL-6, and RELA, made the vital functions in regulating inflammatory response [41, 42]. We have verified that QKF could regulate the key targets and PI3K/Akt/NF- κ B signaling pathway to explain the molecular mechanism of QKF treatment on DOP.

5. Conclusion

In summary, QKF could recuperate the bone loss and improve bone mass of trabecular bone in STZ-induced mouse models by downregulating the expression of IL-6, TNF- α , IKBKB, and IL-1 β to alleviate the inflammation. The results might be mediated by the PI3K/Akt/NF- κ B pathway based on the prediction from network pharmacology and experiment validation. This study may provide new insights into the molecular mechanisms of QKF in the treatment of DOP.

Data Availability

The datasets used and/or analyzed during the current study are available from the corresponding author on reasonable request.

Additional Points

Strengths and Limitations. These results demonstrate that QKF inhibits high glucose-induced osteoporosis by regulating the key targets and PI3K/Akt/NF- κ B signaling pathway. The potential mechanisms of QKF on DOP development need to be further confirmed by multiple targets and multiple pathways.

Ethical Approval

All animal experiments were approved by the Experimental Animal Administration Committee of Changchun

University of Chinese Medicine (batch number 20190134) and carried out in accordance with the institutional guidelines.

Conflicts of Interest

The authors declare that there were no conflicts of interest regarding the publication of this paper.

Authors' Contributions

LT, LD, and GW performed the experiments. YG, XL, and YZ performed the network pharmacology analysis. LT and JM analyzed the data and drafted the manuscript. WZ and YW supervised the experiments and the manuscript. WZ and XW designed and revised the manuscript. All authors read and approved the final version of the manuscript. Lulu Tian and Lu Ding contributed equally to this work.

Acknowledgments

This project was supported by grants from the National Key Research and Development Program of China (2019YFC1709904) and the Jilin Scientific and Technological of Chinese Medicine Program (20160204010YY and 2015ZFFZC14).

References

- [1] Y. Ren, M. Yang, X. Wang, B. Xu, Z. Xu, and B. Su, "ELAV-like RNA binding protein 1 regulates osteogenesis in diabetic osteoporosis: involvement of divalent metal transporter 1," *Molecular and Cellular Endocrinology*, vol. 546, article S0303720722000065, p. 111559, 2022.
- [2] F. Koromani, S. Ghatan, M. van Hoek et al., "Type 2 diabetes mellitus and vertebral fracture risk," *Current Osteoporosis Reports*, vol. 19, no. 1, article 646, pp. 50–57, 2021.
- [3] C. He, M. Liu, Q. Ding, F. Yang, and T. Xu, "Upregulated miR-9-5p inhibits osteogenic differentiation of bone marrow mesenchymal stem cells under high glucose treatment," *Journal of Bone and Mineral Metabolism*, vol. 40, no. 2, article 1280, pp. 208–219, 2022.
- [4] A. R. Gortazar and J. A. Ardura, "Osteocytes and diabetes: altered function of diabetic osteocytes," *Current Osteoporosis Reports*, vol. 18, no. 6, article 641, pp. 796–802, 2020.
- [5] K. F. Moseley, Z. Du, S. E. Sacher, V. L. Ferguson, and E. Donnelly, "Advanced glycation endproducts and bone quality: practical implications for people with type 2 diabetes," *Current Opinion in Endocrinology, Diabetes, and Obesity*, vol. 28, no. 4, pp. 360–370, 2021.
- [6] P. Liu, W. Wang, Z. Li et al., "Ferroptosis: a new regulatory mechanism in osteoporosis," *Oxidative Medicine and Cellular Longevity*, vol. 2022, Article ID 2634431, 10 pages, 2022.
- [7] X. Ying, X. Chen, H. Liu et al., "Silibinin alleviates high glucose-suppressed osteogenic differentiation of human bone marrow stromal cells via antioxidant effect and PI3K/Akt signaling," *European Journal of Pharmacology*, vol. 765, article S0014299915302363, pp. 394–401, 2015.
- [8] S. Khosla, P. Samakkarnthai, D. G. Monroe, and J. N. Farr, "Update on the pathogenesis and treatment of skeletal fragility in type 2 diabetes mellitus," *Nature Reviews. Endocrinology*, vol. 17, no. 11, article 555, pp. 685–697, 2021.
- [9] C. Caffarelli, M. D. Tomai Pitinca, A. Al Refaie, E. Ceccarelli, and S. Gonnelli, "Ability of radiofrequency echographic multi-spectrometry to identify osteoporosis status in elderly women with type 2 diabetes," *Aging Clinical and Experimental Research*, vol. 34, no. 1, article 1889, pp. 121–127, 2022.
- [10] L. C. Hofbauer, B. Busse, R. Eastell et al., "Bone fragility in diabetes: novel concepts and clinical implications," *The Lancet Diabetes and Endocrinology*, vol. 10, no. 3, article S2213858721003478, pp. 207–220, 2022.
- [11] S. C. Jordan, J. Choi, I. Kim et al., "Interleukin-6, a cytokine critical to mediation of inflammation, autoimmunity and allograft rejection: therapeutic implications of IL-6 receptor blockade," *Transplantation*, vol. 101, no. 1, pp. 32–44, 2017.
- [12] J. Dai, C. Huang, J. Wu, C. Yang, K. Frenkel, and X. Huang, "Iron-induced interleukin-6 gene expression: possible mediation through the extracellular signal-regulated kinase and p38 mitogen-activated protein kinase pathways," *Toxicology*, vol. 203, no. 1-3, article S0300483X04003361, pp. 199–209, 2004.
- [13] B. Xie, S. Chen, Y. Xu et al., "The impact of glucagon-like peptide 1 receptor agonists on bone metabolism and its possible mechanisms in osteoporosis treatment," *Frontiers in Pharmacology*, vol. 12, p. 697442, 2021.
- [14] Y. Jia, J. Sun, Y. Zhao et al., "Chinese patent medicine for osteoporosis: a systematic review and meta-analysis," *Bioengineered*, vol. 13, no. 3, pp. 5581–5597, 2022.
- [15] D. Lee, Y. M. Kim, H. W. Kim et al., "Schisandrin C affects glucose-stimulated insulin secretion in pancreatic β -Cells and glucose uptake in skeletal muscle cells," *Molecules*, vol. 26, no. 21, p. 6509, 2021.
- [16] Z. R. Li, R. B. Jia, D. Luo, L. Lin, Q. Zheng, and M. Zhao, "The positive effects and underlying mechanisms of Undaria pinnatifida polysaccharides on type 2 diabetes mellitus in rats," *Food & Function*, vol. 12, no. 23, pp. 11898–11912, 2021.
- [17] G. Karsenty, "The complexities of skeletal biology," *Nature*, vol. 423, no. 6937, article BFnature01654, pp. 316–318, 2003.
- [18] J. M. Huan, W. G. Su, W. Li et al., "Summarizing the effective herbs for the treatment of hypertensive nephropathy by complex network and machine learning," *Evidence-based Complementary and Alternative Medicine*, vol. 2021, Article ID 5590743, 12 pages, 2021.
- [19] W. Zhang, M. Lv, Y. Shi, Y. Mu, Z. Yao, and Z. Yang, "Network pharmacology-based study of the underlying mechanisms of Huangqi Sijunzi decoction for Alzheimer's disease," *Evidence-based Complementary and Alternative Medicine*, vol. 2021, Article ID 6480381, 13 pages, 2021.
- [20] Y. Ning, Y. Rao, Z. Yu, W. Liang, and F. Li, "Skin permeation profile and anti-inflammatory effect of anemonin extracted from weilingxian," *Pharmazie*, vol. 71, no. 3, pp. 134–138, 2016.
- [21] H. Zhang, W. W. Xing, Y. S. Li et al., "Effects of a traditional Chinese herbal preparation on osteoblasts and osteoclasts," *Maturitas*, vol. 61, no. 4, article S0378512208002570, pp. 334–339, 2008.
- [22] C. C. Guo, L. H. Zheng, J. Y. Fu et al., "Antiosteoporotic effects of Huangqi Sanxian decoction in cultured rat osteoblasts by proteomic characterization of the target and mechanism," *Evidence-based Complementary and Alternative Medicine*, vol. 2015, Article ID 514063, 10 pages, 2015.

- [23] A. Gomes, S. Haldar, B. Giri et al., "Experimental osteoporosis induced in female albino rats and its antagonism by Indian black scorpion (*Heterometrus bengalensis* C.L. Koch) venom," *Toxicon*, vol. 53, no. 1, article S0041010108005497, pp. 60–68, 2009.
- [24] Y. H. Park, M. An, J. K. Kim, and Y. H. Lim, "Antiobesity effect of ethanolic extract of *Ramulus mori* in differentiated 3T3-L1 adipocytes and high-fat diet-induced obese mice," *Journal of Ethnopharmacology*, vol. 251, article S0378874119331666, p. 112542, 2020.
- [25] C. Ma, C. Zhang, and X. Li, "Intervention and effect analysis of *Achyranthes bidentata* blume combined with aerobic exercise to interfere with type 2 diabetes," *Pakistan Journal of Pharmaceutical Sciences*, vol. 31, no. 3(Special), pp. 1151–1156, 2018.
- [26] C. Kim, H. Ha, J. H. Lee, J. S. Kim, K. Song, and S. W. Park, "Herbal extract prevents bone loss in ovariectomized rats," *Archives of Pharmacol Research*, vol. 26, no. 11, article BF02980200, pp. 917–924, 2003.
- [27] Z. Zhang, L. Zhang, and H. Xu, "Effect of *Astragalus* polysaccharide in treatment of diabetes mellitus: a narrative review," *Journal of Traditional Chinese Medicine*, vol. 39, no. 1, pp. 133–138, 2019.
- [28] S. Yang, H. Wang, Y. Yang et al., "Baicalein administered in the subacute phase ameliorates ischemia-reperfusion-induced brain injury by reducing neuroinflammation and neuronal damage," *Biomedicine & Pharmacotherapy*, vol. 117, article S0753332219307553, p. 109102, 2019.
- [29] C. Guo, R. J. Yang, K. Jang, X. L. Zhou, and Y. Z. Liu, "Protective effects of pretreatment with quercetin against lipopolysaccharide-induced apoptosis and the inhibition of osteoblast differentiation via the MAPK and Wnt/ β -catenin pathways in MC3T3-E1 cells," *Cellular Physiology and Biochemistry*, vol. 43, no. 4, pp. 1547–1561, 2017.
- [30] F. Tang, P. Zhang, W. Zhao et al., "Research on the mechanism of kaempferol for treating senile osteoporosis by network pharmacology and molecular docking," *Evidence-based Complementary and Alternative Medicine*, vol. 2022, Article ID 6741995, 12 pages, 2022.
- [31] S. F. Li, J. J. Tang, J. Chen et al., "Regulation of bone formation by baicalein via the mTORC1 pathway," *Drug Design, Development and Therapy*, vol. 9, pp. 5169–5183, 2015.
- [32] A. Mukherjee and P. Rotwein, "Selective signaling by Akt 1 controls osteoblast differentiation and osteoblast-mediated osteoclast development," *Molecular and Cellular Biology*, vol. 32, no. 2, pp. 490–500, 2012.
- [33] Y. H. Peng, P. Wang, X. Q. He, M. Z. Hong, and F. Liu, "Micro ribonucleic acid-363 regulates the phosphatidylinositol 3-kinase/threonine protein kinase axis by targeting NOTCH1 and forkhead box C2, leading to hepatic glucose and lipids metabolism disorder in type 2 diabetes mellitus," *J Diabetes Investig*, vol. 13, no. 2, pp. 236–248, 2022.
- [34] A. I. El-Makawy, F. M. Ibrahim, D. M. Mabrouk, S. H. Abdel-Aziem, H. A. Sharaf, and M. F. Ramadan, "Efficiency of turnip bioactive lipids in treating osteoporosis through activation of osterix and suppression of cathepsin K and TNF- α signaling in rats," *Environmental Science and Pollution Research International*, vol. 27, no. 17, article 8540, pp. 20950–20961, 2020.
- [35] J. Wang, Y. Chen, Y. Yang et al., "Endothelial progenitor cells and neural progenitor cells synergistically protect cerebral endothelial cells from hypoxia/reoxygenation-induced injury via activating the PI3K/Akt pathway," *Molecular Brain*, vol. 9, no. 1, article 193, p. 12, 2016.
- [36] P. Cai, Y. Lu, Z. Yin, X. Wang, X. Zhou, and Z. Li, "Baicalein ameliorates osteoporosis via AKT/FOXO1 signaling," *Aging (Albany NY)*, vol. 13, no. 13, article 203227, pp. 17370–17379, 2021.
- [37] G. Zhu, H. Cai, L. Ye et al., "Small proline-rich protein 3 regulates IL-33/ILC2 axis to promote allergic airway inflammation," *Frontiers in Immunology*, vol. 12, p. 758829, 2022.
- [38] H. Tian, F. Chen, Y. Wang et al., "Nur77 prevents osteoporosis by inhibiting the NF- κ B signalling pathway and osteoclast differentiation," *Journal of Cellular and Molecular Medicine*, vol. 26, no. 8, pp. 2163–2176, 2022.
- [39] V. Pivodova, J. Frankova, P. Dolezel, and J. Ulrichova, "The response of osteoblast-like SaOS-2 cells to modified titanium surfaces," *The International Journal of Oral & Maxillofacial Implants*, vol. 28, no. 5, pp. 1386–1394, 2013.
- [40] F. Poutoglidou, C. Pourzitaki, M. E. Manthou et al., "The inhibitory effect of tocilizumab on systemic bone loss and tendon inflammation in a juvenile collagen-induced arthritis rat model," *Connective Tissue Research*, pp. 1–13, 2022.
- [41] Z. Linlin, L. Ciai, S. Yanhong et al., "A multi-target and multi-channel mechanism of action for Jiawei Yinhuo Tang in the treatment of social communication disorders in autism: network pharmacology and molecular docking studies," *Evidence-based Complementary and Alternative Medicine*, vol. 2022, Article ID 4093138, 17 pages, 2022.
- [42] L. Qi, J. Jiang, G. Yu et al., "Dietary curcumin supplementation ameliorates placental inflammation in rats with intra-uterine growth retardation by inhibiting the NF- κ B signaling pathway," *The Journal of Nutritional Biochemistry*, vol. 104, article S0955286322000444, p. 108973, 2022.

Research Article

Alpha-Amylase Inhibits Cell Proliferation and Glucose Uptake in Human Neuroblastoma Cell Lines

Kateryna Pierzynowska ^{1,2,3} Sofia Thomasson,¹ and Stina Oredsson ¹

¹Department of Biology, Lund University, Sölvegatan 35, 22362 Lund, Sweden

²Department of Animal Physiology, The Kielanowski Institute of Animal Nutrition and Physiology Polish Academy of Sciences, Instytutcka 3, 05110 Jabłonna, Poland

³SGPlus-Group, Alfågelgränden 24, 23132 Trelleborg, Sweden

Correspondence should be addressed to Kateryna Pierzynowska; katerina.goncharova@biol.lu.se and Stina Oredsson; stina.oredsson@biol.lu.se

Received 21 November 2021; Revised 17 June 2022; Accepted 11 July 2022; Published 25 July 2022

Academic Editor: Fu-Gui Zhang

Copyright © 2022 Kateryna Pierzynowska et al. This is an open access article distributed under the Creative Commons Attribution License, which permits unrestricted use, distribution, and reproduction in any medium, provided the original work is properly cited.

The present article describes a study of the effects of alpha-amylase (α -amylase) on the human neuroblastoma (NB) cell lines SH-SY5Y, IMR-32, and LA-N-1. NB is the most common malignancy diagnosed in infants younger than 12 months. Some clinical observations revealed an inverse association between the risk of NB development and breastfeeding. α -Amylase which is present in breast milk was shown to have anticancer properties already in the beginning of the 20th century. Data presented here show that pancreatic α -amylase inhibits cell proliferation and has a direct impact on glucose uptake in the human NB cell lines. Our results point out the importance of further research which could elucidate the α -amylase mode of action and justify the presence of this enzyme in breast milk as a possible inhibitor of NB development. α -Amylase can be thus recognized as a potential safe and natural mild/host anticancer agent minimizing chemotherapy-related toxicity in the treatment of NB.

1. Introduction

Neuroblastoma (NB) is the most common extracranial paediatric tumor, and it is the most common malignancy diagnosed in infants younger than 12 months. The incidence rate of NB is almost twice that of leukaemia (the second neonatal cancer) in the mentioned paediatric group [1–4]. Regarding clinical presentation and prognosis, NB demonstrates a variety of patterns, from spontaneous regression to aggressive metastatic tumors [5, 6]. The clinical response differs dramatically in different risk groups. The same variable pattern is observed regarding the five-year survival rates, where low- and intermediate-risk cases have survival rates over 90%, while high-risk patients have a survival rate of only 40–50%, despite the intensification of treatments and incorporation of immunotherapies. It is worth mentioning that high-risk NB is found in about 40% of cases and is often accompanied with chemoresistance and tumor relapse [5, 6]. The goal of current strate-

gies for NB treatment is to decrease therapy- and minimize chemotherapy-related toxicity for patients from low and intermediate NB risk groups, whereas concerning high risk NB cases, present and upcoming trials are devoted to the development of novel immunotherapies, inhibitors of aberrant pathways (such as *MYC* and *ALK*), and radioisotope-containing regimens.

The current treatment of NB is based on stratification into low, medium, and high risk and includes observation, surgery, radiation therapy, ¹³¹I meta-iodobenzylguanidine therapy, chemotherapy, targeted therapy as well as high-dose chemotherapy, and radiation therapy with stem cell rescue [6, 7]. Various immunotherapy strategies are also discussed in the context of NB [8, 9].

In 2002, Daniels et al. [10] conducted a large study showing that breastfeeding was associated with a 41% (22–56%) reduction in risk of NB (odds ratio 0.6). Only two more studies with small *n* (*n* < 45) investigated the relationship between breastfeeding and NB and confirmed the

conclusions of Daniels et al., which have been published [11, 12]. Numerous factors and agents affecting cancer cell proliferation are being investigated, but the mechanisms of inverse relationship between breastfeeding and NB still remain unclarified and the existence and importance of this relationship is overlooked.

Recent studies from our lab have shown the possible role of alpha-amylase (α -amylase), which is present in excessive amounts in breast milk, in the regulation of glucose metabolism [13–15]. Changes in glucose metabolism is recognized as being one of the hallmarks of cancer. Thus, α -amylase may have a role in the regulation of cell proliferation including that of cancer cells. There are some reports about anti-proliferative effects of α -amylase *in vivo* with unknown mechanism [16–19].

Recently, we have shown that α -amylase inhibits cell proliferation and glucose uptake in human NB cell line SH-SY5Y [20]. Thus, the aim of our study was to confirm and extend our previous observations and determine if α -amylase treatment has any impact on the human NB cell lines SH-SY5Y, IMR-32, and LA-N-1, which partly correspond to the low-, medium-, and high-risk NB, respectively, and possess divergent genetic aberrations, by investigating effects on cell proliferation and glucose uptake. An investigation of the potential of the anticancer properties of α -amylase could result in the possibility to suggest a supplemental treatment with lower toxicity to current NB treatments, which is of undoubted importance for the modern cure of this disease.

2. Materials and Methods

2.1. Cell Line Routine Culturing Conditions. The SH-SY5Y and IMR-32 cell lines were purchased from American Type Culture Collection (ATCC® CRL-2266™ and ATCC® CCL-127™, respectively, LGC Standards, Middlesex, UK), and LA-N-1 cell line was purchased from the European Collection of Authenticated Cell Cultures (ECACC 06041201, Salisbury, UK). The cell lines were tested for mycoplasma during the experimental period, and all were found to be negative (Eurofins Scientific, Cologne, Germany). Upon arrival, cell lines were thawed, amplified, and frozen in ampules in liquid nitrogen. Cells were seeded at a density range from 15000 cells/cm² to 30000 cells/cm² in tissue culture flasks (Nunc, Thermo Fisher Scientific, Roskilde, Denmark) containing 0.16 ml medium/cm² and kept in a humidified incubator with 5% CO₂ in air at 37°C. The cell lines were cultured in DMEM/Ham's F12 medium (Avantor VWR cooperation, Lund, Sweden) supplemented with 10% heat-inactivated fetal bovine serum (FBS) (Sigma-Aldrich Sweden AB, Stockholm, Sweden), 1 mM Na-pyruvate (Sigma-Aldrich Sweden AB), 1 mM nonessential amino acids (Avantor VWR cooperation), 100 µg/ml streptomycin (Avantor VWR cooperation), 100 U/ml penicillin (Avantor VWR cooperation), 10 ng/ml epidermal growth factor (Lonza, Basel, Switzerland), and 2 mM L-glutamine (Avantor VWR cooperation). Cells were routinely passaged once a week. 0.05% trypsin/1 mM EDTA was used for cell detachment.

2.2. α -Amylase. Porcine α -amylase was purchased from Merck KGaA (catalogue number 10102814001, Darmstadt, Germany). The amylolytic activity in the solution was determined using ethylidene-pNP-G7 (4,6-ethylidene-p-nitrophenyl- α , D-maltoheptaoside) as the substrate, according to the manufacturer's instructions (Infinity Amylase Liquid Stable Reagent; Thermo Fisher Scientific, Middletown, Virginia, USA), with modifications for a microtiter plate reader. The activity of the original amylase solution was found to be 1000 U/l. A dilution series of the α -amylase stock in 0.9% NaCl was made to be able to investigate the effect of α -amylase on the neuroblastoma cell lines SH-SY5Y, LA-N-1, and IMR-32.

2.3. Dose-Response Assay. Cells were detached, counted in a hemocytometer, and resuspended to a final concentration of 0.11×10^6 cells/ml. A 180 µl aliquot of the cell suspension was added per well in 96-well plates, and the plates were incubated for 24 h before addition of α -amylase. A dilution series of α -amylase was made in 0.9% NaCl, and 20 µl aliquots were added to achieve the final concentrations shown in Figure 1. Controls received 20 µl 0.9% NaCl. After 72 h of incubation, 20 µl of 3-(4,5-dimethylthiazolyl-2)-2,5-diphenyltetrazolium bromide (MTT) (Sigma-Aldrich Stockholm AB) solution (5 mg/ml in phosphate-buffered saline) was added to each well, and the plates were returned to the CO₂ incubator for 1 h. Thereafter, the MTT-containing medium was removed and the blue formazan product was dissolved by the addition of 100 µl of 100% dimethyl sulfoxide per well. The plates were swirled gently for 15 min to dissolve the precipitate. The absorbance was measured at 540 nm using a Multiskan™ FC microplate spectrophotometer and the software SkanIt for Multiskan FC 3.1. Ink (Thermo Fisher Scientific). The results were analyzed using the GraphPad 9 software (La Jolla, California, USA). The presented IC₅₀ values with 95% confidence interval are based on at least 3 dose-response experiments.

2.4. Digital Holographic Imaging and Analysis. To monitor the effect of α -amylase on motility, accumulated distance, and proliferation of neuroblastoma cells, the phase holographic microscope M4 (Phase Holographic Imaging AB, Lund, Sweden) was used. Cells were detached with 0.05% trypsin/1 mM EDTA and counted in a hemocytometer. SH-SY5Y cells were seeded at a density of 20000 cells/cm², and LA-N-1 cells were seeded at a density of 30000 cells/cm² in 6-well plates (Nunc, Thermo Fisher Scientific). After 24 h of incubation, the cell medium was aspirated, and 4 ml of fresh cell medium was added to each well. Subsequently, three wells were treated with 2 U/l α -amylase and the three remaining wells were treated with the equivalent volumes of 0.9% NaCl. After adding α -amylase, specific HoloLids™ (Phase Holographic Imaging AB) replaced the standard 6-well plate lid and the plate was placed on the stage of the M4 HoloMonitor inside a CO₂ cell culturing incubator. Images were acquired every 5 minutes for 72 h using AppSuite™ (Phase Holographic Imaging AB). Following image acquisition, the time-lapses were used to analyze kinetic

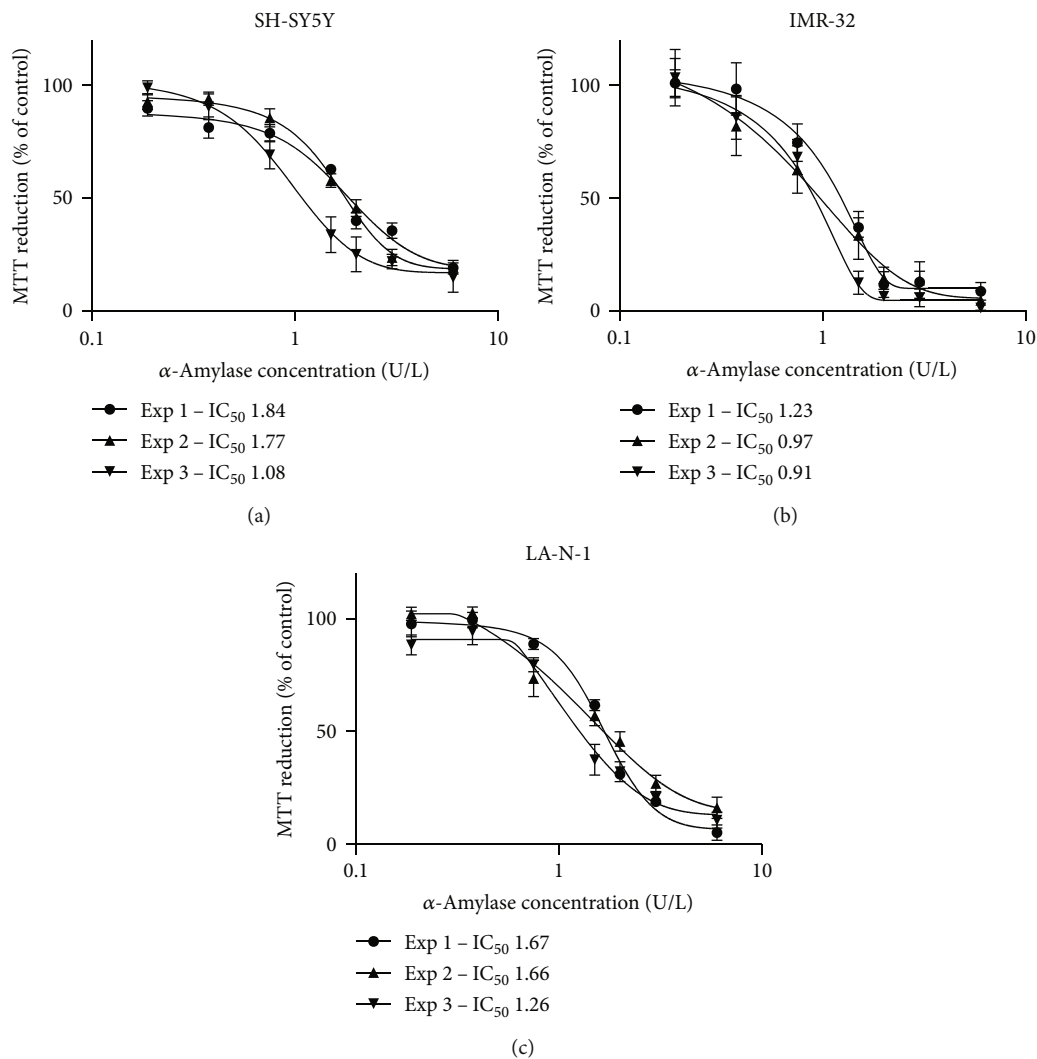


FIGURE 1: Treatment of NB cells with α -amylase decreases the cell number dose dependently. Human NB cells (a) SH-SY5Y, (b) IMR-32, and (c) LA-N-1 were incubated with porcine pancreatic α -amylase for 72 h, and then, an MTT assay was used for indirect determination of cell number. The IC_{50} of each repeat is presented on the right side of the graph. The results are expressed as percent of control. The data are derived from 6 wells per treatment from three different experiments and presented as mean \pm SD.

motility and proliferation of single cells and videos made using AppSuite™ (Phase Holographic Imaging AB).

2.5. Investigation of Glucose Uptake. For the detection of cellular glucose uptake, SH-SY5Y cells were seeded at a density of 20000 cells/cm², and LA-N-1 and IMR-32 cells were seeded at a density of 30000 cells/cm² in 12-well plates (Nalge Nunc International, Penfield, New York, USA) in 2 ml of regular growth medium and then incubated for 24 h. α -Amylase was administered 24 h after seeding as a sterile solution in 0.9% NaCl, to a final concentration of 2 U/L. Control received the same volume 0.9% NaCl. After 1 h of incubation without or with α -amylase, 2 μ l of ³H-radiolabelled deoxy-D-glucose (1 mCi/ml, catalogue number NET549A001MC, PerkinElmer, Boston, MA, USA) was added per well. The plates were incubated for 24 h. After incubation, cell lysates were prepared and mixed with

10 ml Ready Safe Liquid Scintillation Cocktail for Aqueous Samples (Beckman Coulter, Brea, CA, USA) in Poly-Q™ vials (Beckman Coulter). The vials were shaken for 2 min and stored for 48 h in the dark to reduce chemical quenching before analysis. ³H-glucose uptake was determined by liquid scintillation counting in a (Beckmann LS 6500 LSC multi-purpose liquid scintillation counter (Beckmann Coulter)). All experiments were repeated at least three times.

2.6. Immunocytochemistry. Cells seeded at a density of 20000 cells/cm² (SH-SY5Y) or 30000 cells/cm² (LA-N-1 and IMR-32) in 6-well plates and treated with 2 U/L α -amylase for 72 h were used to investigate the effect of α -amylase on the expression of glucose transporter-1 (GLUT1) and glucose transporter-2 (GLUT2) receptors using immunocytochemistry. After 72 h of incubation, the cell medium was aspirated, and the cells were fixed with 3.7% formaldehyde in PBS

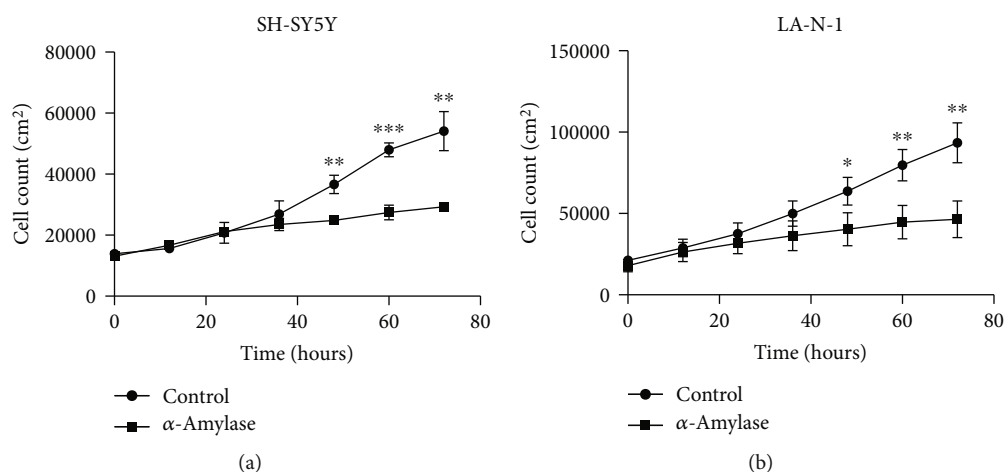


FIGURE 2: α -Amylase treatment inhibits the proliferation of (a) SH-SY5Y and (b) LA-N-1 cells. α -Amylase was added to the final concentration of 2 U/l (control received 0.9% NaCl) at 24 h after seeding. The cell number was determined by digital holographic microscopy. The curves are drawn from cell count data obtained at the indicated times after start of the time-lapse. The data are derived from three images per well and 6 wells per treatment from two different experiments. Data are represented as mean \pm SD. * indicates a statistical significance between α -amylase treated and control in the corresponding time points when $p < 0.05$ and ** when $p < 0.01$.

(Merck KGaA). Subsequently, 400 μ l of blocking buffer (PBS with 1% bovine serum albumin (BSA)) was added to each well and the samples were incubated for a minimum of 2 h. After incubation, the blocking buffer was removed and 400 μ l recombinant Alexa Fluor[®] 488 Anti-Glucose Transporter GLUT1 antibody (1:400, ab195359, Abcam, Waltham, MA, USA) or recombinant Anti-Glucose Transporter GLUT2 antibody (1:400, ab234440, Abcam, Waltham, MA, USA) was added to separate wells and the samples incubated in the dark overnight. After washing, the secondary antibody Alexa Fluor 488[™] anti-rabbit (1:800, A11034, Thermo Fisher Scientific) was added to the wells with GLUT2 unconjugated antibodies. Simultaneously, Alexa Fluor[™] 594 phalloidin (1:200, A12381, Thermo Fisher Scientific) was added to all wells. Both antibodies were diluted to a final volume of 400 μ l per well and were incubated for 1.5 h shielded from light. Finally, 400 μ l 4',6-diamidino-2-phenylindole (DAPI) (1 μ g/ml, Thermo Fisher Scientific) was added to each well and the samples were incubated for 1.5 minutes in darkness. All wells were washed three times with PBS after each staining step, and all staining agents were diluted in blocking buffer. Finally, coverslips were mounted using Mowiol (Sigma-Aldrich Sweden AB). Samples were stored at 4°C and protected from light before microscopy. Confocal images were taken with a Leica SP8 DLS inverted confocal laser scanning microscope using an oil immersion 63x/1.4 objective lens (Leica Microsystems, Wetzlar, Germany).

2.7. Statistical Analyses. All data are presented as mean \pm SD. A two-tailed Student's *t*-test with Holm-Sidak correction for multiple comparisons or two-way ANOVA with a Sidak correction for multiple comparisons was used to estimate differences. A Shapiro-Wilk test was used to assess the normality of distribution. In all statistical analyses, $p \leq 0.05$ was consid-

ered significant. All analyses were carried out using Prism, version 9.3 (GraphPad Software, Inc., San Diego, CA, USA).

3. Results

3.1. Dose-Response Curves for NB Cells Treated with Alpha-Amylase. The antiproliferative effect of treating the human NB SH-SY5Y, IMR-32, and LA-N-1 cell lines with α -amylase was initially evaluated in dose-response experiments. Treatment with α -amylase at a final concentration above 0.2 U/l resulted in decreased MTT reduction, i.e., reduced cell number, with IC₅₀ values 1.53 ± 0.23 U/l for SH-SY5Y, 1.04 ± 0.17 for IMR-32, and 1.56 ± 0.42 for LA-N-1 cell lines after 72 h of incubation (Figure 1). These data gave us the basis for the treatment concentration of α -amylase in further studies.

3.2. Cell Proliferation. Growth curves for NB cells treated with 2 U/l α -amylase were established by digital holography. α -Amylase treatment significantly reduced number of SH-SY5Y cells by 32% ($p = 0.0125$) and LA-N-1 cells by 37% ($p = 0.0036$), already after 48 h of incubation (Figures 2(a) and 2(b), respectively). This decline in cell count was observed until the end of the time-lapse and reached 46% ($p = 0.0026$) and 50% ($p = 0.014$) for SH-SY5Y and LA-N-1 cells, respectively (Figure 2).

3.3. Treatment with Pancreatic α -Amylase Inhibits Cell Movement in SH-SY5Y and LA-N-1 Cell Lines. Cell motility and accumulated distance data from control and amylase-treated wells collected every 5 minutes after start of the time-lapse were compared using Student's paired *t*-test. Motility and accumulated distance were not significantly different for α -amylase-treated SH-SY5Y cells (Figures 3(a) and 3(c), respectively) when compared to control. However, α -amylase treatment significantly reduced the motility and

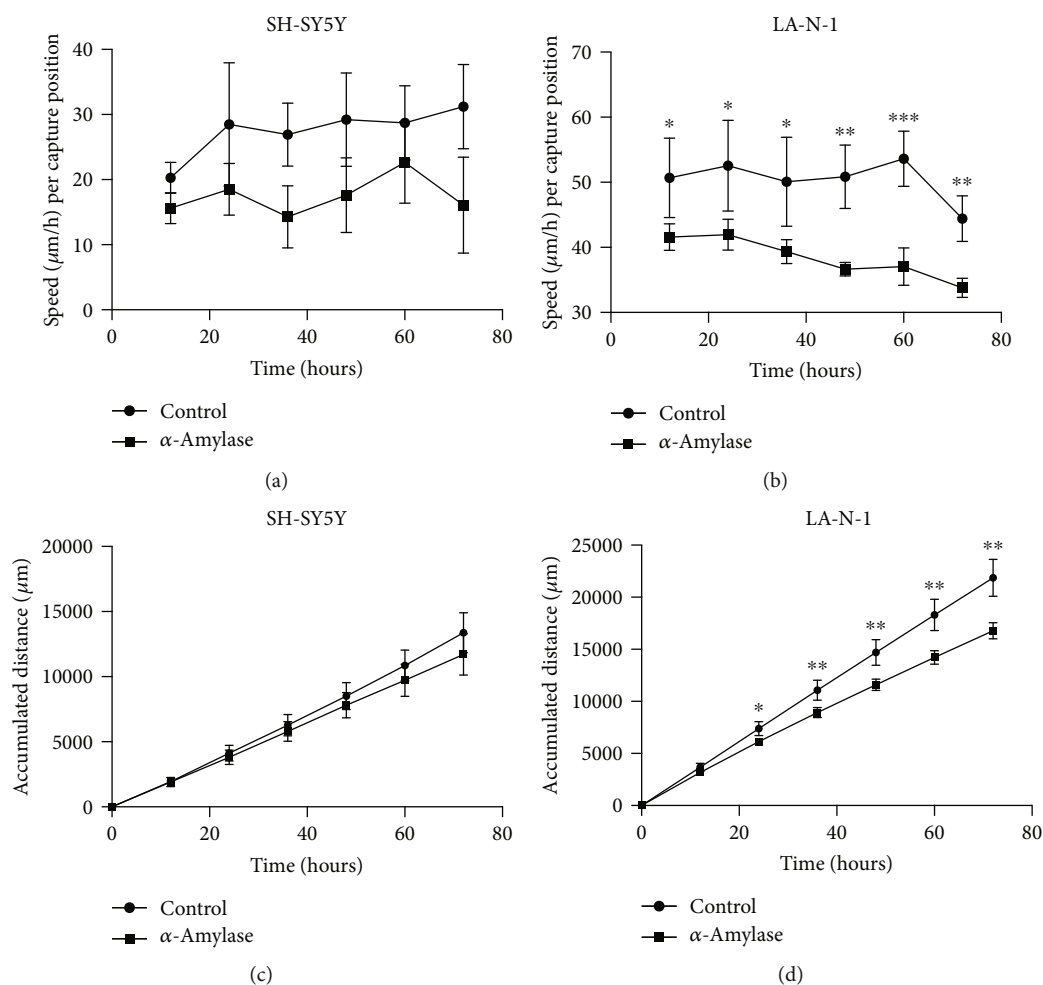


FIGURE 3: The motility and accumulated distance of (a, c) SH-SY5Y and (b, d) LA-N-1 cells treated with α -amylase. α -Amylase was added to the final concentration of 2 U/l (control received 0.9% NaCl) at 24 h after seeding. The data are derived from three images per well and 6 wells per treatment from two different experiments. Data are represented as mean \pm SD. * indicates a statistical significance between α -amylase treated and control in the corresponding time points when $p < 0.05$ and ** when $p < 0.01$.

accumulated distance of LA-N-1 cell line, where motility (Figure 3(b)) was reduced by 18% ($p = 0.0304$) at 12 h of treatment and this decline reached 24% ($p = 0.014$) at 72 h of treatment which is reflected in the reduced accumulated distance in α -amylase-treated cells compared to control (Figure 3(d)).

3.4. Treatment with α -Amylase Inhibits ^3H -Glucose Uptake. Addition of α -amylase to the medium (2 U/l) significantly decreased the uptake of ^3H -glucose in IMR-32 and LA-N-1 cells after 24 h of incubation (Figure 4). The glucose uptake in α -amylase-treated IMR-32 cells at 24 h of treatment was 55% of control values ($p = 0.0020$) and 82% of control in LA-N-1 cells ($p = 0.0027$) (Figure 4). Although there was a trend to decreased glucose uptake in SH-SY5Y cells treated with α -amylase for 24 h, it was not significant.

3.5. Glucose Transporter Expression. Immunocytochemistry was performed to analyze the expression of GLUT1 and GLUT2 in SH-SY5Y (Figure 5), IMR-32 (Figure 6), and LA-N-1 cells (Figure 7) and also if α -amylase treatment

affected the expression. Expression of both GLUT1 and GLUT2 was clearly demonstrated for all cell lines (Figures 5–7) in both control and α -amylase-treated cultures. Visual inspection does not reveal any differences in expression, and semiquantitative evaluation of expression was not performed.

4. Discussion

In this pilot study, the effect of treating human NB cells with pancreatic α -amylase was investigated. Pancreatic amylase was studied as a potential anticancer agent in the beginning of the 20th century [16–18] for the treatment of tumors at different locations in the body. Then, after almost a century of silence, interest in this enzyme in the context of cancer was raised again as Novak and Trnka reported improved survival of mice treated with amylase after transplantation of melanoma cells [19]. More recently, salivary α -amylase was shown to have antiproliferative effects in primary cell cultures of rat mammary epithelial cells and human breast cancer cells [21]. Moreover, breast cancer survivors have

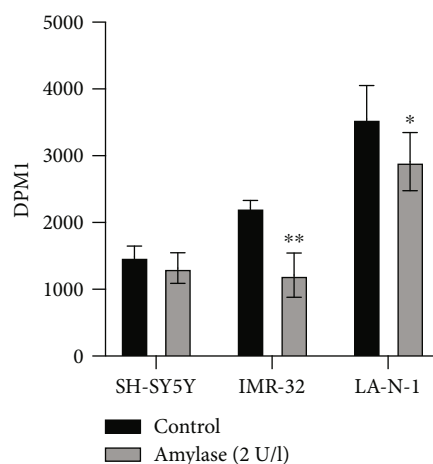


FIGURE 4: ^3H -glucose uptake in SH-SY5Y, IMR-32, and LA-N-1 cells treated with α -amylase. α -Amylase was added to the final concentration of 2 U/l (control received 0.9% NaCl) at 24h after seeding. One hour later, ^3H -glucose was added to the medium. After 24h of incubation in the presence of ^3H -glucose, the uptake was determined by liquid scintillation counting. Data are represented as mean of six independent samples \pm SD. * indicates a statistical significance between α -amylase treated and control when $p < 0.05$ and ** when $p < 0.01$.

an elevated blood level of salivary α -amylase [22], which has been recognized as a stress marker. However, it is unknown if the elevated salivary α -amylase activity is the consequence of cancer and stress or if it is an attempt of the organism to cure itself.

As previously mentioned, numerous factors and agents affecting NB are being investigated, but the mechanisms of the inverse relationship between breastfeeding and NB described by Daniels et al. [10] still remain unclarified and the existence and importance of this relationship are overlooked. An internalization and transcytosis of pancreatic amylase by enterocytes resulting in increased serum amylase level were shown by Cloutier et al. [23]. Thus, it is possible that breast milk α -amylase may increase the blood level of α -amylase in breastfed infants.

We initiated our study with dose-response curve experiments where the dose range was chosen based on serum amylase in humans. The antiproliferative effect was observed at concentrations below the normal human serum range of α -amylase (40-120 U/l), which is comparable to the low level of α -amylase found in infant serum during the first eight months after birth [24, 25]. We found IC_{50} values of 1.53 ± 0.23 U/l for SH-SY5Y, 1.04 ± 0.17 for IMR-32, and 1.56 ± 0.42 for LA-N-1, thus showing that observed effects could be reached by small doses within the physiological range of serum amylase activity in infants. A possible explanation for the variation in results is that the neuroblastoma cell lines contain two cellular phenotypic variants of undifferentiated mesenchymal cells and committed adrenergic cells [26]. The cell types have divergent gene expression profiles and are epigenetically regulated which allows for interconversion between the two phenotypes [27]. Additionally, the cell lines possess different genetic aberrations. The LA-N-1 cell line carries genetic aberrations such as a mutated *p53* gene, *MYCN* amplification, and silenced caspase 8 expression [28-30]. The SH-SY5Y and IMR-32 cell lines carry wild-type *p53* combined with a silenced caspase 8 expression

[29, 30]. The IMR-32 cell line also carries an amplification of the *MYCN* gene, and the SH-SY5Y cell line has trisomy 1q [31, 32]. Similar variation in α -amylase sensitivity among cell lines has also been observed in breast cancer cell lines [21]. Despite the diverse genetic abnormalities and cellular phenotypic variants in the cell lines, α -amylase treatment had an antiproliferative effect on all three cell lines. The levels of α -amylase activity observed in breast milk (about 9-10 kU/l) and in the postprandial duodenal aspirates of infants (about 5 kU/l) are high considering the absence of starch in the infants' diet [33-37], but they are significantly lower when compared to those found in the duodenal lumen of healthy adults [38]. One should remember that preprandial duodenal fluid samples in healthy term newborns do not contain any amylase at least during the first month of life [39], and in fact, all healthy term newborns which are not breastfed are exocrine pancreatic insufficient [40]. Thus, the mothers' milk seems to be an important source of α -amylase, which can enter the circulation and may affect NB development or have some other yet unknown functions unrelated to carbohydrate digestion.

The inhibition of cell proliferation by α -amylase treatment of SH-SY5Y and LA-N-1 cells was also proven by time-lapse imaging using digital holographic microscopy (significance found after 48 h of treatment). Interestingly, the digital holographic microscopy revealed a significant effect on cell motility and accumulated distance of LA-N-1 cells, but not SH-SY5Y cells, already after 24 h of α -amylase treatment. Unfortunately, IMR-32 cell line is not suitable for digital holographic microscopy due to growth peculiarities such as tight cell crowding; thus, data on cell growth, motility, and migration for this particular line was not obtained.

As a recent study from our laboratory shows the possible role of α -amylase in the regulation of glucose metabolism [13-15] and it is well known that changes in glucose metabolism are recognized as being one of the hallmarks of cancer, the effect of α -amylase on glucose uptake in SH-SY5Y, IMR-

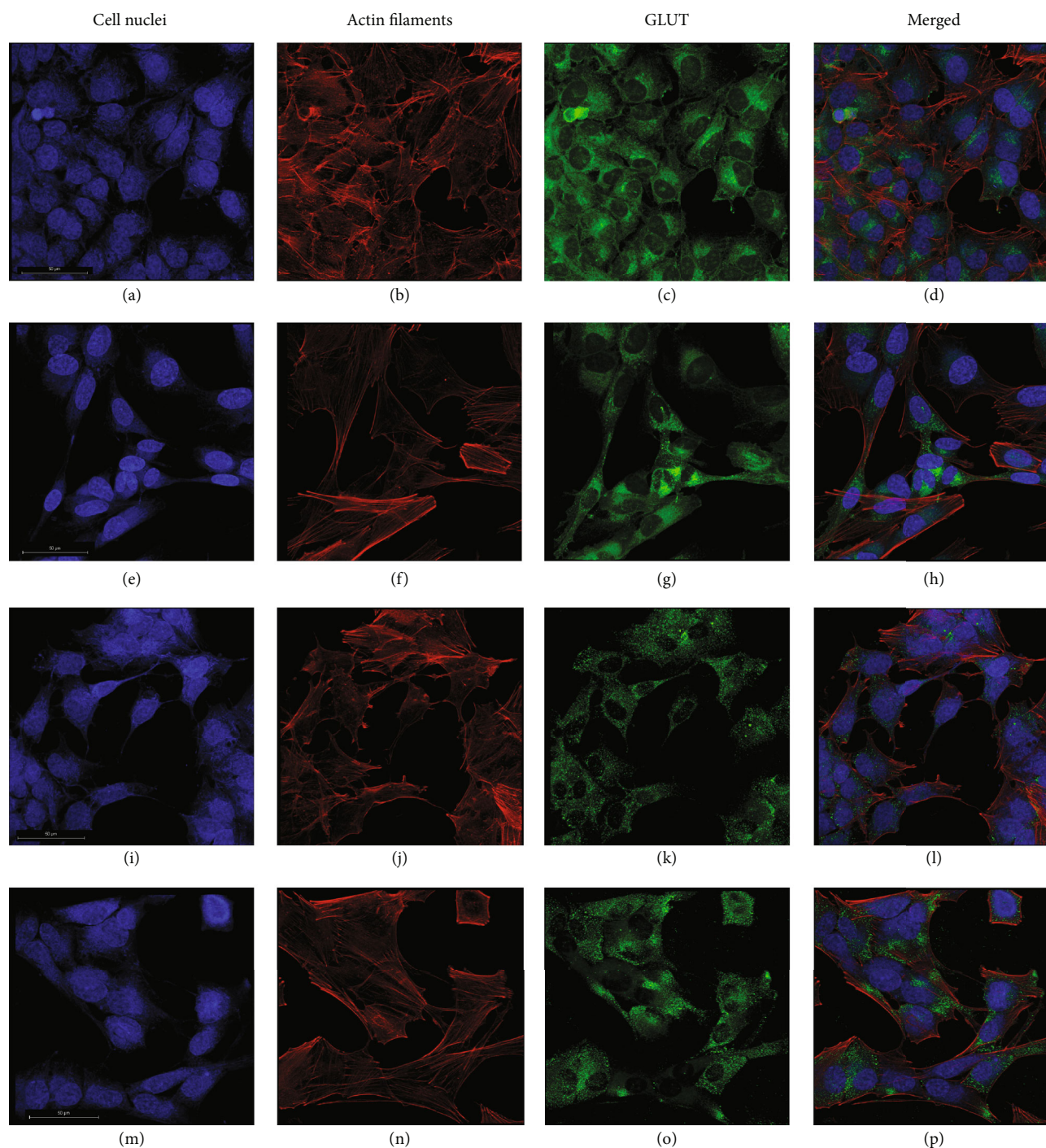


FIGURE 5: Images of the expression of GLUT1 and GLUT2 in control SH-SY5Y cells and cells treated with α -amylase for 72 h. α -Amylase was added to the final concentration of 2 U/l (control received 0.9% NaCl) at 24 h after seeding. GLUT1: (a–d) control; (e–h) α -amylase. GLUT2: (i–l) control; (m–p) α -amylase. NB cells were fixed in 3.7% formaldehyde and stained to visualize cell nuclei (DAPI, blue), actin filaments (Alexa Flour™ 594, red), and GLUT1 or GLUT2 (Alexa Flour™ 488, green). The scale bar is 50 μ m.

32, and LA-N-1 cells was investigated. Here, we show that the cellular glucose uptake in IMR-32 and LA-N-1 cells was significantly inhibited already after 24 h of incubation with α -amylase while there was only a trend for inhibition in SH-SY5Y cells. We have seen that ^3H -glucose uptake was decreased in SH-SY5Y after 72 h of treatment [20]. This

decreased uptake of glucose may be the cause for the inhibition of cell proliferation and cell motility.

Glucose transporter inhibitors are well-recognized targets for anticancer therapy [41, 42]. Some novel anticancer agents, such as the α -tocopherol derivative ESeroS-G, show the ability to target energy metabolism of cancer cells and

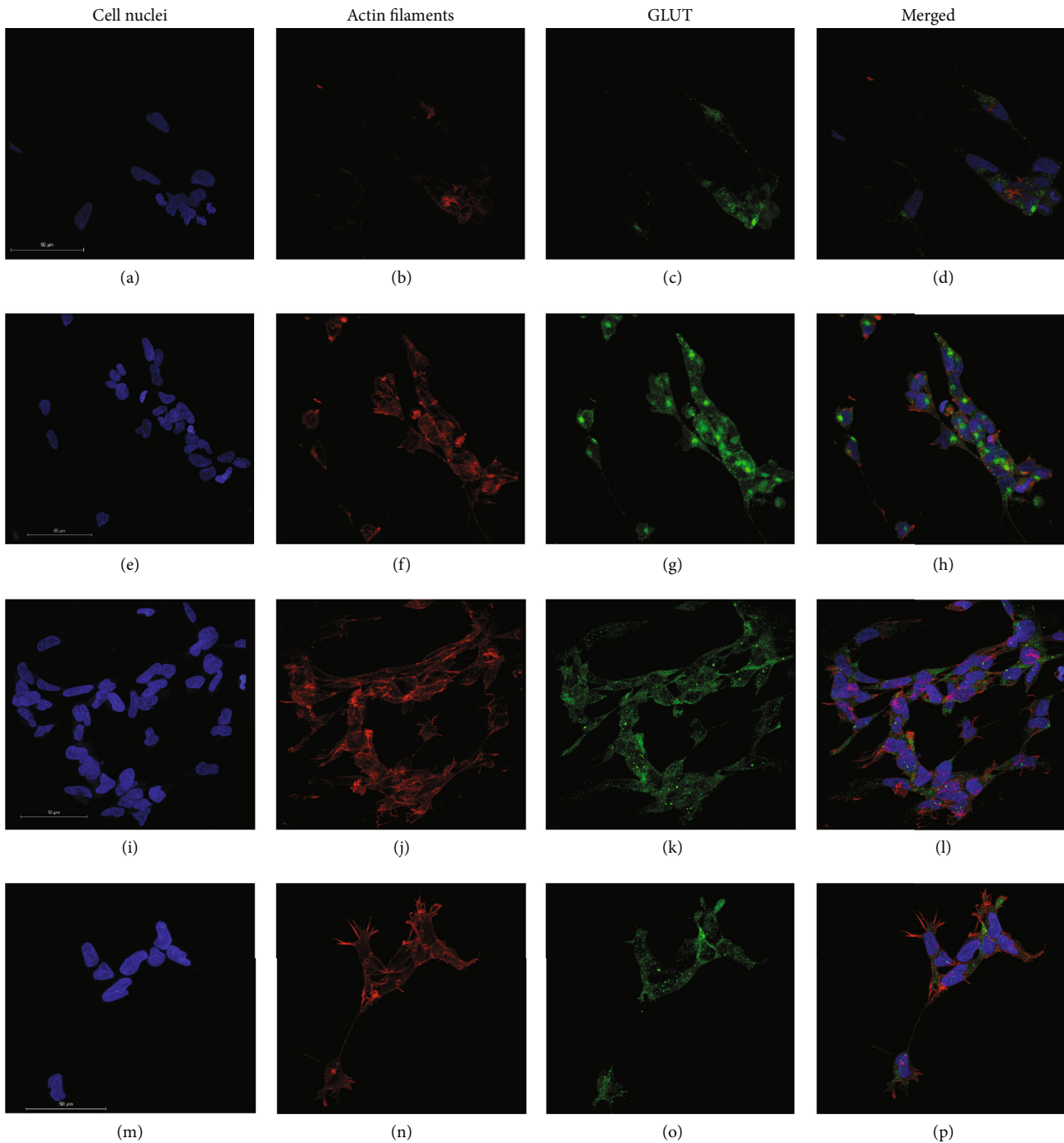


FIGURE 6: Images of the expression of GLUT1 and GLUT2 in IMR-32 cells treated with α -amylase for 72 h. α -Amylase was added to the final concentration of 2 U/l (control received 0.9% NaCl) at 24 h after seeding. GLUT1: (a–d) control; (e–h) 2 U/l α -amylase. GLUT2: (i–l) control; (m–p) 2 U/l α -amylase. NB cells were fixed in 3.7% formaldehyde and stained to visualize cell nuclei (DAPI, blue), actin filaments (Alexa Flour™ 594, red), and GLUT1 or GLUT2 (Alexa Flour™ 488, green). The scale bar is 50 μ m.

inhibit their migration [43]. Recently, α -amylase was shown to actively participate in the regulation of cell proliferation and turnover in the duodenum [44], and the regulatory abilities of this molecule in the intestine are obvious. It is known that SH-SY5Y cells express both GLUT1 and GLUT2 transporters. Previously, we have shown α -amylase-dependent changes in insulin secretion in pancreatic β cells, which express GLUT2 [15], thus supporting our notion that at least

glucose uptake by GLUT2 may be affected by α -amylase in neuroblastoma cells. α -Amylase's inhibitory effect on glucose uptake could be exerted in various ways such as blocking the glucose transporters or affecting the expression of the transporters. Thus, we have chosen immunocytochemistry as an initial step to evaluate GLUT1 and GLUT2 expression in the cell lines and to investigate if α -amylase treatment influenced the expression level. The preliminary data do

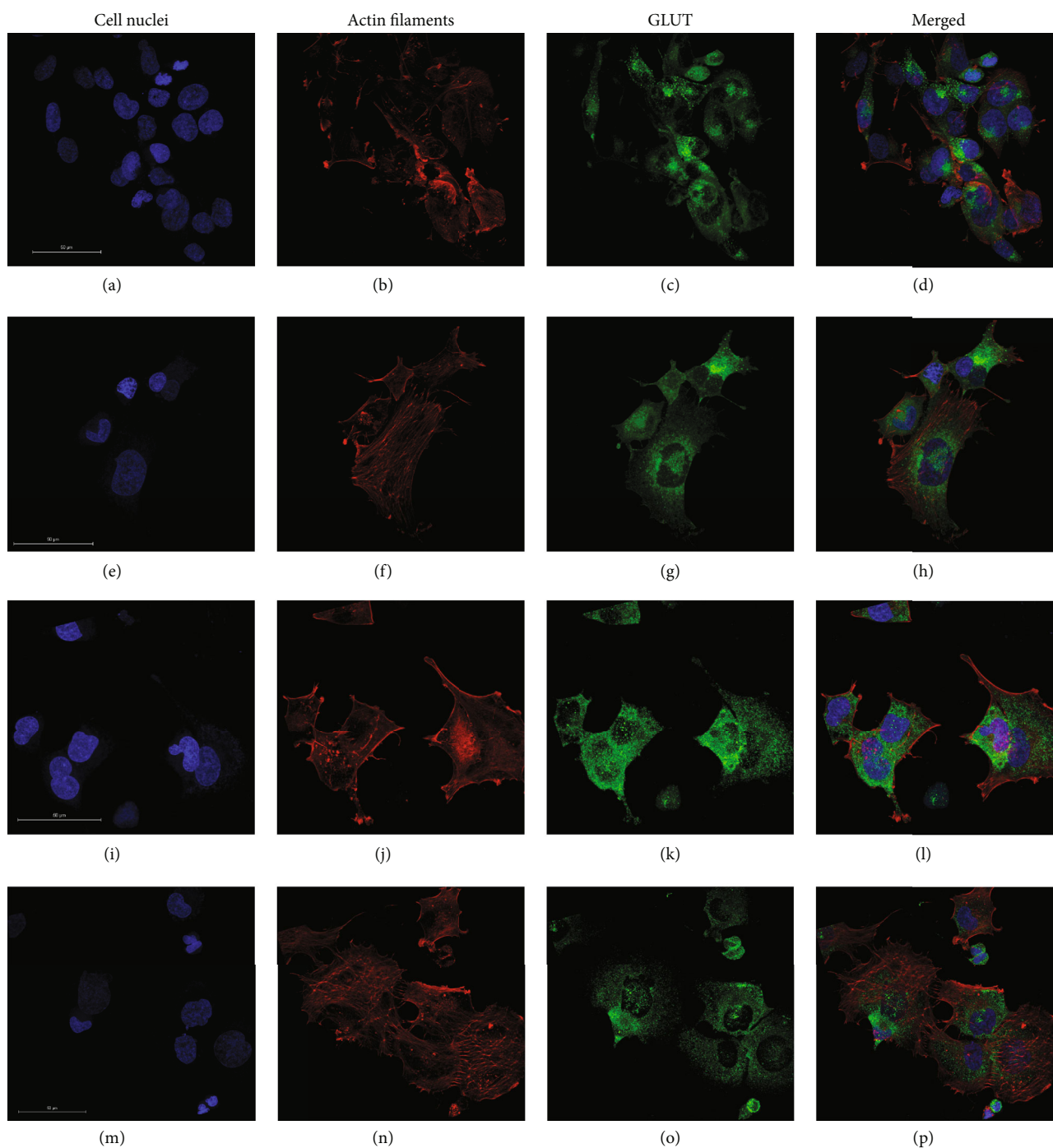


FIGURE 7: Images of the expression of GLUT1 and GLUT2 in LA-N-1 cells treated with α -amylase for 72 h. α -Amylase was added to the final concentration of 2 U/l (control received 0.9% NaCl) at 24 h after seeding. GLUT1: (a–d) control; (e–h) 2 U/l α -amylase. GLUT2: (i–l) control; (m–p) 2 U/l α -amylase. NB cells were fixed in 3.7% formaldehyde and stained to visualize cell nuclei (DAPI, blue), actin filaments (Alexa Flour™ 594, red), and GLUT1 or GLUT2 (Alexa Flour™ 488, green). The scale bar is 50 μ m.

not reveal any difference in GLUT1 and GLUT2 expression in SH-SY5Y, IMR-32, and LA-N-1 cells and there appeared to be no effect of α -amylase treatment. However, only the qualitative assessment was performed and the data obtained should be supported by quantitative investigations. Nevertheless, the demonstrated expression of both GLUT1 and GLUT2 in all NB cell lines used in the study is an important

finding which highlights the mechanisms of glucose transport in this type of tumor.

Some limitations of our studies include the usage of porcine pancreatic α -amylase instead of human salivary α -amylase which is present in breast milk, which might lead to a discrepancy in results [33]. However, salivary α -amylase and pancreatic α -amylase share 97% homology and both

isoenzymes can diffuse into the bloodstream, which supports the use of pancreatic α -amylase [45]. Human salivary α -amylase treatment at similar concentrations has previously been studied in breast cancer cells [21]. Additionally, the effect of α -amylase treatment is not evaluated on a healthy human cell line as a control. The detailed investigation of changes in glucose transporter expression after amylase treatment should be performed as well. However, despite the mentioned limitations, the current work demonstrates the novel important concept of α -amylase as a homeostatic agent and an important player in the metabolic regulations throughout the whole body during the entire lifespan.

5. Conclusions

The described study was designed as a proof-of-concept study, and the mechanisms underlying the observed effects remain to be thoroughly elucidated. However, the ability of α -amylase to inhibit cell proliferation and cell motility in human NB cells is obvious and this enzyme should be investigated as a possible mild, nontoxic alternative or/and supplementation to the current NB treatment strategies.

Data Availability

All data relevant to the study are included in the article.

Conflicts of Interest

Kateryna Pierzynowska is employed by the SGPlus-group, Trelleborg, Sweden. Sofia Thomasson and Stina Oredsson declare no competing interests.

Acknowledgments

The present study was supported by grants from the Royal Physiographic Society of Lund (40616/2019/09/25) and Anara AB, Trelleborg, Sweden.

References

- [1] S. Davis, M. A. Rogers, and T. W. Pendergrass, "The incidence and epidemiologic characteristics of neuroblastoma in the United States," *American Journal of Epidemiology*, vol. 126, no. 6, pp. 1063–1074, 1987.
- [2] J. G. Gurney, J. A. Ross, D. A. Wall, W. A. Bleyer, R. K. Severson, and L. L. Robison, "Infant cancer in the US: histology-specific incidence and trends, 1973 to 1992," *Journal of Pediatric Hematology/Oncology*, vol. 19, no. 5, pp. 428–432, 1997.
- [3] G. M. Brodeur and J. M. Marris, "Neuroblastoma," in *Principles and Practice of Pediatric Oncology*, P. A. Pizzo and B. G. Poplack, Eds., pp. 933–970, Lippincott Williams & Wilkins, Philadelphia, 5th edition, 2006.
- [4] J. M. Maris, M. D. Hogarty, R. Bagatell, and S. L. Cohn, "Neuroblastoma," *Lancet*, vol. 369, no. 9579, pp. 2106–2120, 2007.
- [5] K. Yamamoto, S. Ohta, E. Ito et al., "Marginal decrease in mortality and marked increase in incidence as a result of neuroblastoma screening at 6 months of age: cohort study in seven prefectures in Japan," *Journal of Clinical Oncology*, vol. 20, no. 5, pp. 1209–1214, 2002.
- [6] E. Hiyama, T. Iehara, T. Sugimoto et al., "Effectiveness of screening for neuroblastoma at 6 months of age: a retrospective population-based cohort study," *Lancet*, vol. 371, no. 9619, pp. 1173–1180, 2008.
- [7] M. S. Irwin and J. R. Park, "Neuroblastoma: paradigm for precision medicine," *Pediatric Clinics of North America*, vol. 62, no. 1, pp. 225–256, 2015.
- [8] M. Boes, "Cancer immunotherapy: moving beyond checkpoint inhibition," *Oncotarget*, vol. 9, no. 93, pp. 36545–36546, 2018.
- [9] M. Ishfaq, T. Pham, C. Beaman, P. Tamayo, A. L. Yu, and S. Joshi, "BTK inhibition reverses MDSC-mediated immunosuppression and enhances response to anti-PDL1 therapy in neuroblastoma," *Cancers*, vol. 13, no. 4, p. 817, 2021.
- [10] J. L. Daniels, A. F. Olshan, B. H. Pollock, N. R. Shah, and D. O. Stram, "Breast-feeding and neuroblastoma, USA and Canada," *Cancer causes & control: CCC*, vol. 13, no. 5, pp. 401–405, 2002.
- [11] V. B. Smulevich, L. G. Solionova, and S. V. Belyakova, "Parental occupation and other factors and cancer risk in children: I. Study methodology and non-occupational factors," *International Journal of Cancer*, vol. 83, no. 6, pp. 712–717, 1999.
- [12] L. Hardell and A. C. Dreifaldt, "Breast-feeding duration and the risk of malignant diseases in childhood in Sweden," *European Journal of Clinical Nutrition*, vol. 55, no. 3, pp. 179–185, 2001.
- [13] S. G. Pierzynowski, P. C. Gregory, R. Filip, J. Woliński, and K. Pierzynowska, "Glucose homeostasis dependency on acini-islet-acinar (AIA) axis communication: a new possible pathophysiological hypothesis regarding diabetes mellitus," *Nutrition & Diabetes*, vol. 8, no. 1, p. 55, 2018.
- [14] K. G. Pierzynowska, L. Lozinska, J. Woliński, and S. Pierzynowski, "The inverse relationship between blood amylase and insulin levels in pigs during development, bariatric surgery, and intravenous infusion of amylase," *PLoS One*, vol. 13, no. 6, article e0198672, 2018.
- [15] K. Pierzynowska, S. Oredsson, and S. Pierzynowski, "Amylase-dependent regulation of glucose metabolism and insulin/glucagon secretion in the streptozotocin-induced diabetic pig model and in a rat pancreatic beta-cell line, BRIN-BD11," *Journal Diabetes Research*, vol. 2020, pp. 1–10, 2020.
- [16] F. H. Wiggin, "Case of multiple fibrosarcoma of the tongue, with remarks on the use of trypsin and amylopsin in the treatment of malignant disease," *Journal of the American Medical Association*, vol. XLVII, no. 24, pp. 2003–2008, 1906.
- [17] R. A. Goeth, "Pancreatic treatment of cancer, with report of a cure," *JAMA*, vol. 48, no. 12, p. 1030, 1907.
- [18] W. L. Little, "A case of malignant tumor, with treatment," *Journal of the American Medical Association*, vol. 1907, no. 50, p. 1724, 1908.
- [19] J. Novak and F. Trnka, "Proenzyme therapy of cancer," *Anti-cancer Research*, vol. 25, no. 2A, pp. 1157–1177, 2005.
- [20] K. Pierzynowska and S. Oredsson, "ESPGHAN 54th Annual Meeting Abstracts," *Pediatric Gastroenterology and Nutrition*, vol. 74, no. S2, pp. 1–1172, 2022.
- [21] M. Fedrowitz, R. Hass, C. Bertram, and W. Löscher, "Salivary α -amylase exhibits antiproliferative effects in primary cell cultures of rat mammary epithelial cells and human breast cancer cells," *Journal of Experimental & Clinical Cancer Research*, vol. 30, no. 1, p. 102, 2011.
- [22] C. Wan, M. È. Couture-Lalande, T. A. Narain, S. Lebel, and C. Bielajew, "Salivary alpha-amylase reactivity in breast cancer

- survivors," *International Journal of Environmental Research and Public Health*, vol. 13, no. 4, p. 353, 2016.
- [23] M. Cloutier, D. Gingras, and M. Bendayan, "Internalization and transcytosis of pancreatic enzymes by the intestinal mucosa," *The Journal of Histochemistry and Cytochemistry*, vol. 54, no. 7, pp. 781–794, 2006.
- [24] K. Nakajima, T. Nemoto, T. Muneyuki, M. Kakei, H. Fuchigami, and H. Munakata, "Low serum amylase in association with metabolic syndrome and diabetes: a community-based study," *Cardiovascular Diabetology*, vol. 10, no. 1, p. 34, 2011.
- [25] M. Otsuki, H. Yuu, S. Saeki, and S. Baba, "The characteristics of amylase activity and the isoamylase pattern in serum and urine of infants and children," *European Journal of Pediatrics*, vol. 125, no. 3, pp. 175–180, 1977.
- [26] T. van Groningen, J. Koster, L. J. Valentijn et al., "Neuroblastoma is composed of two super-enhancer-associated differentiation states," *Nature Genetics*, vol. 49, no. 8, pp. 1261–1266, 2017.
- [27] T. van Groningen, N. Akogul, E. M. Westerhout et al., "A NOTCH feed-forward loop drives reprogramming from adrenergic to mesenchymal state in neuroblastoma," *Nature Communications*, vol. 10, no. 1, p. 1530, 2019.
- [28] S. Hopkins-Donaldson, J. L. Bodmer, K. B. Bouloud, C. B. Brognara, J. Tschopp, and N. Gross, "Loss of caspase-8 expression in highly malignant human neuroblastoma cells correlates with resistance to tumor necrosis factor-related apoptosis-inducing ligand-induced apoptosis," *Cancer Research*, vol. 60, no. 16, pp. 4315–4319, 2000.
- [29] A. M. Davidoff, J. C. Pence, N. A. Shorter, J. D. Iglehart, and J. R. Marks, "Expression of p53 in human neuroblastoma and neuroepithelioma-derived cell lines," *Oncogene*, vol. 7, no. 1, pp. 127–133, 1992.
- [30] R. Huang, N.-K. V. Cheung, J. Vider et al., "MYCN and MYC regulate tumor proliferation and tumorigenesis directly through BMI1 in human neuroblastomas," *The FASEB Journal*, vol. 25, no. 12, pp. 4138–4149, 2011.
- [31] J. L. Harenza, M. A. Diamond, R. N. Adams et al., "Transcriptomic profiling of 39 commonly-used neuroblastoma cell lines," *Scientific Data*, vol. 4, no. 1, article 170033, 2017.
- [32] T. C. Neuroblastoma and C. Lines, "Neuroblastoma," *Journal Human Cell Culture*, vol. 1, pp. 21–53, 2002.
- [33] T. Lindberg and G. Skude, "Amylase in human milk," *Pediatrics*, vol. 70, no. 2, pp. 235–238, 1982.
- [34] P. Hegardt, T. Lindberg, J. Börjesson, and G. Skude, "Amylase in human milk from mothers of preterm and term infants," *Journal of Pediatric Gastroenterology and Nutrition*, vol. 3, no. 4, pp. 563–566, 1984.
- [35] O. Dewit, B. Dibba, and A. Prentice, "Breast-milk amylase activity in English and Gambian mothers: effects of prolonged lactation, maternal parity, and individual variations," *Pediatric Research*, vol. 28, no. 5, pp. 502–506, 1990.
- [36] S. G. Pierzynowski, B. R. Weström, J. Svendsen, L. Svendsen, and B. W. Karlsson, "Development and regulation of porcine pancreatic function," *International Journal of Pancreatology*, vol. 18, no. 2, pp. 81–94, 1995.
- [37] L. A. Heitlinger, P. C. Lee, W. P. Dillon, and E. Lebenthal, "Mammary amylase: a possible alternate pathway of carbohydrate digestion in infancy," *Pediatric Research*, vol. 17, no. 1, pp. 15–18, 1983.
- [38] H. Worning, S. Müllertz, E. H. Thaysen, and H. O. Bang, "pH and concentration of pancreatic enzymes in aspirates from the human duodenum during digestion of a standard meal. In patients with duodenal ulcer and in patients subjected to different gastric resections," *Scandinavian Journal of Gastroenterology*, vol. 2, no. 1, pp. 23–28, 1967.
- [39] E. Lebenthal and P. C. Lee, "Development of functional responses in human exocrine pancreas," *Pediatrics*, vol. 66, no. 4, pp. 556–560, 1980.
- [40] M. R. Struyvenberg, C. R. Martin, and S. D. Freedman, "Practical guide to exocrine pancreatic insufficiency - breaking the myths," *BMC Medicine*, vol. 15, no. 1, p. 29, 2017.
- [41] Y. Peng, S. N. Xing, H. Y. Tang et al., "Influence of glucose transporter 1 activity inhibition on neuroblastoma in vitro," *Gene*, vol. 689, pp. 11–17, 2019.
- [42] E. S. Reckzeh and H. Waldmann, "Small-molecule inhibition of glucose transporters GLUT-1–4," *Chembiochem*, vol. 21, no. 1–2, pp. 45–52, 2020.
- [43] L. Zhao, X. Zhao, K. Zhao et al., "The α -tocopherol derivative ESeroS-GS induces cell death and inhibits cell motility of breast cancer cells through the regulation of energy metabolism," *European Journal of Pharmacology*, vol. 745, pp. 98–107, 2014.
- [44] K. Date, T. Yamazaki, Y. Toyoda, K. Hoshi, and H. Ogawa, " α -Amylase expressed in human small intestinal epithelial cells is essential for cell proliferation and differentiation," *Journal of Cellular Biochemistry*, vol. 121, no. 2, pp. 1238–1249, 2020.
- [45] E. Azzopardi, C. Lloyd, S. R. Teixeira, R. S. Conlan, and I. S. Whitaker, "Clinical applications of amylase: novel perspectives," *Surgery*, vol. 160, no. 1, pp. 26–37, 2016.

Review Article

Nutraceuticals: Pharmacologically Active Potent Dietary Supplements

Subhash Chandra ¹, **Sarla Saklani**,¹ **Pramod Kumar**,² **Bonglee Kim** ³,
and **Henrique D. M. Coutinho** ⁴

¹Department of Pharmaceutical Chemistry, School of Sciences, Hemvati Nandan Bahuguna Garhwal (A Central) University, 246174, Srinagar Garhwal, Uttarakhand, India

²Department of Pharmaceutical Sciences, HNB Garhwal University, Srinagar Garhwal, India

³College of Korean Medicine, Kyung Hee University, Seoul 02447, Republic of Korea

⁴Department of Biological Chemistry, Regional University of Cariri (URCA), Crato, Brazil

Correspondence should be addressed to Subhash Chandra; subhashkothiyal@gmail.com, Bonglee Kim; bongleekim@khu.ac.kr, and Henrique D. M. Coutinho; hdmcoutinho@gmail.com

Received 25 February 2022; Revised 24 May 2022; Accepted 7 June 2022; Published 4 July 2022

Academic Editor: Madiha Ahmed

Copyright © 2022 Subhash Chandra et al. This is an open access article distributed under the Creative Commons Attribution License, which permits unrestricted use, distribution, and reproduction in any medium, provided the original work is properly cited.

A growing demand exists for nutraceuticals, which seem to reside in the grey area between pharmaceuticals and food. Nutraceuticals, up today, do not have a specific definition distinct from those of other food-derived categories, e.g., food supplements, herbal products, functional foods, and fortified foods. They have, however, a pharmacological beneficial effect on health. Many studies have been recently addressed to assess their safety, efficacy, and regulation. The object of writing this review article is that we need to pay more attention to natural and organic foods. The bases of nutraceutical components (food supplements) are known for potent and powerful clinical evidence effects on the treatment of hypertension and type 2 diabetes.

1. Introduction

Nutraceutical use is growing fast and is well accepted by people for its all-natural origin. Nutraceuticals cannot replace pharmaceuticals but can be used in the prevention and cure of some pathological conditions. According to Stephen DeFelice (1989), a nutraceutical is a food or part of food capable of providing beneficial health effects, including the prevention and the treatment of disease, which is not applicable to food supplements [1]. Nutraceuticals are obtained from foods of plant or animal origin, and worldwide research focused on their mechanism of action, safety, and clinical data. These are therapeutic agents that do not propose themselves as an alternative to drugs but instead can be helpful to prevent a cluster of conditions that could occur together (metabolic syndrome), e.g., type 2 diabetes, stroke, heart disease, and cardiovascular disease. Nutraceuticals are a challenge for the future of prevention and therapy and a

triggering tool in the medicine area. The possibility of preventing or supporting a pharmacological treatment, which is nowadays mainly based on pharmaceuticals, can be a powerful tool to face pathological, chronic, and long-term diseases in subjects who do not qualify for pharmacological therapy [2].

The excessive demand for natural healthcare has dramatically improved the price of hospital treatment, so humans have used herbal nutritional food, dietary supplements, and nutraceuticals for the usage of phytotherapy or nutritional therapy to replace or get rid of radiotherapy or chemotherapy [3]. This superior and practical know-how had been assisted to standardize production methods and clinical practices for nutraceutical markets. The Indians, Chinese, Japanese, Egyptians, and Sumerians have provided clinical evidence, suggesting that nutraceutical or food supplements can be efficaciously used as remedies to treat/prevent exclusive forms of ailment [4]. Nutraceutical food

affords better fitness with greater benefits, which claims to prevent subacute and continual ailment and improve fitness with put off the getting older technique and boom lifestyle expectancy [5].

The term nutraceutical is largely used to indicate the usage and effectiveness of a variety of herbal products [6]. The “nutritional elements” products are herbs, vitamins, proteins, minerals, fat, fiber, and amino acids (Tables 1 and 2). The dietary meal nutrient ingredients can be collections, isolates, or concentrates and may be found in lots of stages along with tablets, capsules, suspension and emulsion drugs, soft gel, gel cap, suspension, emulsion, drinks, or powders [7]. The nutritional meal complement, including the vitamin B complement, is normally sold in pill shape. The nutraceuticals are broadly utilized in human fitness, e.g., cancer treatment, Vita. E, Vita. D, soy, green tea, selenium, and lycopene (Table 2), which describe nutraceuticals as meals or nourishment supplements that produce medical or fitness advantages, inclusive of the prevention/treatment of any type of sickness [8].

This special issue is dedicated to the role and perspectives of nutraceuticals in human health, examined from different angles, ranging from analytical aspects to clinical trials and from efficacy studies to beneficial effects on health conditions.

1.1. Sources and Methodology. The literature data was collected via Core Collection, Web of Science, Google Scholar, Scopus, Science Direct, PubMed, MDPI, Clarivate Analytical, Google Academic, and Scientific Electronic Library Online (SciELO) from 1990-21. The search terms were nutraceuticals, food supplements, medicinal food, and functional food. These articles were considered on the basis of their nutraceutical and therapeutical uses with scientific proof.

2. Nutraceutical Hypothesis

These are based on the meal assets, MOA, useful food, chemical nature [9, 10], fatty acids, dietary fiber, proteins, vitamins, minerals, carbohydrates, spices, probiotics, prebiotics, polyunsaturated fatty acids, polyphenols, amino acids, antioxidants, antimicrobial, antidiabetic, analgesics, anti-inflammatory, carotenoids, dairy-primarily based elements, nutritional lipids, oils, phytochemicals, plant extracts, peptides, soy-primarily based substances, and premixes.

Essentially, the nutraceuticals are mainly categorized into two elements [11].

- (1) Potential nutraceuticals
- (2) Established nutraceuticals [12]

2.1. Functional Ingredients. Functional foods are typically classified as traditional foods that have been enriched with an ingredient (bioactive in many cases) that is able to provide additional benefits to human health. Functional foods are those ingredients that are used after clinical intelligence and knowledge. They have used especially healthy life and more resistant survival [13]. Functional foods are fed on to eat evidently as opposed to any dosage form as alike tablet,

tablet, and liquid dosage form. On occasion, extra complementary nutrients are covered, which include vitamin D in milk. The Canadian health organization describes or outlines approximately functional foods, the ones are “regular meals that have components or elements introduced to offer it a selected scientific or physiological advantage, apart from a merely dietary effect.” According to Japan, all practical ingredients must be present and occurring of their herbal shape [14] in place of a tablet, capsule, and powder [15] consumed in the food plan as every so often or every day [16] and ought to modify a biological system in wish of preventing/controlling disease or disorder-like situations [17].

2.2. Medicinal Foods. The medicinal or clinical foods are not present as a chip consequence to clients. The “Food & Drug Administration” contemplates medical nourishment to be “formulated, to be fed on or administered internally under the supervision of a physician and which is meant for the particular nutritional control of a disease or circumstance for which one-of-a-kind dietary necessities, on the idea of recognized scientific ideas, are established by way of medical evaluation.” The clinical food ingredients are designed to satisfy nutritional requirements for humans identified or observed out with unique contamination and ingested through oral or tube feeding. These ingredients are regulated by using FDA and authorized by scientific direction.

3. Phytochemicals as Nutraceutical Ingredients

Plants comprise primary and secondary metabolites, which showed and play various styles of functions. The primary metabolites, which play a vital position in mobile strategies, may be simple sugar, carbohydrates, nucleic acids, lipids, and amino acids. Secondary metabolites are used in pressure and deterrent. Plants grow and expand the special varieties of secondary metabolites, which can be used in beneficial positions for people and residing organisms. Its miles are referred to as plant herbal products (Figures 1 and 2).

3.1. Carotenoids. The carotenoids are observed in exceptional colorings and nature, e.g., carrots orange, corn yellow, tomato red, salmon, flamingos, goldfish, and autumn leaves, while “chlorophyll” has gone via the leaves, simplest carotenoids and phenols continue to be. The bell peppers of various colorations offer a ramification of various carotenoids:

Orange carotenoids: alpha, beta, and gamma carotene.
Red carotenoids: lycopene and astaxanthin.
Yellow carotenoids: lutein and zeaxanthin.

Plants produce more than six hundred carotenoids, and the handiest 50 carotenoids in the human weight-reduction plan are absorbed into the bloodstream. The α , β , and some other carotenoids (“not lycopene or lutein”) may be transformed to vitamin A. Hypervitaminosis of vitamin A cannot be because of immoderate α - and β -carotene intakes since the switch and absorption rates are too gradual. Each of the carotenes (α -carotene and β -carotene) is protecting against liver and lung cancers in the cell way of life and animal research. The most lipid-rich (LDL) cholesterol particles

TABLE 1: Nutraceutical foods and their therapeutic uses.

Nutraceutical/nutrients	Therapeutic uses	References
Ketogenic/Atkins diets (high protein and fat diet with low carbohydrates)	Benefits against diabetes, cancer, epilepsy, and Alzheimer's disease	[55, 56]
Minimally refined grains, cereals, and fortified grains	Reduce diabetes, prevent gastrointestinal cancers	[57]
Phytoestrogens (soya flour and linseeds)	Enhance estrogen levels, prevent hot flushes & cancers	[57]
Edible mushrooms (Tonnage, Lentinus, Pleurites, Auricularia, Flammulina, Tremella, Hericium, & Grifola)	Immunomodulatory, lipid-lowering, and antitumor activity	[58]
Glucosamine sulfate and chondroitin sulfate	Osteoarthritis	[59]
Peptides/hydrolysates (casein, buckwheat proteins, & whey proteins)	ACE inhibitor, reduce cholesterol and hypertension, improve constipation & obesity	[60]
Dairy foods/bio yoghurts (probiotics, Lactobacillus acidophilus, & Bifidobacterium)	Promote gut health,	[61]
Fatty acids (LCPUFAs)	Important for foetal & infant development	[62]

TABLE 2: Essential micro- or macronutrients/vitamins and their therapeutic uses.

Vitamins	Therapeutic uses
Vitamin A	Maintain healthy skin, mucus membrane and vision, body growth and development, anticancer, skin disorder, and antioxidant
Vitamin D	Formation of teeth and bones (which helps the body to absorb and use calcium)
Vitamin E	Boost the immune system, antioxidant (formation of nerve tissue, blood cells, muscles, and lungs)
Vitamin K	Clotting of blood
H ₂ O (soluble vitamins & acids)	
Vitamin C	Maintain good skin, gums, bones, & teeth, wound healing & reduce cold & cough, antioxidant
Vitamin B1	Essential in neurological functions and convert food into energy
Vitamin B2	Energy production, maintain healthy skin, eyes, & nerve
Vitamin B3	Convert food into energy and maintain brain function
Vitamin B6	Produce proteins and convert protein into energy
Vitamin B12	Produce the DNA of cells, form red blood cells, maintain CNS and amino acid synthesis, metabolism of fats, proteins, and carbohydrates
Folic acid	Essential for preventing birth defects, formation of RBC ("red blood cell"), produce DNA of cells, heart disease protector
Pantothenic acid	Cholesterol, fatty acids & steroid synthesis, acetylcholine intraneuronal synthesis
Vitamin-like compounds	
Biotin	Used in different biotransformation processes
L-Carnitine	Formation of certain organic acid excretion and phosphorylation, fatty acid oxidation
Choline	Lipotropic agent; these are used for treatment of fatty liver and interrupted fat metabolism
Vitamin F	Synthesis of prostaglandins, leukotrienes & different hydroxyl fatty acids, membrane development
Inositol lipotropic agents	Formation & movement of potassium & sodium, transportation of amino acid
Taurine	Conjugation of bile acid, CNS neuromodulation, retinal photoreceptor activity, antioxidant activity in WBC, platelet aggregation, cardiac contractility, sperm growth & motility, insulin growth & development activity

are transported by means of carotenoids into blood movement and get hold of the maximum LDL receptors.

3.2. *Lycopene*. Lycopene is found in watermelon, tomatoes, pink grapefruit, papaya, and guava and additionally offers red color. It is a potent antioxidant compound that reduces damage to DNA and proteins and additionally offers better pores and skin safety in opposition to extremely violet light than β -carotene. It is utilized in most cancer protection

and decreases LDL levels of cholesterol and suppresses insulin-like increase elements, which stimulates tumor boom.

3.3. β -Carotene. β -Carotene is a much less lively antioxidant, however robust in opposition to singlet oxygen, their components can fairly enrich β -carotene content and LDL cholesterol without affecting different carotenes, they are able to increase the pastime of herbal killer "T-cells, β -cells, and

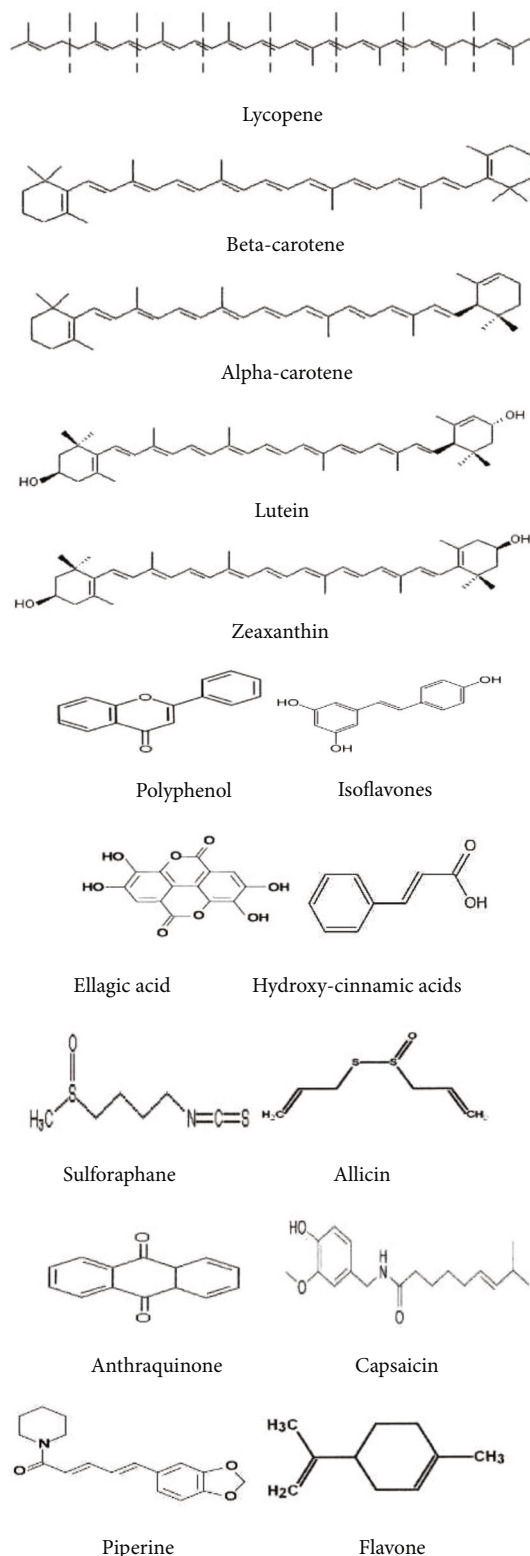


FIGURE 1: Some of the important bioactive phytonutrients.

NK cells,” and energizing “DNA” mend enzymes and grant higher cornea safety in opposition to extremely violet light than lycopene.

3.4. *α-Carotene*. *α-Carotene* is 10 instances stronger and a more effective anticarcinogenic compound in assessment than *β-carotene*, because of the let out of immunogenic cytokines (IL-1 and TNF- α).

3.5. *Lutein*. Lutein produces yellow color in nature through the exceptional types of resources, e.g., corn, avocado, and egg yolk. It protects and therapies the attention, from macular degeneration and cataracts, which shield against colon cancer. Its maximum concentration or quantity is located in kale, spinach, watercress, and parsley.

3.6. *Astaxanthin*. Astaxanthin gives different colors to salmon, shrimp, and crab. It is a potent antioxidant rather than any other carotenoid. It is also improved T-cell manufacturing and cytokine, which releases and crosses the “blood-brain barrier” (BBB) brain antioxidant and authorizes it to liberate trapped absolutely to vitamin C.

3.7. *Saponins*. Saponins are a legume’s own family medicinal plant, the ones that occur in chickpeas and soybeans and eliminate LDL cholesterol. They are effective in opposition to colon cancers and a few other crucial troubles.

3.8. *Terpineol*. Terpineol produces carrot flavor from carrots, and the origin cellular pattern is detained in most cancer stalls. They are water-insoluble chemical compounds, classified as hydrocarbon constituents by isoprene units and a high class of secondary metabolites [18, 19]. It is used in exhibiting antimicrobial and cytotoxic potential [20, 21].

3.9. *Limuloids*. Limuloids are present in orange membranes and peels, which are 45 times more potent anticarcinogenic than hesperidins. It detoxifies cancer agents and promotes most cancers’ cellular apoptosis, one-limonene smells “piney” like turpentine, d-limonene smells like orange, and it is able to be used as a solvent and cleanser.

3.10. *Anthocyanins*. Anthocyanins are water-soluble, anti-inflammatory glycosides and acryl-glycosides; they make roses red, cherries, strawberries, blueberries, and violet-blue. Blueberries increase anthocyanin contents when ripened and are easily damaged by heat (cooking).

3.11. *Flavonoids*. Flavonoids (flavone-like) are antioxidant and anti-inflammatory nature chemical compounds, which are present in dark chocolate and red wine and absent in white wine, due to their different extraction methods, where red wine is prepared or made by the fermentation method, although ultrafiltration is every now and then used to reduce astringency and bitterness. It is used for those patients, who are suffering from radiation and chemotherapy [22].

3.12. *Ruthin*. It is determined in asparagus, buckwheat, and citrus quit end result, which is not misplaced in drying grapes to raisins and strengthens arteriole partitions.

3.13. *Quercetin*. Quercetin (“flavanol”) which is the mighty antioxidant is present in green tea, red onions, buckwheat, and red grapes, which is distinctly available in the skins of apples and decreases LDL oxidation and is a vasodilator

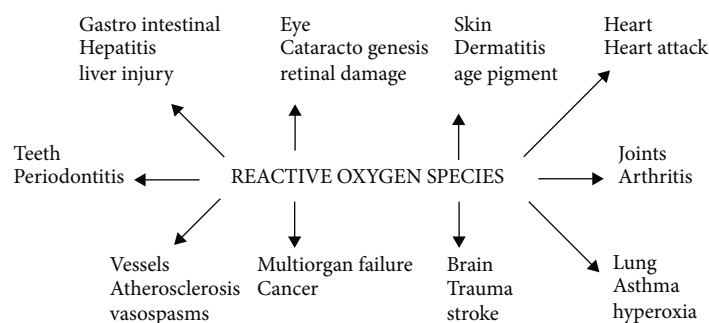


FIGURE 2: Clinical condition involving reactive oxygen species.

and blood thinner and might kill viruses. It is used to relieve allergy, inhibit catechol-O-methyl transferase (COMT) enzymes, reduce epinephrine, inhibit heart stroke protein and antihistaminic activity, and also promote apoptosis in cancer and other cells.

3.14. Tannins. Tannins (polyphenolics) are used to tan and defend leather-based seen in the 18th century A.D., which makes cranberries and pomegranates sour. It together with vitamin C helps to construct and improve collagen. It prevents UTI (“urinary tract infection”) with the useful resource of stopping microorganisms (bacteria) from adhering to the partitions. While blended with anthocyanins (“as in pomegranate juice”), it damage down oxidized LDL cholesterol within the bloodstream and in the atherosclerotic plate. It available in maximum energetic shape is black tea, which includes 90% catechin and epicatechin in natural grapes.

3.15. Phenolic Acids. The phenolic compounds (proanthocyanidins, resveratrol, and ellagic acid) are found in red wine, grape juice, and raisins, which are fantastically found in cranberry juice, reducing oxidation of LDL cholesterol and adherence of bacteria to enamel/teeth and cellular lining of the bladder, thereby lowering UTI (“urinary tract infections”) and tooth fairy. The sugar-coat nature compounds lessen the nonstick homes of phenolic. The phenolic acid formation of most cancers sells nitrosamines from dietary nitrate and nitrites.

3.16. Ellagic Acid. Ellagic acid is determined in strawberries and raspberries but is 50% greater in raspberries; it reduces esophageal and colorectal cancers, which retard the process of DNA adducts, retard stage 1, and potentiate phase-2 adjuvant.

3.17. Chlorogenic Acid. Chlorogenic acid is present in high excessive amounts in blueberries, tomatoes, and bell peppers, alongside the ester of caffeic acid (“hydroxyl cinnamic acid”), which diminish mutagenicity of polycyclic fragrant hydrocarbons and showed potent antioxidant activity.

3.18. Ferulic Acid. Ferulic acid is plentiful inside the cellular walls of seeds of whole wheat, brown rice, oats, apple, artichoke, orange pineapple, and peanut. Its miles are used as an antioxidant and anticancer, a precursor to vanillin and antitumor activity in breast and liver cancers.

4. Dietary Supplements

On the premise of the US (“DSHEA”) “Dietary Supplements Health & Education Act” 1994, the nutritional additives are those that include fatty acids, fiber, protein, vitamin, amino acid, and mineral, which are referred to as dietary ingredients or dietary supplements [6, 23].

LCPUFAs are crucial for foetal and infant growth and development because of their essential position in cellular growth and biotransformation or metabolism, membrane shape, and function [24]. The LCPUFAs (“flaxseed, flaxseed oil, walnuts, canola oil, and soybean oil”) result in brain growth and irrevocable damage due to both of them being wealthy in arachidonic acid and docosahexaenoic acid, primarily based on the clinical evidence and epidemiology that dietary ω -3 type polyunsaturated fatty acid decreases the risk of heart ailment [25]. The main five essential fatty acids for human consumption are saturated palmitic acid, stearic acid, monounsaturated oleic acid, polyunsaturated linoleic, and linolenic acids [26]. The newly synthesized secure, less expensive, and sustainable plant origin of these fatty acids is arachidonic acid, eicosatetraenoic acid, and docosahexaenoic acid [27]. Today’s and greater currently eicosatetraenoic acid and docosahexaenoic acid were fabricated in *Brassica juncea* with an excessive capitulate [28].

4.1. Amino Acids. The amino acids are playing a significant role in anti-inflammatory, immunomodulatory, and antioxidant properties [29]. These are used in protein biosynthesis and many others, e.g., L-arginine is used for infant or children growth, pregnant women, and synthesis of agmatine, urea, creatine, polyamines, and nitric oxide. It is also useful for antihypertensive and antiproliferative effects on vascular smooth muscles. Glutamine is essential for metabolic stress, burn injury, muscle wasting, weight loss, and other infections with depletion of plasma. It has been shown to gain patients and decreases the mortality rate [30] by elevating the level of amino acids in staple meals which include rice, wheat, corn, and different flora [16, 31].

5. Micronutrients

5.1. Vitamins. These are micronutrients/food supplements, which play a significant role in our daily life for better health

TABLE 3: Minerals and their therapeutic uses.

Minerals	Therapeutic uses
Macronutrients (major minerals)	
Calcium (Ca)	Development of teeth & bones, maintain bone strength, nerve, muscle, and glandular functions
Magnesium (Mg)	Nerve, muscle & bone formation, help to “prevent premenstrual syndrome (PMS)”
Phosphorous (P)	Build strong bones and teeth, formation of gene material, energy production & storage
Sodium (Na)	Nerve transmission, proper fluid balance, muscle contraction
Chloride (Cl)	Fluid balance & stomach acid
Potassium (K)	Nerve transmission & muscle contraction
Sulfur (S)	Found in protein molecules
Microelements (trace minerals)	
Chromium (Cr)	insulin helps to convert carbohydrates & fats into energy
Iron (Fe)	Energy production by carrying oxygen to tissues
Cobalt (Co)	Essential for vitamin B12, formation of B12 coenzymes
Copper (Cu)	Production of hemoglobin & collagen, healthy functioning of heart, energy production, absorption of iron from digestive tract
Iodine (I)	Thyroid functioning
Selenium (Se)	Antioxidant, essential for heart muscle functioning
Zinc (Zn)	Cell reproduction, child growth & development, wound healing, production of sperm & testosterone
Fluoride (F)	Formation of bones & teeth and prevent tooth decay

and are essential for metabolic pathway, as an enzyme cofactor forerunner [32].

5.2. Minerals. Minerals are those chemical compounds which are vital for the normal growth and development of all residing organisms (humans, animals, and plants). They protect our bodies from various types of diseases. A right and healthy amount of mineral intake/consumption is crucial to maintaining an exact diet nutritionally, which will reduce the major disease such as cardiovascular and degenerative disease, diabetes, digestive disorder, and cancer [33, 34] (Table 3).

6. Nutraceuticals as Clinical Study

6.1. Healthy Fats (MUFA ω -9 and PUFAs ω -3 and ω -6). Monounsaturated fatty acids and polyunsaturated fatty acids are linked or connected with a reduced chance of coronary heart disease [35].

6.2. Monounsaturated Fatty Acids (MUFA/ ω -9). On the basis of 7 nations’ statistics, the death rate from “CHD” became specifically low in Mediterranean nations, wherein the olive oil has been used, which is exceedingly enhanced with MUFA and fats. The protective impact of MUFA in competition with CHD became additionally supported via using a retrogression investigation of information from the “nurse health” look at of 80082 females observed for much less than 14 years and additionally found a fantastic affiliation amongst consumption of MUFA and CHD danger [36–38]. We have got presently stated in asymptomatic excessive cardiovascular chance topics that consumption of traditional Mediterranean weight-reduction plan augmented with virgin olive oil actively regulates the articulation of lead

chromosome concerned in vascular irritation, foam cell process, and thrombosis inside the course of an antiatherothrombotic profile [39].

6.3. Polyunsaturated Fatty Acids (PUFAs). ALA (“ α -linolenic acid”) and LA (“linoleic acid”) belong to the ω -three (“omega-3”) and ω -6 (“omega-6”) collection of PUFA separately. The resources of omega three and omega six are seafood and fatty fish, optimum vegetable oils, grains, and walnuts. PUFA omega-three fatty acids show potent primary and secondary prevention or cure of cardiovascular disorder [40]. Polyunsaturated fatty acids are traditionally useful for human health [41, 42] which is based on the two types of omega-3 and omega-6 series. The health benefit of the ω -three and ω -six ratio in macroalgae allows their use in the method of practical meals and convenience food. These fatty acids lessen the possibility of chest, colon, prostate, and renal cancers, and other effects are suppressing inflammation, asthma, and rheumatoid arthritis [43]. It is especially used in cardiovascular and inflammatory diseases and skin health [44].

6.4. Cholesterol Reduction. All agents reduce LDL cholesterol absorption in the intestinal gut and additionally reduce plasma LDL concentrations. A metaevaluation of forty-one trials showed that consumption of 2 gm/day of stanols or sterols decreased LDL concentration by using about ten-eleven% [45]. The “American Heart Association” and “European Current Dietary Guideline” aid plant sterols as a healing option for people with improved levels of cholesterol [46, 47]. In a pooled evaluation of ten prospective cohorts, each 10 gm/day increment of energy-adjusted general nutritional fiber becomes associated with a 14% lower hazard of

coronary activities and a 27% decrease in the hazard of coronary loss of life [48].

6.5. Coenzyme Q-10 (CoQ-10). CoQ-10 is an herbal food substance, and its miles are used for functional food and dietary supplements. It is an internal lipophilic substance, which is a crucial or useful substance of mitochondrial strength biotransformation and additionally effective for antioxidants and effective for human fitness [49–51]. CoQ-10 limited deterioration of viscoelasticity and reduce the wrinkle 7 microrelief lines and improved/increased skin smoothness/fairness.

7. Effectiveness and Safety

7.1. Regulatory Aspects. The regulation of nutraceuticals presents a noteworthy challenge to the globalization of nutraceuticals, with a murky and somewhat dissimilar definition of these products that are used in different countries. In general, the goals of nutraceutical regulation have been focused on safety and labeling with a lesser emphasis, as compared to pharmaceuticals, on product claims and intended use. The first step in food regulation in Europe was established in 1997 with the Green Paper after that the safety and use of food were set by the United Nations Food and Agricultural Organization (FAO) and the World Health Organization (WHO) in the *Codex Alimentarius* (FAO/WHO1992). In the USA, the FDA, which focuses on safety aspects and food supplements, acknowledges the term nutraceutical and applies a different set of regulations to them than those of conventional foods and drugs. As per the Dietary Supplement Health and Education Act established in 1994 (DSHEA), it is the manufacturer's responsibility to ensure that a nutraceutical is safe before it is marketed. The Food and Drug Administration Modernization Act of 1997 contains sections that enable health claims and nutrient content claims on food labeling to be authorized based on an authoritative statement from the Academy of Sciences or other federal authorities after notifying the FDA at least four months before the introduction of the supplement on the market [52].

The government of India established the Food Safety and Standards Act (FSSA) in 2006 to introduce a legislation system. FSSA does not separate functional foods, nutraceuticals, and dietary supplements; instead, each is indicated as food for a special dietary application. In 2015, India notified the World Trade Organization of a draft regulation for nutraceuticals and foods for special diets and medical purposes. In general, many countries, such as Australia or China, regulate nutraceuticals simply as a category of food, and the national regulations are valid for food application. Moreover, a health claim should be authorized and attributed only after a complete clinical study is proposed to the appropriate authority for approval with the aim of substantiating its safety and efficacy with respect to the claimed beneficial health effect based on an understanding of the mechanism of action and the absence of undesired side effects.

7.2. Impact of Placebo Effect. The impact of nutraceuticals is just like pharmaceuticals and a part of the effectiveness of nutraceuticals, which can be attributed to the placebo effect.

People have used nutraceuticals as a healing illness and are often able to recover on their own. The Nobel Prize winner (Linus Pauling and Abraham Hoffer) suggested that the provision of these nutrients might also in truth encourage the restoration mechanism; ill individuals may additionally require more nutrients to cause the mechanism [8].

8. Future Prospective

The increasing demand for nutraceuticals, such as food for fitness and health, is responsible for their positive and therapeutic uses for different kinds of diseases. The development and growth of new functional food or specially nutraceutical industry seem destined to occupy the landscape in the new millennium. The enzymes are used in various nutraceutical processes and play a crucial part in nutraceuticals. The next area of high consideration is the interaction between nutraceuticals and FDA. The therapeutic effectiveness of nutraceuticals remains to be determined as like drugs [11].

It is a big challenge for nutraceuticals, for the future prevention and therapy of triggering tools in the medicine area. The future possibility of nutraceuticals to prevent or support a pharmacological therapy is now recently based on pharmaceuticals, which can be a powerful tool to face pathological, chronic, and long-term diseases. The clinical study data evaluation is based on the beneficial effect of nutraceuticals, through "*in vitro* and *in vivo*" representation, which may be dispensed in an individual nutritive supplementation observed in animals [53, 54].

9. Conclusions

Nutraceuticals provide benefits in the prevention and treatment of various diseases. With increasing incidences of lifestyle-related health problems, they have emerged as an essential component of the diet for the common consumer. Nutraceuticals are now serving as a primary dietary supplement for health-conscious masses in India. Nutraceuticals (nutritional supplements) have fast become a staple in the healthcare market in numerous forms, including tablets, syrups, gums, and capsules. The combined and concerted action of nutrient and biologically active compounds is flagged as an indicator of a possible beneficial role for health. Nutraceutical use is growing fast and is well accepted by people for its all-natural origin. The demand for fewer synthetic pharmaceuticals is triggering this interest and stimulating also the industry to develop and put on the market new products which claim beneficial health effects. Nutraceuticals cannot replace pharmaceuticals but can be a strong high-value tool for prevention and aid in therapy of some pathological conditions. The present review provides comprehensive knowledge about all these aspects related to nutraceutical sources, formulations, scopes, challenges, quality control, stability, and safety evaluation in brief.

Abbreviations

ALA: α -Linolenic acid
BBB: Blood-brain barrier

CHD: Coronary heart disease
 COMT: Catechol-O-methyl transferase
 CoQ-10: Coenzyme Q-10
 DNA: Deoxyribonucleic acid
 DSHEA: Dietary Supplements Health and Education Act
 FAO: Food and Agricultural Organization
 FDA: Food and Drug Administration
 FSSA: Food Safety and Standards Act
 LA: Linoleic acid
 LDL: Low-density lipoprotein
 MDPI: Multidisciplinary digital publishing institute
 MOA: Mechanism of action
 MUFA: Monounsaturated fatty acids
 NK cell: Natural killer cell
 PubMed: Public/publisher Medline
 PUFA: Polyunsaturated fatty acids
 SciELO: Scientific electronic library online
 TNF: Tumor necrosis factor
 UTI: Urinary tract infection
 Vita: Vitamin
 WHO: World Health Organization.

Data Availability

The data used to support the findings of this study are available from the corresponding authors upon request.

Conflicts of Interest

The authors do not have any warfare of hobby or monetary or any other case.

Acknowledgments

This research was supported by the Basic Science Research Program through the National Research Foundation of Korea (NRF) funded by the Ministry of Education (NRF-2020R1I1A2066868), the National Research Foundation of Korea (NRF) grant funded by the Ministry of Science, ICT and Future Planning (No. 501100003621), a grant of the Korea Health Technology R&D Project through the Korea Health Industry Development Institute (KHIDI), funded by the Ministry of Health and Welfare, Republic of Korea (grant number: HF20C0116), and a grant of the Korea Health Technology R&D Project through the Korea Health Industry Development Institute (KHIDI), funded by the Ministry of Health and Welfare, Republic of Korea (grant number: HF20C0038).

References

- [1] P. Daliu, A. Santini, and E. Novellino, "From pharmaceuticals to nutraceuticals: bridging disease prevention and management," *Expert Review of Clinical Pharmacology*, vol. 12, pp. 1–7, 2019.
- [2] A. Durazzo, M. Lucarini, and A. Santini, "Nutraceuticals in human health," *Foods*, vol. 9, no. 3, article 370, 2020.
- [3] M. M. Berger, F. Spertin, and A. Shenkin, "Clinical Immune and metabolic effects of trace element supplements in burns, a double-blind placebo-controlled trial," *Clinical Nutrition*, vol. 15, no. 2, pp. 94–96, 1996.
- [4] C. S. Ramaa, A. R. Shirode, and A. S. Mundada, "Nutraceuticals- an emerging era in the treatment and prevention of cardiovascular diseases," *Current Pharmaceutical Biotechnology*, vol. 7, pp. 15–23, 2006.
- [5] D. Bagchi and H. G. Preuss, "Nutraceutical and functional food industries, aspects on safety and regulatory requirements," *Toxicology Letters*, vol. 1, no. 150, pp. 1-2, 2004.
- [6] S. H. Zeisel, "Regulation of nutraceuticals," *Science*, vol. 285, pp. 1853–1855, 1999.
- [7] M. Whitman, "Understanding the perceived need for complementary and alternative nutraceuticals, lifestyle issues," *Clinical Journal of Oncology Nursing*, vol. 5, no. 5, pp. 190–194, 2001.
- [8] V. Brower, "Nutraceuticals: poised for a healthy slice of the healthcare market," *Nature Biotechnology*, vol. 16, no. 8, pp. 728–731, 1998.
- [9] A. N. Kalia, *Textbook of Industrial Pharmacognosy*, CBS publisher and distributor, New Delhi, 2005.
- [10] C. K. Kokate, A. P. Purohit, and S. B. Gokhale, "Nutraceutical and Cosmeceutical," *Pharmacognosy*, 21st edition, Pune, India: Nirali Prakashan, 2002.
- [11] M. Pandey, R. K. Verma, and S. A. Saraf, "Nutraceuticals: new era of medicine and health," *Asian Journal of Pharmaceutical and Clinical Research*, vol. 3, pp. 11–15, 2010.
- [12] D. Lipi, B. Eshani, and R. Utpal, "Role of nutraceuticals in human health," *Journal of Food Science and Technology*, vol. 49, no. 2, pp. 173–183, 2012.
- [13] Food and Agriculture Organization of the United Nations (FAO), "Report on Functional Foods, Food Quality and Standards Service (AGNS)," 2007.
- [14] D. Bagchi, "Nutraceuticals and functional foods regulations in the United States and around the world," *Toxicology*, vol. 221, pp. 1–3, 2006.
- [15] D. S. L. Felice, "Rationale and proposed guidelines for the nutraceutical research and education act, NREA," 2002.
- [16] A. Rajasekaran, G. Sivagnanam, and R. Xavier, "Nutraceuticals as therapeutic agents, a review research," *Research Journal of Pharmacy and Technology*, vol. 1, no. 4, pp. 328–340, 2008.
- [17] C. H. Halsted, "Dietary supplements, and functional foods: 2 sides of a coin," *The American Journal of Clinical Nutrition*, vol. 77, no. 4, pp. 1001S–1007S, 2003.
- [18] S. Perveen, *Introductory chapter: terpenes and terpenoids. In Terpenes and Terpenoids*, Perveen, S., Ed.; Intech Open, London, UK, 2018.
- [19] M. Qverland, L. T. Mydland, and A. Skrede, "Marine macroalgae as sources of protein and bioactive compounds in feed for monogastric animals," *Journal of the Science of Food and Agriculture*, vol. 99, pp. 13–24, 2019.
- [20] M. Suzuki, Y. Takahashi, Y. Mitome, T. Itoh, T. Abe, and M. Masuda, "Brominated metabolites from an Okinawan Laurencia intricate," *Phytochemistry*, vol. 60, no. 8, pp. 861–867, 2002.
- [21] D. Iliopoulou, V. Roussis, C. Pannecouque, E. De Clercq, and C. Vagias, "Halogenated sesquiterpenes from the red alga Laurencia obtuse," *Tetrahedron*, vol. 58, pp. 6749–6755, 2002.
- [22] S. Saklani and S. Chandra, "Evaluation of antioxidant activity, quantitative estimation of phenols, anthocynins and flavonoids of wild edible fruits of Garhwal Himalaya," *Journal of Pharmacy Research*, vol. 4, no. 11, pp. 4083–4086, 2011.

- [23] E. K. Kalra, "Nutraceutical-definition and introduction," *Aaps Pharmsci*, vol. 5, pp. 27-28, 2003.
- [24] T. L. Psota, S. K. Gebauer, and E. P. Kris, "Dietary omega-3 fatty acid intake and cardiovascular risk," *The American Journal of Cardiology*, vol. 98, no. 4, pp. 3-18, 2006.
- [25] S. P. Singh, X. R. Zhou, Q. Liu, and S. Stymne, "Metabolic engineering of new fatty acids in plants," *Current Opinion in Plant Biology*, vol. 8, no. 2, pp. 197-203, 2005.
- [26] A. Abbadi and F. Domergue, "Biosynthesis of very long-chain polyunsaturated fatty acids in transgenic oilseeds: constraints on their accumulation," *Plant Cell*, vol. 16, pp. 2734-2748, 2004.
- [27] G. Wu, M. Truksa, and N. Datla, "Stepwise engineering to produce high yields of very long-chain polyunsaturated fatty acids in plants," *Nature Biotechnology*, vol. 23, pp. 1013-1017, 2005.
- [28] E. M. Windle, "Glutamine supplementation in critical illness, evidence, recommendations, and implications for clinical practice in burn care," *Journal Of Burn Care & Research*, vol. 27, no. 6, pp. 764-772, 2006.
- [29] K. P. Lawrence, P. F. Long, and A. R. Young, "Mycosporine-like amino acids for skin photoprotection," *Current Medicinal Chemistry*, vol. 25, no. 40, pp. 5512-5527, 2018.
- [30] G. Galili, H. Karchi, and O. Shaul, "Production of transgenic plants containing elevated levels of lysine and threonine," *Biochemical Society Transactions*, vol. 22, no. 4, pp. 921-925, 1994.
- [31] D. Dureja, D. Kaushik, and V. Kumar, "Developments in nutraceuticals," *Indian Journal of Pharmacology*, vol. 35, pp. 363-372, 2003.
- [32] C. Joao, L. Adriana, and P. Diana, "A comprehensive review of the nutraceutical and therapeutic applications of red seaweeds (Rhodophyta)," *Life*, vol. 10, no. 3, article 19, 2020.
- [33] M. Fenech and L. R. Ferguson, "Vitamins/minerals, and genomic stability in humans," *Mutation Research/Fundamental and Molecular Mechanisms of Mutagenesis*, vol. 475, no. 1-2, pp. 1-6, 2001.
- [34] M. Kersting, U. Alexy, and W. Sichert-Hellert, "Dietary intake and food sources of minerals in 1 to 18 year old German children and adolescents," *Nutrition Research*, vol. 21, no. 4, pp. 607-616, 2001.
- [35] A. T. Erkkilae, U. S. Schwab, V. D. de Mello et al., "Effects of fatty and lean fish intake on blood pressure in subjects with coronary heart disease using multiple medications," *European Journal of Nutrition*, vol. 47, no. 6, pp. 319-328, 2008.
- [36] F. B. Hu, M. J. Stampfer, and J. E. Manson, "Dietary fat intake and the risk of coronary heart disease in women," *New England Journal of Medicine*, vol. 337, no. 21, pp. 1491-1499, 1997.
- [37] K. L. Esrey, L. Joseph, and S. A. Grover, "Relationship between dietary intake and coronary heart disease mortality: lipid research clinics prevalence follow-up study," *Journal of Clinical Epidemiology*, vol. 49, pp. 211-216, 1996.
- [38] B. M. Posner, J. L. Cobb, A. J. Belanger, L. A. Cupples, and J. Stokes 3rd., "Dietary lipid predictors of coronary heart disease in men. The Framingham study," *Archives of Internal Medicine*, vol. 151, no. 6, pp. 1181-1187, 1991.
- [39] V. Llorente-Cortes, R. Estruch, and M. P. Mena, "Effect of Mediterranean diet on the expression of pro-atherogenic genes in a population at high cardiovascular risk," *Atherosclerosis*, vol. 208, pp. 442-450, 2010.
- [40] S. P. Whelton, J. He, P. K. Whelton, and P. Muntner, "Meta-analysis of observational studies on fish intake and coronary heart disease," *The American Journal of Cardiology*, vol. 93, no. 9, pp. 1119-1123, 2004.
- [41] A. P. Simopoulos, "Omega-3 fatty acids in health and disease and in growth and development," *The American Journal of Clinical Nutrition*, vol. 54, no. 3, pp. 438-463, 1991.
- [42] C. H. S. Ruxton, S. C. Reed, M. J. A. Simpson, and K. J. Millington, "The health benefits of omega-3 polyunsaturated fatty acids: a review of the evidence," *Journal of Human Nutrition and Dietetics*, vol. 17, no. 5, pp. 449-459, 2004.
- [43] A. Wiktorowska-Owczarek, M. Berezińska, and J. Z. Nowak, "Pufas: structures, metabolism and functions," *Advances in Clinical and Experimental Medicine*, vol. 24, pp. 931-941, 2015.
- [44] G. L. Capella, "Strategies for leukotriene modulation in dermatology: even more visionary perspectives? Anupdate," *Anti-Inflammatory & Anti-Allergy Agents in Medicinal Chemistry*, vol. 10, pp. 407-417, 2012.
- [45] M. B. Katan, S. M. Grundy, P. Jones, M. Law, and R. Paoletti, "Efficacy and safety of plant stanols and sterols in the management of blood cholesterol levels," *Mayo Clinic Proceedings*, vol. 78, pp. 965-978, 2003.
- [46] A. H. Lichtenstein, L. J. Appel, and M. Brands, "Summary of American Heart Association diet and lifestyle recommendations revision 2006," *Arteriosclerosis, Thrombosis, and Vascular Biology*, vol. 26, no. 10, pp. 2186-2191, 2006.
- [47] European Commission, "General view of the scientific committee on food on the long-term effects of the intake of elevated levels of phytosterols from multiple dietary sources, with particular attention to the effects of beta-carotene," 2002.
- [48] B. Lina, V. Gemma, and P. Teresa, "Nutraceuticals and atherosclerosis: human trials," *Cardiovascular Therapeutics*, vol. 28, 215 pages, 2010.
- [49] F. L. Crane, "Biochemical functions of coenzyme Q10," *Journal of the American College of Nutrition*, vol. 20, no. 6, pp. 591-598, 2001.
- [50] G. P. Littarru and L. Tiano, "Clinical aspects of coenzyme Q10: an update," *Nutrition*, vol. 26, no. 3, pp. 250-254, 2010.
- [51] K. Zmitek, T. Pogacnik, L. Mervic, J. Zmitek, and I. Pravst, "The effect of dietary intake of coenzyme Q10 on skin parameters and condition: results of a randomized, placebo-controlled, double-blind study," *Biofactors*, vol. 43, pp. 132-140, 2017.
- [52] A. Santini, S. M. Cammarata, and G. Capone, "Nutraceuticals: opening the debate for a regulatory framework," *British Journal of Clinical Pharmacology*, vol. 84, no. 4, pp. 659-672, 2018.
- [53] B. Omri, M. Amraoui, A. Tarek et al., "Arthrosporin Platensis (spirulina) supplementation on laying hens' performance: eggs physical, chemical, and sensorial qualities," *Foods*, vol. 8, article 386, 2019.
- [54] B. Omri, B. Larbi Manel, Z. Jihed, R. Romano, A. Santini, and H. Abdouli, "Effect of a combination of fenugreek seeds, linseeds, garlic and copper sulfate on laying hens performances, egg physical and chemical qualities," *Foods*, vol. 8, article 311, 2019.
- [55] S. G. Sukkar and M. Muscaritoli, "A clinical perspective of low carbohydrate ketogenic diets: a narrative review," *Frontiers in Nutrition*, vol. 8, article 642628, 2021.
- [56] L. Crosby, B. Davis, and S. Joshi, "Ketogenic diets and chronic disease: weighing the benefits against the risks," *Frontiers in Nutrition*, vol. 8, article 702802, 2021.

- [57] J. L. Slavin, "Whole grains, refined grains and fortified refined grains: what's the difference," *Asia Pacific Journal of Clinical Nutrition*, vol. 9, pp. S23–S27, 2000.
- [58] G. Hetland, J. M. Tangen, and F. Mahmood, "Antitumor, anti-inflammatory and antiallergic effects of *Agaricus blazei* mushroom extract and the related medicinal Basidiomycetes mushrooms, *Hericium erinaceus* and *Grifola frondosa*: a review of preclinical and clinical studies," *Nutrients*, vol. 12, no. 1339, pp. 2–19, 2020.
- [59] D. O. Clegg, D. J. Reda, C. L. Harris et al., "Glucosamine, chondroitin sulfate, and the two in combination for painful knee osteoarthritis," *New England Journal of Medicine*, vol. 354, no. 8, pp. 795–808, 2006.
- [60] S. Minj and S. Anand, "Whey proteins and its derivatives: bio-activity, functionality, and current applications," *Dairy*, vol. 1, pp. 233–258, 2020.
- [61] R. Nyanzi, P. J. Jooste, and E. M. Buys, "Invited review: Probiotic yogurt quality criteria, regulatory framework, clinical evidence, and analytical aspects," *Journal of Dairy Science*, vol. 104, no. 1, pp. 1–19, 2021.
- [62] "Clinical studies on the benefits of long-chain polyunsaturated fatty acids (LCPUFAs) for term infants," *Journal of Modern Pharmacy*, vol. 8, no. 3, article 33, 2001.

Research Article

The Leaf Extract of *Mitrephora chulabhorniana* Suppresses Migration and Invasion and Induces Human Cervical Cancer Cell Apoptosis through Caspase-Dependent Pathway

Wutigri Nimlamool ¹, Sunee Chansakaow ², Saranyapin Potikanond ¹, Nitwara Wikan ¹, Phateep Hankittichai ¹, Jirapak Ruttanapattanakul ¹, and Phatarawat Thaklaewphan ¹

¹Department of Pharmacology, Faculty of Medicine, Chiang Mai University, Chiang Mai 50200, Thailand

²Department of Pharmaceutical Sciences, Faculty of Pharmacy, Chiang Mai University, Chiang Mai 50200, Thailand

Correspondence should be addressed to Wutigri Nimlamool; wutigri.nimlamool@cmu.ac.th

Received 22 January 2022; Revised 11 April 2022; Accepted 20 April 2022; Published 12 May 2022

Academic Editor: Madiha Ahmed

Copyright © 2022 Wutigri Nimlamool et al. This is an open access article distributed under the Creative Commons Attribution License, which permits unrestricted use, distribution, and reproduction in any medium, provided the original work is properly cited.

Cervical cancer is rated to be the leading cause of cancer-related death in women worldwide. Since screening test and conventional treatments are less accessible for people in developing countries, an alternative use of medicinal plants exhibiting strong anticancer activities may be an affordable means to treat cervical cancer. *Mitrephora chulabhorniana* (MC) is the newly identified species; however, its biological functions including anticancer activities have been largely unexplored. Hence, in this study, we were interested in investigating anticancer effects of this plant on the human cervical cell line (HeLa). MC extract was profiled for phytochemicals by TLC. This plant was tested to contain alkaloids, flavonoids, and terpenes. HeLa cells were treated with MC extract to investigate the anticancer activities. Cytotoxicity and viability of cells treated with MC were determined by MTT assay and Trypan blue exclusion assay. Cell migration was tested by wound healing assay, and cell invasion was determined by Transwell assay. The level of caspase 7, caspase 9, and PARP was determined by western blot analysis. We found that the leaf extract of MC strongly reduced cancer cell survival rate. This finding was consistent with the discovery that the extract dramatically induced apoptosis of cervical cancer cells through the activation of caspase 7 and caspase 9 which consequently degraded PARP protein. Furthermore, MC extract at lower concentrations which were not cytotoxic to the cancer cells showed potent inhibitory activities against HeLa cervical cancer cell migration and invasion. *Mitrephora chulabhorniana* possesses its pharmacological properties in inhibiting cervical cancer cell migration/invasion and inducing apoptotic signaling. This accumulated information suggests that *Mitrephora chulabhorniana* may be a beneficial source of potential agents for cervical cancer treatment.

1. Background

In 2020, among six hundred thousand of new cases and three hundred thousand deaths caused by cancer, cervical cancer was ranked the fourth as a most commonly diagnosed cancer and a leading cause of mortality in women [1]. Despite the fact that cervical cancer incidences and deaths are declining in developed countries, it remains a leading

cause of cancer-related deaths in women in developing regions [2, 3]. Moreover, IARC HPV Information Center has reported that cervical cancer's morbidity and mortality are definitely on the rise. Consistent with the world trend, cervical cancer has become the second leading cancer for women in Thailand [4].

The currently used cytotoxic therapy which exerts mainly on cisplatin-based combination chemotherapeutic

drugs has greatly produced beneficial response [5, 6]. However, the effective medicine options for cancer are exceptionally limited since the treatment is usually less effortable for the population, especially for developing countries. Therefore, the investigation is aimed at discovering novel active anticancer compounds from natural sources that can effectively cure the disease with reasonable cost is needed. Recently, nature-derived agents have emerged as alternative means for treating certain diseases or conditions. In particular, there are numerous antitumor agents derived from natural products [7]. A variety of plants in Thailand is valuable sources of biologically active compounds [8–13]. Many of them have been encouraged as potential chemotherapeutic candidates. For instance, we previously disclosed that some plants predominant in Thailand exhibited their strong activities against cervical cancer and ovarian cancer cell lines with the defined possible molecular mechanisms of action [11, 14, 15]. As a pace towards the discovery of possible anticancer compounds, we focused on studying a new species of plant (*Mitrephora chulabhorniana*) in the largest family of the magnolia which contains certain plant members that exhibit anticancer properties.

Mitrephora chulabhorniana (Annonaceae), known as Phrom Chulabhorn in Thai, is a remarkable new species discovered in a karst area in southern Thailand [16]. Different secondary metabolites including alkaloids, diterpenoids, dihydrobenzofuran lignans, and polyphenolic compounds have been reported to be concentrated in *Mitrephora* plants [17–24]. Phytochemicals derived from this genus exhibited a wide range of biological properties including antimicrobial [24], antifungal [25], antitumor [26], and cytotoxicity against human cancer cell lines [19, 20, 22, 27]. However, pharmacological activity of the new species, *M. chulabhorniana*, has not yet been explored, especially for its anticancer properties. Therefore, we aimed to evaluate whether *M. chulabhorniana* extract exhibits moderate to potent cytotoxicity against human cervical cancer, HeLa cells. To the top of our knowledge, data from our study were the first evidence to demonstrate that the extract from *M. chulabhorniana* possesses cytotoxic activities in inducing programmed cell death via activating the caspase-dependent cell death signaling pathway. Our discovery provided biological understanding of mechanism of action and may lead to the identification of possible active compounds as candidate agents for cervical cancer treatment.

2. Materials and Methods

2.1. Reagents and Chemicals. Dulbecco's modified Eagle's medium (DMEM), fetal bovine serum (FBS), Trypan blue solution, and antibiotics were purchased from Gibco™ (USA). Phosphate-buffered saline (PBS), DMSO, 3-(4,5-dimethylthiazol-2-yl)-2,5-diphenyltetrazolium bromide (MTT), 4', 6-diamidino-2'-phenylindole dihydrochloride (DAPI), and Matrigel® Matrix were procured from Corning (USA). Primary antibodies against caspase 7, cleaved caspase 7, caspase 9, cleaved caspase 9, PARP, cleaved PARP, and actin were supplied by Cell Signaling Technology (USA). Secondary antibodies including an anti-mouse IgG conju-

gated with IRDye®800CW and an anti-rabbit IgG conjugated with IRDye®680RT were obtained from LI-COR Biosciences (USA). Annexin V/PI kit was purchased from ImmunoTools (Germany).

2.2. Preparation of Alcoholic *Mitrephora chulabhorniana* (MC) Extract

2.2.1. Plant Material. *Mitrephora chulabhorniana* was collected from Surat Thani province, Thailand. The plant material was identified by the taxonomist. The voucher specimen was deposited in the Faculty of Science, Chiang Mai University (number 162). The leaves of MC were collected and dried in the hot air oven until the moisture was less than 10%. Then, the dried leaves were pulverized. The coarse powder of the samples was separately extracted by maceration. Specifically, 200 g of dried powder of MC leaves was extracted using 2 liters of methanol as a solvent. Maceration was performed three times, and the extract mixture was filtered through Whatman No. 1 filter paper (Sigma-Aldrich, St. Louis, MO). The filtrate was concentrated using a rotary evaporator (Eyela N-1000, Japan) to obtain a brownish syrupy mass.

2.3. Phytochemical Screening and Chemical Profile by Thin-Layer Chromatography. Investigation of the chemical components of the MC extract was performed by thin-layer chromatography (TLC). Chloroform:ethyl acetate:methanol (5:3:2) was used as the mobile phase. Each sample was applied to a normal phase silica gel GF254 (Merck®). After development in the chamber, the TLC plates were dried with a hairdryer. The components were detected under 254 nm and 365 nm ultraviolet (UV) light. The developed plate was sprayed with respective spray reagents (anisaldehyde, DPPH spraying reagent) and dried at 100°C in a hot air oven. Rf values were used to compare the distances of the unknown spots and calculated as follows: Rf = migration distance of spot/migration distance of solvent. The extract was subjected to certain analysis phytochemical tests to determine the major chemical nature of the extract. In particular, different assays were conducted to detect the existence of alkaloids, tannins, hydrolysable tannins, condensed tannins, glycosides (including flavonoid), terpenoids, and proteins.

2.4. Cell Lines and Determination of Cytotoxicity by Cell Viability Assay. Human HeLa cell line (HeLa 229 (ATCC®CCL-2.1TM)) and mouse 3T3-L1 fibroblast (CL-173) used in this study were obtained from the American Type Culture Collection (ATCC) (USA). These two types of cells were cultivated in DMEM containing 10% (v/v) FBS and antibiotics (100 U/mL penicillin and 100 µg/mL streptomycin) in a 37°C humidified incubator with 5% (v/v) CO₂. Cell viability and the optimal dose (the half maximal inhibitory concentration, IC₅₀) of MC extract for HeLa and 3T3-L1 cells were determined using MTT assay as described previously [15, 28]. Specifically, the cells were grown for 24 h in complete media before treated with MC extract. The cells were seeded into 96-well plates at a density of 1 × 10⁴ cells/well in 0.2 mL of complete media. After 24 h of incubation,

the cells were exposed with various concentration of MC extract (0-1000 $\mu\text{g}/\text{mL}$) for 48 h. Treatment with DMSO (0-0.5%) was included as vehicle control. At the end of the treatment, 25 μL of MTT solution (5 mg/mL) was added to each well, and the plate was incubated for 1 h at 37°C. The absorbance was measured at 450 nm wavelength using a microplate absorbance reader (BioTek Instruments, USA) relative to that of untreated control in triplicate experiments.

2.5. Trypan Blue Exclusion Assay. On the basis that viable cells contain strong membrane integrity whereas dead cells lost their membrane permeability, we used Trypan blue to stain dead cells since this dye can freely diffuse into them. Cells at a density of 0.05×10^6 cells/well were seeded in 24-well plates and incubated with MC extract at its IC_{50} concentrations (125 $\mu\text{g}/\text{mL}$) or DMSO at 0.0625% as a vehicle control. Cells were harvested after 0, 6, 24, and 48 h of incubation. Trypan blue solution was added to the cell suspensions in a ratio of 1:1. Total cells and dead cells (stained in blue) were counted using haemocytometer. The percentage of living cells and dead cells was calculated.

2.6. Wound Healing Assay for Examining Cell Migration. Inhibition of migration activity in HeLa cells treated with MC extract was measured by wound-healing assay. The cells were seeded in 24-well plates in complete media until it reached 95-100% confluent. A 200 μL pipette tip was used to scrape the cell monolayer in a vertical and horizontal cross-line to create a "scratch" to each well. The center of the cross, where the 2 scratch lines meet, was used to position the center of the wound gap. The wells were washed once with growth medium to clear any detached cells and then refilled with the media (untreated (UT)) or treatment media (media containing MC extract at 15, 30, and 60 $\mu\text{g}/\text{mL}$ or DMSO at 0.03125%). Cell migration (wound closure) was examined using a phase-contrast microscope at 0 h (immediately after scratch), 24 h, and 48 h. Wound closure was measured, and cell migration was quantified. Each treatment was done in triplicate, and each experiment was repeated at least three times.

2.7. Cell Invasion Assay. The effects of MC extract on HeLa cell invasion were explored by Transwell invasion assay using Cell Culture Inserts (SPL Life Sciences, Korea). The polycarbonate invasion chambers (8 μm pore size) were coated with Matrigel® Matrix per well and incubated at room temperature (RT) for 1-4 h. Then, HeLa cells at a density of 0.25×10^6 cells per well were seeded on Matrigel in serum-free media alone (control) or serum-free media with the presence of 15, 30, or 60 $\mu\text{g}/\text{mL}$ of MC extract. The invasion chambers were put into the wells (the lower chambers) containing DMEM with 10% FBS and incubated for 24 h. Cells were then fixed with absolute methanol for 5 min at RT and stained with 0.5% crystal violet for 15 min. After three washes with water, cells in the invasion chambers were removed with cotton swab, and the images of the stained cells attached at the other site of the invasion chamber were taken and analyzed with the ImageJ software.

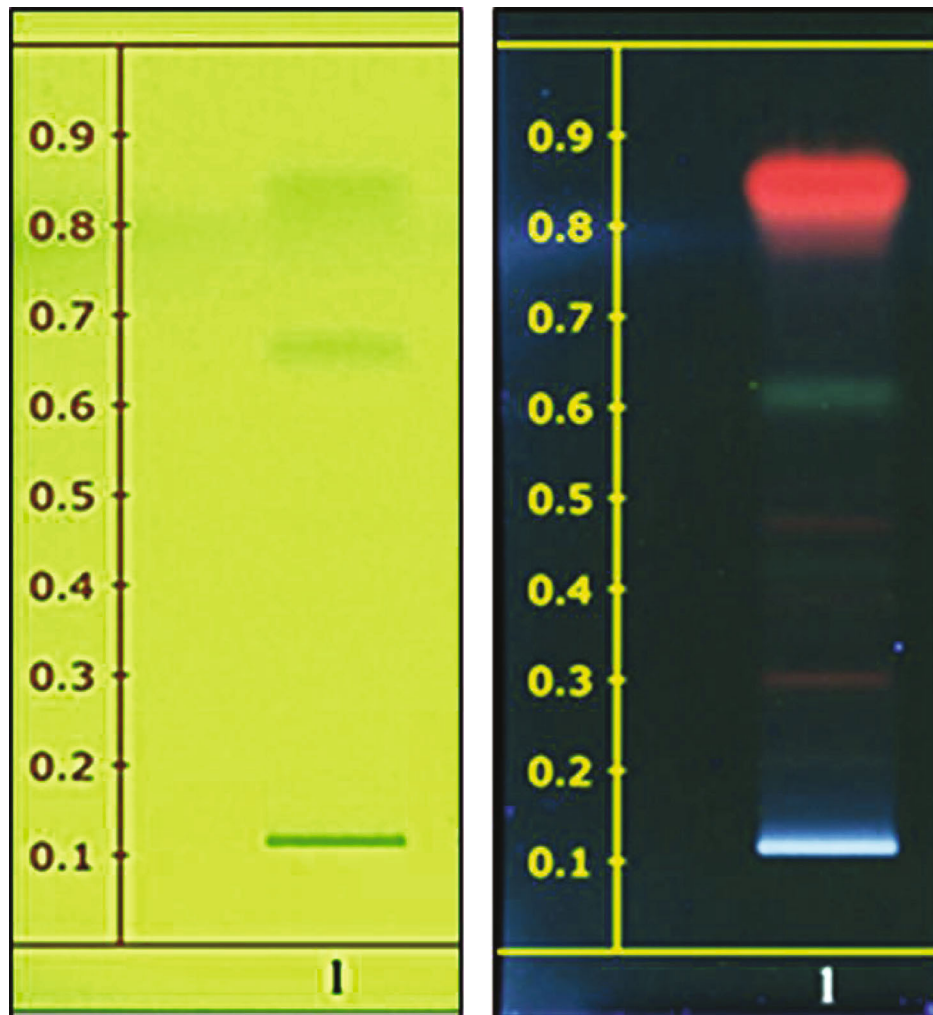
2.8. Apoptosis Assay by Annexin V/PI Staining and Flow Cytometry. Cell apoptosis was examined using FITC-annexin V (ImmunoTools, Germany) and propidium iodide (PI) (Sigma, United States). After treatment with MC extract at different concentrations (62.5, 125, and 250 $\mu\text{g}/\text{mL}$) for 24 h, cells (approximately 1×10^6 cells/mL) were harvested by trypsinization and washed in PBS one time by centrifugation. The supernatants were discarded, and cells were resuspended in 1x annexin-binding buffer. Then, Annexin V and PI were added to the cell suspension, and cells were incubated at RT for 15 min. To determine the percentage of apoptotic cell death, stained cells were analyzed immediately by flow cytometry using a flow cytometer DxFLX from Beckman Coulter (Indianapolis, IN, United States). Data analysis was performed using the CytExpert for the DxFLX software.

2.9. Western Blot Analysis. HeLa cell lysates were prepared by adding 1x reducing Laemmli buffer into the sample dishes. Samples were collected and heated at 98°C for 10 min and then separated in a 10% gel by SDS-PAGE and electroblotted onto nitrocellulose. Membranes were blocked with 5% nonfat dry milk in TBS-T (0.02 mol/L Tris-HCl, pH 7.6, 0.137 mol/L NaCl, and 0.1% (wt/vol) Tween 20) at room temperature for 1 h. Membranes were then incubated with primary antibodies at 4°C overnight. After three washes with TBS-T, membranes were incubated with secondary antibodies for 2 h at RT. The western blot protein bands were illustrated by using an Odyssey® CLx Imaging System (LI-COR Biosciences, USA).

2.10. Statistical Analysis. Data were analyzed by one-way ANOVA followed by the Tukey-Kramer multiple comparisons test and expressed as the mean \pm standard deviation (SD). *p* values less than 0.05 were considered statistically significant.

3. Results

3.1. Phytochemical Screening for the Leaves of *M. chulabhorniana* (MC). The chemical profile was performed with the suitable mobile phase and visualized under UV 254 nm and 365 nm. The TLC chromatogram of the methanolic extract was observed as shown in Figure 1. The methanolic extract of the leaves of *M. chulabhorniana* did not consist of apigenin, kaempferol, quercetin, and rutin compared to the standard R_f value of known flavonoid standards. In this study, TLC chromatogram did not indicate the chemical components, but the fingerprinting can be used to analyze the quantification of herbal products and identification for further study (Figure 1). However, our phytochemical test for major chemical groups revealed that the methanolic extract of the leaves of *M. chulabhorniana* contained alkaloids, flavonoids, and terpenes (Supplementary Table 1). On the basis that MC extract possesses anticancer properties, complete identification and characterization of certain active compounds responsible for anticancer activities of this plant should be further evaluated.



(a)

(b)

FIGURE 1: Continued.

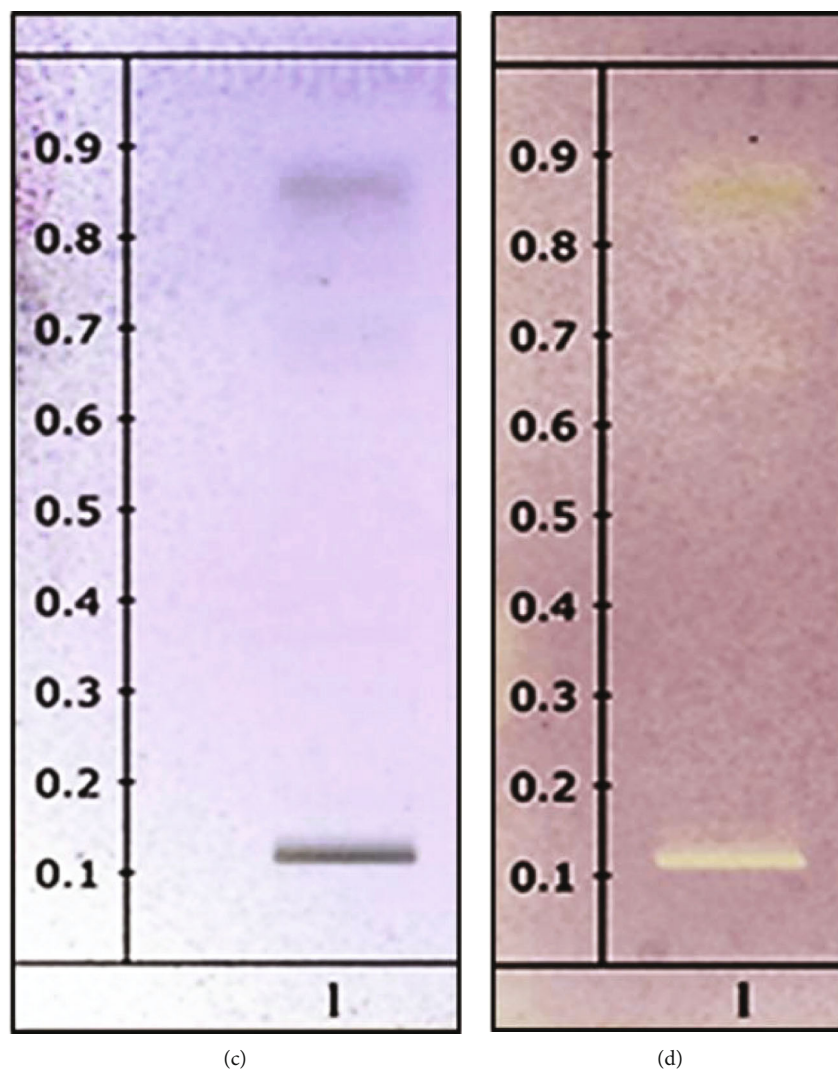


FIGURE 1: TLC chromatogram of methanolic extract of *M. chulabhorniana*. (a) Methanolic extract of leaves observed under UV at 254 nm. (b) Methanolic extract of leaves observed under UV at 365 nm. (c) Methanolic extract of leaves observed by using anisaldehyde-sulfuric acid spraying reagent. (d) Methanolic extract of leaves observed by using DPPH spraying reagent. Data are representatives of three individual replicates.

3.2. *Mitrephora chulabhorniana* (MC) Extract Inhibits the Growth of HeLa Cervical Cancer Cells. To evaluate the effects of the leaf extract of MC on cervical cell growth, HeLa cells were directly treated with 0, 0.98, 1.95, 3.91, 7.81, 15.63, 31.25, 62.5, 125, 250, 500, and 1000 $\mu\text{g}/\text{mL}$ of MC extract for 48 h in complete media before subjected to MTT assay. As shown in Figure 2(a), incubation of HeLa cells with MC extract for 48 h inhibited the growth of cells in a dose-dependent manner. The concentration of MC extract that reduced HeLa cell growth to 50% was approximately 125 $\mu\text{g}/\text{mL}$. Therefore, the half-maximal inhibitory concentration (IC_{50}) of MC extract was 125 $\mu\text{g}/\text{mL}$. MC extract at 250 $\mu\text{g}/\text{mL}$ reduced cell growth to be below 40%, and this cytotoxic effect of MC extract was seen to be similar to the groups treated with the extract at 500 or 1000 $\mu\text{g}/\text{mL}$. We observed that DMSO had no effect on growth and viability of HeLa cells (data not shown).

When the effect of MC extract on cell viability was tested in a different cell line, 3T3, which was a fibroblast cell line, we found that MC extract at 125 $\mu\text{g}/\text{mL}$ had no significant effect on 3T3 cell growth (Figure 2(b)). Specifically, MC extract at 250 $\mu\text{g}/\text{mL}$ started to decrease 3T3 cell growth to approximately 60%. These results suggest that HeLa cervical cancer cells are more sensitive to MC treatment than a non-cancerous 3T3 fibroblast cells. Additionally, MTT screening was conducted in four other cancer cell lines. Those included HN31 cell (a metastatic squamous cell carcinoma of pharynx from lymph node site), HepG2 cell (an immortal cell line derived from the liver tissue), SKOV3 cell (an ovarian cancer cell line derived from the ascites), and TOV21G (ovarian primary malignant adenocarcinoma). MTT results in these four cancer cell lines (Supplementary Figure 1) showed that in response to MC extract treatment, all four cancer cell lines exhibited a dose-dependent decrease in cell

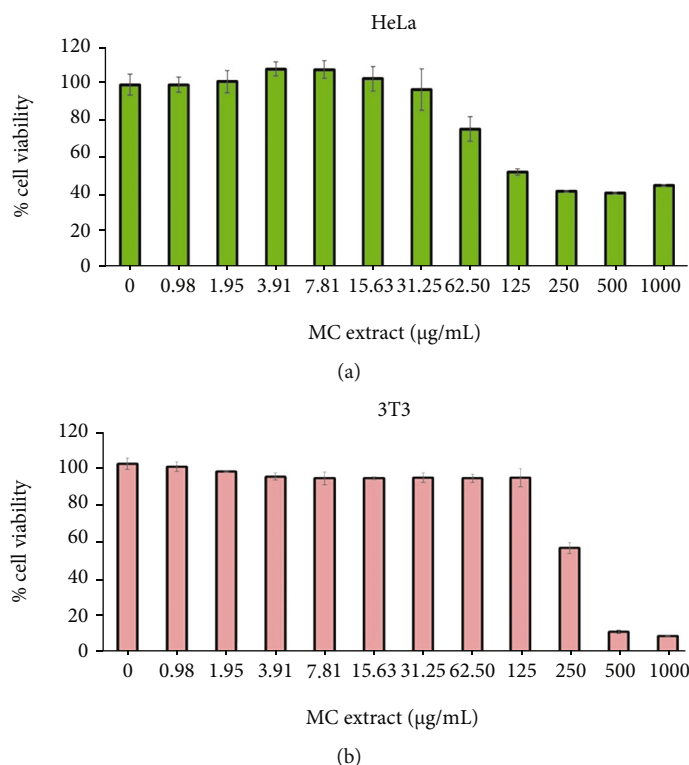


FIGURE 2: Effects of the leaf extract of MC on HeLa cervical cell and fibroblast cell viability. (a) MTT assay for testing cell viability of HeLa cells treated by MC extract at varied concentrations (0-1000 µg/mL) for 48 h. (b) MTT assay for cell viability of 3T3 fibroblast cell for 48 h. Data are representatives of three individual replicates.

viability. Among these cancer cell lines, when we assayed percent cell viability and nuclear fragmentation, HeLa cervical cancer cells were the most sensitive to the extract at same concentrations.

3.3. MC Extract Induces Morphological Changes and Nuclear Fragmentation in HeLa Cervical Cancer Cells. The results from MTT assay showing that MC extract significantly inhibited HeLa cell growth over the course of 48 h led us to hypothesize that MC extract can induce HeLa cervical cell death. Therefore, we designed an experiment to observe the effects of MC on HeLa cancer cell alterations. The morphologies of the untreated and MC treated cells were compared under a phase-contrast microscope. The morphology of HeLa cells drastically changed after treatment with 125 µg/mL of MC extract for 24 h (Figure 3(a)). Specifically, at the beginning of MC extract treatment (0 h), HeLa cells exhibited adherent epithelial characteristics, but after 24 h of MC extract treatment, many cells detached from the surface of the dish, and the remaining cells attaching to the surface presented the round-shape appearance and the changed pattern of light reflection under the phase-contrast microscope (Figure 3(a)). When we stained MC extract-treated HeLa cells with DAPI, we found that at the beginning of the treatment, the nuclei of the cells were intact and exhibited normal morphology (Figure 3(a)). However, the nuclei of HeLa cells presented nuclear fragmentation and a decrease in their volume after 24 h of MC extract treatment (Figure 3(a)). These morphological changes suggest that

MC extract-treated HeLa cells preceded apoptosis. Similar experiments were performed in 3T3 fibroblast cells, and we did not notice any effects of MC extract on the cell morphology and the characteristics of their nuclei at both 0 h and 24 h posttreatment (Figure 3(b)). We also monitored nuclear fragmentation to confirm the effects of the extract at the selected concentration (125 µg/mL) in HN31, HepG2, SKOV3, and TOV21G cells, and we found that these cell lines were less sensitive to MC extract in terms of induction of nuclear fragmentation (Supplementary Figure 2).

3.4. MC Extract Activates Apoptotic Cell Death in HeLa Cervical Cancer Cells. The effects of MC extract on changes of HeLa cell morphology and induction of nuclear fragmentation strongly suggest that MC extract may induce cell death through activating apoptosis signaling. To examine this hypothesis, we first performed Trypan blue exclusion assay to quantify the percent of dead cells after MC extract treatment. Results clearly demonstrated that MC extract at 125 µg/mL could induce number of Trypan blue-positive HeLa cells over the course of 48 h in a time-dependent manner. Specifically, the percent of Trypan blue-positive HeLa cells at 0 h was around 20% which was approximately equal to that of the DMSO vehicle control group (data not shown), and the dead cells were increased to 40%, 60%, and 100% at 6 h, 24 h, and 48 h, respectively (Figure 4.).

To further verify the relevant signaling pathway in which MC extract sensitized HeLa cervical cancer cells to death, we determined apoptotic cell death by staining cells

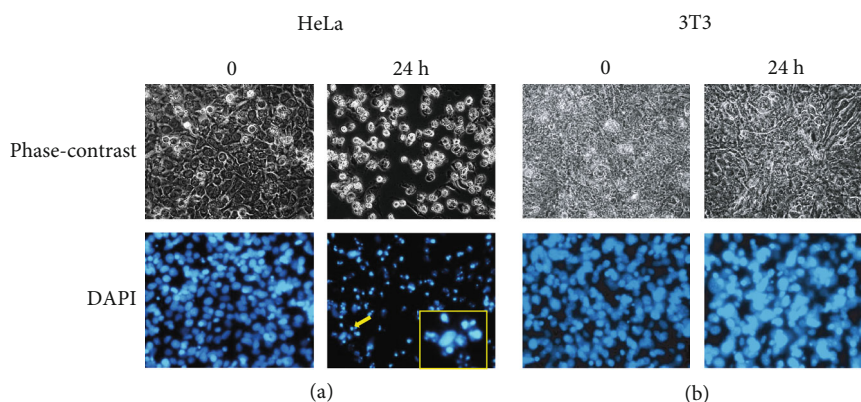


FIGURE 3: Effects of the leaf extract of MC on the cell morphological changes and nuclear fragmentation of HeLa cervical cancer cells and 3T3 fibroblast cells. (a) HeLa cells were treated with 125 $\mu\text{g/mL}$ of MC extract for 24 h. (b) 3T3 fibroblast cells were treated with 125 $\mu\text{g/mL}$ of MC extract for 24 h. Micrographs were taken at 0 and 24 h by a bright-field microscope (phase-contrast) and a fluorescent microscope to observe DNA fragmentation stained by DAPI (blue). Yellow arrow indicates DNA fragmentation, and the indicated cell is magnified in the right corner with yellow border. Data are representatives of three individual replicates.

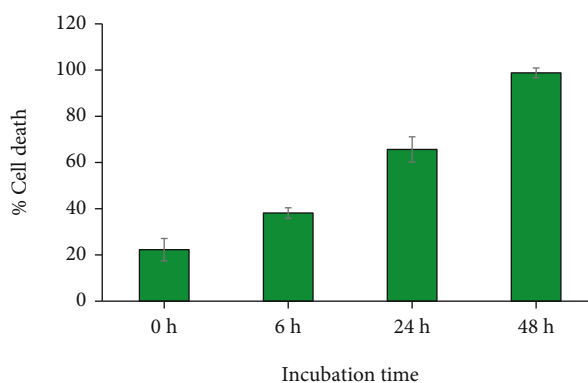


FIGURE 4: Effects of MC extract on HeLa cell death determined by Trypan blue exclusion assay. HeLa cells were treated with 125 $\mu\text{g/mL}$ of MC extract over the course of 48 h, and dead cells were stained by Trypan blue and quantified. Data are representatives of three individual replicates.

with Annexin V/PI and performed flow cytometry analysis. As expected, MC extract induced early and late apoptosis in HeLa cells in a concentration-dependent fashion (Figure 5 (a)). Quantitative analysis demonstrated that total apoptotic cell death was induced to be approximately 20%, 70%, and 90% in cells treated with MC extract at 62.5, 125, and 250 $\mu\text{g/mL}$, respectively (Figure 5(b)). Furthermore, we detected the activation of caspases and their executive substrate, PARP, by western blot analysis. As shown in Figure 5 (c), MC extract could induce the cleavage of full-length caspase 9 and caspase 7. Thus, the full-length (inactive) level of these two enzymes was reduced in a concentration-dependent manner. Consistently, the active forms of caspase 9 and caspase 7 were increased when the concentration of MC extract was increased. Generally, when the executive caspase such as caspase 7 is activated, the enzyme can further degrade several different downstream substrates including PARP protein. As expected, PARP was degraded in HeLa cells treated with MC extract, and the degradation was higher when the concentration of the extract was increased (Figure 5(c)). These data confirm that MC extract

induces apoptotic death of HeLa cervical cancer cells through caspase-dependent pathway. Western blot data from three independent experiments are shown in supplementary figure 3.

3.5. MC Extract Inhibits HeLa Cervical Cancer Cell Migration. Beside the effects of MC extract on inducing apoptosis in human cervical cells, we also evaluated its effects (at low concentrations) on cervical cancer cell migration. The results from scratch wound healing assay showed that MC extract at 60 $\mu\text{g/mL}$ could significantly inhibit HeLa cell migration (approximately 40% inhibition) at 24 h and 48 h (Figure 6). Although the migration rate of the groups treated with MC extract at 15 and 30 $\mu\text{g/mL}$ was not significant, the results exhibited the reduction trend of cell migration over the course of 24 and 48 h (Figure 6).

3.6. MC Extract Suppresses HeLa Cervical Cancer Cell Invasion. Since we observed that MC could inhibit HeLa cervical cancer cell migration, we further hypothesized that the extract may also inhibit cancer cell invasion. Therefore, we

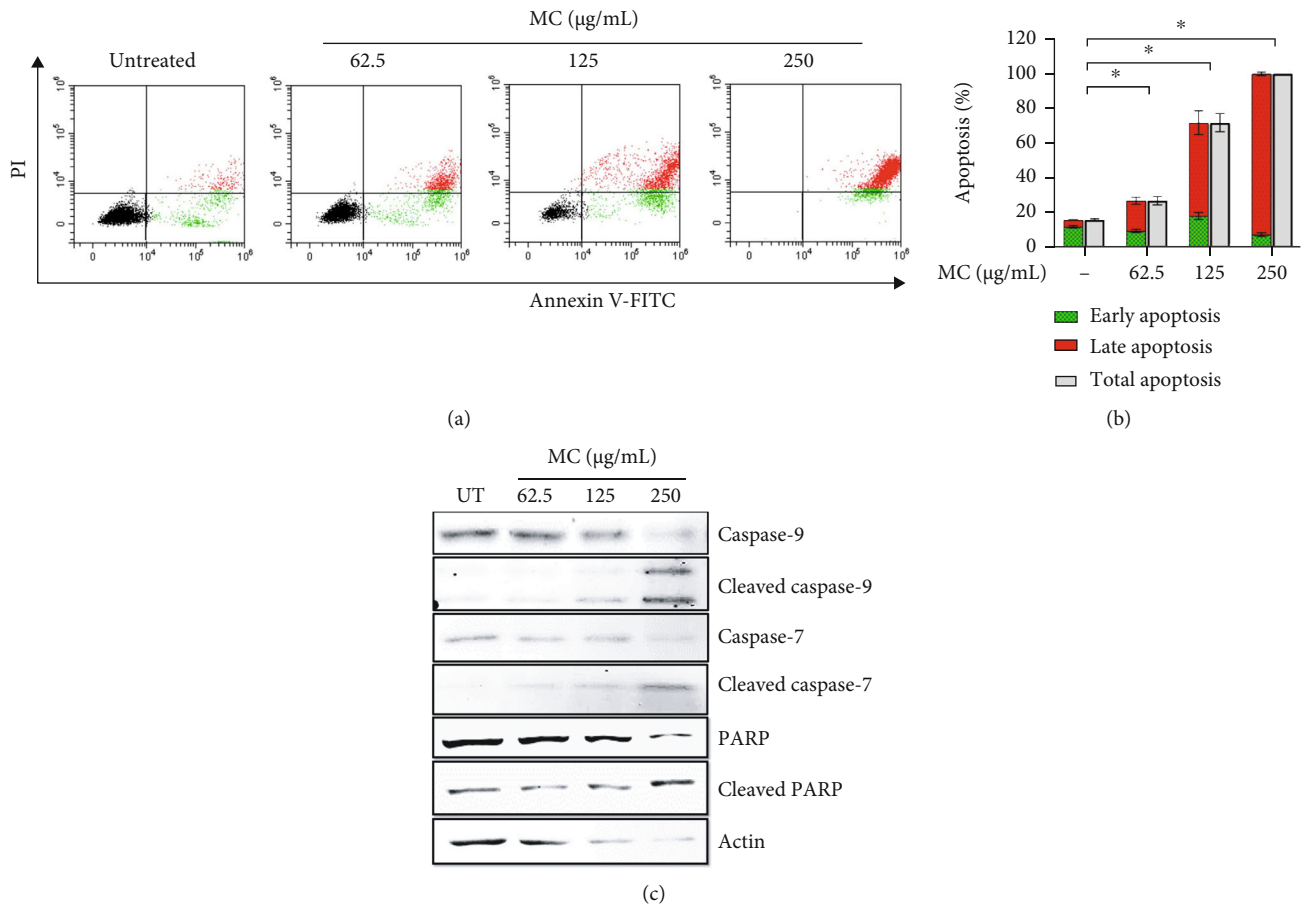


FIGURE 5: Effects of MC extract on stimulating caspase-dependent death signaling pathway. (a) HeLa cells were treated with MC extract at different concentrations (UT: untreated; 62.5, 125, and 250 µg/mL) for 24 h, subjected to Annexin V/PI staining and flow cytometry. (b) Quantitative analysis of apoptotic HeLa cells from Annexin V/PI staining and flow cytometry. (c) Full-length and cleaved caspase 9, caspase 7, and PARP were detected by western blot analysis. Actin was used as an internal control. Data are representatives of three individual replicates.

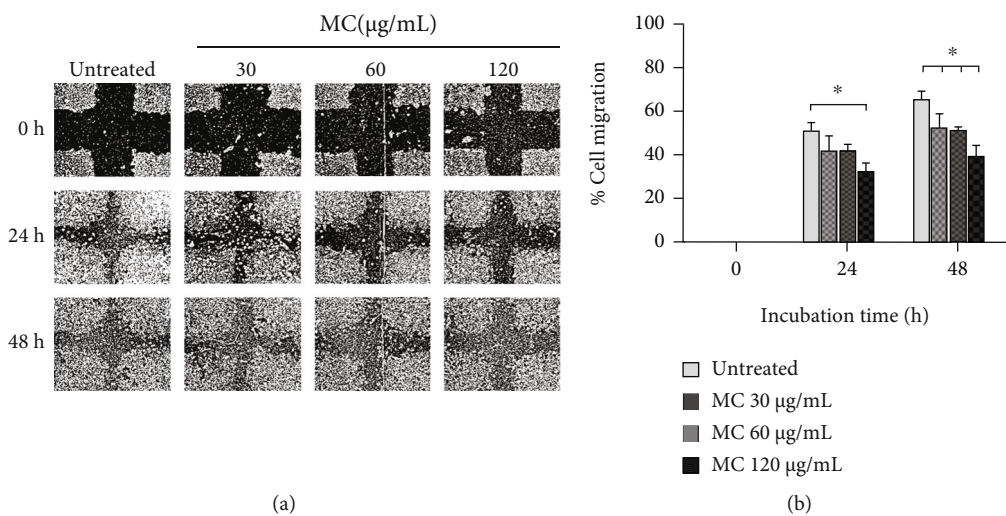


FIGURE 6: Effects of MC on HeLa cell migration. (a) Scratch wound healing assay of HeLa cells treated with MC extract at 15, 30, and 60 µg/mL over 48 h. (b) Quantitative analysis of the percent HeLa cell migration after treated with MC extract at 15, 30, and 60 µg/mL over 48 h. * $p < 0.05$ in comparison to the untreated group. Data are representatives of three individual replicates.

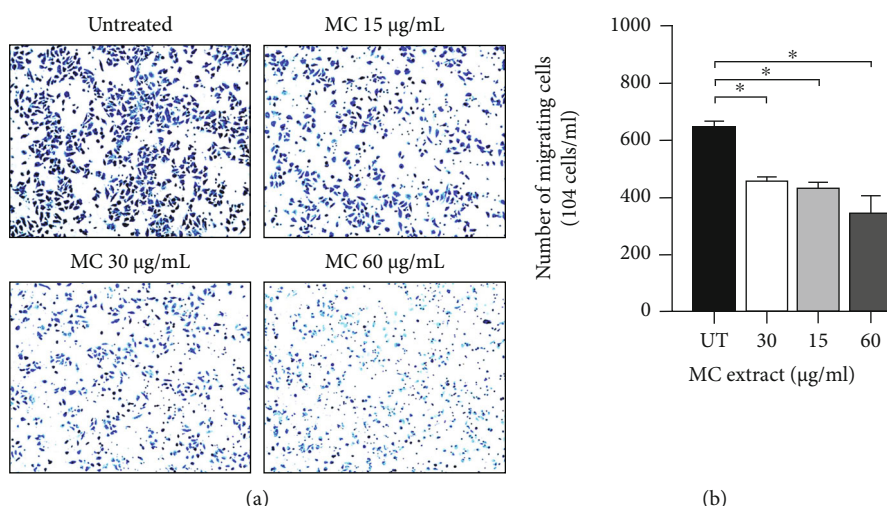


FIGURE 7: Effects of MC extract on HeLa cell invasion. (a) HeLa cells were treated with MC extract at 15, 30, and 60 µg/mL for 24 h and tested for cell invasion by using Transwell invasion assay. (b) Quantitative analysis for the number of the invading HeLa cells after 24 h of MC extract treatment. **p* < 0.05 in comparison to the untreated (UT) group. Data are representatives of three individual replicates.

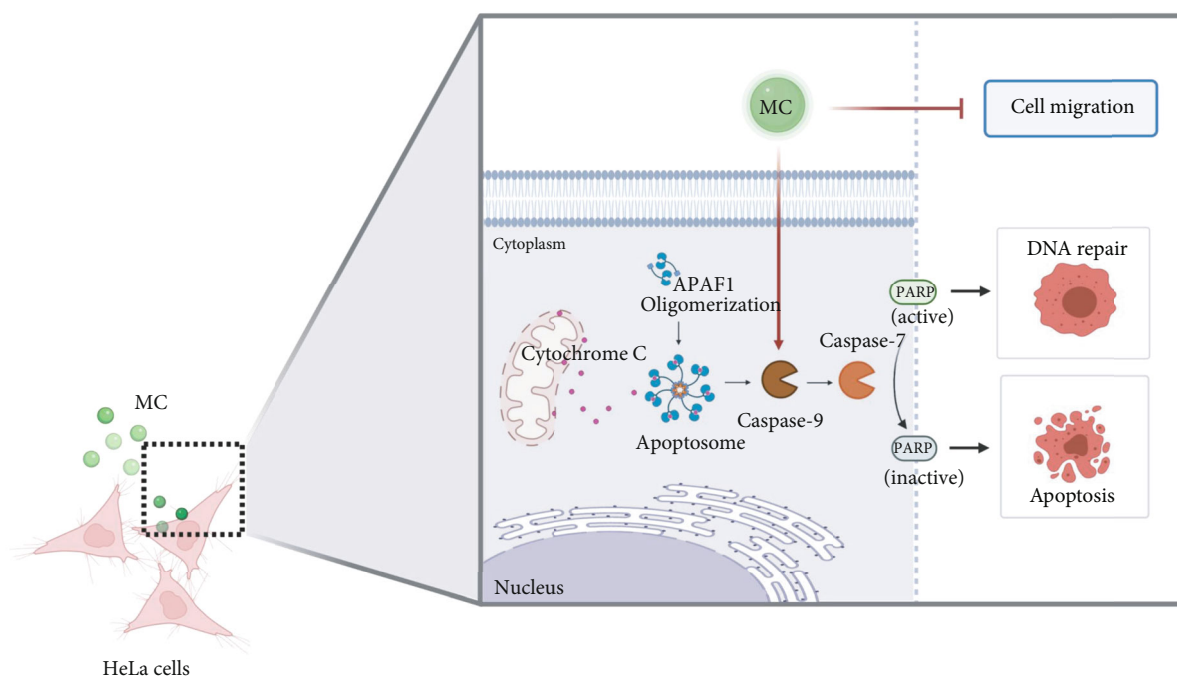


FIGURE 8: Explanatory image proposing that MC extract initiates cell apoptosis signaling and suppress migration/invasion of human cervical cancer cells, HeLa. The graphic was created with <http://biorender.com/>.

performed Transwell invasion assay. Data from this experiment clearly showed that MC extract significantly suppressed numbers of invading cells in a dose-dependent manner. Specifically, about 6.0×10^6 cells/mL of the untreated cells could migrate to the lower chamber, but MC extract at 15, 30, and 60 µg/mL could reduce the number of HeLa cell invasion to approximately 4.5×10^6 cells/mL (25% reduction), 4.0×10^6 cells/mL (30% reduction), and 3.0×10^6 cells/mL (50% reduction), respectively

(Figure 7). These data indicate that MC extract has a potential to suppress cervical cancer cell invasion.

4. Discussion

For cervical cancer, the best way to reduce the burden and the associated death rate of this disease is to screen for HPV lesions through HPV testing and Pap smears and prevent by vaccination [29]. Although screening program and

vaccination have been promoted for preventing the incidence of cervical cancer, this type of cancer is still the leading cause of cancer-related death in young women [30, 31]. This may be due to the fact that routine screening may not be widely available in many underdeveloped countries [32], and vaccination is currently limited to young people [33]. Conventional therapies including radiation, chemotherapy, and surgery are major means for patients; however, most of these conventional treatment can cause adverse effects (ranging from mild to severe) to the patients [34]. Medicinal plants have been extensively studied with the ultimate goal of discovering and developing novel anticervical cancer agents. For instance, the ethanolic extract of *Kaempferia parviflora* which contained certain kinds of methoxyflavones was reported to exhibit strong effects on the growth and survival of cervical cancer cells [14, 15] and ovarian cancer cells [11]. Numerous plants and their active compounds have been approved to be effective for many cancers since they can interfere with cancer homeostasis [35].

One genus that has been reported to show inhibitory effects on cancers is *Mitrephora* [19, 20, 22, 26, 27]. However, anticancer investigation for a new species, *Mitrephora chulabhorniana* (MC), has not been reported. Considering the cytotoxic effects of this genus, we believe that *Mitrephora chulabhorniana* may possess conserved pharmacological activities against cancer cells. Therefore, we focused on exploring the anticancer effects of *Mitrephora chulabhorniana* on cervical cancer cells using HeLa cervical cell line as a model for studying. Data from our study showed that in comparison to a noncancerous cell line, 3T3 fibroblast, MC extract significantly reduced cell viability of HeLa cervical cancer cells with the IC₅₀ being approximately 2-fold lower than that for 3T3 fibroblast cells and four other cancer cell lines, including HN31, HepG2, SKOV3, and TOV21G cells. The reduction in metabolic activity of MC extract-treated HeLa cells assayed by MTT pointed to the possibility that MC extract may cause reduced cell viability through inducing cell death. Our observation by phase contrast microscopy confirmed that MC extract dramatically caused HeLa cell morphological changes over the course of 24 h. Specifically, the morphology of epithelial cells adhering to the culture dish surface changed to the round-shape with different pattern of light reflection, and significant number of cells detached from the surface. These data suggest that MC extract interferes with the normal physiological conditions of HeLa cervical cancer cells. However, the extract at the same concentration did not cause any change in the morphology of 3T3 fibroblast cells over the same treatment duration, confirming that these cells are less sensitive to MC extract in comparison to HeLa cervical cancer cells. We further investigated the morphological changes at the nuclear level by staining the nuclei of the cells with DAPI which is a fluorescent dye used to probe DNA. As expected, HeLa cells treated with MC extract for 24 h exhibited dramatic reduction in the nucleus size, compared to their original volume at 0 h of treatment. Importantly, MC extract strongly induced irregular nuclear structure pattern where it was clearly shown at the higher magnification to be

nuclear fragmentation. Again, 3T3 fibroblast cells were irresponsive to MC extract as seen by their intact nuclei. These results verified that HeLa cervical cancer cells but not 3T3 noncancerous cells are susceptible for cellular stresses in response to MC extract. Nuclear fragmentation is a distinctive characteristic of dying cells, especially the ones undergoing apoptotic cell death [36]. As we anticipated, when MC extract-treated HeLa cells were stained with Trypan blue and counted for the proportion of dead cells, we found that MC extract significantly induced percent cell death in a time-dependent fashion over the course of 48 h. Further investigation at the molecular level indicated that MC extract induced HeLa cervical cancer cell death through activation of caspase-dependent pathway which is a major route of apoptotic cell death [37, 38]. It is possible that the extract may function to decrease the activation of growth and survival signal transduction pathways including MAPK [39] and PI3K/AKT [40] signal transduction pathways in response to growth factors or inflammatory cytokines, and these pathways are required for cancer cell proliferation and survival. Future identification of relevant signal transduction pathways by using molecular techniques as well as rational redesign of a functional protein kinase-substrate interaction [41] is required to accurately probe the cellular function which would explain how MC extract interferes with cervical cancer cell signaling.

Cellular responses upon treatment with MC extract at concentrations close to its IC₅₀ could cause extensive cervical cancer cell death. This event directed us to hypothesize that MC extract at lower concentrations may have inhibitory effects on HeLa cervical cancer cells in other aspects associated with the cancer cell behavior. As it is well-known that migration and invasion are crucial steps of tumor progression [42, 43], we determined whether MC extract can suppress HeLa cell migration and invasion. Scratch wound healing assay and Transwell migration assay evidently demonstrated that MC extract at nontoxic ranges of concentration could effectively inhibit HeLa cervical cancer cell migration and invasion in a dose-dependent pattern. These findings suggest that MC extract may help suppress cervical cancer metastasis.

5. Conclusions

Taken together, like other members of plants in the same genus, our current study provided accumulated evidence that *Mitrephora chulabhorniana* possesses anticancer properties by suppressing cervical cancer cell migration and invasion as well as inducing apoptosis (as shown in schematic Figure 8). This plant may be a good candidate for isolating critical compounds in which we believed to be conserved among the plant's genus. Those potential compounds may include the terpenoids, alkaloids, and flavonoids. Further investigation of this plant and its active compounds for all pharmacology aspects related to cervical cancer cell biology would contribute greatly to the development of alternative anticervical cancer therapeutic agents.

Abbreviations

MC: *Mitrephora chulabhorniana*
 TLC: Thin-layer chromatography
 MTT: 3-(4,5-Dimethylthiazol-2-yl)-2,5-diphenyltetrazolium bromide
 IC₅₀: Half maximal inhibitory concentration value
 DMSO: Dimethyl sulfoxide
 PARP: Poly (ADP-ribose) polymerase.

Data Availability

The data presented in this study are available in this article.

Disclosure

The funders had no role in the design of the study; in the collection, analyses, or interpretation of data; in the writing of the manuscript; or in the decision to publish the results.

Conflicts of Interest

The authors declare no conflict of interest.

Authors' Contributions

W.N. contributed to the conceptualization and methodology. W.N., S.C., S.P., P.H., J.R., and P.T. contributed to the experimental investigation. N.W. and W.N. contributed to the formal analysis. S.P. and N.W. contributed to the resources. W.N., N.W., P.H., J.R., and P.T. contributed to the writing—original draft preparation. S.P. and S.C. contributed to the review and editing. W.N. contributed to the funding acquisition. All authors have read and agreed to the published version of the manuscript.

Acknowledgments

Grateful appreciation is to Asst. Prof. Dr. Tanawat Chaowasku, Faculty of Science Chiang Mai University, for providing the plant samples and identification. This research work was partially supported by the Chiang Mai University. This research project was supported by Fundamental Fund 2022, Chiang Mai University (Funding number FF65/042). This research was also funded by the grants from the Utilization and Genetic Conservation of Local Plants in Complementation to the Plant Germplasm Conservation Project of H.R.H. Princess Maha Chakri Sirindhorn (Grant number R000026449).

Supplementary Materials

Supplementary data associated with this article can be found in the Supporting Information. (*Supplementary Materials*). Supplementary Figure 1: effects of the leaf extract of MC on the cell viability of (A) HN3, a metastatic squamous cell carcinoma of pharynx from lymph node site; (B) HepG2 cell, an immortal cell line derived from the liver tissue; (C) SKOV3, an ovarian cancer cell line derived from the ascites; and (D) TOV21G, ovarian pri-

mary malignant adenocarcinoma. MTT assay of four cancer cell lines treated by MC extract at varied concentrations (0-1 mg/mL) for 48 h. Data are representatives of three individual replicates. Supplementary Figure 2: effects of the leaf extract of MC on the cell morphological changes and nuclear fragmentation of (A) HN31 cells, (B) HepG2 cells, (C) SKOV3 cells, and (D) TOV21G. Cancer cells were treated with 125 µg/mL of MC extract for 24 h. Micrographs were taken at 0 and 24 h by a bright-field microscope (phase-contrast) and a fluorescent microscope to observe DNA fragmentation stained by DAPI (blue). Data are representatives of three individual replicates. Supplementary Figure 3: three individual replicates of western blot analysis of HeLa cells treated with different concentrations of MC extract showing caspase 9, cleaved (activated) caspase 9, caspase 7, cleaved (activated) caspase 7, PARP, cleaved PARP, and actin. DMSO was used as a vehicle control. M=protein markers. Supplementary Table 1: phytochemical tests were evaluated for major chemical groups in MC extract, e.g., flavonoids, alkaloids, glycosides, proteins, and terpenoids using chemical reagents. (+): positive result; (-): negative result. (*Supplementary Materials*)

References

- [1] H. Sung, J. Ferlay, R. L. Siegel et al., "Global cancer statistics 2020: GLOBOCAN estimates of incidence and mortality worldwide for 36 cancers in 185 countries," *CA: a Cancer Journal for Clinicians*, vol. 71, no. 3, pp. 209–249, 2021.
- [2] J. M. Lemp, J. W. De Neve, H. Bussmann et al., "Lifetime prevalence of cervical cancer screening in 55 low- and middle-income countries," *JAMA*, vol. 324, no. 15, pp. 1532–1542, 2020.
- [3] S. Vaccarella, M. Laversanne, J. Ferlay, and F. Bray, "Cervical cancer in Africa, Latin America and the Caribbean and Asia: regional inequalities and changing trends," *International Journal of Cancer*, vol. 141, no. 10, pp. 1997–2001, 2017.
- [4] L. Bruni, G. Albero, B. Serrano et al., *Human Papillomavirus and Related Disease in Thailand Report*, ICO/IARC Information Centre on HPV and Cancer (HPV Information Centre), Barcelona, Spain, 2019.
- [5] L. Kumar, P. Harish, P. S. Malik, and S. Khurana, "Chemotherapy and targeted therapy in the management of cervical cancer," *Current Problems in Cancer*, vol. 42, no. 2, pp. 120–128, 2018.
- [6] P. G. Rose, J. A. Blessing, D. M. Gershenson, and R. McGehee, "Paclitaxel and cisplatin as first-line therapy in recurrent or advanced squamous cell carcinoma of the cervix: a gynecologic oncology group study," *Journal of Clinical Oncology*, vol. 17, no. 9, pp. 2676–2676, 1999.
- [7] N. Bailon-Moscoso, G. Cevallos-Solorzano, J. C. Romero-Benavides, and M. I. Orellana, "Natural compounds as modulators of cell cycle arrest: application for anticancer chemotherapies," *Current Genomics*, vol. 18, no. 2, pp. 106–131, 2017.
- [8] P. Hankittichai, P. Buacheen, P. Pitchakarn et al., "Artocarpus lakoocha extract inhibits LPS-induced inflammatory response in RAW 264.7 macrophage cells," *International Journal of Molecular Sciences*, vol. 21, no. 4, p. 1355, 2020.

- [9] P. Hankittichai, H. J. Lou, N. Wikan, D. R. Smith, S. Potikanond, and W. Nimlamool, "Oxyresveratrol inhibits IL-1 β -induced inflammation via suppressing AKT and ERK1/2 activation in human microglia, HMC3," *International Journal of Molecular Sciences*, vol. 21, no. 17, p. 6054, 2020.
- [10] R. Namsen, N. Rojanasthien, S. Sireeratawong, P. Rojsanga, W. Nimlamool, and S. Potikanond, "Thunbergia laurifolia exhibits antifibrotic effects in human hepatic stellate cells," *Evidence-based Complementary and Alternative Medicine*, vol. 2017, Article ID 3508569, 2017.
- [11] S. Paramee, S. Sookkhee, C. Sakonwasun et al., "Anti-cancer effects of Kaempferia parviflora on ovarian cancer SKOV3 cells," *BMC Complementary and Alternative Medicine*, vol. 18, no. 1, p. 178, 2018.
- [12] P. Thaklaewphan, J. Ruttanapattanakul, S. Monkaew et al., "Kaempferia parviflora extract inhibits TNF- α -induced release of MCP-1 in ovarian cancer cells through the suppression of NF- κ B signaling," *Biomedicine & Pharmacotherapy*, vol. 141, article 111911, 2021.
- [13] J. Ruttanapattanakul, N. Wikan, S. Okonogi et al., "Boesenbergia rotunda extract accelerates human keratinocyte proliferation through activating ERK1/2 and PI3K/Akt kinases," *Biomedicine & Pharmacotherapy*, vol. 133, article 111002, 2021.
- [14] S. Potikanond, S. Sookkhee, M. Na Takuathung et al., "Kaempferia parviflora extract exhibits anti-cancer activity against HeLa cervical cancer cells," *Frontiers in Pharmacology*, vol. 8, 2017.
- [15] B. Suradej, S. Sookkhee, J. Panyakaew et al., "Kaempferia parviflora extract inhibits STAT3 activation and interleukin-6 production in HeLa cervical cancer cells," *International Journal of Molecular Sciences*, vol. 20, no. 17, p. 4226, 2019.
- [16] A. Damthongdee, K. Aongyong, and T. Chaowasku, "Mitrephora chulabhorniana (Annonaceae), an extraordinary new species from southern Thailand," *Brittonia*, vol. 71, no. 4, pp. 381–388, 2019.
- [17] K. Deepralard, T. Pengsuparp, M. Moriyasu, K. Kawanishi, and R. Suttisri, "Chemical constituents of Mitrephora maingayi," *Biochemical Systematics and Ecology*, vol. 10, no. 35, pp. 696–699, 2007.
- [18] W. Jaidee, W. Maneerat, R. J. Andersen, B. O. Patrick, S. G. Pyne, and S. Laphookhieo, "Antioxidant neolignans from the twigs and leaves of Mitrephora wangii HU," *Fitoterapia*, vol. 130, pp. 219–224, 2018.
- [19] C. Li, D. Lee, T. N. Graf et al., "A hexacyclic ent-trachylobane diterpenoid possessing an oxetane ring from Mitrephora glabra," *Organic Letters*, vol. 7, no. 25, pp. 5709–5712, 2005.
- [20] C. Li, D. Lee, T. N. Graf et al., "Bioactive constituents of the stem bark of Mitrephora glabra," *Journal of Natural Products*, vol. 72, no. 11, pp. 1949–1953, 2009.
- [21] B. A. Moharam, I. Jantan, J. Jalil, and K. Shaari, "Inhibitory effects of phylligenin and quebrachitol isolated from Mitrephora vulpina on platelet activating factor receptor binding and platelet aggregation," *Molecules*, vol. 15, no. 11, pp. 7840–7848, 2010.
- [22] K. O. Rayanil, S. Limpanawisut, and P. Tuntiwachwuttikul, "Ent-pimarane and ent-trachylobane diterpenoids from Mitrephora alba and their cytotoxicity against three human cancer cell lines," *Phytochemistry*, vol. 89, pp. 125–130, 2013.
- [23] K. O. Rayanil, W. Sutassanawichanna, O. Suntornwat, and P. Tuntiwachwuttikul, "A new dihydrobenzofuran lignan and potential α -glucosidase inhibitory activity of isolated compounds from Mitrephora teysmannii," *Natural Product Research*, vol. 30, pp. 2675–2681, 2016.
- [24] J. R. Zgoda, A. J. Freyer, L. B. Killmer, and J. R. Porter, "Polyacetylene carboxylic acids from Mitrephora celebica," *Journal of Natural Products*, vol. 64, no. 10, pp. 1348–1349, 2001.
- [25] S. Sanyachareerukul, S. Nantapap, K. Sangrueng, N. Nuntasaeen, W. Pompimon, and P. Meepowpan, "Antifungal of modified neolignans from Mitrephora wangii Hu," *Applied Biological Chemistry*, vol. 59, no. 3, pp. 385–389, 2016.
- [26] D.-H. Meng, Y.-P. Xu, W.-L. Chen, J. Zou, L.-G. Lou, and W.-M. Zhao, "Anti-tumour clerodane-type diterpenes from Mitrephora thorelii," *Journal of Asian Natural Products Research*, vol. 9, no. 7, pp. 679–684, 2007.
- [27] N. Anantachoke, D. Lovacharaporn, V. Reutrakul et al., "Cytotoxic compounds from the leaves and stems of the endemic Thai plant Mitrephora sirikitiae," *Pharmaceutical Biology*, vol. 58, no. 1, pp. 490–497, 2020.
- [28] T. Mosmann, "Rapid colorimetric assay for cellular growth and survival: application to proliferation and cytotoxicity assays," *Journal of Immunological Methods*, vol. 65, no. 1–2, pp. 55–63, 1983.
- [29] M. Safaeian, D. Solomon, and P. E. Castle, "Cervical cancer prevention—cervical screening: science in evolution," *Obstetrics and Gynecology Clinics of North America*, vol. 34, no. 4, pp. 739–760, 2007.
- [30] W. Small Jr., M. A. Bacon, A. Bajaj et al., "Cervical cancer: a global health crisis," *Cancer*, vol. 123, no. 13, pp. 2404–2412, 2017.
- [31] S. Zhang, H. Xu, L. Zhang, and Y. Qiao, "Cervical cancer: epidemiology, risk factors and screening," *Chinese Journal of Cancer Research*, vol. 32, no. 6, pp. 720–728, 2020.
- [32] L. Denny, M. Quinn, and R. Sankaranarayanan, "Chapter 8: screening for cervical cancer in developing countries," *Vaccine*, vol. 24, Supplement 3, 2006.
- [33] D. Saslow, P. E. Castle, J. T. Cox et al., "American Cancer Society guideline for human papillomavirus (HPV) vaccine use to prevent cervical cancer and its precursors," *CA: a Cancer Journal for Clinicians*, vol. 57, no. 1, pp. 7–28, 2007.
- [34] P. Petignat and M. Roy, "Diagnosis and management of cervical cancer," *BMJ*, vol. 335, no. 7623, pp. 765–768, 2007.
- [35] A. Cervantes-Arias, L. Y. Pang, and D. J. Argyle, "Epithelial-mesenchymal transition as a fundamental mechanism underlying the cancer phenotype," *Veterinary and Comparative Oncology*, vol. 11, no. 3, pp. 169–184, 2013.
- [36] B. Monier and M. Suzanne, "Orchestration of force generation and nuclear collapse in apoptotic cells," *International Journal of Molecular Sciences*, vol. 22, no. 19, article 10257, 2021.
- [37] P. Ghose and S. Shaham, "Cell death in animal development," *Development*, vol. 147, no. 14, 2020.
- [38] M. D. Jacobson, M. Weil, and M. C. Raff, "Programmed cell death in animal development," *Cell*, vol. 88, no. 3, pp. 347–354, 1997.
- [39] B. B. Aggarwal, A. B. Kunnumakkara, K. B. Harikumar et al., "Signal transducer and activator of transcription-3, inflammation, and cancer," *Annals of the New York Academy of Sciences*, vol. 1171, no. 1, pp. 59–76, 2009.
- [40] L. H. Wei, M. L. Kuo, C. A. Chen et al., "The anti-apoptotic role of interleukin-6 in human cervical cancer is mediated by up-regulation of Mcl-1 through a PI 3-K/Akt pathway," *Oncogene*, vol. 20, no. 41, pp. 5799–5809, 2001.

- [41] C. Chen, W. Nimlamool, C. J. Miller, H. J. Lou, and B. E. Turk, "Rational redesign of a functional protein kinase-substrate interaction," *ACS Chemical Biology*, vol. 12, no. 5, pp. 1194–1198, 2017.
- [42] V. Bhandari, M. Kausar, A. Naik, and M. Batra, "Unusual metastasis from carcinoma cervix," *Journal of Obstetrics and Gynaecology of India*, vol. 66, no. 5, pp. 358–362, 2016.
- [43] R. Pasricha, A. Tiwari, T. Aggarwal, and P. Lal, "Carcinoma of uterine cervix with isolated metastasis to fibula and its unusual behavior: report of a case and review of literature," *Journal of Cancer Research and Therapeutics*, vol. 2, no. 2, pp. 79–81, 2006.

Review Article

Looking for Responders among Women with Chronic Pelvic Pain Treated with a Comiconized Formulation of Micronized Palmitoylethanolamide and Polydatin

Ugo Indraccolo ¹, Alessandro Favilli,² Arianna Dell'Anna,³ Antonio Di Francesco,⁴ Barbara Dionisi,⁵ Emilio Giugliano,⁶ Filippo Murina,^{7,8} and Erica Stocco⁹

¹Maternal-Infantile Department, Complex Operative Unit of Obstetrics and Gynecology, "Alto Tevere" Hospital of Città di Castello, ASL 1 Umbria, Via L. Angelini 10, 06012 Città di Castello, Italy

²Maternal-Infantile Department, Section of Obstetrics and Gynecology, Azienda Ospedaliera Universitaria Integrata di Verona, Hospital of Woman and Child, Piazzale Stefani 1, 37126 Verona, Italy

³Obstetrics and Gynecology Unit, "Santa Caterina Novella" Hospital of Galatina ASL Lecce, Via Roma, 73013 Galatina, Italy

⁴Obstetrics and Gynecology Unit, "Floraspe Renzetti" Hospital of Lanciano, ASL 2 Abruzzo, Via per Fossacesia 1, 66034 Lanciano, Italy

⁵"Santa Famiglia" Health House of Rome, Via dei Gracchi 134, 00192 Roma, Italy

⁶Maternal-Infantile Department, Complex Operative Unit of Obstetrics and Gynecology, "Santa Maria della Misericordia" Hospital of Rovigo ULSS 5 Veneto, Viale Tre Martiri 140, 45100 Rovigo (PD), Italy

⁷Obstetrics and Gynecology Department Lower Genital Tract Disease Unit "Vittore Buzzi" Hospital University of Milano, Via Castelvetto 32, 20154 Milano, Italy

⁸Vulvodinia Italian Association, Via G.B. Pergolesi 4, 20124 Milano, Italy

⁹Department of Surgical, Oncologic and Gastroenterologic Sciences, First Surgical Clinic, University of Padua, Via Giustiniani 2, 35128 Padova, Italy

Correspondence should be addressed to Ugo Indraccolo; ugo.indraccolo@libero.it

Received 9 January 2022; Accepted 23 April 2022; Published 7 May 2022

Academic Editor: Madiha Ahmed

Copyright © 2022 Ugo Indraccolo et al. This is an open access article distributed under the Creative Commons Attribution License, which permits unrestricted use, distribution, and reproduction in any medium, provided the original work is properly cited.

Background. Palmitoylethanolamide is reported to solve pain and neuroinflammation in different models of chronic and neurodegenerative diseases. Some concerns have been illustrated for cautiously interpreting the available literature on the topic. Specifically, there is a lack of evidence about palmitoylethanolamide and female chronic pelvic pain. Concerns will be best solved by randomized trials. The present study was aimed at finding the best responders to micronized palmitoylethanolamide in female patient with chronic pelvic pain, using the existing literature at individual patient level, to help further randomized trial planning. **Methods.** After a systematic research, eligible studies (the ones enrolled female patients treated for chronic pelvic pain or for dyspareunia, dysuria, dyschezia, and dysmenorrhea with or without chronic pelvic pain) were assessed at individual patient data level. Conditional probabilities were calculated to assess variables conditioning the rates of good responders (pain score points more or equal to 3 reduction), poor responders (2 pain score reduction), and nonresponders at a three-month follow-up. **Results.** Only cases treated with palmitoylethanolamide comiconized with polydatin for a short period can be assessed. Good responders are more than 50%. In chronic pelvic pain, there is a 19.0% conditional probability to find good responders among patients with pain score at enrolment of 6 to 8 and of 6.8% to find poor responders among patients with a pain score at enrolment of 6 to 8. Painful disease does not matter on responders' rates. **Conclusion.** Best responders to comiconized palmitoylethanolamide/polydatin are patients with pain score higher than 6 at enrolment, irrespective of other variables.

1. Introduction

Chronic pelvic pain is a common problem that affects mainly the female population, and it is caused by a dysfunction, damage, or degeneration of the sensory nervous system. This condition leads to a significant discomfort and reduction of the patient quality of life [1].

In recent years, scientific literature has expressed positive opinions about palmitoylethanolamide (PEA). While mast cells and glia cells are acknowledged having pivotal role in chronic inflammatory disorders [2–4], PEA is able to block persistent activation of these cells [5], thereby playing an important role in the resolution of pain and neuroinflammation in different models of chronic and neurodegenerative diseases [6].

The mechanism of action of PEA has been recently summarized by D'Amico et al. [7]. First, it acts as an "ALIA" molecule able to directly downregulate mast cell degranulation. Second, it activates at least two nuclear receptors, the peroxisome proliferator-activated receptor alpha (PPAR α) and the orphan receptor G-protein coupling (GPR55), provoking a somewhat regulation of the proinflammatory behaviour of the cell. Third, PEA plays a so-called entourage action, by enhancing the anti-inflammatory and anti-nociceptive function of other substances (among them, the ones involved in activating the cannabinoid receptors 1 and 2).

The strength points of PEA naïve along with hypothetical weakness have been exposed in several reviews, on the base of experimental data and clinical issues [8–14]. Micronized and ultramicronized palmitoylethanolamide (m-PEA and um-PEA) have been used for preclinical and clinical studies to overcome the concern of PEA bioavailability. Both m-PEA and um-PEA are constituted by a crystalline form with a particle size between 100 and 700 μm [15] characterized by a high surface-volume ratio that allows a better diffusion, distribution, and higher biological efficacy compared to non-micronized PEA [16, 17]. In 2016, however, Gabriëlsson et al. [9] suggested to cautiously interpret the available literature on PEA because of a conflict of interest issue and poor-quality clinical trials. Specifically, the issue of PEA and chronic pelvic pain is still poor to date, while more data have been provided for chronic pain, as reported by Paladini et al. [18] in pooled data meta-analysis.

In a previous aggregate data meta-analysis on female patients with pelvic pain [19], the authors have proved that m-PEA comicronized with transpolydatin (Pol) allows a significant reduction of pain scores in female patients with endometriosis suffering from chronic pelvic pain.

Transpolydatin (Pol) is a natural glucoside of resveratrol, an antioxidant and anti-inflammatory molecule. Pol has been combined with m-PEA in a comicronized form (9 mg of m-PEA and 1 mg of Pol) [m(PEA/Pol)]. Besides endometriosis [19–22], m-PEA/Pol has been used in the treatment of interstitial cystitis/bladder syndrome [23] and dinitrobenzene sulfonic acid- (DNBS-) induced colitis [24].

The U. Indraccolo et al. meta-analysis [19] was unable to detect a subgroup of patients able to show a larger pain reduction, although it suggested that the higher the pain score at enrolment, the greater the pain reduction. Addition-

ally, meta-analyzed data [19] do not report how many responders to the m(PEA/Pol) have been found and if such reduction can be observed in chronic pelvic pain patients with other painful diseases. Moreover, it is unknown if the effectiveness observed in the U. Indraccolo et al. [19] meta-analysis is due to m-PEA, Pol, or both. Understanding how many patients would be responders to m-PEA and if a subgroup of best responders exists among them is needed to plan hypothetical randomized trials on the compound efficacy.

Compounds with PEA and Pol formulations (both associated and alone) are commercialized in some countries as foods for special medical purpose (with heterogeneous regulatory issues [25]). Therefore, in some countries, they can be administered in spite of lacking of registrative trials supporting their efficacy, the route of administration, and their dosage.

The present study was aimed at finding the best responders to m-PEA in female chronic pelvic pain patients, using the existing literature at individual patient level.

2. Methods

A systematic review was planned and registered in the PROSPERO database (CRD42021232156).

The best responders to m-PEA are planned to be assessed in a descriptive way, by pooling individual data from databases of already published articles on the topic. No comparators are planned to be assessed in the present work.

2.1. Systematic Research. In December 7, 2020, a systematic review was drawn on PubMed, Web of Science, Scopus, SciELO, African Journal Online, and Asian Digital Library. The search on each database was done using the following MeSH: palmitoylethanolamide AND chronic pelvic pain; palmitoylethanolamide AND pelvic pain; palmitoylethanolamide AND endometriosis; and palmitoylethanolamide AND dysmenorrhoea. Neither time frame nor language limits were set. Already published systematic reviews and meta-analyses on PEA [18, 19, 26, 27] were also screened for collecting more references on PEA clinical series. More articles were collected by screening the Epitech Group SpA database on spontaneous studies on m-PEA.

Prospective and retrospective studies, randomized trials, and clinical descriptive series, where an arm of cases was treated with m-PEA, were all screened for eligibility at individual patient level.

Eligible studies were the ones in which female patients were treated for chronic pelvic pain or other pelvic pain with or without chronic pelvic pain (even in a subgroup of the sample). After the screening phase of the studies selection (Figure 1), the corresponding authors, of the 11 references [20, 22, 23, 28–36] eligible for inclusion, were contacted to share their full databases by mail or phone. Those databases would be judged eligible for a further analysis if they had at least one case of a female patient with at least a pelvic pain reported as dysmenorrhea, dysuria, dyschezia, dyspareunia (irrespective from deep or superficial dyspareunia or both), and chronic pelvic pain.

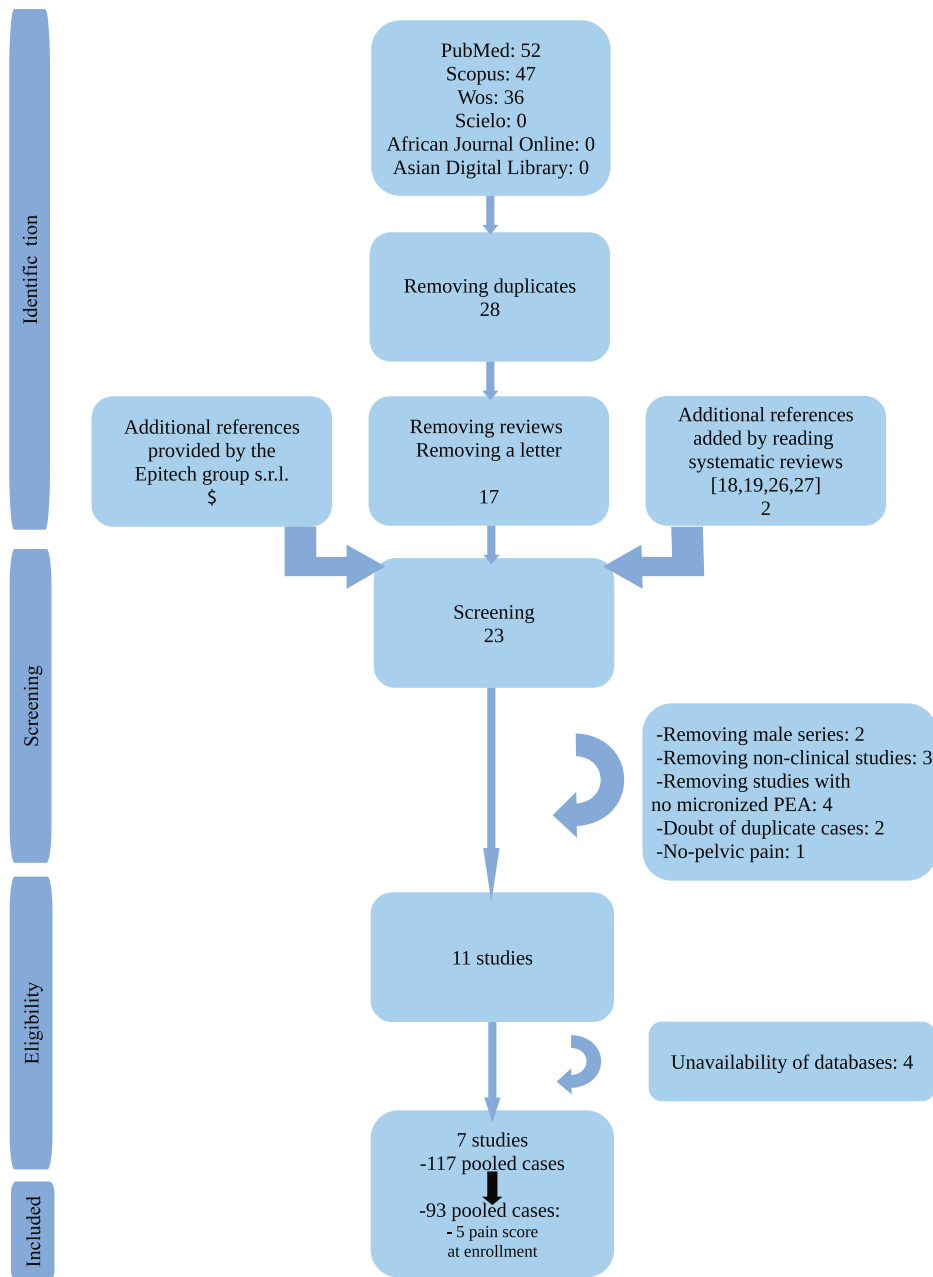


FIGURE 1: Flow chart of the phases of systematic review.

Pain had to be assessed with the visual analogue scale (VAS) or numeric rating scale (NRS). Pain had to have a value score point of 5 or more at enrolment in one or more of the above-mentioned pains and had to be assessed in a three-month follow-up for the same pain. Any other information useful for assessing the characteristics of responders was planned to be collected from single databases.

Responders were defined as patients reporting a reduction of pain, from enrolment to three-month follow-up, of 2 or more scores in one or more symptoms of chronic pelvic pain as dysmenorrhea, dyspareunia, dyschezia, and dysuria. Among responders, we also differentiated poor responders (only 2 VAS or NRS score point reduction from the enrol-

ment value at the three-month follow-up) from good responders (3 or more VAS or NRS score points reduction from the enrolment value at the three-month follow-up).

2.2. Data Synthesis. Cases with no pain score at enrolment of 5 or more in none of the pains were excluded from the whole pooled case database. Rates of good responders, poor responders, and non responders were calculated on the whole. Then, rates of nonresponders, poor responders, and good responders were reported for chronic pelvic pain, dysmenorrhea, dyspareunia, dyschezia, and dysuria groups.

A conditional probability of occurrence of each patient characteristics (independent variables) extracted from the

pooled case database among nonresponders, poor responders, and good responders at three-month follow-up was also provided.

2.3. Statistical Analysis. The pooled case database has been assessed by principal component two-dimensional correspondence analysis for each type of pain: dysmenorrhea, dysuria, dyschezia, dyspareunia, and chronic pelvic pain. The two dimensions were organized among the dependent variables (nonresponders, poor responders, and good responders at three-month follow-up) and all other independent variables theoretically involved in pain perception. Those independent variables were extracted at individual patient level. The correspondence analysis output provides a two-axis map with dependent and independent variables summarized as points with proper coordinates. The higher is the closeness of the independent variables to the point dependent variables, the higher their association. Therefore, by calculating distances among points, it is possible to estimate the unconditioned probabilities of associations of variables. The distances were rescaled to be between 0 and 1, as probability does. Finally, by applying Bayes' theorem, the conditional probability was calculated for each independent variable and each group of responders for all types of pain. Associations are hypothesized if conditional probabilities are found to be more than 0.05 (5%), setting the *P* value for chance of less or equal to 0.05. Therefore, the higher is the probability over the 0.05, the higher the strength of association.

As a complimentary analysis, the percentage of association among good responders and no good responders of each type of pelvic pain with chronic pelvic pain was checked. Such analysis is needed as chronic pelvic pain sensitization can increase pain perception for other pains with acute behaviour.

IBM SPSS 27 was used for principal correspondence analysis, and LibreOffice 7.0 was used to perform other calculations.

2.4. Quality Assessment. A modified GRADE score [37] was used to assess the quality of data, in relation with the specific methodology used for performing the present study. The aim of this scoring system is to give an overall objective judgment of the quality of the available databases for meeting the aims of the current study, as poor-quality study has been reported to be a practical concern in interpreting the literature on PEA [9]. We did not plan to exclude poor studies from the review, as the main aim of the study was not to demonstrate any superiority of m-PEA.

The modified GRADE scoring system has been:

- (1) Type of study: +3 for randomized series, +2 for prospective observational series, +1 for retrospective series, and 0 for small series (less than 5 cases)
- (2) Availability of descriptive data for calculating unconditional probabilities: +3 full items available; +2 more than a half of items available; +1 less than a half of items available; and 0 no additional information than pain score at enrolment and at three months follow-up available

- (3) Numerosity of the eligibility series: +1 if more or equal to 10 and -1 if less than 10
- (4) Presence of comparator arm: -1: no comparator arm and 0: comparator arm is reported, but the quality assessment of the study provided by the Newcastle-Ottawa [38] scale (for observational studies) or by the Jadad et al. [39] scale (for randomized studies) is less than a half of maximum score; +1: comparator arm is reported, and the quality assessment of the study provided by the Newcastle-Ottawa [38] scale (for observational studies) or by the Jadad et al. [39] scale (for randomized studies) is more than, or equal to, a half of maximum score.

The score was attributed by UI and AF. In case of no agreement, discussion among UI and AF led to the final score.

To each pooled case, it was assigned the score given to the study where such case was extracted. The pooled scores were averaged for each kind of subgroup of pain (chronic pelvic pain, dysmenorrhea, dyspareunia, dyschezia, and dysuria). The scoring system of the study can vary from -2 to 8, with mean value of 3. For single subgroup series of pooled data, a quality mean score of more than 3 indicates that the quality is higher than the mean. The mean quality has been provided for each subgroup of pain, along with 95% confidence intervals (CI).

3. Results

Figure 1 reports the phases of systematic review in a flow chart. Studies eligible by viewing the full database were 11, but full databases have been shared by only 7 authors of studies [20, 22, 29–32, 34]. One hundred seventeen cases were collected. According to the inclusion criteria, 24 cases were excluded because patients did not have at least one pain score at enrolment of 5 or more in at least a type of pain. Therefore, 93 pooled cases were assessed.

Table 1 reported the characteristics of each study assessed for inclusion. None of these studies provides data on patients treated with m-PEA alone. All studies reported data on the association of m-PEA/Pol. Quality score attributed to each study is reported in Table 2.

Sixty-four patients had chronic pelvic pain of 5 or more (68.8%), 28 (30.1%) had dyspareunia (unspecified if deep or superficial or both), 15 (16.1%) dyschezia, 19 (20.4%) dysuria, and 34 (36.6%) dysmenorrhea. The quality score for pooled cases is slightly higher than 3 (Table 3). Table 3 reports also the crude numbers and rates of good responders, poor responders, and nonresponders according to each type of pain at the three-month follow-up.

Among available additional information in databases, 10 items have been extracted: patient' age at enrolment, years of pains, years elapsed from pains onset to diagnosis of painful disease, type of painful disease (endometriosis, vulvodynia, and unknown or unreported painful disease), menopausal status, previous surgery, use of analgesics during treatment, hormonal therapies during treatment, transcutaneous electrical

TABLE 1: Description of studies of which databases has been assessed at individual patient level. Included cases are reported in the last column at the right side.

	Treatment	Disease	Pain assessment	Enrolment	Eligible cases	Included cases
Dell’Anna and De Marzi [29]	Um-PEA 200 mg m-(PEA/Pol) 400 mg/40 mg 3 times daily for four months	Endometriosis	NRS	Prospective	Single arm: 16	14
Di Francesco and Pizzagallo [22]	m-(PEA/Pol) 400 mg/40 mg two times daily for six months	Endometriosis	NRS	Randomized	An arm: 10	9
Dionisi and Senatori [30]	m-(PEA/Pol) 400 mg/40 mg two times daily for two months, plus topical adelmidrol	Vulvodynia/ vestibulodynia	NRS	Prospective	Single arm: 34	17
Giugliano et al. [31]	m-(PEA/Pol) 400 mg/40 mg two times daily for three months	Endometriosis	VAS	Prospective	Two arms (but no comparator arm): 19 and 28	15 and 18
Indraccolo and Barbieri [20]	m-(PEA/Pol) 400 mg/40 mg two times daily for three months	Endometriosis	VAS	Small series	4 cases	4
Murina et al. [32]	m-(PEA/Pol) 400 mg/40 mg two times daily for two months	Vestibulodynia	VAS	Randomized	An arm: 10	9
Stocco and Schievano [34]	m-(PEA/Pol) 400 mg/40 mg two times daily for two months	Miscellaneous symptoms	VAS/NRS	Prospective	Single arm: 13 (male and female)	7

m-PEA: micronized palmitoylethanolamide; um-PEA: ultramicronized palmitoylethanolamide; Pol: polydatin.

TABLE 2: Quality score given for each study.

	Type of study	Availability of descriptive data	Numerosity of the series	Presence and appropriateness of comparator arm	Total score of the study
Dell’Anna and De Marzi [29]	2	2	1	-1	4
Di Francesco and Pizzagallo [22]	3	2	-1	0	4
Dionisi and Senatori [30]	2	2	1	-1	4
Giugliano et al. [31]	2	2	1	-1	4
Indraccolo and Barbieri [20]	0	3	-1	-1	1
Murina et al. [32]	3	2	-1	1	5
Stocco and Schievano [34]	2	2	-1	-1	2

No observational study with comparator arm has been found (so the Newcastle-Ottawa scale was not applied). The Giugliano et al. [31] study is a two-arm study; both arms are treated with the m-(PEA/Pol).

nerve stimulation (TENS), and pain value at enrolment. These items were assessed as independent variables.

Figure 2 illustrates the conditional probability of each type of independent variables for the five types of pain (dysmenorrhea, dysuria, dyschezia, dyspareunia, and chronic pelvic pain) for good responders, poor responders, and nonresponders at the three-month follow-up.

In chronic pelvic pain, there is a 19.0% conditional probability to find good responders among patients with pain score at enrolment of 6 to 8; there is a conditional probability of 6.8% to find poor responders among patients with a pain score at enrolment of 6 to 8. Poor responders have a 41.8% conditional probability to use analgesics. The conditional probability that nonresponders associate with any of the variables reported in Figure 2 is less than 5% (not signif-

icant). Additionally, the type of painful disease does not matter on responders’ rates.

In the dysmenorrhea and dysuria group (Figure 3), good responders, poor responders, and nonresponders are not found to be associated to any of the variables assessed. In dyspareunia group (Figure 3), good responders have a conditional probability of 20.6% to undergo TENS, while in the dyschezia group (Figure 3), good responders have a conditional probability of 5.7% to be found among patients with pain score at enrolment of 6 to 8 and of 13.0% to be found among patients with pain score at enrolment of more than 8. Again, the type of painful disease does not matter on responders rates.

Finally, Table 4 reports the percentage of concordance among number of improvement or no-improvement in at least

TABLE 3: Quality score attributed at individual patient level (first column, left side). Additionally, the unconditional probabilities of good responders, poor responders, and nonresponders are reported as crude numbers and rates, according with type of pain.

	Nonresponders	Poor responders	Good responders
Chronic pelvic pain ($N = 64$) -Quality score: 3.6 (3.4-3.8)	14 (21.9%)	17 (26.6%)	33 (51.6%)
Dysmenorrhea ($N = 34$) -Quality score: 3.9 (3.7-4.1)	6 (17.6%)	3 (8.8%)	25 (73.5%)
Dyspareunia ($N = 28$) -Quality score: 4.0 (3.6-4.4)	3 (10.7%)	2 (7.1%)	23 (82.1%)
Dyschezia ($N = 15$) -Quality score: 3.5 (3.0-4.0)	3 (20.0%)	2 (13.3%)	10 (66.7%)
Dysuria ($N = 19$) -Quality score: 3.8 (3.5-4.2)	1 (5.3%)	0	18 (94.7%)

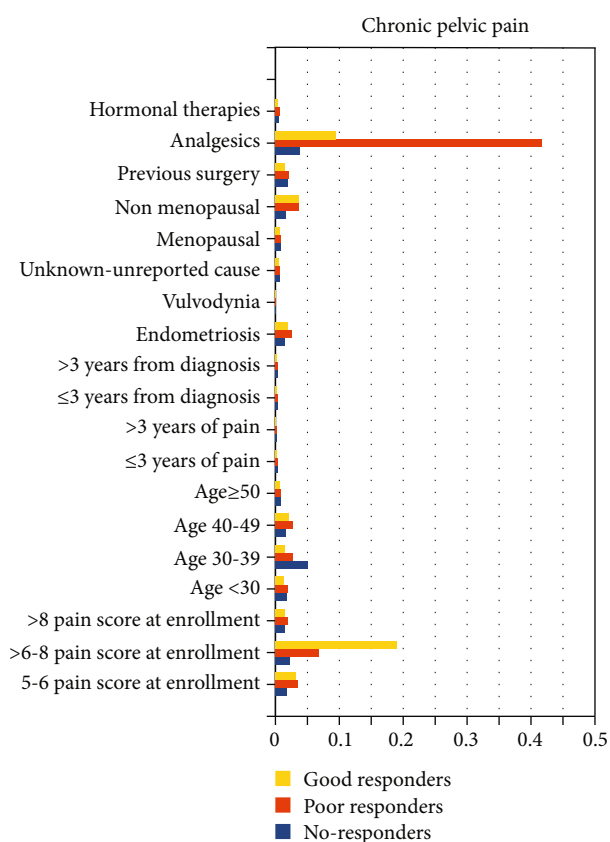


FIGURE 2: Conditional probabilities to be good responders, poor responders, and nonresponders for each variables assessed in chronic pelvic pain group.

one acute pain and chronic pelvic pain at the three-month follow-up. The concordances observed are all over 50%.

4. Discussion

The present review was aimed at finding the best responder female patient to the m-PEA in chronic pelvic pain. Instead, basing on the available literature, the work is able to find the best responder female patient to short-duration treatment with PEA comiconized with Pol at the three-month fol-

low-up, assessing more variables available at individual patients slides. Prior to initiate a randomized trial, such a kind of study would be advisable, to know the proportion of patients needed to be enrolled to obtain an appropriate sample size and their characteristics.

Ninety-three heterogeneous patients had any type of pelvic pain (pain score equal to or more greater than 5). More than 50.0% of them have a very good improvement (3 pain score points or more) of their pain in at least one pain item, and more than 70% are overall responders at the three-month follow-up. All these patients have been treated with m-(PEA/Pol) for two months or more. The improvement of pain scores is not affected by type of painful disease, proving that m-(PEA/Pol) acts on pain and not on the specific painful disease. Those results were achieved from individual patient series with intermediate quality score, extracted from 7 studies of low quality at aggregate level. Five out of 7 studies have not any comparator arm and are not blinded. In our opinion, this is the higher concern as placebo efficacy is a well-known bias for pain killer drugs assessment, sometimes hard to control in clinical trials on pains [40].

In chronic pelvic pain and dyschezia groups of patients, we found that the best responders at the three-month follow-up to the m-(PEA/Pol) therapy are the ones with pain score at enrolment of more than 6. Additionally, good responders to dyspareunia, dysmenorrhea, dysuria, and dyschezia are likely to be good responders also to chronic pelvic pain (Table 4), thereby confirming that pain control by m-(PEA/Pol) would be exerted on pain sensitization [41]. On the other hand, no other factors than higher pain score at enrolment has been linked with pain reduction at the three-month follow-up, excluding the TENS treatment for dyspareunia and the use of analgesics for chronic pelvic pain in poor responders patients.

Therefore, in planning a hypothetical randomized trial aiming to prove the efficacy of the m-(PEA/Pol) combination, chronic pelvic pain of more than 6 pain score point cases should be enrolled. Arranging both a placebo arm and a no-treatment arm [40] would be advisable for ruling out the efficacy of the placebo from the hypothetical efficacy of the m-(PEA/Pol). In all these hypothetical arms, the consumption of analgesics has to be assessed.

The present review does not exclude that poor responders to the m-(PEA/Pol) at the three-month follow-

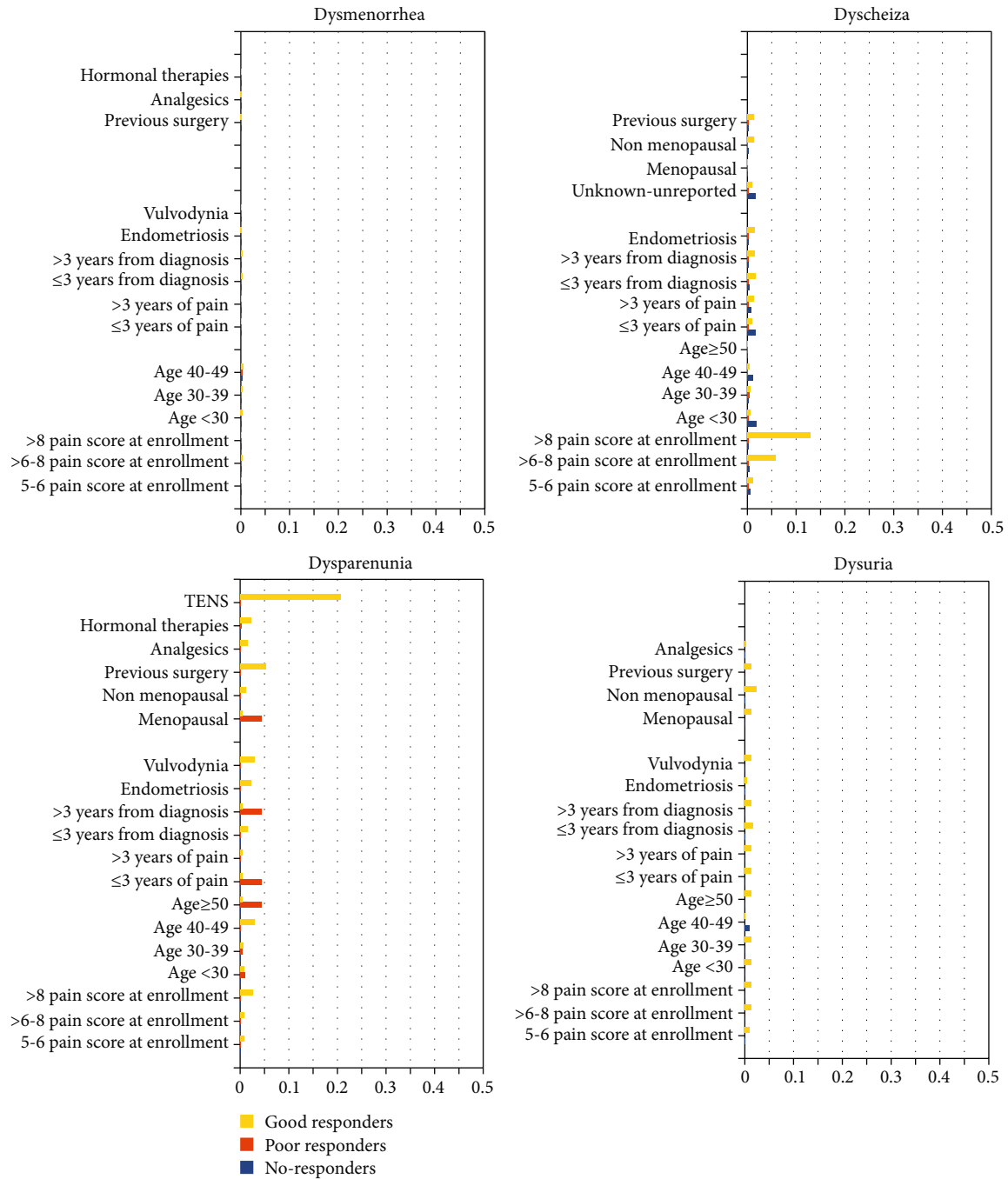


FIGURE 3: Conditional probabilities to be good responders, poor responders, and nonresponders for each variables assessed in dysmenorrhea, dyschezia, dyspareunia, and dysuria groups.

up would be able to become good responders after more than three-month therapy. Poor responders seem being 10-25% (Table 3). The experimental design of the reviewed studies available in literature are mainly focused on a three month follow-up. Therefore, further data on more than three months therapy are needed. Additionally, dyspareunia has been assessed without considering deep or superficial dyspareunia complained by patients with endometriosis or vulvodynia. TENS has been only administered to patients with vulvodynia in the Murina et al. study [32], explaining

why good responders in the dyspareunia group associate with TENS treatment. While the specific localization of dyspareunia was not reported in the pooled case database, it is likely that good responders to the combination complained of superficial dyspareunia, as superficial dyspareunia is complained in vulvodynia cases.

A limitation of the study comes from missing information from unavailable databases. It would be very interesting to assess unavailable databases [23, 28, 33, 35, 36] at individual patient level because missing studies assess the

TABLE 4: Rates of concordances among chronic pelvic pain and other type of pain of acute behaviour.

	Good responders in both	No good responders in both	Percentage of association
Dysmenorrhea and chronic pelvic pain ($N = 19$)	9	8	17/19 89.5%
Dyspareunia and chronic pelvic pain ($N = 16$)	9	3	12/16 75.0%
Dyschezia and chronic pelvic pain ($N = 14$)	5	5	10/14 71.4%
Dysuria and chronic pelvic pain ($N = 8$)	3	3	6/8 75.0%

effectiveness of m-(PEA/Pol) in painful bladder syndrome/interstitial cystitis [23, 33], primary dysmenorrhea [38], and more painful cases of endometriosis [28, 35]. All these studies demonstrate significant improvement of pain. The Tartaglia et al. study [36] and the Cobellis et al. [28] study are also randomized trials. The results would suggest a good degree of efficacy for m-(PEA/Pol) along with very good effectiveness.

A further limitation of the present study is that the number of pooled patients with pain is low for pelvic pains of acute behaviour (dyspareunia, dysmenorrhea, dyschezia, and dysuria). Therefore, number of cooccurrence of chronic pelvic pain and other type of pain is very low, as reported in Table 4. While the probabilistic approach to the analysis does not need many data, a randomized trial would take into consideration that cooccurrence of chronic pelvic pain, and other types of pelvic pain, is an uncommon event.

As no data has been registered in chronic pelvic pain for m-PEA without Pol, it is still unclear how effective is the combination of m-(PEA/Pol) versus single micronized agent administration (specifically, the m-PEA). m-PEA has been reported to be effective for other kinds of chronic pain [42]. The item should be a matter of further investigation.

Quite stringent criteria for quality assessment could lead to underrating some study basing on a questionable subjective view. The step is needed for being as soon honest as possible for the interpretation of the available literature at individual patient level, thereby addressing the issue of poor-quality studies exposed by Gabrielsson et al. [9]. Moreover, the individual patient approach is able to overcome the confusion between effectiveness and efficacy of PEA.

In conclusion, short-duration treatments with m-(PEA/Pol) would allow an improvement of pain score in chronic pelvic pain patients of 3/4 of cases. Half of treated patients would improve by at least 3 points of pain score, while 1/4 would improve of 2 points of pain score. The improvement is not conditioned by any painful disease. Best responders in chronic pelvic pain are patients with pain score at enrolment between 6 and 8. Other acute pelvic pains (dyspareunia, dyschezia, dysuria, and dysmenorrhea) would benefit from treating chronic pelvic pain. These evidences came from low-quality study and from pooled case databases of intermediate quality. They strongly suggest that efficacy and effectiveness of the m-(PEA/Pol) short-time treatments for chronic pelvic pain in female patients have to be proved against placebo and no-treatment in randomized trial.

Data Availability

The articles cited for the organizing database [16, 18, 24–27, 29] report the corresponding authors' names and contacts. Authors can be contacted for information on data.

Conflicts of Interest

All authors disclose no conflict of interest.

Authors' Contributions

Ugo Indraccolo planned the study, performed systematic research and calculations, and wrote the article. Alessandro Favilli gave his contribution in assessing the articles and giving final quality score along with Ugo Indraccolo. All other authors shared their databases allowing the final assessment. They are listed alphabetically.

Acknowledgments

The authors are grateful to Epitech Group SpA, who was able to favour contacts among the authors by using its internal database of articles on PEA and its contacts with corresponding authors of eligible studies. Specifically, the authors thank Dr. T. Cenacchi for her kindly scientific support for assessing and editing the final version of the article. Epitech Group SpA provided financial support for covering language editing and publication fees.

References

- [1] R. R. Myers, W. M. Campana, and V. I. Shubayev, "The role of neuroinflammation in neuropathic pain: mechanisms and therapeutic targets," *Drug Discovery Today*, vol. 11, no. 1-2, pp. 8–20, 2006.
- [2] S. J. Galli, N. Gaudenzio, and M. Tzai, "Mast cells in inflammation and disease: recent progress and ongoing concerns," *Annual Review of Immunology*, vol. 38, no. 1, pp. 49–77, 2020.
- [3] S. Wernersson and G. Pejler, "Mast cell secretory granules: armed for battle," *Nature Reviews. Immunology*, vol. 14, no. 7, pp. 478–494, 2014.
- [4] T. C. Theoharides, K. D. Alysandratos, A. Angelidou et al., "Mast cells and inflammation," *Biochimica et Biophysica Acta*, vol. 2012, pp. 21–33, 2012.

- [5] S. D. Skaper, L. Facci, and D. Giusti, "Mast cells, glia and neuroinflammation: partners in crime?," *Immunology*, vol. 141, no. 3, pp. 314–327, 2014.
- [6] E. Palazzo, L. Luongo, F. Guida et al., "Role of N-acyl ethanolamines in the neuroinflammation: ultramicro-nized palmitoylethanolamide in the relief of chronic pain and neurodegenerative diseases," *Neuropsychiatry*, vol. 9, pp. 2035–2046, 2019.
- [7] R. D'Amico, D. Impellizzeri, S. Cuzzocrea, and R. Di Paola, "ALIAMides update: palmitoylethanolamide and its formulations on management of peripheral neuropathic pain," *International Journal of Molecular Sciences*, vol. 21, no. 15, p. 5330, 2020.
- [8] L. Rankin and C. J. Fowler, "The basal pharmacology of palmitoylethanolamide," *International Journal of Molecular Sciences*, vol. 21, no. 21, p. 7942, 2020.
- [9] L. Gabrielsson, S. Mattson, and C. J. Fowler, "Palmitoylethanolamide for the treatment of pain: pharmacokinetics, safety and efficacy," *British Journal of Clinical Pharmacology*, vol. 82, no. 4, pp. 932–942, 2016.
- [10] S. Petrosino and V. Di Marzo, "The pharmacology of palmitoylethanolamide and first data on the therapeutic efficacy of some of its new formulations," *British Journal of Pharmacology*, vol. 174, no. 11, pp. 1349–1365, 2017.
- [11] E. Gugliandolo, A. F. Peritore, C. Piras, S. Cuzzocrea, and R. Crupi, "Palmitoylethanolamide and related ALIAMides: prohomeostatic lipid compounds for animal health and well-being," *Veterinary Sciences*, vol. 7, no. 2, article 78, 2020.
- [12] S. Beggiato, M. C. Tomasini, and L. Ferraro, "Palmitoylethanolamide (PEA) as a potential therapeutic agent in Alzheimer's disease," *Frontiers in Pharmacology*, vol. 10, p. 821, 2019.
- [13] G. Mattace Raso, R. Russo, A. Calignano, and R. Meli, "Palmitoylethanolamide in CNS health and disease," *Pharmacological Research*, vol. 86, pp. 32–41, 2014.
- [14] P. Clayton, M. Hill, N. Bogoda, S. Subah, and R. Venkatesh, "Palmitoylethanolamide: a natural compound for health management," *International Journal of Molecular Sciences*, vol. 22, no. 10, p. 5305, 2021.
- [15] S. D. Skaper, L. Facci, M. Fusco et al., "Palmitoylethanolamide, a naturally occurring disease-modifying agent in neuropathic pain," *Inflammopharmacology*, vol. 22, no. 2, pp. 79–94, 2014.
- [16] D. Impellizzeri, G. Bruschetta, M. Cordaro et al., "Micronized/ultramicro-nized palmitoylethanolamide displays superior oral efficacy compared to nonmicronized palmitoylethanolamide in a rat model of inflammatory pain," *Journal of Neuroinflammation*, vol. 11, no. 1, p. 136, 2014.
- [17] S. Petrosino, M. Cordaro, R. Verde et al., "Oral ultramicro-nized palmitoylethanolamide: plasma and tissue levels and spinal antihyperalgesic effect," *Frontiers in Pharmacology*, vol. 9, p. 249, 2018.
- [18] A. Paladini, M. Fusco, T. Cenacchi, C. Schievano, A. Piroli, and G. Varrassi, "Palmitoylethanolamide, a special food for medical purposes, in the treatment of chronic pain: a pooled data meta-analysis," *Pain Physician*, vol. 19, no. 2, pp. 11–24, 2016.
- [19] U. Indraccolo, S. R. Indraccolo, and F. Mignini, "Micronized palmitoylethanolamide/trans-polydatin treatment of endometriosis-related pain: a meta-analysis," *Annali Dell'istituto Superiore Di Sanita*, vol. 53, pp. 125–134, 2017.
- [20] U. Indraccolo and F. Barbieri, "Effect of palmitoylethanolamide-polydatin combination on chronic pelvic pain associated with endometriosis: preliminary observations," *European Journal of Obstetrics, Gynecology, and Reproductive Biology*, vol. 150, no. 1, pp. 76–79, 2010.
- [21] R. Di Paola, R. Fusco, E. Gugliandolo et al., "Co-micronized palmitoylethanolamide/polydatin treatment causes endometriotic lesion regression in a rodent model of surgically induced endometriosis," *Frontiers in Pharmacology*, vol. 7, p. 382, 2016.
- [22] A. Di Francesco and D. Pizzagallo, "Use of micronized palmitoylethanolamide and trans-polydatin in chronic pelvic pain associated with endometriosis. An open-label study," *G Ital Ostet E Ginecol*, vol. 36, pp. 353–358, 2014.
- [23] M. Cervigni, L. Nasta, C. Schievano, N. Lampropoulou, and E. Ostaro, "Micronized palmitoylethanolamide-polydatin reduces the painful symptomatology in patients with interstitial cystitis/bladder pain syndrome," *BioMed Research International*, vol. 2019, Article ID 9828397, 6 pages, 2019.
- [24] A. P. Peritore, R. D'Amico, M. Cordaro et al., "PEA/polydatin: anti-inflammatory and antioxidant approach to counteract DNBS-induced colitis," *Antioxidants*, vol. 10, no. 3, article 464, 2021.
- [25] J. T. Dweyer, P. M. Coates, and M. J. Smith, "Dietary supplements: regulatory challenges and research resources," *Nutrients*, vol. 10, no. 1, article 41, 2018.
- [26] B. B. Artukoglu, C. Beyer, A. Zuloft-Shani, E. Brener, and M. H. Bloch, "Efficacy of palmitoylethanolamide for pain: a meta-analysis," *Pain Physician*, vol. 20, no. 5, pp. 353–362, 2017.
- [27] M. P. Davis, B. Behm, Z. Mehta, and C. Fernandez, "The potential benefits of palmitoylethanolamide in palliation: a qualitative systematic review," *The American Journal of Hospice & Palliative Care*, vol. 36, no. 12, pp. 1134–1154, 2019.
- [28] L. Cobellis, M. A. Castaldi, V. Giordano et al., "Effectiveness of the association micronized N-palmitoylethanolamine (PEA)-transpolydatin in the treatment of chronic pelvic pain related to endometriosis after laparoscopic assessment: a pilot study," *European Journal of Obstetrics, Gynecology, and Reproductive Biology*, vol. 158, no. 1, pp. 82–86, 2011.
- [29] A. Dell'Anna and C. A. De Marzi, "Mast cells and microglia: new therapeutic targets for the treatment of endometriosis-associated symptomatology," *Giornale Italiano Di Ostetricia E Ginecologia*, vol. 39, no. 4-5, pp. 193–201, 2017.
- [30] B. Dionisi and R. Senatori, "Aliamides in the treatment of vulvodinia," *Giornale Italiano Di Ostetricia E Ginecologia*, vol. 37, no. 3, pp. 121–126, 2015.
- [31] E. Giugliano, E. Cagnazzo, I. Soave, G. Lo Monte, J. M. Wenger, and R. Marci, "The adjuvant use of N-palmitoylethanolamine and transpolydatin in the treatment of endometriotic pain," *European Journal of Obstetrics, Gynecology, and Reproductive Biology*, vol. 168, no. 2, pp. 209–213, 2013.
- [32] F. Murina, A. Graziottin, R. Felice, G. Radici, and C. Tognocchi, "Vestibulodynia: synergy between palmitoylethanolamide + transpolydatin and transcutaneous electrical nerve stimulation," *Journal of Lower Genital Tract Disease*, vol. 17, no. 2, pp. 111–116, 2013.
- [33] M. Sommariva, C. Schievano, and O. Saleh, "Micronized palmitoylethanolamide reduces bladder chronic pelvic pain due to different etiologies and improves bladder function," *Pelviperrineology*, vol. 36, pp. 92–96, 2017.
- [34] E. Stocco, C. Schievano, and G. Dodi, "Chronic pelvic pain: preliminary study with PEA-m + polydatin in patients referred

- to a proctologic-pelvic floor clinic," *Pelviperrineologia*, vol. 33, pp. 34–38, 2014.
- [35] E. Stochino Loi, A. Pontis, V. Cofelice et al., "Effect of ultramicrosized-palmitoylethanolamide and co-microsized palmitoylethanolamide/polydatin on chronic pelvic pain and quality of life in endometriosis patients: an open-label pilot study," *International Journal of Women's Health*, vol. 11, pp. 443–449, 2019.
- [36] E. Tartaglia, M. Armentano, B. Giugliano et al., "Effectiveness of the association N-palmitoylethanolamine and transpolydatin in the treatment of primary dysmenorrhea," *Journal of Pediatric and Adolescent Gynecology*, vol. 28, no. 6, pp. 447–450, 2015.
- [37] G. Guyatt, A. D. Oxman, E. A. Akl et al., "GRADE guidelines: 1. Introduction-GRADE evidence profiles and summary of findings tables," *Journal of Clinical Epidemiology*, vol. 64, no. 4, pp. 383–394, 2011.
- [38] G. A. Wells, B. Shea, D. O'Connell et al., "The Newcastle-Ottawa scale (NOS) for assessing the quality of nonrandomised studies in meta-analyses," *Ottawa Hospital Research Institute*, vol. 2, no. 1, pp. 1–12, 2021.
- [39] A. R. Jadad, R. A. Moore, D. Carroll et al., "Assessing the quality of reports of randomized clinical trials: is blinding necessary?," *Controlled Clinical Trials*, vol. 17, no. 1, pp. 1–12, 1996.
- [40] L. Vase and K. Wartolowska, "Pain, placebo, and test of treatment efficacy: a narrative review," *British Journal of Anaesthesia*, vol. 123, no. 2, pp. e254–e262, 2019.
- [41] S. D. Skaper, L. Facci, and P. Giusti, "Glia and mast cells as targets for palmitoylethanolamide, an anti-inflammatory and neuroprotective lipid mediator," *Molecular Neurobiology*, vol. 48, no. 2, pp. 340–352, 2013.
- [42] A. Gatti, M. Lazzari, V. Gianfelice, A. Di Paolo, E. Sabato, and A. F. Sabato, "Palmitoylethanolamide in the treatment of chronic pain caused by different etiopathogenesis," *Pain Medicine*, vol. 13, no. 9, pp. 1121–1130, 2012.

Research Article

Oridonin Attenuates Cisplatin-Induced Acute Kidney Injury via Inhibiting Oxidative Stress, Apoptosis, and Inflammation in Mice

Hyemin Gu ¹, Mi-Gyeong Gwon ¹, Jong Hyun Kim ², Jaechan Leem ³,
and Sun-Jae Lee ¹

¹Department of Pathology, School of Medicine, Daegu Catholic University, Daegu 42472, Republic of Korea

²Department of Biochemistry, School of Medicine, Daegu Catholic University, Daegu 42472, Republic of Korea

³Department of Immunology, School of Medicine, Daegu Catholic University, Daegu 42472, Republic of Korea

Correspondence should be addressed to Jaechan Leem; jcim@cu.ac.kr

Received 28 November 2021; Revised 25 February 2022; Accepted 30 March 2022; Published 16 April 2022

Academic Editor: Madiha Ahmed

Copyright © 2022 Hyemin Gu et al. This is an open access article distributed under the Creative Commons Attribution License, which permits unrestricted use, distribution, and reproduction in any medium, provided the original work is properly cited.

The use of cisplatin, a chemotherapy drug, is often limited due to its renal side effects such as acute kidney injury (AKI). However, there are no validated medications to prevent or treat cisplatin-induced AKI. Oridonin is the major bioactive component of *Isodon rubescens* (*Rabdosia rubescens*) and exhibits anticancer, antioxidative, and anti-inflammatory effects. Recent studies have shown that oridonin alleviated a variety of inflammatory diseases, including renal diseases, in rodents. This study was aimed at investigating the potential renoprotective effect of oridonin on cisplatin-induced AKI. Male C57BL/6 mice were administered with cisplatin (20 mg/kg) with or without oridonin (15 mg/kg). Oridonin administration to mice after cisplatin injection attenuated renal dysfunction and histopathological changes. Upregulation of tubular injury markers was also suppressed by oridonin. Mechanistically, oridonin suppressed lipid peroxidation and reversed the decreased ratio of reduced to oxidized glutathione in cisplatin-injected mice. The increase in cisplatin-induced apoptosis was also alleviated by the compound. Moreover, oridonin inhibited cytokine overproduction and attenuated immune cell infiltration in cisplatin-injected mice. Altogether, these data demonstrated that oridonin alleviates cisplatin-induced kidney injury via inhibiting oxidative stress, apoptosis, and inflammation.

1. Introduction

Acute kidney injury (AKI) is characterized by a sudden decrease in renal function and is one of the major global health problems [1]. The severity of AKI is positively associated with in-hospital mortality, length of hospital stay, and medical care costs [2]. In the long term, AKI is also related to an increased risk of cardiovascular events, progression to chronic kidney disease, and long-term mortality [2]. The primary causes of AKI include renal ischemia-reperfusion, sepsis, and nephrotoxins. Among them, nephrotoxic drugs are increasingly considered as substantial contributors to AKI in hospitalized patients [3]. Cisplatin is a widely used chemotherapy drug to treat many types of cancer, including breast, testicular, and ovarian cancers [4]. Although the drug

has potent antitumor effects, its serious side effects often limit its clinical use [4]. Nephrotoxicity is an important side effect of cisplatin therapy, and the nephrotoxic effects of cisplatin are dose-dependent and cumulative [5]. Unfortunately, despite the limited clinical application of cisplatin due to renal side effects, there are no validated drugs that prevent or treat its nephrotoxicity.

Oridonin is a diterpenoid compound found in *Isodon rubescens* (*Rabdosia rubescens*) [6]. Accumulating evidence suggest that oridonin has potent anticancer, antioxidative, and anti-inflammatory activities [7–9]. Although many studies have focused on elucidating the antitumor effect of oridonin [7], emerging evidence suggest that the compound inhibits renal ischemia-reperfusion injury in mice via suppressing inflammatory pathways [10, 11]. Moreover,

oridonin attenuated diabetes-associated renal inflammation and injury in rats [12], suggesting that the compound has a protective action against both acute and chronic kidney injury. However, it has not yet been determined whether oridonin has a beneficial action on cisplatin nephrotoxicity. Thus, in the current study, we examined the effect of oridonin on cisplatin-induced kidney injury and explored the mechanism.

2. Materials and Methods

2.1. Animal Experiments. Male C57BL/6 mice were obtained from HyoSung Science (Daegu, Korea) and maintained at a temperature of 20–24°C and humidity of 60–70%. The mice were grouped into three groups ($n = 8$ per group): the control group, the CP group, and the CP+Ori group. The CP group received a single intraperitoneal injection of cisplatin (20 mg/kg; Sigma-Aldrich, St. Louis, MO, USA). The CP+Ori group was given an intraperitoneal administration of oridonin (15 mg/kg; dissolved in DMSO; Sigma-Aldrich) daily for 3 consecutive days, starting from 1 hour after cisplatin injection. The control group received intraperitoneal injections of an equal volume of DMSO daily for 3 consecutive days. All mice were sacrificed 72 hours after a single dose of cisplatin. The doses of oridonin and cisplatin were selected based on the results of previous studies [10, 13]. All animal procedures were approved by the Institutional Animal Care and Use Committee of the Daegu Catholic University Medical Center (DCIAFCR-200626-12-Y).

2.2. Plasma and Tissue Biochemical Assays. Serum creatinine and blood urea nitrogen (BUN) levels were assessed using an automatic analyzer (Hitachi, Osaka, Japan). Serum tumor necrosis factor- α (TNF- α) and interleukin-6 (IL-6) levels were analyzed using ELISA kits (R&D Systems, Minneapolis, MN, USA). Malondialdehyde (MDA) levels were analyzed using a MDA assay kit (Sigma-Aldrich). Reduced glutathione (GSH) and oxidized glutathione (GSSG) levels were measured using a GSH assay kit (Enzo Life Sciences, Farmingdale, NY, USA). All analyses were conducted following the manufacturers' protocols.

2.3. Histological and Immunohistochemistry (IHC) Staining. Formalin-fixed tissues were dehydrated, cleared, and embedded in paraffin. The tissue blocks were sectioned and stained with hematoxylin and eosin (H&E) or periodic acid-Schiff (PAS). Tubular injury score was assessed in 5 randomly selected fields per sample, as previously described [14, 15]. For IHC, primary antibodies against neutrophil gelatinase-associated lipocalin (NGAL; Santa Cruz Biotechnology, Santa Cruz, CA, USA), kidney injury molecule-1 (KIM-1; Santa Cruz Biotechnology), 4-hydroxy-2-nonenal (4-HNE; Invitrogen, Carlsbad, CA, USA), F4/80 (Santa Cruz Biotechnology), and CD4 (Novus Biologicals, Littleton, CO, USA) antibodies were used. Mouse IgG1 isotype control antibody (R&D Systems) was used as a primary antibody for negative control. Positive areas were examined in 5 randomly selected fields at 400x magnification per sample using a computerized image analyzer (i-Solution DT software; IMT i-Solu-

tion, Coquitlam, BC, Canada), and the results were presented as percentage of the positively stained area with respect to the total area analyzed. Positive cells were examined in 10 randomly selected fields at 1000x magnification per sample.

2.4. Western Blot Analysis. Western blot analysis was conducted using primary antibodies against cleaved caspase-3 (Cell Signaling Technology, Danvers, MA, USA), caspase-3 (Cell Signaling Technology), TNF- α (Abcam, Cambridge, MA, USA), and glyceraldehyde-3-phosphate dehydrogenase (GAPDH; Cell Signaling Technology), as previously described [15]. Protein bands were visualized using enhanced chemiluminescence reagents (Thermo Fisher Scientific, Waltham, MA, USA).

2.5. qPCR Analysis. Total RNA isolation was performed using the TRIzol reagent (Sigma-Aldrich). Total RNA was reverse-transcribed into cDNA using the PrimeScript RT Reagent Kit (TaKaRa, Tokyo, Japan). For qPCR analysis, the Power SYBR Green PCR Master Mix (Thermo Fisher Scientific) and the Thermal Cycler Dice Real Time System III (TaKaRa) were used. Primers are shown in Table 1. GAPDH was used as a reference gene. Data were analyzed using $2^{-\Delta\Delta CT}$ method.

2.6. TUNEL Assay. Apoptosis was examined using a TUNEL assay kit (Roche Diagnostics, Indianapolis, IN, USA) following the manufacturer's protocol. Briefly, the kidney sections were deparaffinized, rehydrated, and permeabilized for 30 min at room temperature with proteinase K in 10 mM Tris-HCl, pH 7.4. After washing, the sections were incubated in the TUNEL reaction mixture for 1 h at 37°C. DAPI was used for nuclear staining. Positive cells were examined in 10 randomly selected fields at 600x magnification per sample.

2.7. Statistical Analysis. Data are presented as mean \pm SEM. Differences among the groups were analyzed with one-way ANOVA and Bonferroni's post hoc tests. A p value less than 0.05 was considered statistically significant.

3. Results

3.1. Oridonin Ameliorated Renal Dysfunction and Structural Damage in Cisplatin-Injected Mice. To assess renal function, serum creatinine and BUN levels, indicators of renal function [16], were measured in all experimental groups. Intraperitoneal injection of cisplatin increased serum levels of the indicators (Figures 1(a) and 1(b)). Cisplatin-injected mice exhibited significant tubular damage, including tubular dilatation and cast formation, as shown by histological examination (Figures 1(c) and 1(d)). However, these changes were significantly attenuated by oridonin (Figures 1(a)–1(d)).

Renal tubular injury is a hallmark of cisplatin-induced kidney injury [17]. To more clearly assess the action of oridonin on cisplatin-induced tubular injury, the renal expression of NGAL and KIM-1, tubular injury markers [18], was examined using IHC staining. Expression of the markers was elevated after cisplatin injection (Figures 2(a)–2(c)).

TABLE 1: List of primers used in this study.

Target genes	Primer sequences	Accession no.
NGAL	F: 5' - GACCTAGTAGCTGCTGAAACC -3' R: 5' - GAGGATGGAAGTGACGTTGTAG -3'	NM_130741
KIM-1	F: 5' - TCCACACATGTACCAACATCAA -3' R: 5' - GTCACAGTGCCATTCCAGTC -3'	NM_001161356
TNF- α	F: 5' -GACGTGGAAGTGGCAGAAGAG-3' R: 5' -CCGCCTGGAGTTCTGGAA-3'	NM_013693
IL-6	F: 5' -CCAGAGATACAAAGAAATGATGG-3' R: 5' -ACTCCAGAAGACCAGAGGAAAT-3'	NM_031168
IL-1 β	F: 5' - GCAACTGTTCTGAACTCAACT -3' R: 5' - ATCTTTTGGGGTCCGTCAACT -3'	NM_008361
GAPDH	F: 5' -ACTCCAATCAGGCAAATTC-3' R: 5' -TCTCCATGGTGGTGAAGACA-3'	NM_001289726

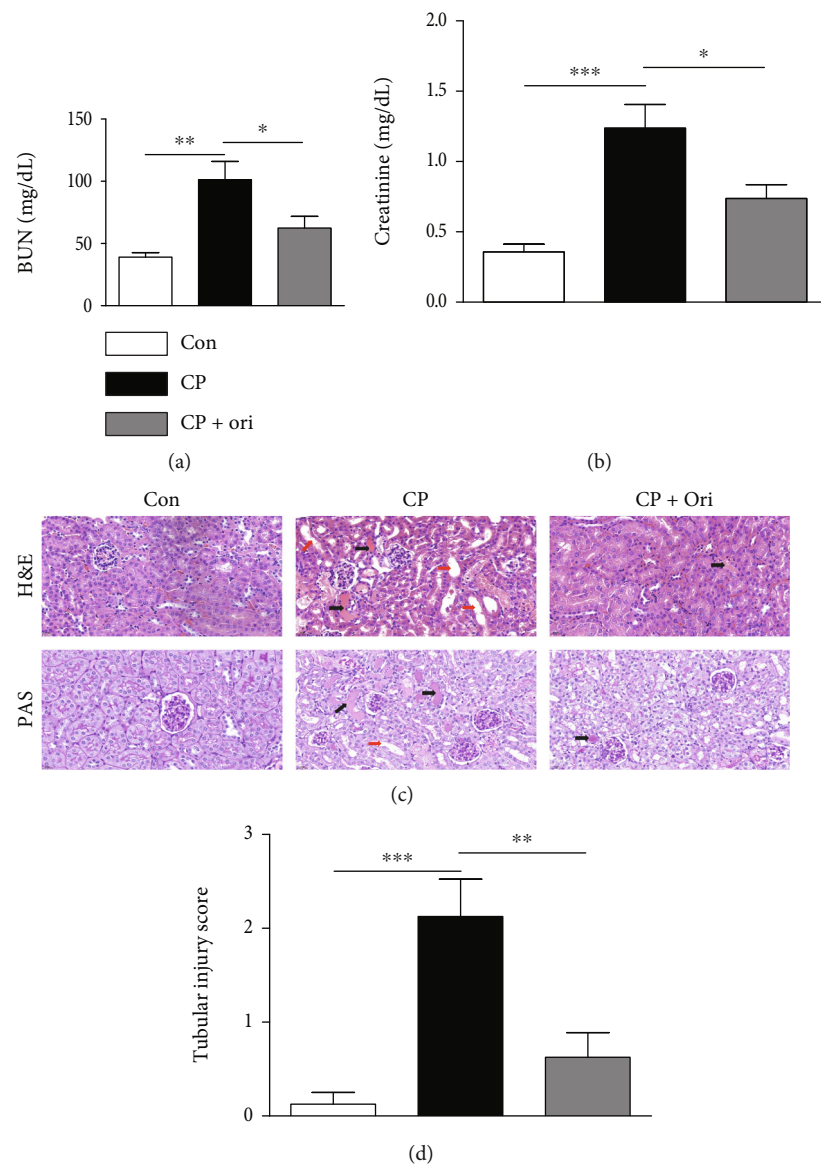


FIGURE 1: Effect of oridonin on renal function and histological abnormalities in cisplatin-injected mice. (a) Serum creatinine levels. (b) BUN levels. (c) H&E and PAS staining of kidney sections. Scale bar = 40 μ m. Red arrows indicate tubular dilatation. Black arrows indicate cast deposition in the lumens of tubules. (d) Tubular injury score. $n = 8$ per group. * $p < 0.05$, ** $p < 0.01$, and *** $p < 0.001$.

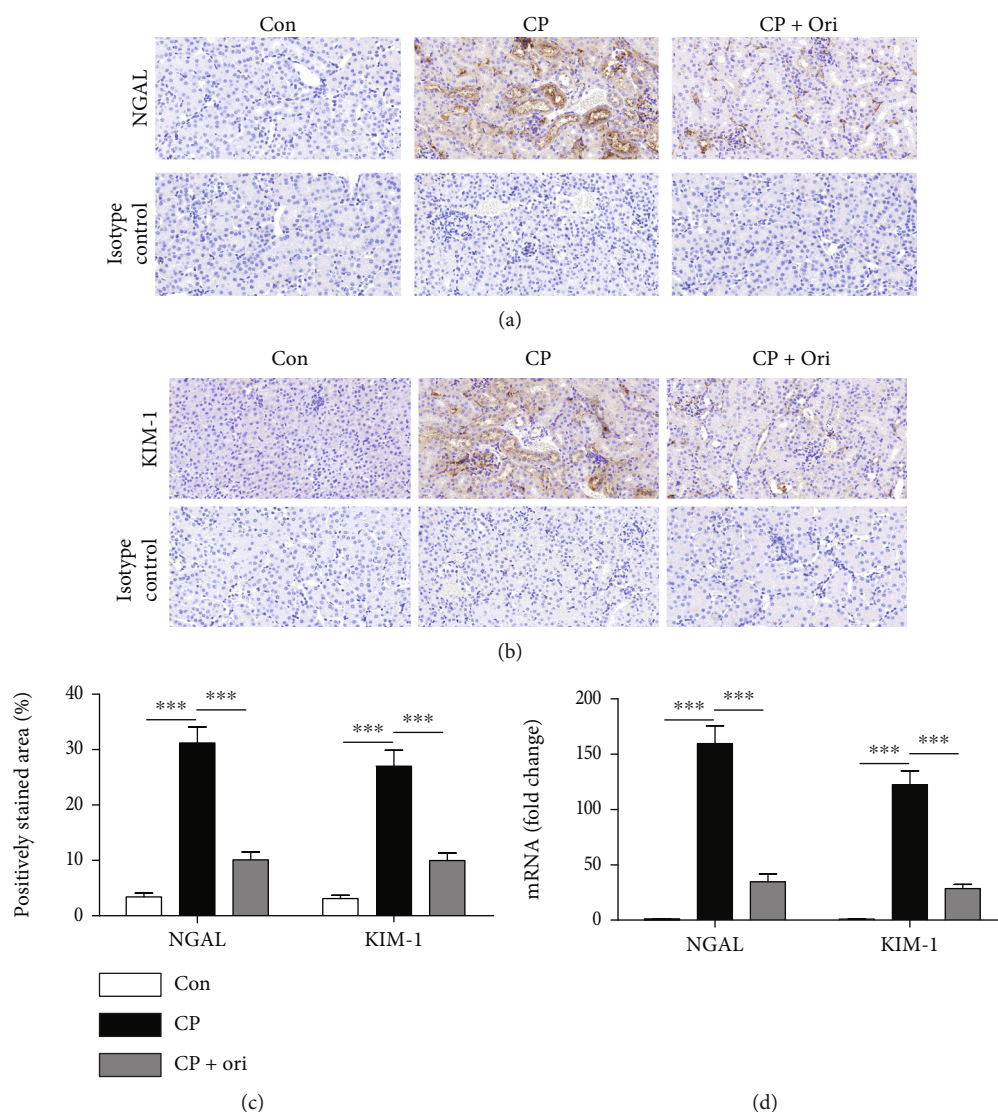


FIGURE 2: Effect of oridonin on NGAL and KIM-1 expression. (a) IHC staining for NGAL. Scale bar = 40 μm . (b) IHC staining for KIM-1. Scale bar = 40 μm . (c) Quantification of positive staining for NGAL and KIM-1. (d) Relative mRNA levels of NGAL and KIM-1. $n = 8$ per group. *** $p < 0.001$.

Moreover, their mRNA levels were also increased (Figure 2(d)). However, the upregulation of the markers was significantly inhibited by oridonin (Figures 2(a)–2(d)).

3.2. Oridonin Suppressed Oxidative Stress. Oxidative stress is a crucial mechanism of cisplatin nephrotoxicity [19]. Therefore, we examined renal expression of 4-HNE, a lipid peroxidation product [20], in all experimental groups. Cisplatin injection increased 4-HNE expression in the renal cortex compared to control group (Figures 3(a) and 3(b)). Amounts of MDA, another lipid peroxidation product [20], were also increased after cisplatin injection (Figure 3(c)). However, oridonin significantly lowered the increased levels of lipid peroxidation products induced by cisplatin (Figures 3(a)–3(c)). In addition, after cisplatin injection, GSSG levels (Figure 3(d)) were increased in kidneys, while GSH levels (Figure 3(e)) and GSH/GSSG ratios (Figure 3(f)) were decreased. These alterations were significantly reversed by oridonin

(Figures 3(d)–3(f)), indicating that the compound suppressed cisplatin-induced oxidative stress.

3.3. Oridonin Attenuated Apoptotic Cell Death. Because apoptosis of tubular cells is frequently observed in cisplatin-induced kidney injury [5], TUNEL assay was conducted to assess the effect of oridonin on apoptosis. Cisplatin injection increased the number of TUNEL-positive cells in the kidney (Figures 4(a) and 4(b)). Caspase-3 cleavage was also increased (Figures 4(c) and 4(d)). However, cisplatin-induced apoptosis was significantly inhibited by oridonin (Figures 4(a)–4(d)).

3.4. Oridonin Inhibited Inflammatory Responses. Inflammation also contributes to the pathophysiology of cisplatin nephrotoxicity [5]. Cisplatin-injected mice had elevated serum TNF- α and IL-6 levels compared to controls (Figure 5(a)). Renal levels of TNF- α , IL-6, and IL-1 β mRNA

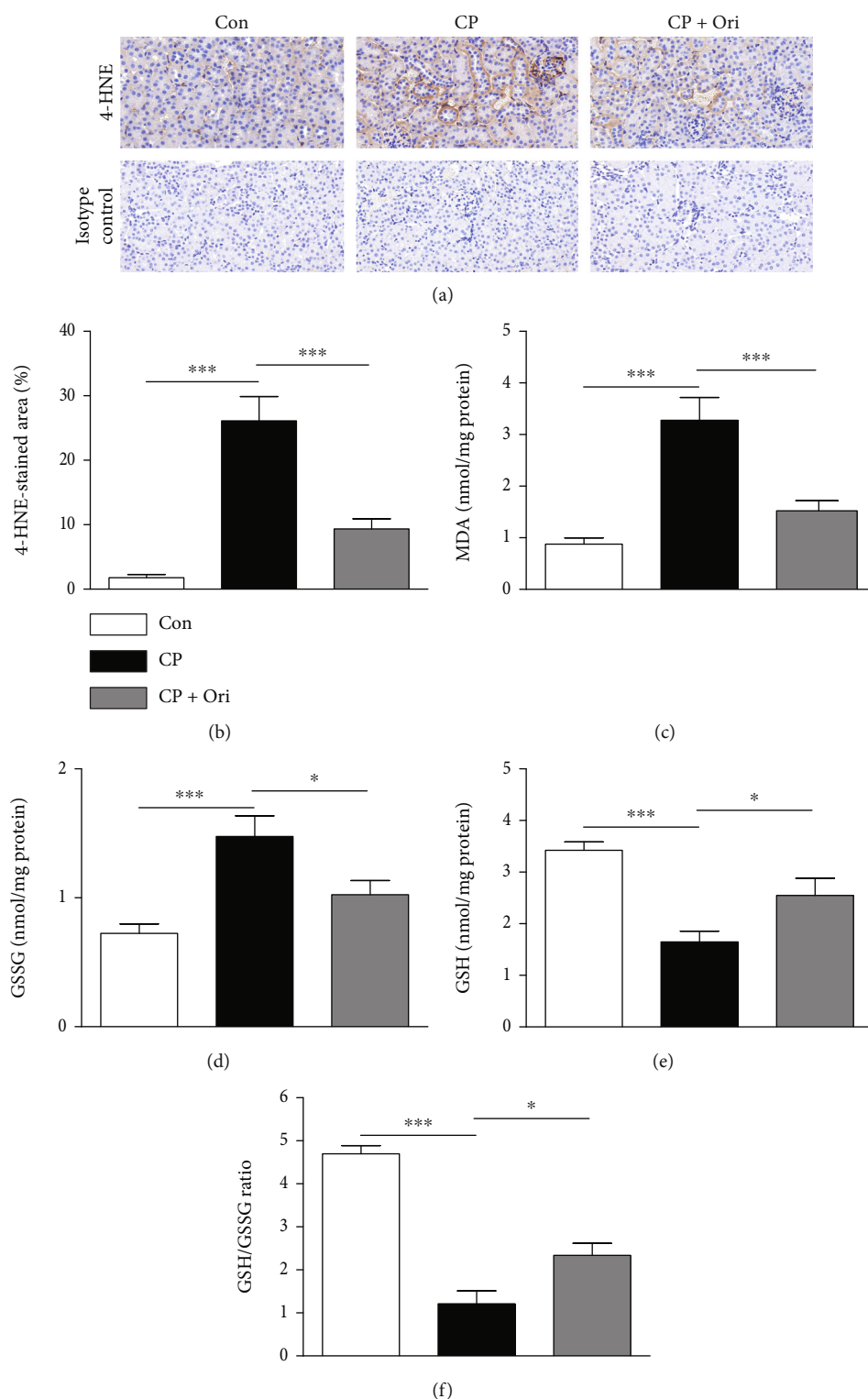


FIGURE 3: Effect of oridonin on oxidative stress. (a) IHC staining for 4-HNE. Scale bar = 40 μ m. (b) Quantification of positive staining for 4-HNE. (c) Renal MDA levels. (d) Renal GSSG levels. (e) Renal GSH levels. (f) GSH/GSSG ratios. $n = 8$ per group. * $p < 0.05$ and *** $p < 0.001$.

was also increased after cisplatin injection (Figure 5(b)). Increase protein levels of TNF- α were also detected by Western blot analysis (Figures 5(c) and 5(d)). However, oridonin significantly lowered serum and tissue levels of the cytokines (Figures 5(a)–5(d)).

Because immune cells infiltrate into the kidney and secrete large amounts of cytokines during cisplatin-induced kidney injury [5], we next performed IHC staining with antibodies against F4/80 and CD4 to detect macrophages and CD4⁺ T cells, respectively. The number of

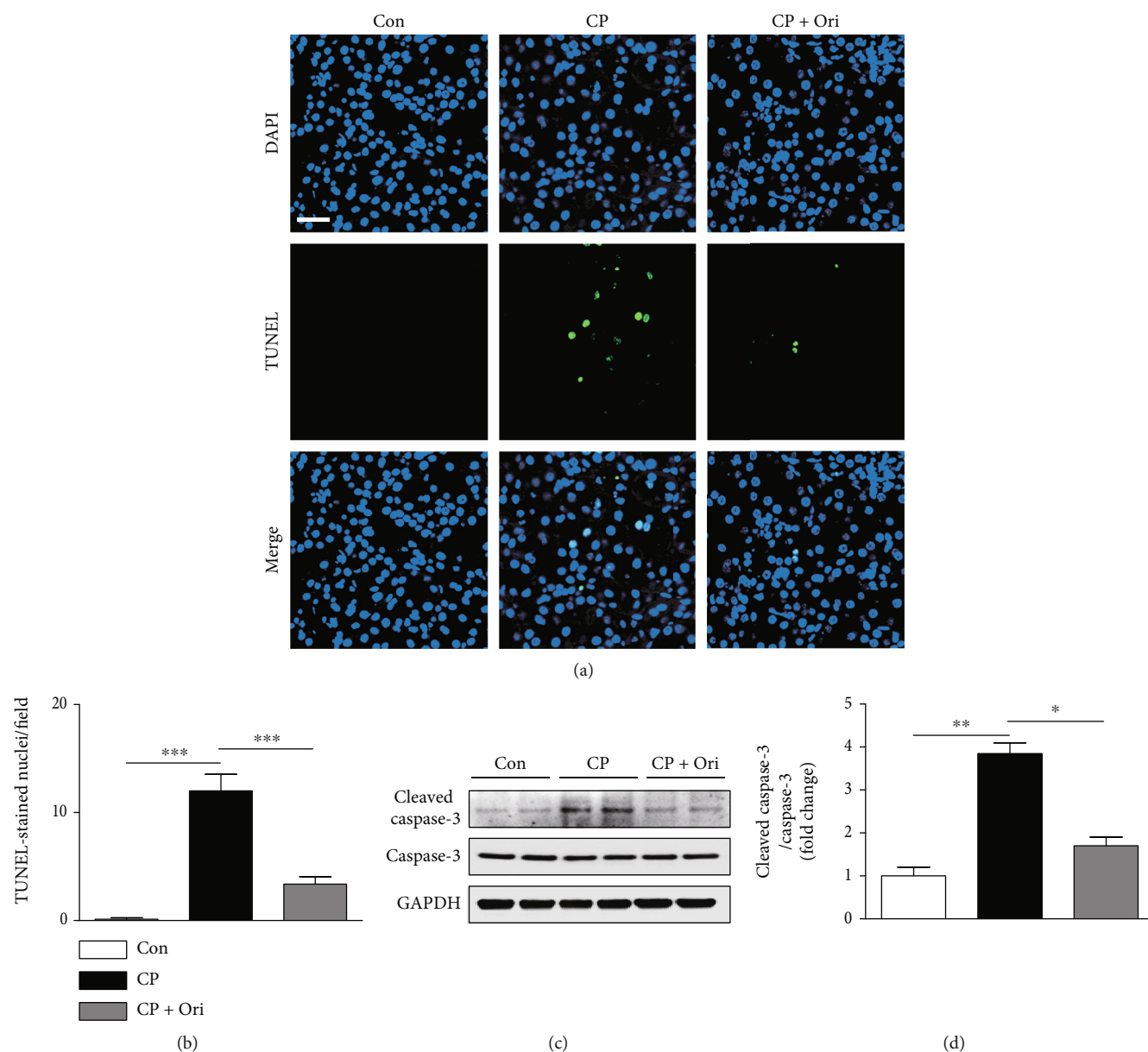


FIGURE 4: Effect of oridonin on tubular cell apoptosis. (a) TUNEL assay on kidney sections. Scale bar = 10 μm . To detect nuclei, DAPI was used. (b) Number of TUNEL-stained nuclei per field. (c) Western blotting of cleaved caspase-3. (d) Quantification of Western blot results for cleaved caspase-3. $n = 8$ per group. * $p < 0.05$, ** $p < 0.01$, and *** $p < 0.001$.

macrophages was increased after cisplatin injection but was significantly alleviated by oridonin (Figures 6(a) and 6(b)). Administration of oridonin also decreased the number of CD4⁺ T cells in cisplatin-injected mice (Figures 7(a) and 7(b)).

4. Discussion

In the current study, we demonstrated the therapeutic effect of oridonin on cisplatin-induced kidney injury. Mechanistically, oridonin inhibited oxidative stress, tubular cell apoptosis, and inflammation in cisplatin-injected mice.

Early studies on the function of oridonin have mainly focused on its anticancer effect [7]. Indeed, oridonin has

been shown to exert anticancer activity on many types of cancers [21–23]. However, subsequent studies suggest that in addition to its anticancer effect, oridonin has several other favorable effects including antioxidative and anti-inflammatory effects [8, 9]. Therefore, we hypothesized that oridonin may have a beneficial effect on cisplatin nephrotoxicity. In the current study, administration of oridonin ameliorated renal dysfunction and histopathological alterations, suggesting that the compound has a therapeutic action on cisplatin-induced kidney injury. Besides nephrotoxic medications, ischemia-reperfusion injury is also a major cause of AKI [24]. Recent studies have demonstrated the protective effect of oridonin on renal ischemia-reperfusion injury [10, 11]. These findings suggest that the beneficial action of

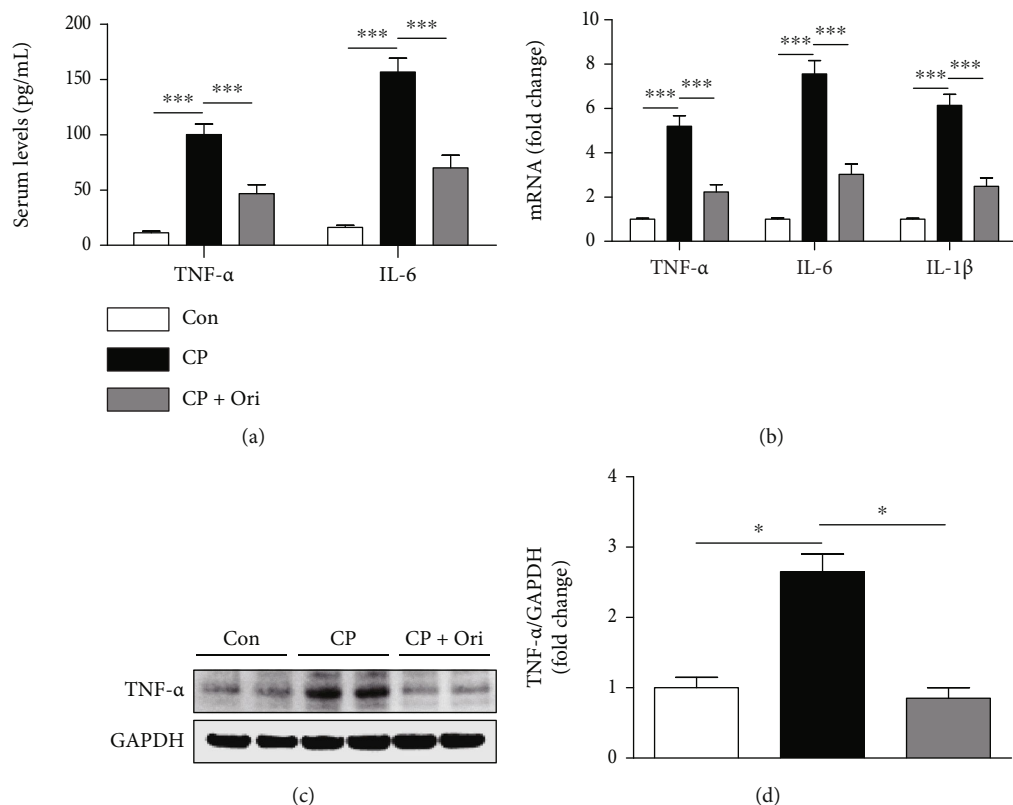


FIGURE 5: Effect of oridonin on cytokine production. (a) Serum levels TNF- α and IL-6. (b) Relative mRNA levels of TNF- α , IL-6, and IL-1 β . (c) Western blotting of TNF- α . (d) Quantification of Western blot results for TNF- α . $n = 8$ per group. * $p < 0.05$ and *** $p < 0.001$.

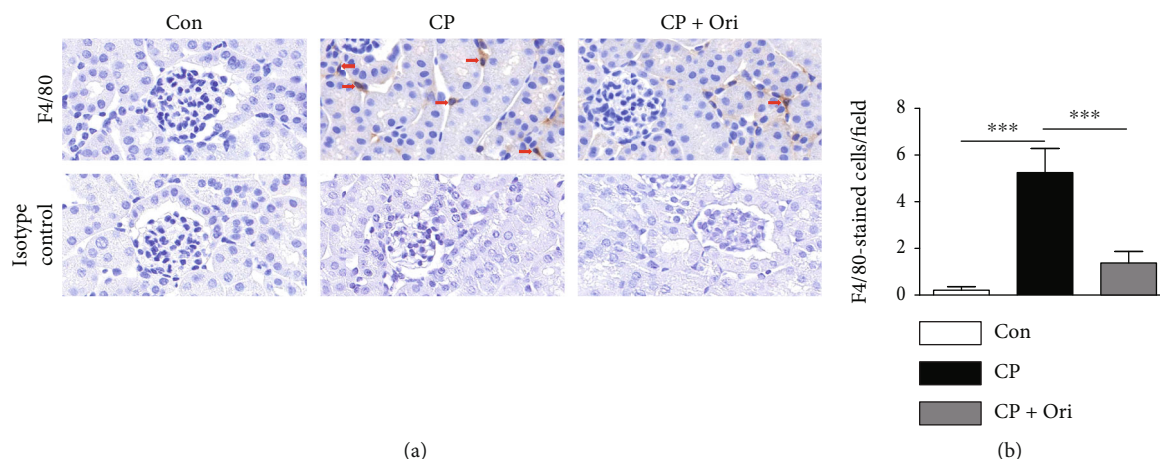


FIGURE 6: Effect of oridonin on macrophage infiltration. (a) IHC staining for F4/80. Scale bar = 20 μ m. Red arrows indicate positive cells. (b) Number of F4/80-positive cells per field. $n = 8$ per group. *** $p < 0.001$.

oridonin is not limited to cisplatin-induced AKI but may also be applied to other types of AKI.

Oxidative stress has been known to play a critical role in various diseases, including cardiovascular diseases, metabolic diseases, and neurodegenerative diseases [25]. Animal studies have shown that cisplatin nephrotoxicity is alleviated by administration of various antioxidants, such as coenzyme Q10 [26], vitamin C [27], vitamin E [28], resveratrol [29], and melatonin [30], suggesting that oxidative stress is also an

important mechanism of cisplatin nephrotoxicity. Importantly, various natural compounds have antioxidative activity [31, 32]. Antioxidative effect of oridonin has also been reported in several studies [8, 9]. Oridonin suppressed reactive oxygen species generation in lipopolysaccharide- (LPS-) treated human renal tubular epithelial cells [33]. In the present study, administration of oridonin decreased the amounts of 4-HNE and MDA in kidneys of cisplatin-injected mice. These molecules are well-known lipid peroxidation products and

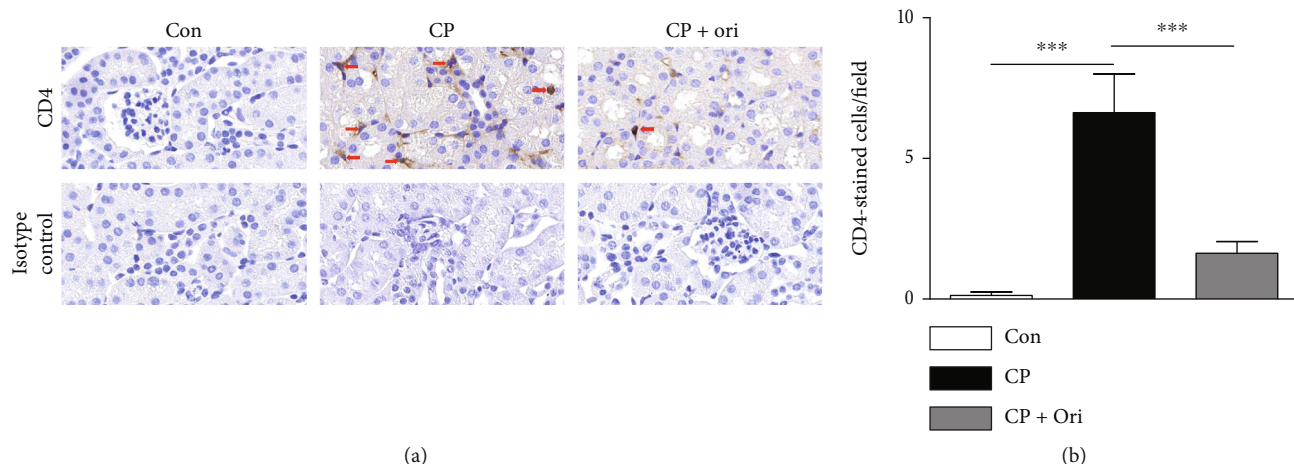


FIGURE 7: Effect of oridonin on CD4⁺ T cell infiltration. (a) IHC staining for CD4. Scale bar = 20 μ m. Red arrows indicate positively stained cells. (b) Number of CD4-positive cells per field. $n = 8$ per group. *** $p < 0.001$.

have been shown to be increased in cisplatin nephrotoxicity [34, 35]. Moreover, cisplatin injection lowered the GSH/GSSG ratio, indicating increased oxidative stress [36, 37]. However, oridonin significantly reversed the decreased GSH/GSSG ratio. Therefore, the therapeutic action of oridonin on cisplatin-induced kidney injury is possibly attributed to its antioxidative effect.

Tubular cell apoptosis is frequently observed and is mainly caused by oxidative stress in cisplatin-induced kidney injury [38]. In the current study, cisplatin injection resulted in caspase-3 activation and apoptosis, which were inhibited by oridonin. Cisplatin can activate proapoptotic proteins, which cause the translocation of cytochrome c into the cytoplasm [19]. Then, the mediator induces the assembly of a multiprotein complex, resulting in activation of executioner caspases. Therefore, our data suggest that oridonin attenuated cisplatin-induced apoptosis through suppressing caspase-3 pathway. Consistent with our findings, oridonin inhibited hypoxia-induced apoptosis in a rat cardiomyoblast cell line [39]. Oridonin also protected human keratinocytes and dermal fibroblasts against hydrogen peroxide-induced apoptosis [40, 41]. Furthermore, the compound inhibited hepatocyte apoptosis to ameliorate acute liver injury in mice [42].

Excessive cytokine secretion and immune cell infiltration are characteristic features of cisplatin-induced AKI [43–45]. Oridonin inhibited cisplatin-induced systemic and renal inflammation, as evidenced by reductions in both serum and renal levels of cytokines. Increased infiltration of macrophages and CD4⁺ T cells was also alleviated by oridonin. Consistently, emerging evidence suggest that the beneficial action of oridonin on renal ischemia-reperfusion injury is associated with suppression of macrophage-mediated inflammation [10, 11]. It has been also reported that oridonin can modulate the activation and proliferation of T cells to alleviate inflammatory diseases such as inflammatory bowel disease [46, 47] and asthma [48]. In addition, oridonin inhibited LPS-induced cytokine production in human gingival fibroblasts [49] and mouse endometrial epithelial cells [50]. Inflammatory responses in IL-1 β -stimulated human osteoarthritis chondrocytes were also suppressed by oridonin [51].

Oridonin has broad potential for drug development due to its wide range of pharmacological activities [8, 52]. However, oridonin has low solubility and poor bioavailability, which limits its clinical application. Therefore, much effort should be focused on the development of strategies, such as structural modification and new dosage form, to overcome these shortcomings [52].

In conclusion, we showed that oridonin ameliorated cisplatin-induced kidney injury in mice and that its therapeutic effect was due to attenuation of oxidative stress, apoptosis, and inflammation. The compound has been shown to increase the susceptibility of cancer cells to chemotherapy drugs including cisplatin [53, 55]. Therefore, oridonin may be a useful therapeutic agent for AKI in cancer patients undergoing chemotherapy.

Data Availability

The data used to support the findings of this study are included within the article.

Conflicts of Interest

All authors declare no conflict of interest.

Authors' Contributions

Hyemin Gu and Mi-Gyeong Gwon These authors equally contributed to this work.

Acknowledgments

This study was supported by the Basic Science Research Program through the National Research Foundation of Korea (NRF), funded by the Ministry of Science, ICT, and Future Planning (MSIP) (NRF-2020R1C1C1003348 and NRF-2020R1F1A1076475).

References

- [1] J. Gameiro, J. A. Fonseca, C. Outerelo, and J. A. Lopes, "Acute kidney injury: from diagnosis to prevention and treatment strategies," *Journal of Clinical Medicine*, vol. 9, no. 6, p. 1704, 2020.
- [2] G. M. Chertow, E. Burdick, M. Honour, J. V. Bonventre, and D. W. Bates, "Acute kidney injury, mortality, length of stay, and costs in hospitalized patients," *Journal of the American Society of Nephrology*, vol. 16, no. 11, pp. 3365–3370, 2005.
- [3] S. L. Goldstein, "Medication-induced acute kidney injury," *Current Opinion in Critical Care*, vol. 22, no. 6, pp. 542–545, 2016.
- [4] S. Dasari and P. B. Tchounwou, "Cisplatin in cancer therapy: molecular mechanisms of action," *European Journal of Pharmacology*, vol. 740, pp. 364–378, 2014.
- [5] P. D. Sánchez-González, F. J. López-Hernández, J. M. López-Novoa, and A. I. Morales, "An integrative view of the pathophysiological events leading to cisplatin nephrotoxicity," *Critical Reviews in Toxicology*, vol. 41, no. 10, pp. 803–821, 2011.
- [6] M. S. Sarwar, Y.-X. Xia, Z.-M. Liang, S. W. Tsang, and H.-J. Zhang, "Mechanistic pathways and molecular targets of plant-derived anticancer ent-kaurane diterpenes," *Biomolecules*, vol. 10, no. 1, p. 144, 2020.
- [7] N. A. Abdullah, N. F. Md Hashim, A. Ammar, and N. Muhamad Zakuan, "An insight into the anti-angiogenic and anti-metastatic effects of oridonin: current knowledge and future potential," *Molecules*, vol. 26, no. 4, p. 775, 2021.
- [8] X. Li, C.-T. Zhang, W. Ma, X. Xie, and Q. Huang, "Oridonin: a review of its pharmacology, pharmacokinetics and toxicity," *Frontiers in Pharmacology*, vol. 12, article 645824, 2021.
- [9] J. Xu, E. A. Wold, Y. Ding, Q. Shen, and J. Zhou, "Therapeutic potential of oridonin and its analogs: from anticancer and antiinflammation to neuroprotection," *Molecules*, vol. 23, no. 2, p. 474, 2018.
- [10] R.-Z. Tan, Y. Yan, Y. Yu et al., "Renoprotective effect of oridonin in a mouse model of acute kidney injury via suppression of macrophage involved inflammation," *Biological & Pharmaceutical Bulletin*, vol. 44, no. 5, pp. 714–723, 2021.
- [11] Y. Yan, R.-Z. Tan, P. Liu et al., "Oridonin alleviates IRI-induced kidney injury by inhibiting inflammatory response of macrophages via AKT-related pathways," *Medical Science Monitor*, vol. 26, article e921114, 2020.
- [12] J. Li, L. Bao, D. Zha et al., "Oridonin protects against the inflammatory response in diabetic nephropathy by inhibiting the TLR4/p38-MAPK and TLR4/NF- κ B signaling pathways," *International Immunopharmacology*, vol. 55, pp. 9–19, 2018.
- [13] J.-Y. Kim, J. Jo, J. Leem, and K.-K. Park, "Inhibition of p300 by garcinol protects against cisplatin-induced acute kidney injury through suppression of oxidative stress, inflammation, and tubular cell death in mice," *Antioxidants*, vol. 9, no. 12, p. 1271, 2020.
- [14] J.-Y. Kim, H.-L. Hong, G. M. Kim, J. Leem, and H. H. Kwon, "Protective effects of carnolic acid on lipopolysaccharide-induced acute kidney injury in mice," *Molecules*, vol. 26, no. 24, p. 7589, 2021.
- [15] J.-Y. Kim, J. Leem, and H.-L. Hong, "Protective effects of SPA 0355, a thiourea analogue, against lipopolysaccharide-induced acute kidney injury in mice," *Antioxidants*, vol. 9, no. 7, p. 585, 2020.
- [16] J.-Y. Kim, S.-J. Lee, Y.-I. Maeng, J. Leem, and K.-K. Park, "Protective effects of bee venom against endotoxemia-related acute kidney injury in mice," *Biology*, vol. 9, no. 7, p. 154, 2020.
- [17] S. J. Holditch, C. N. Brown, A. M. Lombardi, K. N. Nguyen, and C. L. Edelstein, "Recent advances in models, mechanisms, biomarkers, and interventions in cisplatin-induced acute kidney injury," *International Journal of Molecular Sciences*, vol. 20, no. 12, p. 3011, 2019.
- [18] J.-Y. Kim, J. Leem, and E. J. Jeon, "Protective effects of melatonin against aristolochic acid-induced nephropathy in mice," *Biomolecules*, vol. 10, no. 1, p. 11, 2020.
- [19] N. Pabla and Z. Dong, "Cisplatin nephrotoxicity: mechanisms and renoprotective strategies," *Kidney International*, vol. 73, no. 9, pp. 994–1007, 2008.
- [20] J.-Y. Kim, J. Leem, and H.-L. Hong, "Melittin ameliorates endotoxin-induced acute kidney injury by inhibiting inflammation, oxidative stress, and cell death in mice," *Oxidative Medicine and Cellular Longevity*, vol. 2021, Article ID 8843051, 2021.
- [21] J.-H. Jiang, J. Pi, H. Jin, and J.-Y. Cai, "Oridonin-induced mitochondria-dependent apoptosis in esophageal cancer cells by inhibiting PI3K/AKT/mTOR and Ras/Raf pathways," *Journal of Cellular Biochemistry*, vol. 120, no. 3, pp. 3736–3746, 2019.
- [22] L. Xu, Y. Bi, Y. Xu et al., "Oridonin inhibits the migration and epithelial-to-mesenchymal transition of small cell lung cancer cells by suppressing FAK-ERK1/2 signalling pathway," *Journal of Cellular and Molecular Medicine*, vol. 24, no. 8, pp. 4480–4493, 2020.
- [23] J. Zhou, Y. Li, X. Shi et al., "Oridonin inhibits tumor angiogenesis and induces vessel normalization in experimental colon cancer," *Journal of Cancer*, vol. 12, no. 11, pp. 3257–3264, 2021.
- [24] N. Shiva, N. Sharma, Y. A. Kulkarni, S. R. Mulay, and A. B. Gaikwad, "Renal ischemia/reperfusion injury: an insight on in vitro and in vivo models," *Life Sciences*, vol. 256, article 117860, 2020.
- [25] Y. Gao, L. Fang, X. Wang et al., "Antioxidant activity evaluation of dietary flavonoid hyperoside using *saccharomyces cerevisiae* as a model," *Molecules*, vol. 24, no. 4, p. 788, 2019.
- [26] A. A. Fouad, A. I. Al-Sultan, S. M. Refaie, and M. T. Yaoubi, "Coenzyme Q10 treatment ameliorates acute cisplatin nephrotoxicity in mice," *Toxicology*, vol. 274, no. 1–3, pp. 49–56, 2010.
- [27] M.-F. Chen, C.-M. Yang, C.-M. Su, and M.-L. Hu, "Vitamin C protects against cisplatin-induced nephrotoxicity and damage without reducing its effectiveness in C57BL/6 mice xenografted with Lewis lung carcinoma," *Nutrition and Cancer*, vol. 66, no. 7, pp. 1085–1091, 2014.
- [28] M. Darwish, A. M. Abo-Youssef, M. M. Khalaf, A. A. Abo-Saif, I. G. Saleh, and T. M. Abdelghany, "Vitamin E mitigates cisplatin-induced nephrotoxicity due to reversal of oxidative/nitrosative stress, suppression of inflammation and reduction of total renal platinum accumulation," *Journal of Biochemical and Molecular Toxicology*, vol. 31, no. 1, 2017.
- [29] Q. Hao, X. Xiao, J. Zhen et al., "Resveratrol attenuates acute kidney injury by inhibiting death receptor-mediated apoptotic pathways in a cisplatin-induced rat model," *Molecular Medicine Reports*, vol. 14, no. 4, pp. 3683–3689, 2016.
- [30] J. W. Kim, J. Jo, J.-Y. Kim, M. Choe, J. Leem, and J.-H. Park, "Melatonin attenuates cisplatin-induced acute kidney injury

- through dual suppression of apoptosis and necroptosis,” *Biology*, vol. 8, no. 3, p. 64, 2019.
- [31] M. Mohany, M. M. Ahmed, and S. S. Al-Rejaie, “Molecular mechanistic pathways targeted by natural antioxidants in the prevention and treatment of chronic kidney disease,” *Antioxidants*, vol. 11, no. 1, p. 15, 2022.
- [32] M. E. Embuscado, “Bioactives from culinary spices and herbs: a review,” *Journal of Food Bioactives*, vol. 6, 2019.
- [33] J.-H. Huang, C.-C. Lan, Y.-T. Hsu et al., “Oridonin attenuates lipopolysaccharide-induced ROS accumulation and inflammation in HK-2 cells,” *Evidence-based Complementary and Alternative Medicine*, vol. 2020, Article ID 9724520, 2020.
- [34] D. Meng, P. Zhang, L. Zhang et al., “Detection of cellular redox reactions and antioxidant activity assays,” *Journal of Functional Foods*, vol. 37, pp. 467–479, 2017.
- [35] M.-G. Gwon, H. Gu, J. Leem, and K.-K. Park, “Protective effects of 6-Shogaol, an active compound of ginger, in a murine model of cisplatin-induced acute kidney injury,” *Molecules*, vol. 26, no. 19, p. 5931, 2021.
- [36] J.-Y. Kim, J. Jo, K. Kim et al., “Pharmacological activation of Sirt 1 ameliorates cisplatin-induced acute kidney injury by suppressing apoptosis, oxidative stress, and inflammation in mice,” *Antioxidants*, vol. 8, no. 8, p. 322, 2019.
- [37] J.-Y. Kim, J. Leem, and K.-K. Park, “Antioxidative, antiapoptotic, and anti-inflammatory effects of apamin in a murine model of lipopolysaccharide-induced acute kidney injury,” *Molecules*, vol. 25, no. 23, p. 5717, 2020.
- [38] M. Jiang, Q. Wei, N. Pabla et al., “Effects of hydroxyl radical scavenging on cisplatin-induced p53 activation, tubular cell apoptosis and nephrotoxicity,” *Biochemical Pharmacology*, vol. 73, no. 9, pp. 1499–1510, 2007.
- [39] L. Gong, H. Xu, X. Zhang, T. Zhang, J. Shi, and H. Chang, “Oridonin relieves hypoxia-evoked apoptosis and autophagy via modulating microRNA-214 in H9c2 cells,” *Artificial Cells, Nanomedicine, and Biotechnology*, vol. 47, no. 1, pp. 2585–2592, 2019.
- [40] S. Bae, E.-J. Lee, J. H. Lee et al., “Oridonin protects HaCaT keratinocytes against hydrogen peroxide-induced oxidative stress by altering microRNA expression,” *International Journal of Molecular Medicine*, vol. 33, no. 1, pp. 185–193, 2014.
- [41] E.-J. Lee, H. J. Cha, K. J. Ahn, I.-S. An, S. An, and S. Bae, “Oridonin exerts protective effects against hydrogen peroxide-induced damage by altering microRNA expression profiles in human dermal fibroblasts,” *International Journal of Molecular Medicine*, vol. 32, no. 6, pp. 1345–1354, 2013.
- [42] Y. Deng, C. Chen, H. Yu et al., “Oridonin ameliorates lipopolysaccharide/D-galactosamine-induced acute liver injury in mice via inhibition of apoptosis,” *American Journal of Translational Research*, vol. 9, no. 9, pp. 4271–4279, 2017.
- [43] J.-Y. Kim, J. Jo, J. Leem, and K.-K. Park, “Kahweol ameliorates cisplatin-induced acute kidney injury through pleiotropic effects in mice,” *Biomedicine*, vol. 8, no. 12, p. 572, 2020.
- [44] H. Liang, H. Z. Liu, H. B. Wang, J. Y. Zhong, C. X. Yang, and B. Zhang, “Dexmedetomidine protects against cisplatin-induced acute kidney injury in mice through regulating apoptosis and inflammation,” *Inflammation Research*, vol. 66, no. 5, pp. 399–411, 2017.
- [45] J.-Y. Kim, J.-H. Park, K. Kim, J. Jo, J. Leem, and K.-K. Park, “Pharmacological inhibition of caspase-1 ameliorates cisplatin-induced nephrotoxicity through suppression of apoptosis, oxidative stress, and inflammation in mice,” *Mediators of Inflammation*, vol. 2018, Article ID 6571676, 2018.
- [46] S. Wang, Y. Zhang, P. Saas et al., “Oridonin’s therapeutic effect: suppressing Th1/Th17 simultaneously in a mouse model of Crohn’s disease,” *Journal of Gastroenterology and Hepatology*, vol. 30, no. 3, pp. 504–512, 2015.
- [47] Q. Q. Liu, H. L. Wang, K. Chen et al., “Oridonin derivative ameliorates experimental colitis by inhibiting activated T-cells and translocation of nuclear factor-kappa B,” *Journal of Digestive Diseases*, vol. 17, no. 2, pp. 104–112, 2016.
- [48] J. Wang, F. Li, J. Ding et al., “Investigation of the anti-asthmatic activity of oridonin on a mouse model of asthma,” *Molecular Medicine Reports*, vol. 14, no. 3, pp. 2000–2006, 2016.
- [49] T. Yu, W. Xie, and Y. Sun, “Oridonin inhibits LPS-induced inflammation in human gingival fibroblasts by activating PPAR γ ,” *International Immunopharmacology*, vol. 72, pp. 301–307, 2019.
- [50] M. Zhou, Y. Yi, and L. Hong, “Oridonin ameliorates lipopolysaccharide-induced endometritis in mice via inhibition of the TLR-4/NF- κ B pathway,” *Inflammation*, vol. 42, no. 1, pp. 81–90, 2019.
- [51] T. Jia, M. Cai, X. Ma, M. Li, J. Qiao, and T. Chen, “Oridonin inhibits IL-1 β -induced inflammation in human osteoarthritis chondrocytes by activating PPAR- γ ,” *International Immunopharmacology*, vol. 69, pp. 382–388, 2019.
- [52] Y. Zhang, S. Wang, M. Dai, J. Nai, L. Zhu, and H. Sheng, “Solubility and bioavailability enhancement of oridonin: a review,” *Molecules*, vol. 25, no. 2, p. 332, 2020.
- [53] H. Yang, Y. Gao, X. Fan, X. Liu, L. Peng, and X. Ci, “Oridonin sensitizes cisplatin-induced apoptosis via AMPK/Akt/mTOR-dependent autophagosome accumulation in A549 cells,” *Frontiers in Oncology*, vol. 9, p. 769, 2019.
- [54] X. Li, W. Chen, K. Liu et al., “Oridonin sensitizes hepatocellular carcinoma to the anticancer effect of sorafenib by targeting the Akt pathway,” *Cancer Management and Research*, vol. - Volume 12, pp. 8081–8091, 2020.
- [55] H.-Q. Bu, J. Luo, H. Chen et al., “Oridonin enhances antitumor activity of gemcitabine in pancreatic cancer through MAPK-p38 signaling pathway,” *International Journal of Oncology*, vol. 41, no. 3, pp. 949–958, 2012.

Research Article

***Datura stramonium* Leaf Extract Exhibits Anti-inflammatory Activity in CCL₄-Induced Hepatic Injury Model by Modulating Oxidative Stress Markers and iNOS/Nrf2 Expression**

**Bakht Nasir,¹ Ashraf Ullah Khan,^{1,2} Muhammad Waleed Baig,¹ Yusuf S. Althobaiti^{3,4},
Muhammad Faheem,⁵ and Ihsan-Ul Haq¹**

¹Department of Pharmacy, Faculty of Biological Sciences, Quaid-i-Azam University, Islamabad 45320, Pakistan

²Faculty of Pharmaceutical Sciences, Abasyn University Peshawar, Peshawar 25000, Pakistan

³Department of Pharmacology and Toxicology, College of Pharmacy, Taif University, P.O. Box 11099, Taif 21944, Saudi Arabia

⁴Addiction and Neuroscience Research Unit, Taif University, P.O. Box 11099, Taif 21944, Saudi Arabia

⁵Riphah Institute of Pharmaceutical Sciences, Riphah International University, Islamabad 45320, Pakistan

Correspondence should be addressed to Yusuf S. Althobaiti; ys.althobaiti@tu.edu.sa and Ihsan-Ul Haq; ihsn99@yahoo.com

Received 31 December 2021; Accepted 7 February 2022; Published 16 March 2022

Academic Editor: Abdul Rehman Phull

Copyright © 2022 Bakht Nasir et al. This is an open access article distributed under the Creative Commons Attribution License, which permits unrestricted use, distribution, and reproduction in any medium, provided the original work is properly cited.

Background. Inflammation is a frequent phenomenon in the pathogenesis of hepatic disorders leading to fibrosis and cirrhosis. Phytopharmaceuticals developed from traditional medicine can provide effective therapeutic alternatives to conventional medications. *Datura stramonium* (DS) has reported traditional uses in inflammatory diseases. In this study, we have tried to validate its potential as a source of anti-inflammatory agents. **Methods.** Powdered leaf part of DS was extracted using ethyl acetate (EA) to provide the extract (DSL-EA). Lymphocyte and macrophage viability and acute toxicity assays established the safety profile, while nitric oxide (NO) scavenging assay estimated the *in vitro* anti-inflammatory potential. Noninvasive anti-inflammatory, antidepressant, and antinociceptive activities were monitored using BALB/c mice using low and high doses (150 and 250 mg/kg). Major inflammatory studies were performed on Sprague-Dawley male rats using CCL₄-induced liver injury model. Disease induction was initiated by intraperitoneal injections of CCL₄ (1 mL/kg of 30% CCL₄ in olive oil). The rats were divided into six groups. The anti-inflammatory potential of DSL-EA in low and high doses (150 and 300 mg/kg, respectively) was assessed through hematological, biochemical, liver antioxidant defense, oxidative stress markers, and histological studies as well as the expression of Nrf2 and iNOS. **Results.** DSL-EA exhibited prominent *in vitro* NO scavenging (IC₅₀: 7.625 ± 0.51 μg/mL) and *in vivo* anti-inflammatory activity in paw and anal edema models. In CCL₄ model, hematological investigations revealed vasotonic effects. Liver functionality was significantly ($P < 0.001 - 0.05$) improved in DSL-EA-treated rats. The activity level of endogenous antioxidant enzymes in liver tissues was improved in a manner identical to silymarin. The extract reduced the percent concentration of oxidative stress markers in liver tissues. Furthermore, DSL-EA displayed restorative effects on histological parameters (H and E and Masson's trichrome staining). Immunohistochemistry studies showed marked decline in Nrf2 expression, while overexpression of iNOS was also observed in disease control rats. The damage was distinctly reversed by the extract.

1. Introduction

Oxygen and nitrogen are found abundantly in any aerobic system. These molecules are involved in numerous physiological and metabolic processes, and they undergo chemical changes within the system [1]. These molecules go into a

readily reactive state when these are transformed into unpaired moieties within the body. Few examples of such reactive species are singlet oxygen, superoxide anion, nitric oxide, hydroxyl radical, etc. [2]. The terms reactive oxygen species (ROS) and reactive nitrogen species (RNS) were used to describe these moieties since there are numerous free

oxygen and nitrogen radicals and nonradicals involved in the overall process. These molecules are formed within the living system as a result of various exogenous and endogenous factors [3]. Generation of these species in appropriate amount plays a key role in normal physiological functions, i.e., body's defense against microbes and signal transduction, but the problem arises when these are produced in excessive amounts ultimately resulting in oxidative stress. These molecules, due to their chemical nature, are involved in DNA damage, lipid peroxidation, and oxidation of numerous cellular molecules including cellular membranes, the inevitable consequence being cellular injury [4]. Out of the many endogenous sources leading to generation of free radicals, drugs, pollutants, radiations, and chemicals are the most common ones [5]. The pathological conditions resulting from such oxidative insults include liver cirrhosis, cancer, Alzheimer's disease, diabetes mellitus, rheumatoid arthritis, and multiple sclerosis [6, 7]. The liver is not just responsible for metabolism but also the largest organ involved in detoxification and life sustainability [8]. Our body relies on the liver for breakdown of toxins produced inside the body or ingested from outside; this makes the liver particularly vulnerable to long-term exposure of oxidative stress [9]. Liver fibrosis is a serious health condition, and if not treated promptly, it leads to several liver ailments including liver cirrhosis and hepatocellular carcinoma (HCC) [10]. Different factors are responsible for the development and progression of liver diseases; the involvement of exogenous toxins and drugs cannot be overruled. Carbon tetrachloride (CCL_4) has been widely employed as a toxin in liver injury models. The mode of action of CCL_4 -induced toxicity is production of oxidative stress leading to steatosis and centrilobular necrosis, while prolonged exposure causes chronic liver injury resulting in liver fibrosis [11].

Phytochemicals from different medicinal plants are known to possess significant antioxidant properties. Some of the important antioxidant phytochemicals include phenolics and flavonoids, terpenoids, vitamins, alkaloids, saponins, minerals, and certain pigments. These diverse groups of compounds help the body to combat various oxidative stress-mediated diseases [12, 13]. Antioxidants protect the body tissues by scavenging the highly reactive oxygen compounds [14]. Apart from the antioxidant nature of plants, the underlying mechanisms of the protective action against liver injuries may include their anti-inflammatory, antinecrosis, and regulatory action on lipid metabolism as well as their antiapoptotic effects [15]. Genus *Datura* (family Solanaceae) consists of medicinally important species including but not limited to *D. stramonium*, *D. ferox*, *D. innoxia*, and *D. metel* [16]. These species are being used for medicinal and recreational purposes since time immemorial. *Datura* species have several traditional and ethnopharmacological uses, i.e., antiasthmatic, anesthetic, sedative, antihemorrhoidal, expectorant, demulcent, and antitumor [16, 17]. *D. stramonium* Linn. is the most common species within genus *Datura* native to Asia but found abundantly in tropical, subtropical, and temperate regions around the world [18]. It is well recognized as a valuable remedy in numerous ailments including inflammation, rheumatoid arthritis, wounds,

ulcers, gout, asthma and bronchitis, fever, and toothache [19]. *D. stramonium* is chosen for the current study because of ample evidence in the literature substantiating its potential as a source of anti-inflammatory agents [20]. Our study aims to look for a scientific validation of the ethnomedicinal use of *D. stramonium* extracts in inflammatory disorders using acute and chronic *in vivo* models. This study will provide a comprehensive insight into the potential of selected plant extract in alleviating liver inflammation and its role in modulating the oxidative stress markers.

2. Results

In the previously published study covering the initial phase of our project, the ethyl acetate leaf extract of *D. stramonium* (DSL-EA) was qualitatively and quantitatively evaluated for the presence of pharmacologically significant secondary metabolites including flavonoids and phenolics. Several *in vitro* antioxidant and anticancer studies were also undertaken which substantiated the medicinal worth of the selected plant species [16]. In this study, the anti-inflammatory potential of DSL-EA is appraised. The details of a series of assays performed to scientifically validate the folkloric use of this medicinal plant are given in the following sections.

2.1. Nitric Oxide Scavenging Potential. Nitric oxide scavenging action was determined to further establish the efficacy profile of selected extract before initiating the acute and sub chronic *in vivo* studies. The highest concentration of DLS-EA used in this assay was $20 \mu\text{g/mL}$, and it inhibited NO production to a significant level. The response tapered down at lower concentrations proving a concentration-dependent scavenging response. Maximum % NO production of $67.62 \pm 0.45\%$ was observed at the lowest tested concentration of DSL-EA, i.e., $2.5 \mu\text{g/mL}$, while only $27.35 \pm 0.12\%$ NO production was estimated at $20 \mu\text{g/mL}$. The IC_{50} value recorded was $7.625 \pm 0.51 \mu\text{g/mL}$.

2.2. Toxicity Studies

2.2.1. Lymphocyte and Macrophage Toxicity Assay. Cytotoxicity against normal human lymphocytes was tested as reported in our previous study [16]. Cytotoxicity against isolated macrophages from rat peritoneum was also determined. The percent cell viability was determined by performing methyl thiazole tetrazolium (MTT) assay. The results were expressed in terms of % viable cells in the test wells having predetermined concentration of DSL-EA and designated controls. The results have shown that DSL-EA, even at a maximum concentration of $20 \mu\text{g/mL}$, resulted in cell viability greater than 90%.

2.3. Acute In Vivo Studies

2.3.1. Acute Toxicity Study. Acute toxicity was checked after a single booster dose ($150\text{--}2000 \text{ mg/kg}$) to rats divided into different groups. The rats were kept under surveillance for a period of two weeks. No deaths were recorded during the said time period, and the rats did not experience any

abnormal changes in the behavior. Normal physiology and all the senses were intact which showed that DSL-EA was safe to be administered up to a highest dose of 2000 mg/kg with no risk of any kind of toxicity.

2.3.2. Noninvasive In Vivo Tests

(1) *Paw Edema*. The anti-inflammatory potential of DSL-EA was evaluated by calculating its edema inhibitory effect in carrageenan-induced hind paw edema test. As evident from the results in Figure 1, DSL-EA has alleviated the edema caused by carrageenan in a dose- and time-dependent manner with high dose of DSL-EA (300 mg/kg) showing more than 70% inhibitory effect. Low dose of the extract (150 mg/kg) exhibited moderate activity with the effect peaking at the 4th hour, i.e., $51.63 \pm 5.49\%$ reduction noted in hind paw edema.

(2) *Anal Edema*. Croton oil-induced anal edema test was also performed for further validation of the anti-inflammatory potential of DSL-EA. A substantial steady decline in percent edema volume was observed over the course of the study duration, and maximum activity in terms of edema inhibition was observed at the 4th hour in case of DSL-EA-HD, i.e., $67.62 \pm 7.56\%$. Low dose of the extract curbed the edema by slightly less than 43% as of the 4th hour reading. Ibuprofen was the standard drug used in the study, and it showed $80.1 \pm 5.1\%$ edema inhibition at the 3rd hour. The details can be seen in Figure 1.

(3) *Tail Suspension Test*. The potential antidepressant action of extract was estimated using tail suspension test. Fluoxetine was the standard drug used in this assay, and it significantly reduced the immobility time in mice (66.66 ± 11.37 sec) in comparison to the vehicle control group (168.33 ± 14.04 sec). DSL-EA-HD reduced the immobility time only slightly (117 ± 6.93), and somewhat insignificant effect was observed in the case of DSL-EA-LD (136.66 ± 11.37). The results are stacked in Figure 1.

(4) *Hotplate Test*. The analgesic property of DSL-EA was also determined against thermally induced pain using hotplate method. The antinociceptive effect was evaluated by observing the % increase in latency period, and the results were compared with standard drug, i.e., tramadol. The maximum antinociceptive action of tramadol was observed at the 3rd hour, i.e., $91.66 \pm 9.74\%$ increase in latency period. DSL-EA-HD moderately elevated the latency period with maximum increment of $59.4 \pm 7.6\%$ observed at the 4th hour. DSL-EA-LD yielded slightly less significant response with a maximum of $49.5 \pm 5.8\%$ noted at the 4th hour as shown in Figure 1.

2.4. *Chronic In Vivo Study (CCL₄-Induced Hepatic Injury in Sprague-Dawley Rats)*. Following intraperitoneal administration of predetermined doses of CCL₄ to the rats in groups III-VI (disease control, silymarin treated, DSL-EA low dose (LD), and DSL-EA high dose (HD)) and induction of hepatic toxicity, groups were treated with respective drugs

and samples. The efficacy of low and high doses of DSL-EA alleviation of the hepatic toxicity was measured through extensive hematological, biochemical, and histological examinations. The effects produced by crude extract were compared with the controls used in the study.

2.4.1. *CCL₄-Induced Hematological Variations*. The results of CCL₄-induced hematological variations are shown in Table 1. As obvious from the data, CCL₄ has caused significant aberrations, i.e., decline in red blood cells (RBC) ($6.07 \pm 0.32 \times 10^6/\text{mm}^3$) and hemoglobin (HGB) (8.02 ± 1.02 g/dL) while significant hike in white blood cells (WBC) ($13.12 \pm 0.03 \times 10^3/\text{mm}^3$), neutrophils ($62.04 \pm 1.31\%$), monocytes ($12.12 \pm 1.03\%$), eosinophils ($0.90 \pm 0.22\%$), and basophils ($0.81 \pm 0.05\%$) in disease control rats. The hematological parameters of DSL-EA-treated groups are significantly different from the disease control group ($P < 0.05, 0.01, \text{ and } 0.001$). DSL-EA crude extract normalized the aberrations in a dose-dependent manner fairly identical to silymarin given at 50 mg/kg dose.

2.4.2. *Effect on Biochemical Parameters*. The deleterious effects of CCL₄ on the liver and kidneys were further confirmed by numerous biochemical tests performed using serum acquired from rats of each study group. Liver function tests showed significantly higher level of liver enzymes ($P < 0.05, 0.01, \text{ and } 0.001$) in comparison to other study groups. Alanine transaminase (ALT), aspartate aminotransferase (AST), alkaline phosphatase (ALP), and bilirubin levels recorded in serum of disease control rats were $188.73 \pm 3.24, 231.98 \pm 2.32, 172.74 \pm 4.41$ (U/L), and 2.99 ± 0.04 mg/dL, respectively. Furthermore, albumin level was markedly lower in the disease control group, i.e., 4.28 ± 0.09 g/L. Low and high doses of DSL-EA crude extract dose dependently reverted the harm done to liver functionality by CCL₄ administration. High-dose treatment yielded significant alleviation ($P < 0.05, 0.01, \text{ and } 0.001$) of the liver toxicity in a manner identical to positive control. Creatinine level was also elevated in the disease control group (1.08 ± 0.04 mg/dL). There was no statistically significant difference ($P < 0.05, 0.01, \text{ and } 0.001$) between the positive control, DSL-EA-LD, and DSL-EA-HD groups when their serum creatinine levels were compared. The results are further elaborated in Table 2.

2.4.3. *Effect on Endogenous Antioxidant Enzymes and GSH Levels*. The effect of DSL-EA treatment on endogenous antioxidant enzymes and glutathione (GSH) levels of the study groups is presented in Figure 2. A significant ($P < 0.05, 0.01, \text{ and } 0.001$) reduction in activity level of glutathione S-transferase (GST), GSH, superoxide dismutase (SOD), catalase, and peroxidase (POD) was observed in the disease control group further confirming the damage inflicted by CCL₄ dosing. High-dose treatments with DSL-EA curbed the damage and elevated the level of antioxidant enzymes and GSH to a similar extent as observed in silymarin-treated group. The % enzyme activity levels in liver tissues are presented in Figure 2.

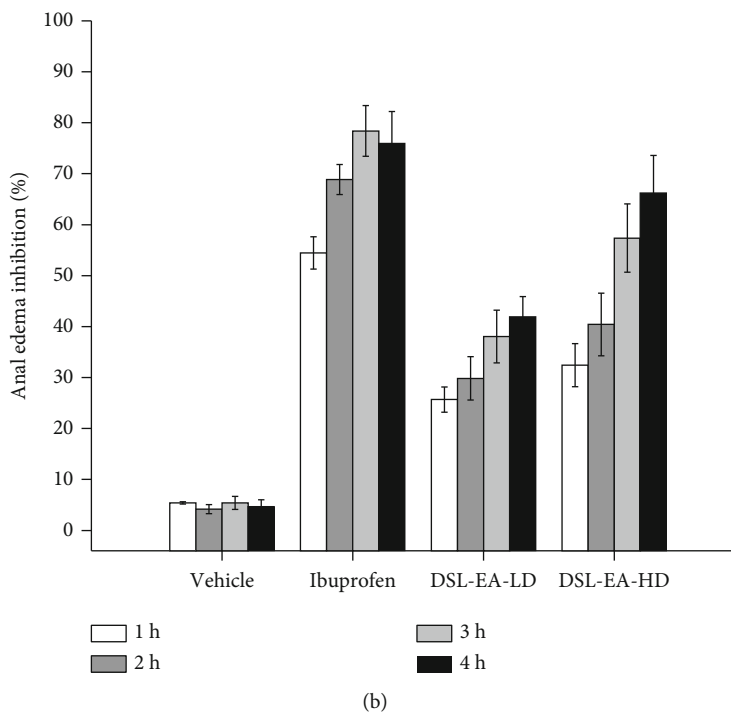
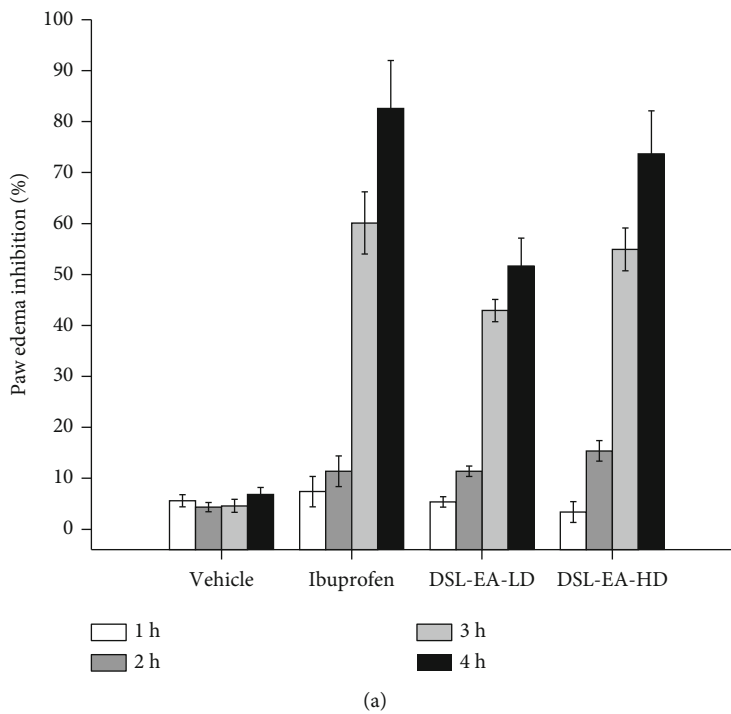


FIGURE 1: Continued.

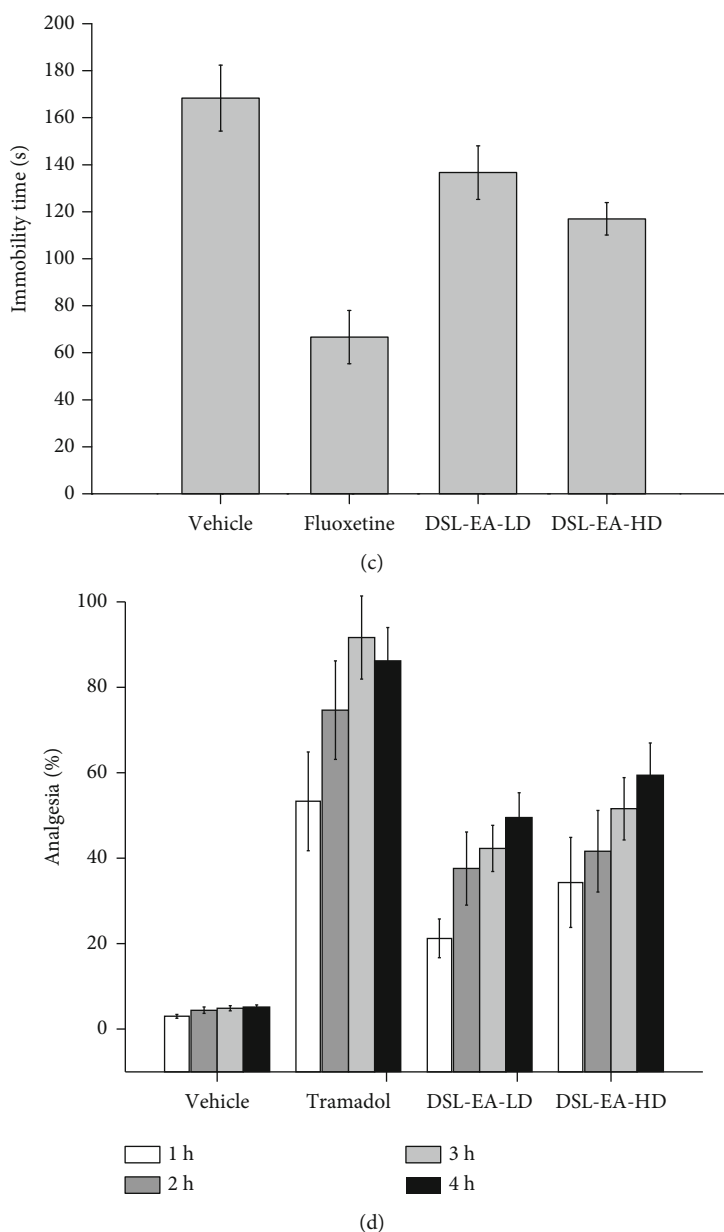


FIGURE 1: Percent paw edema inhibition (a), percent anal edema inhibition (b), immobility time in seconds (c), and percent analgesia (d) by DSL-EA extract in BALB/c mice. Data shown is presented as mean \pm SD ($n = 6$). DSL-EA-LD: low-dose ethyl acetate extract of *D. stramonium*; DSL-EA-HD: high-dose ethyl acetate extract of *D. stramonium*.

2.4.4. Effect on Oxidative Stress Markers. The oxidative stress markers investigated in the current study were NO, malondialdehyde (MDA), and myeloperoxidase (MPO), and their levels were greatly elevated in liver tissues of the disease control group. NO levels were assessed both in plasma and liver tissue since it is an important mediator of inflammation influenced by iNOS gene. As presented in Figure 3, % NO levels both in plasma and tissue homogenates were excessively elevated in the disease control group. DSL-EA-HD and silymarin decreased the NO levels in a significant ($P < 0.05$, 0.01, and 0.001) and comparable manner, while DSL-EA-LD treatments also yielded very good results.

There was statistically significant ($P < 0.05$, 0.01, and 0.001) difference between the % MDA level of the disease

control rats and DSL-EA-treated groups. Dose-dependent decline in the oxidative stress was observed in treatment groups which further support the results of % enzyme activity and antioxidant status as discussed earlier. Low-dose treatment with DSL-EA also resulted in moderate improvement of the overall oxidative status of test rats. The details are presented in Figure 3.

The MPO expression levels in liver tissue act as marker of neutrophilic infiltration during inflammation. As expected in CCL₄-induced liver injury, the MPO expression was markedly increased in the liver tissues of the disease control rats. Silymarin, DSL-EA-LD, and DSL-EA-HD decreased the % MPO activity in a statistically significant and comparable manner ($P < 0.05$, 0.01, and 0.001) as

TABLE 1: Effect of the DSL-EA-LD and DSL-EA-HD on the complete blood profile.

Hematological parameters	Normal control (mean \pm SEM)	Vehicle control (mean \pm SEM)	Disease control (mean \pm SEM)	Silymarin treated (mean \pm SEM)	DSL-EA-LD (mean \pm SEM)	DSL-EA-HD (mean \pm SEM)
HGB (g/dL)	12.86 \pm 0.45	12.67 \pm 0.92	8.02 \pm 1.02 ^{###}	11.98 \pm 0.087*	10.34 \pm 0.23*	12.10 \pm 1.03*
RBC ($\times 10^6$ /mm ³)	10.01 \pm 0.34	10.2 \pm 0.04	6.07 \pm 0.32 ^{###}	9.98 \pm 0.22*	8.78 \pm 0.43*	10.06 \pm 0.23*
WBC ($\times 10^3$ /mm ³)	8.078 \pm 1.21	8.11 \pm 0.04	13.12 \pm 0.03 ^{###}	8.98 \pm 0.03*	9.43 \pm 0.23*	8.34 \pm 0.32*
Neutrophils (%)	33.7 \pm 4.06	31.3 \pm 1.07	62.04 \pm 1.31 ^{###}	45.8 \pm 0.72**	59.87 \pm 1.23*	36.14 \pm 0.32**
Monocytes (%)	5.83 \pm 0.70	5.43 \pm 0.70	12.12 \pm 1.03 ^{###}	7.09 \pm 0.35*	8.92 \pm 1.12*	7.64 \pm 1.09*
Eosinophils (%)	0.78 \pm 0.10	0.73 \pm 0.05	0.90 \pm 0.22 ^{###}	0.78 \pm 0.12**	0.852 \pm 0.01**	0.761 \pm 0.05**
Basophils (%)	0.45 \pm 0.02	0.461 \pm 0.12	0.81 \pm 0.05 ^{###}	0.57 \pm 0.14*	0.598 \pm 0.051*	0.521 \pm 0.12*

All values are expressed as mean \pm SEM ($n=6$), * $P < 0.05$, ** $P < 0.01$, and *** $P < 0.001$ as compared to the disease control group. The results were analyzed by the two-way ANOVA followed by Dunnett's test. HGB: hemoglobin; RBC: red blood cells; WBC: white blood cells.

TABLE 2: Effect of the DSL-EA-LD and DSL-EA-HD on the biochemical parameters.

Biochemical parameters	Normal control (mean \pm SEM)	Vehicle control (mean \pm SEM)	Disease control (mean \pm SEM)	Silymarin treated (mean \pm SEM)	DSL-EA-LD (mean \pm SEM)	DSL-EA-HD (mean \pm SEM)
ALT (U/L)	25.32 \pm 1.1	25.9 \pm 1.50	188.73 \pm 3.24 ^{###}	56.45 \pm 1.24**	78.62 \pm 2.81**	51.32 \pm 2.18**
AST (U/L)	28.9 \pm 1.53	30.1 \pm 2.40	231.98 \pm 2.32 ^{###}	76.2 \pm 4.12**	96.71 \pm 3.12***	80.35 \pm 4.00**
ALP (U/L)	45.12 \pm 2.10	47.56 \pm 1.90	172.74 \pm 4.41 ^{###}	67.54 \pm 1.21**	92.42 \pm 2.32**	62.81 \pm 2.90**
Bilirubin (mg/dL)	1.023 \pm 0.02	1.1 \pm 0.011	2.99 \pm 0.04 ^{###}	1.870 \pm 0.09***	2.09 \pm 0.087***	1.54 \pm 0.71***
Albumin (g/L)	16.34 \pm 1.32	15.32 \pm 0.87	4.28 \pm 0.09 ^{###}	12.45 \pm 0.10**	8.12 \pm 0.84**	13.5 \pm 0.09**
Creatinine (mg/dL)	0.276 \pm 0.03	0.284 \pm 0.10	1.08 \pm 0.04 ^{###}	0.41 \pm 0.089*	0.73 \pm 0.13*	0.378 \pm 0.10*

Values are expressed as mean \pm SEM ($n=6$), * $P < 0.05$, ** $P < 0.01$, and *** $P < 0.001$ as compared to the disease control group. The results were analyzed by the two-way ANOVA followed by Dunnett's test. ALT: alanine transaminase; AST: aspartate aminotransferase; ALP: alkaline phosphatase; U/L: units per liter; mg/dL: milligrams per deciliter; g/L: grams per liter.

shown in Figure 3. The reduced MPO activity greatly helps in curbing neutrophilic infiltration and inflammation in liver tissues.

2.4.5. Effects on Histopathology (H&E and Masson's Trichrome Staining). Histological examination has further ratified the findings of biochemical tests performed previously. Liver tissues of the normal and vehicle control groups were having normal morphological features, i.e., unharmed hepatocytes, central veins, and sinusoids. The disease control group incurred severe liver injury due to CCL₄ injections. The most obvious signs of liver damage were immune cell infiltration, fibrosis, necrosed hepatocytes, and edema as evident in Figure 4 (hematoxylin-eosin (H&E) staining). In an identical manner to effects of DSL-EA observed in biochemical parameters, there was a significant ($P < 0.05$, 0.01, and 0.001) dose-dependent restorative effect on liver tissues. There was no significant difference between the liver histology score of silymarin and DSL-EA-HD-treated groups.

The excessive accumulation of collagen and subsequent liver damage, i.e., fibrosis, was confirmed by Masson's trichrome staining. The results were in complete accordance with H&E-stained slides of liver tissue. Marked reduction in accumulation of extracellular matrix proteins (collagen)

was observed in DSL-EA-HD-treated rats and likewise in the positive control group. Low dose of the extract also resulted in alleviating the injury caused by CCL₄ compared to the disease control group as shown in Figure 5.

2.4.6. Effect on Nrf2 and iNOS Expression Using Immunohistochemistry. The expression of nuclear factor erythroid 2 (Nrf2) and inducible nitric oxide synthase (iNOS) was investigated using immunostaining. There was marked reduction in Nrf2 expression in CCL₄-treated disease control group confirming the diminished resistance to oxidative stress. The expression level of iNOS on the other hand was increased due to obvious signs of tissue damage in the disease control rats. As shown in Figure 6, DSL-EA treatments have restored the normal Nrf2 and iNOS expression levels in a significant manner ($P < 0.05$, 0.01, and 0.001). As observed in hematological and biochemical investigations, the effect was dose dependent, with DSL-EA-HD- and silymarin-treated groups revealing identical immunoreactivity scores (Figure 6).

3. Discussion

Medicine derived from natural origin has gained immense interest and popularity in recent years owing to their great

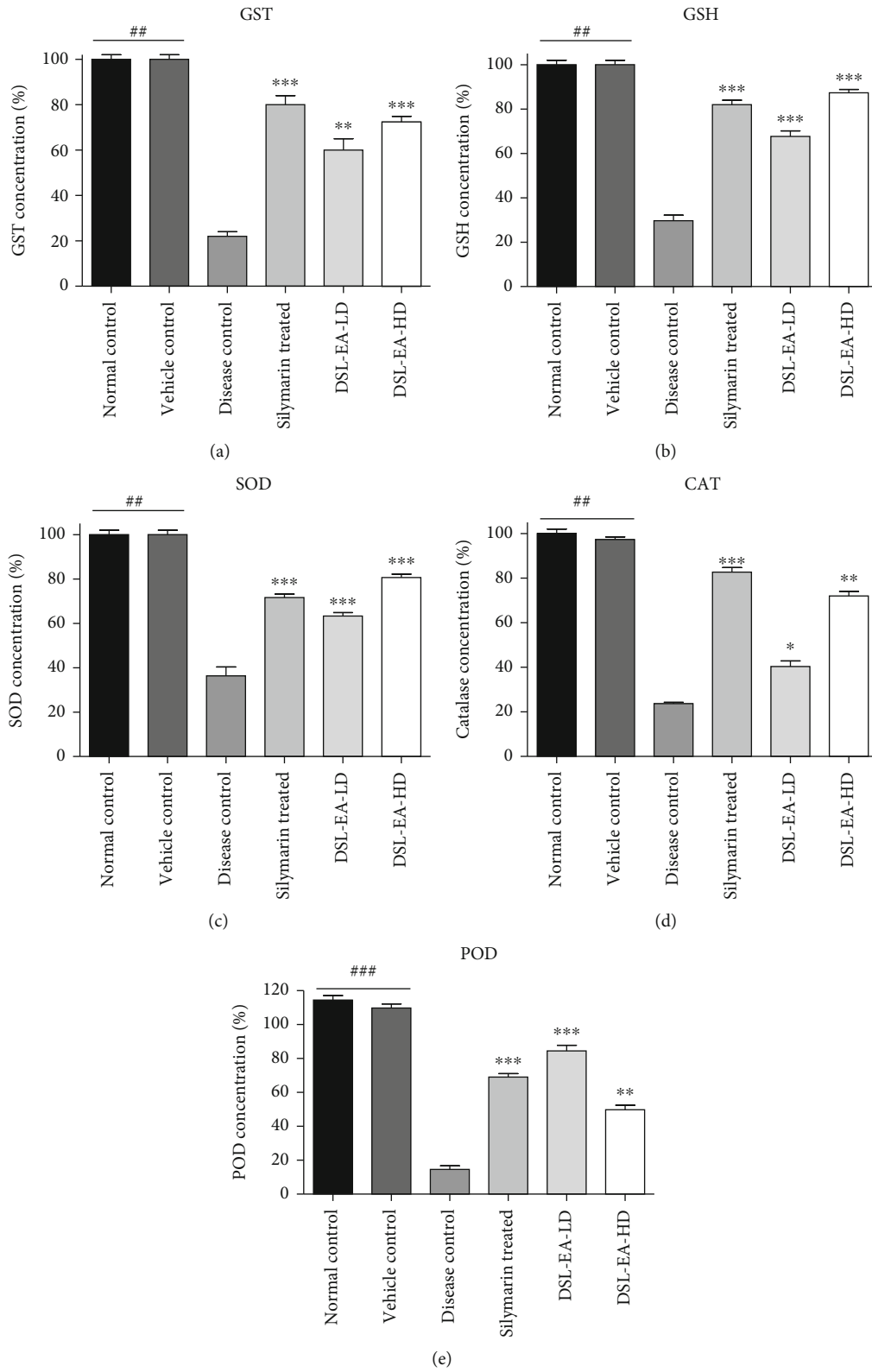


FIGURE 2: Effect of DSL-EA-LD and HD on glutathione S-transferase (GST) (a), glutathione (GSH) (b), superoxide dismutase (SOD) (c), catalase (d), and peroxidase (POD) (e) levels in liver tissue compared to the disease control group. All values are expressed as mean \pm SEM ($n = 6$), * $P < 0.05$, ** $P < 0.01$, and *** $P < 0.001$ as compared to the disease control group.

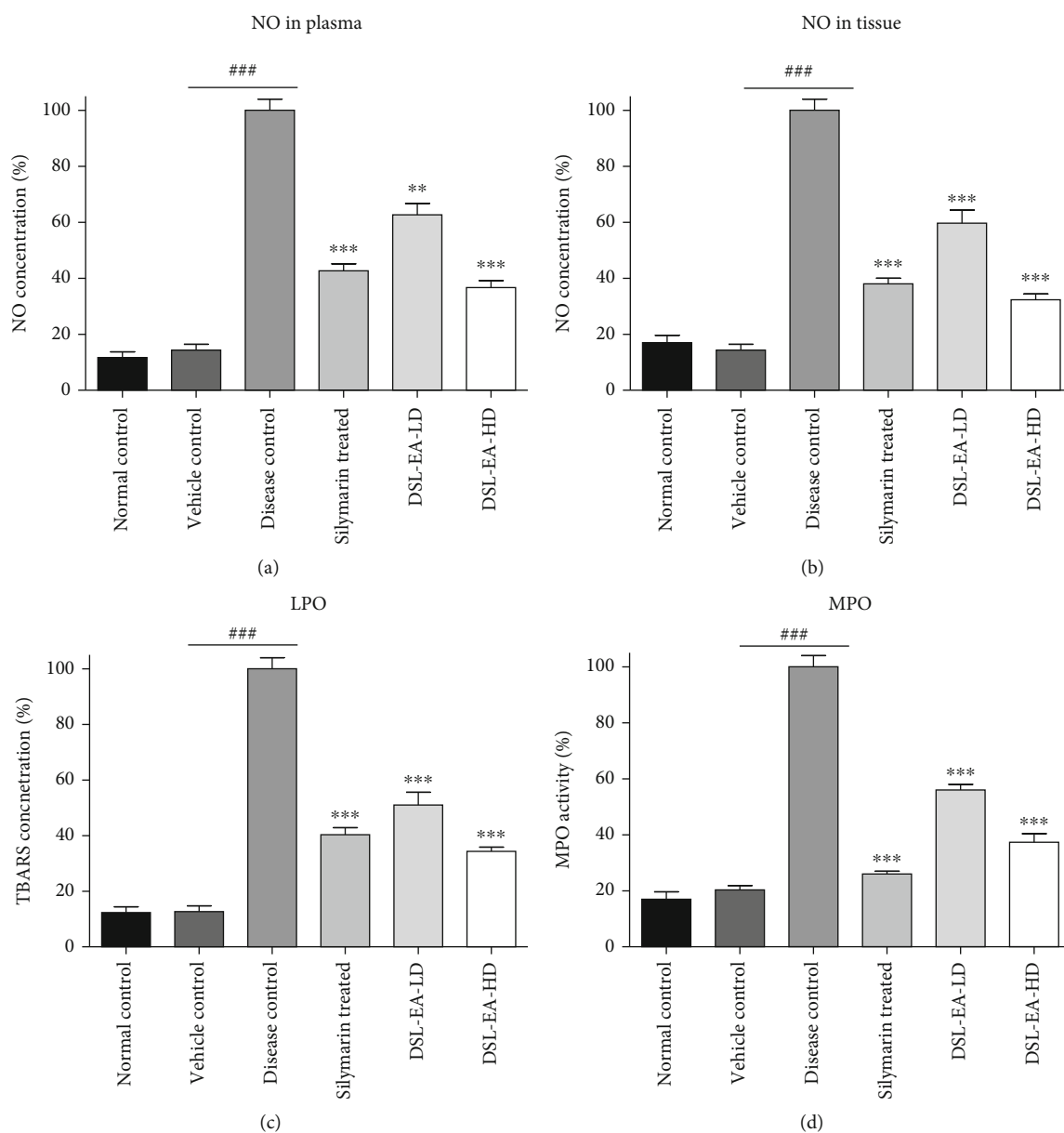


FIGURE 3: Effect of the DSL-EA-LD and HD on the oxidative stress markers such as nitric oxide (NO) in plasma (a), NO in liver tissue (b), malondialdehyde (MDA) (c), and myeloperoxidase (MPO) (d) concentration in liver tissues compared to the disease control group. All values are expressed as mean \pm SEM ($n = 6$), * $P < 0.05$, ** $P < 0.01$, and *** $P < 0.001$. LPO: lipid peroxidation assay.

potential to prevent and treat several health issues linked to oxidative stress in a much safer and effective way [21]. Plants are considered the earliest source of drug discovery, and plant-based drugs have played a vital role in the healthcare system around the world [22]. Most medicinal plants have been known to be useful in mitigating more than one disease condition. This is because plants do possess a cocktail of constituents each possessing its own pharmacological effects. These constituents act via diverse mechanisms, and some of these have synergistic effects, while others have distinct therapeutic effects elicited through numerous receptors. Many such constituents are known to possess anti-inflammatory actions and are capable of repairing the injured cells or limiting the deleterious effects of inflammatory products [23].

Datura stramonium was chosen for the current study based on evidence regarding its reputation as a potential source of anti-inflammatory agents [20, 24]. In the initial phase of our study [16], pharmacologically significant secondary metabolites were estimated in the ethyl acetate leaf extract (DSL-EA) of selected plant followed by *in vitro* antioxidant and anticancer assessment. The toxicity profile of the extract was checked, and once the safety index was established, the extract was utilized in assessing the *in vivo* anti-inflammatory activity using CCl_4 -induced hepatic injury model in the rats.

Phytochemical investigations of DSL-EA revealed the presence of phenolics and flavonoids as reported in our previous paper [16], and these polyphenolic moieties play a vital

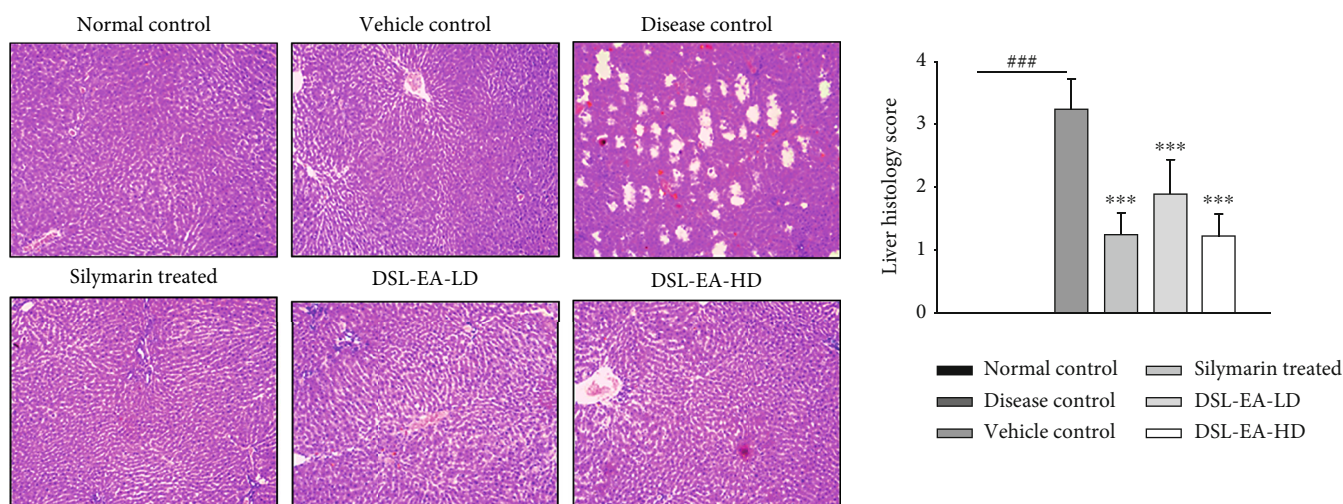


FIGURE 4: Hematoxylin-eosin (H and E) staining of the liver tissue. The restorative effect of the DSL-EA-LD and HD on liver tissues following CCL₄-induced liver injury. The extracts markedly improved the histological parameters such as immune cell infiltration, fibrosis, and edema compared to the disease control. All values are expressed as mean ± SEM (n = 6), *P < 0.05, **P < 0.01, and ***P < 0.001 as compared to the disease control group.

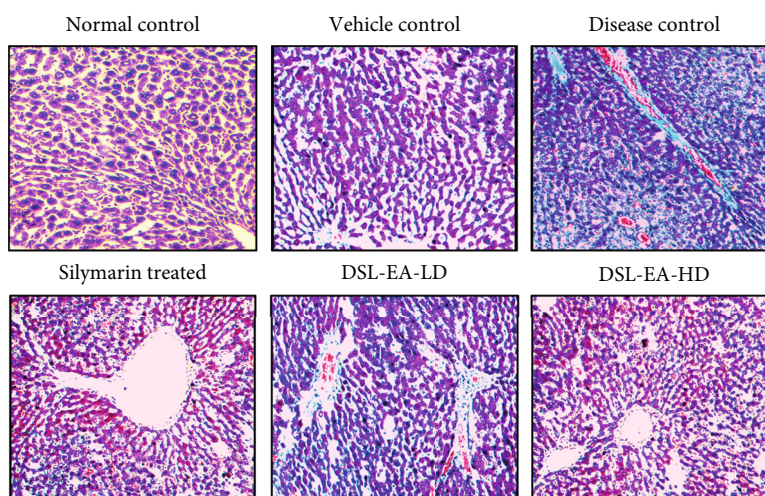


FIGURE 5: Masson's trichrome staining of the liver tissues. The extracts markedly improved the histological parameters and inhibited the liver fibrosis compared to the disease control.

role in the overall antioxidant defense mechanism of plants owing to the presence of hydroxyl, methoxy, ketonic, and phenolic functional groups in their chemical structure [25]. These compounds are widely reported to have free radical scavenging and lipid peroxidation inhibitory activities [16]. Polyphenolic compounds have a wide array of pharmacological benefits including but not limited to their anticancer, antioxidant, anti-inflammatory, antiangiogenic, and tumor suppressive actions [26–30]. Moreover, the hepatoprotective effect of polyphenols, i.e., gallic acid, rutin, apigenin, and catechin, has been widely documented in multimodal pre-clinical *in vitro* and *in vivo* studies [31–34].

Advancements in molecular biology have strengthened and rejuvenated the research interest of scientists in already established evidence of close association between inflamma-

tion and cancer [35, 36]. Once triggered by endogenous or exogenous stimuli, restoration of normal tissue physiology and elimination of toxins are achieved by inflammatory response of the body. However, in chronic cases, it can lead to serious disease conditions, the most worrying pathological state being cancer. Epidemiological data also indicates that one-fourth of all cancers are linked to chronic unresolved inflammatory disorders [37]. Chronic inflammatory disorders may pave way to situations that foster genomic lesions and cancer progression. The host combats such deleterious insults by numerous mechanisms, one prominent effector mechanism is the generation of free radicals, i.e., reactive oxygen species (ROS), superoxide (O₂•), hydroxyl radical (OH•), and reactive nitrogen species (RNS), i.e., nitric oxide (NO•) and peroxynitrite (ONOO⁻). These molecules are

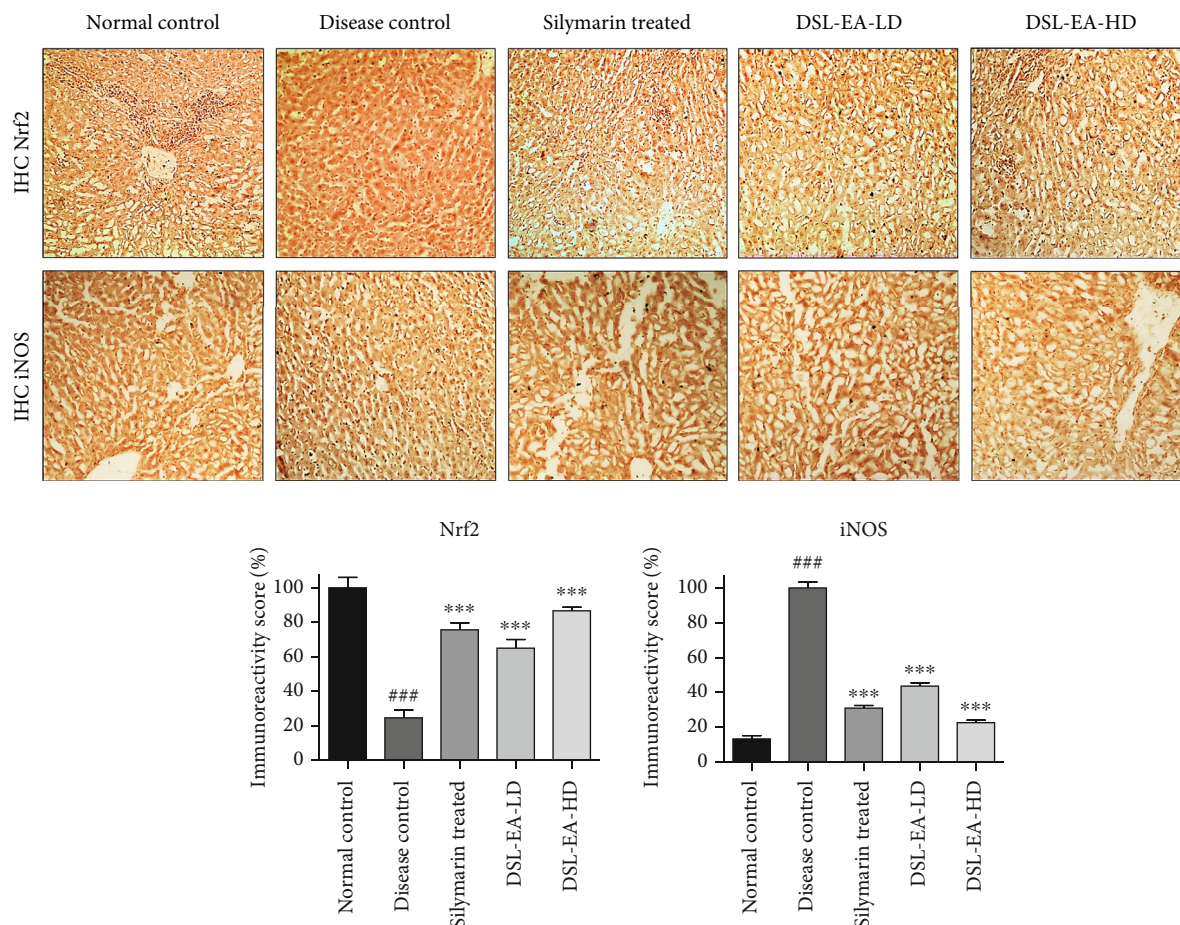


FIGURE 6: Effect of the DSL-EA-LD and HD treatment on expression level of nuclear factor erythroid 2(Nrf2) and inducible nitric oxide synthase (iNOS) in the liver tissue using immunohistochemistry analysis. The DSL-EA-LD and HD induced the expression of Nrf2 while inhibited the iNOS expression compared to the disease control. IHC: immunohistochemistry. All values are expressed as mean \pm SEM ($n = 6$), * $P < 0.05$, ** $P < 0.01$, and *** $P < 0.001$ as compared to the disease control group.

produced by the activities of host enzymes, i.e., NADPH oxidase, myeloperoxidase, and nitric oxide synthases. These enzymes are regulated by signaling pathways involved in inflammation. Unregulated ROS and RNS production leads to oxidative stress and damage to DNA bases that ultimately results in elevated risk of DNA damage [38].

The nitric oxide scavenging potential of DSL-EA in LPS-challenged murine macrophages was estimated, and at concentration of 2.5-20 $\mu\text{g}/\text{mL}$, significant inhibition of NO production was observed. Macrophages activated by immune response generate NO at a higher rate at inflammatory sites which then play a major role as immune regulators and neurotransmitters in various tissues [39, 40]. Scavenging the excessive NO radicals thus constitutes a prominent therapeutic approach for curbing inflammatory disorders.

The toxicity profile of DSL-EA was evaluated, and no significant cytotoxic action was observed against isolated normal human lymphocytes [16]. Cytotoxicity was further gauged by quantifying DSL-EA's action against macrophages isolated from rat peritoneum. As discussed in the Results, even at the highest used concentration, DSL-EA did not kill the isolated macrophages which further proves

the selective nature of its cytotoxic action. Keeping in view the escalating demand to discover new anti-inflammatory and anticancer drug moieties, it is quite imperative to identify potent molecules with clinically proven safety profile.

Following *in vitro* screening of the extract, acute toxicity was assessed in the rats at doses ranging from 150 to 2000 mg/kg. Observation of no harmful and damaging effects on any of the groups over a period of two weeks further confirmed the safety of DSL-EA within the specified dose range, and it led to the designing of noninvasive single day and subchronic anti-inflammatory *in vivo* assays. Two of the most widely recognized mice models to evaluate the anti-inflammatory potential of potential medicinal agents are carrageenan-induced paw edema and croton oil-induced anal edema inhibition tests [41]. Mediators effecting acute inflammatory responses generally work in three different phases with histamine and serotonin being released in first phase (first 1.5 hr), and second phase involves bradykinin release (1.5-2 hr), while prostaglandins are involved in the third and last phase (2.5-6 hr) [42]. Carrageenan-induced edema is a biphasic model, and edema induction in the first two hours is due to bradykinin, serotonin, and

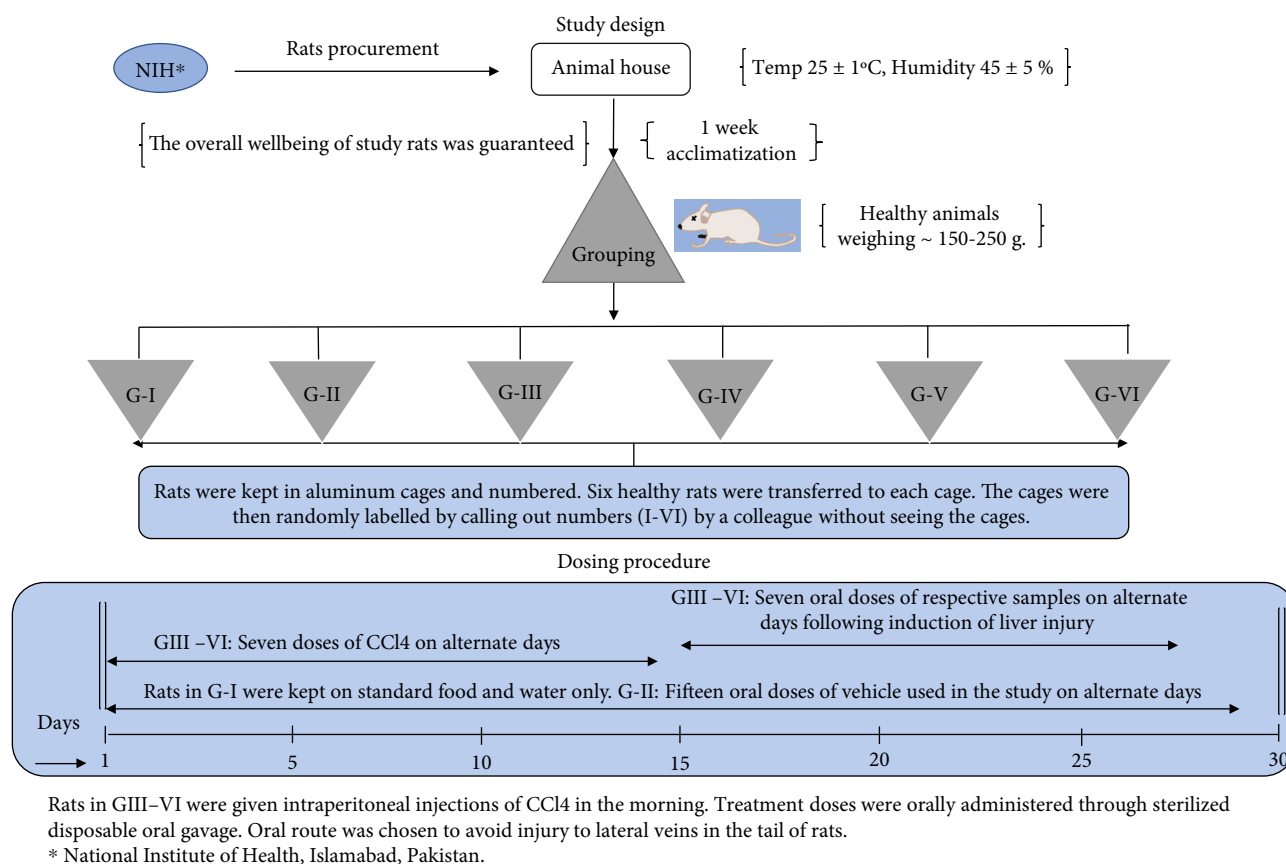


FIGURE 7: A schematic diagram of study design and experimental timeline of the *in vivo* anti-inflammatory assay performed using male Sprague-Dawley rats. Clip art images in the figure were made using ChemDraw Professional v20.0.

histamine release, while in the latter stages (3-5 hr), prostaglandins are primarily responsible for edema [43]. Moreover, croton oil-induced inflammatory responses are primarily characterized by edema, greater vascular permeability, neutrophil infiltration, and prostaglandin production [44]. Considerable reduction in edema volume was observed at the 4th hour following administration of predetermined doses of DSL-EA in both models of inflammation used in the current study. The anti-inflammatory response was in a dose-dependent manner, and previously published data support our findings [20, 42]. It can be inferred from the pattern of observed edema inhibitory action that the leaf extract has a tendency to limit the production of certain inflammatory mediators and proinflammatory cytokines.

Inflammation is reckoned to play a critical role in promoting susceptibility to depression, so treating inflammation, regardless of its type and cause, can be of great therapeutic benefit in improving the overall health status [45]. There is ample data to support the notion that depression is accompanied by elevated oxidative and nitrosative stress, and it also has a strong association with chronic inflammatory response [46, 47]. Several pathways are involved in carrying signals to the brain in the event of peripheral inflammation, i.e., cytokine transport system, vagus nerve and leaky regions in the blood-brain barrier [48], and peripheral cytokines are then disturb the synthesis and reuptake of neurotransmitters including, serotonin,

dopamine, and norepinephrine [49]. In the current study, tail suspension test was used to predict the effect of DSL-EA on the behavior of test animals when they were exposed to testing conditions. Tail suspension test is a commonly used behavioral test in rodents and is used to assess the clinical effectiveness of antidepressant agents [50]. The efficacy of test samples is usually scaled by observing the reduction in immobility time, i.e., the state of helplessness displayed by test animals. DSL-EA HD, when compared with the positive control (fluoxetine), displayed mild effect, while slight reduction in the immobility time was observed in the low-dose group animals. *D. stramonium* has reported ethnomedicinal uses in epilepsy and depression when used internally, while in the form of ointments, it was utilized by ancient communities in rheumatism and burns [51], but there is lack of latest comprehensive data about its antidepressant potential. Hot plate test is a prominent nociceptive test using thermal stimuli to assess the centrally mediated analgesic action of test samples [52]. Scientific evidence supports the notion that drug molecules causing increase latency period possibly possess central analgesic activity [53]. Ethnopharmacological use of *D. stramonium* leaves as an antinociceptive agent was further validated by conducting the hot plate assay using mice model. Moderate elevation in latency period was observed in the case of DSL-EA HD, while low dose revealed slight antinociceptive response as per readings taken at 4th hour of the experiment. *D. stramonium* leaves have been

used traditionally for the management of pain externally as topical preparations [54]; the plant also has reported pharmacological use as an analgesic in variety of inflammatory disorders and pain [19, 55]. Our observations have further reinforced this ethnomedicinal and folklore use of *D. stramonium*. Promising results in toxicity studies and acute *in vivo* assays braced the plan to perform chronic *in vivo* anti-inflammatory assay using carbon tetrachloride (CCL_4) as inducer of hepatic injury. The liver is continuously exposed to exogenous moieties derived from food, drugs, chemicals, and microbiota in the gut even under normal physiological conditions. Liver parenchymal and nonparenchymal cells are susceptible to harm instigated by oxidative stress, and prolonged stress can lead to changes in the composition of parenchymal cells as well as hepatic extracellular matrix. The cascade of events then causes recruitment of inflammatory and immune cells at the site of injury which further result in activation of nonparenchymal cells, i.e., stellate and hepatic Kupffer cells [56]. This is followed by a significant elevation in the levels of cytokines, chemokine, and growth hormones leading to liver fibrosis, the gateway to numerous hepatic abnormalities including HCC [57]. Regardless of the intrinsic dissimilarities between numerous etiological factors responsible for fibrosis, cirrhosis, and HCC, the preservation of wound healing response triggered by parenchymal cell death and the subsequent inflammatory cascade is a common denominator [58]. CCL_4 is a toxicant linked to liver damage via generation of oxidative stress and injury of cellular components [59]. In the current study, the effect of DSL-EA extract in CCL_4 -induced liver inflammation was assessed through a series of hematological, biochemical, enzymatic, and histological studies. Moreover, immunohistochemistry studies were also incorporated to further scrutinize the anti-inflammatory potential of tested sample. Hematological investigations are a useful prognostic tool for underlying inflammatory conditions and consequent oxidative stress in vital organs including liver. CCL_4 is known to cause hematological aberrations including lysis of RBCs and anemia following its metabolism and ROS production [60]. Distinctly decreased RBCs and hemoglobin levels and higher WBCs count in the disease control rats indicated the harm toxic effects of chemical toxin used in the study. The DSLA-EA-treated groups revealed almost identical results to the positive control "silymarin" used in the study. The presence of pharmacologically significant secondary metabolites including polyphenols, terpenoids, withanolides, steroidal glycosides, and alkaloids might be responsible for the vasotonic effects of DSL-EA. Estimation of serum levels of enzymes, i.e., ALT, AST, and ALP, are considered as important indicators of the functional integrity of hepatocellular membranes. These are cytosolic enzymes and seep out into the plasma in the event of hepatic injury accounting for their raised levels in the serum [14, 61] as observed in the disease control rats in our study due to CCL_4 intoxication. Elevated bilirubin level in serum is also an indication of underlying liver damage and subsequent obstruction in bile excretion, thus serving as a useful confirmative test [62]. Similarly, reduced level of serum albumin is also an indication of ROS-mediated inflammatory condition

within the body due to protein oxidation and lipid peroxidation-type reactions [63]. DSL-EA's effect on the said parameters was quite remarkable, and there was significant difference between the findings of the DSL-EA-treated groups and disease control rats. While the mechanism of restorative effect on liver functionality is not clear, this might be accredited to free radical scavenging and lipid peroxidation inhibitory potential of polyphenolic compounds present in the plant [26]. Oxidative stress due to CCL_4 intoxication damages the antioxidant defense mechanism by deactivating the cellular antioxidant enzymes. Trichloromethyl peroxy radicals ($\text{CCl}_3\text{OO}\cdot$) derived from CCL_4 cause lipid peroxidation and inhibition of oxidative enzymes, thus leading to over accumulation of $\text{O}_2\cdot^-$ and H_2O_2 resulting in massive outpouring of free radicals causing hepatic injury [64]. The major antioxidant enzymes responsible for neutralization of free radicals are GST, SOD, CAT, and POD. Moreover, a nonenzymatic antioxidant, GSH, also plays a major role in shielding hepatocytes by scavenging hydrogen peroxides and lipid peroxides as well as through its role as a substrate in catalytic action of glutathione peroxide [65]. The restoration of mentioned antioxidant defense system by DSL-EA, specifically in high-dose group, was remarkable, and the results were almost comparable to positive control used in the study. The findings of *in vitro* antioxidant and anti-inflammatory assays in our study are further validated with these results. Medicinally important phytoconstituents of *D. stramonium* leaf, i.e., terpenes [66], essential oils [42], polyphenols, steroids, tannins [67], and steroidal glycosides [68], might be responsible for the restorative effects observed in our study.

Oxidative stress markers addressed in the current study are NO, MDA, and MPO levels. A debilitated antioxidant defense setup results in dire consequences including greatly increased lipid peroxidation and loss of cellular membrane integrity. There are several end products of lipid peroxidation including MDA. Furthermore, there exists a close association between MPO enzyme level and oxidative stress [69]. Increase in MPO level serves as an indirect indicator of neutrophilic infiltration and inflammation [70]. Finally, in inflammatory conditions, NO is synthesized in excessive amount, surpassing the normal physiological NO level by almost 1000 folds, and this exceedingly higher NO production can result in ROS-mediated tissue damage [71]. Estimating the effect of DSL-EA on the levels of abovementioned markers thus provided a stout indication of its overall anti-inflammatory potential. The results observed were in accordance with the findings of biochemical and antioxidant enzyme level. MDA and MPO levels in liver tissue were greatly elevated, and NO production was also observed to be higher both in plasma and liver tissue of disease control rats, indicating the antioxidant defense system to be in dire straits due to CCL_4 intoxication. Considerable reduction in % concentration of MDA and NO was observed in the DSL-EA-treated groups (more effective reduction in high-dose group). Our results further support the findings of previously reported potential of *D. stramonium* leaf extract in curbing oxidative stress [16]. MPO level was also reduced in the treatment groups as compared to

significantly elevated level in the disease control rats. Bio-transformation of CCl_4 is carried out by endoplasmic reticulum (ER) which is one of the chief cellular organelle responsible for normal cellular functions [72, 73]. CCl_4 is known to disrupt the normal function of ER within the hepatocytes leading to centrilobular necrosis and fatty degeneration of the liver [74]. CCl_4 intoxication is normally associated with damaged ER and cellular membrane, immune cell infiltration, and necrosed hepatocytes, and all these collectively result in severely disfigured hepatocyte ultrastructure [75]. In the present study, H and E staining of the liver tissue of disease control group revealed immune cell infiltration, fibrosis, necrosed hepatocytes, and edema. DSL-EA in a manner identical to silymarin restored the normal histoarchitecture of liver tissues. The findings are in true agreement with a range of investigations performed in the current study proving significant anti-inflammatory action of the plant extract. Masson's trichrome staining is used effectively to measure the extent of liver fibrosis and necrosis by detecting collagen in liver tissues [76]. The presence of hyperplastic fibrous tissue due to CCl_4 -induced liver damage was confirmed by Masson's staining. Clear improvement was observed in the DSL-EA-treated groups in terms of detected collagen content and fibrosis, further confirming the results of preceding investigations done in the current study. Numerous *in vivo* studies have proved the pivotal role played by Nrf2 in inflammatory diseases including liver damage. Nrf2^{-/-} animals used in these studies have shown aggravated tissue damage and symptoms of inflammation. It is thus postulated that Nrf2 signaling pathway has a definite protective role in inflammatory disorders [77, 78]. Nrf2 signaling helps in curbing the inflammatory insults by regulation of endogenous antioxidant enzymes and proinflammatory cytokines [78]. The progression of an early phase liver injury to fibrosis usually is preceded by an inflammatory phase with building up of continuous oxidative stress, and under these circumstances, there is upregulation of iNOS and consequential generation of greater amounts of NO [79]. In our study, reduced Nrf2 and elevated iNOS expressions were observed in liver tissue of the CCl_4 -treated disease control rats using immunohistochemistry analysis. Nrf2 expression was elevated by DSL-EA in a dose-independent manner and both low- and high-dose groups exhibited identical improvement. The expression level of iNOS on the other hand was distinctly reduced by high dose of the extract and the positive control used in the study.

Outcomes of our study have scientifically validated the folkloric usage of *D. stramonium* in inflammatory diseases. Notwithstanding the fact that animal models have several common features to human physiology and much has been learned about human development by using animal models, due diligence exercise must be undertaken while extrapolating outcomes of an animal model to clinical studies.

4. Materials and Methods

4.1. Plant Collection and Preparation of Extract. *D. stramonium* was collected in August 2016 from district Mansehra in Khyber Pakhtunkhwa province of Pakistan. The plant

was identified by Prof. Dr. Rizwana Aleem Qureshi, Department of Plant Sciences, Faculty of Biological Sciences, Quaid-i-Azam University, Islamabad, Pakistan. Following identification, a dried sample of *D. stramonium* was deposited at the Herbarium of Quaid-i-Azam University, Islamabad, with voucher number PHM-504. The plant was washed with water, segregated into parts (root, stem, fruit, and leaf), and shade dried at a properly ventilated place. Fully dried plant parts were grinded into fine powder and weighed. Ultrasonication-assisted maceration was performed for successive extraction using four different solvents with increasing order of polarity (n-hexane, ethyl acetate, methanol, and distilled water). The entire extraction process was repeated twice. Prior to rotary evaporation, the extracts were filtered using Whatman No. 1 filter paper and later dried in vacuum oven at 40°C. Numerous bench top assays were performed by weighing out and preparing samples of various concentrations. The extracts were stored at -20°C until further use.

4.2. Chemicals and Reagents. All chemicals and reagents consumed in our study were of analytical grade and were purchased from authentic vendors. Solvents, i.e., ethyl acetate and dimethylsulfoxide (DMSO), were purchased from Merck (Darmstadt, Germany). Potassium dihydrogen phosphate, dipotassium hydrogen phosphate, ferrous chloride, sodium hydroxide, aluminum chloride, ascorbic acid, quercetin, gallic acid, rutin, caffeic acid, kaempferol, myricetin, and (+)-catechin were acquired from Sigma-Aldrich (Steinheim, Germany). Folin-Ciocalteu reagent was purchased from Sigma-Aldrich (Steinheim, Germany). Sodium carbonate, sulphuric acid, hydrogen peroxide, potassium ferricyanide, sodium dihydrogen phosphate, and disodium hydrogen phosphate were purchased from Merck KGaA (Darmstadt, Germany). Tween 80, thiobarbituric acid, trichloroacetic acid, ferric chloride, and phenazine methosulphate were acquired from Sigma (Chemicals Co. St. Louis, USA). The chemicals and standard drugs were freshly made before use. Primary and secondary antibodies used for Nrf2 and iNOS proteins were procured from Santa Cruz (Santa Cruz Biotechnology, Inc.). All other chemicals were obtained from Sigma (Chemicals Co. St. Louis, USA).

4.3. Animals. Sprague-Dawley rats and BALB/c mice were acquired from the National Institute of Health, Islamabad, Pakistan (NIH).

4.4. In Vitro Anti-inflammatory Assay

4.4.1. Nitric Oxide Scavenging Potential. The selected extract was also analyzed for its nitric oxide (NO) scavenging potential in murine macrophages using the Griess reagent method reported previously [80]. The experiment was performed in a 96-well plate, isolated macrophages were seeded at a density of 1×10^6 per well, and the plate was kept at 37°C for 24 hr in a 5% CO_2 incubator. The cells were then treated with various concentrations (2.5 to 20 $\mu\text{g}/\text{mL}$) of test samples and controls and incubated for another two hours under similar conditions. It was followed by addition of 1 mg/mL LPS (10 μL) to the medium, and the cells were incubated

for further 18 hr. The Griess reagent (100 μ L) was then mixed with an equal volume of culture medium and absorbance was recorded at 540 nm. The positive control used in this assay was piroxicam, while LPS was taken as a blank. Quantification of nitrite in the media was done using the sodium nitrite standard curve ($y = 0.0083x + 0.0017$, $R_2 = 0.9999$). The inhibitory capacity of DSL-EA against LPS-induced NO generation by macrophages was obtained from the estimated value of "x" in the regression equation.

Ethyl acetate leaf extracts of *D. stramonium* were selected for estimation of *in vivo* anti-inflammatory activity based on its pharmacologically significant primary and secondary metabolites as well proficient *in vitro* antioxidant and NO scavenging capacity.

4.5. Toxicity Assays

(2.4.1) Lymphocyte and Macrophage Toxicity Assays

Toxicity against human lymphocytes used in the study was checked as reported in our previous publication [16].

The toxicity was also assessed against macrophages isolated from rat peritoneum. The percent cell viability assessment of DSLA-EA was done using MTT assay [81]. The experiment was performed in a 96-well plate, and isolated macrophages were seeded at a density of 1×10^6 per well. The cells were then exposed to different concentrations (2.5 to 20 μ g/mL) of test samples and controls and incubated at 37°C in a 5% CO₂ incubator. Following 24 hr incubation period, 20 μ L MTT solution (1 mg/mL normal saline) was introduced into each well and kept in incubator under identical conditions for 2 hr. Succinate dehydrogenase in mitochondria of alive cells converted MTT into formazan crystals which are purple in color. These crystals were taken and solubilized in DMSO (100 μ L). The absorbance of resulting solution was estimated at 570 nm. Doxorubicin (1-100 μ M) was the positive control, while PBS was used as a negative control in this assay. Percent cell viability was determined using the following formula.

$$\% \text{cell viability} = \frac{\text{Ab sample} - \text{Ab blank}}{\text{Ab conrol} - \text{Ab blank}} \times 100. \quad (1)$$

4.6. Acute In Vivo Studies

4.6.1. In Vivo Acute Toxicity in Rats. To determine the safety profile of extract, acute toxicity assay was performed. Sprague-Dawley rats (6-8 weeks old), weighing approximately 150-250 g, were randomly divided into test and control groups ($n = 6$). Test groups received single booster oral dose of different strengths (150, 300, 500, 1000, and 2000 mg/kg). The control group received normal saline (10 mL/kg). Animals were kept under observation for two weeks, and any symptoms of toxicity and/or deaths were recorded. The guidelines provided by the Organization for Economic Cooperation and Development (OECD) were followed during the study.

4.6.2. Noninvasive Acute In Vivo Tests. The acute *in vivo* activity indicated that the extract was safe to administer in

the range of 150-2000 mg/kg concentrations. Therefore, DSL-EA in two different doses, i.e., 150 mg/kg (low) and 300 mg/kg (high), dissolved in 10% DMSO in olive oil were used to determine the acute *in vivo* anti-inflammatory, anti-depressant, and antinociceptive activity in BALB/c mice. Healthy male mice, 6-8 weeks old, weighing between 25 and 30 g were used in the study. Mice were kept in standard metallic cages and provided with standard diet and water *ad libitum*. Mice were randomly divided into five groups with six mice in each group, and their description is given as follows.

- (i) Group I: normal control (untreated, standard food only)
- (ii) Group II: vehicle control (10% DMSO in olive oil)
- (iii) Group III: positive control (standard drug specific for each test)
- (iv) Group IV: DSL-EA LD (DSL-EA [150 mg/kg])
- (v) Group V: DSL-EA HD (DSL-EA [300 mg/kg])

The experimental details of each noninvasive experiment are provided in the following section.

(1) Carrageenan-Induced Hind Paw Edema Test. The experiment was carried out by following a previously reported procedure with slight modifications [82]. The controls and sample groups were given oral doses of respective samples one hour before the administration of 0.05 mL of carrageenan (1% in sterile water for injection) into the subplanter region of right hind paw. Ibuprofen (the positive control) was also given orally at a dose of 10 mg/kg. Edema volume was estimated by measuring the thickness of right hind paw immediately after the carrageenan injection. Measurement of paw thickness was done at regular intervals for up to 4 hours. The results were expressed as percent edema inhibition using the following formula.

$$EV = PVa - PVi, \quad (2)$$

where EV is edema volume, PV_i is initial paw volume (before carrageenan administration), and PV_a is paw volume following carrageenan injection.

$$\text{Percent edema inhibition} = \left[\frac{EVc - EVt}{EVc} \right] \times 100, \quad (3)$$

where EV_c is edema volume of control mice and EV_t is edema volume of test sample mice.

(2) Croton Oil-Induced Anal Edema Inhibition. Anti-inflammatory potential of DSL-EA was further evaluated by estimating the croton oil-induced anal edema inhibitory response in Balb/c mice. A previously reported procedure was followed [83], and as elaborated previously, different control and treatment groups received respective doses of standard drug and test samples one hour before the induction of acute inflammation. A cotton swab swabbed in the

inducer was introduced gently into the anus of the mice for 10 seconds. The inducer used in this assay was croton oil (200 μ L of 6% croton oil in diethyl ether). The anal edema was measured using a Vernier caliper each hour for four hours following induction. The anti-inflammatory potential of samples, if present, was indicated by reduction in anal edema of treatment groups when compared with the control group. The formula used to calculate percent inhibition in anal edema is given as follows.

$$\% \text{inhibition} = \left(\frac{\text{Control animal edema volume} - \text{test group edema volume}}{\text{Control animal edema volume}} \right) \times 100. \quad (4)$$

(3) *Tail Suspension Test.* Tail suspension test has been effectively used to determine the antidepressant action of tested samples. Slightly modified version of a previously reported protocol was followed in the current study [50]. One hour after administration of extracts and specified samples to relevant groups, mice were individually suspended from their tails using an adhesive tape placed 1 cm from the tip of the tail. The mice were suspended in such a way that they were at 7.5 cm above the surface of a working table. The experiment was carried out in a quiet room and the total duration of the test was 6 minutes. Immobility time was recorded for each group, i.e., that situation during the study when the mice stayed passively hung without any motion or urge to move. The positive control used in this test was fluoxetine given intraperitoneally (i.p) (20 mg/kg). Samples possessing antidepressant action are expected to reduce the immobility time of the mice.

(4) *Hotplate Analgesic Assay.* Hotplate analgesic assay is a well-established and reliable procedure to determine the antinociceptive response in rodents [84]. Before administering the test samples, the mice were individually placed on a heated plate set at $55 \pm 2^\circ\text{C}$ and the paw licking and jumping actions were recorded, the time at which the mice start showing these responses was recorded (T_a), and an average of two readings is normally taken. A cutoff time was set at 30 seconds to prevent tissue damage. One hour after administration of test samples and controls to relevant study groups, each animal was placed again on the heated plate and reaction time, i.e., the time taken to initiate jumping and paw licking while being on the hotplate, was noted (T_b). The reaction times were recorded at regular interval of one hour for up to 4 hours. The positive control used in this test was tramadol (12.5 mg/kg via i.p route). The results are expressed as mean \pm SD of percent analgesia. The percent analgesic or antinociceptive activity was estimated using the following formula.

$$\text{Percent analgesic activity} = \frac{T_b - T_a}{T_a} \times 100. \quad (5)$$

4.7. In Vivo Study (CCL_4 -Induced Toxicity in Sprague-Dawley Rats)

4.7.1. Experimental Design

(1) *Animal Model.* Thirty-six (36) male Sprague-Dawley rats, 6-8 weeks old with weights in the range of ~150-250 g, were selected for the current study. Aluminum cages with wood shavings as bedding were used to retain the animals, and the temperature was maintained at $25 \pm 1^\circ\text{C}$ and air humidity at $45 \pm 5\%$ with a 12 h light/dark cycle. The rats were fed with standard feed and water ad libitum prior to their experimental use.

(2) *Experimental Protocol.* The rats were randomly divided into six groups after a one-week acclimatization period, each group consisted of six rats. Predetermined high and low doses (as indicated by acute toxicity study) of DSL-EA and standard drug used as positive control were orally administered via sterile oral gavage to specified groups. The maximum volume to be administered orally was kept constant at 1 mL. The vehicle used for making suspensions of the extract was 10% DMSO in olive oil. The study had four controls, i.e., normal, vehicle, disease and positive control groups. All doses to respective groups were given in the morning on alternate days.

- (i) Group I: normal control (untreated, standard food only)
- (ii) Group II: vehicle control (10% DMSO in olive oil)
- (iii) Group III: disease control (1 mL/kg of 30% CCL_4 in olive oil)
- (iv) Group IV: positive control (1 mL/kg of 30% CCL_4 +silymarin [50 mg/kg] dissolved in the vehicle)
- (v) Group V: DSL-EA LD (1 mL/kg of 30% CCL_4 +DSL-EA [150 mg/kg])
- (vi) Group VI: DSL-EA HD (1 mL/kg of 30% CCL_4 +DSL-EA [300 mg/kg])

The current *in vivo* experiment lasted for 30 days. Group I rats received no treatment of any kind and were fed and watered ad libitum. Group II animals were given oral doses of the vehicle used in the study to assess any effect it might have on experimental rats. The rats in groups III-VI received intraperitoneal injections (7 doses) of the inducer (30% CCL_4 in olive oil) used in current study. Following disease induction, the rats in groups IV, V, and VI were given 7 doses of silymarin, DSL-EA LD, and DSL-EA HD, respectively, on alternate days. The experiment ended on 29th day and thereafter the rats were kept for 24 hrs before sacrificing and taking blood, serum, and tissue samples for analysis. The study design is elaborated further in Figure 7.

4.7.2. *CCL_4 -Induced Toxicity.* As discussed previously, the rats used in the study were randomly distributed into 6 groups, and CCL_4 model was adopted to induce liver injury [14, 85]. Hepatotoxicity was induced by injecting 0.2 mL

CCL_4 into the peritoneal cavity of the rats in groups III-VI on alternate days.

4.7.3. Collection of Blood Samples and Serum Separation. At the end of the assay, the rats were unfed for 24 h, anesthetized by chloroform inhalation, and subsequently euthanized by cervical dislocation. The blood was collected from abdominal aorta for the assessment of hematological and biochemical parameters. Serum was separated from the collected blood samples by centrifugation for 15 min at 4°C (6000 rpm). Serum was stored at -20°C until analyzed for biochemical tests.

The excised and flash frozen liver portions of the rats from each study group were homogenized using $10\times$ buffer (100 mM potassium phosphate buffer and 1 mM ethylenediaminetetraacetic acid; pH 7.4). Homogenates were then centrifuged for 30 min at 4°C ($12,000\times g$). The resultant supernatant was carefully separated and used for the analysis of endogenous antioxidant enzymes and numerous biochemical parameters.

4.7.4. Estimation of Hematological Parameters. The levels of red blood cells (RBC) and white blood cells (WBC) were estimated by using Neubauer hemocytometer (Feinoptik, Germany). Hemoglobin level was measured with the aid of Sahli's hemoglobin meter. Differential WBC count (% neutrophils, monocytes, eosinophils, and basophils) was also determined following a previously reported method [86].

4.7.5. Assessment of Biochemical Parameters. For the analysis of biochemical parameters, serum separated from the blood samples was used for analysis of alanine transaminase (ALT), aspartate aminotransferase (AST), alkaline phosphatase (ALP), bilirubin, creatinine, and albumin using AMP diagnostic kits (Stattogger Strasse 31b 8045 Graz, Austria) as per the instruction of the manufacturers.

4.7.6. Determination of Endogenous Antioxidant Enzymes and GSH. The level of endogenous antioxidant enzymes, i.e., glutathione S-transferase (GST), superoxide dismutase (SOD), peroxidase (POD), and catalase (CAT) as well as glutathione (GSH), in serum was found using a slightly modified version of a protocol reported earlier [14].

4.7.7. Expression of Biomarkers of Oxidative Stress (MDA, MPO, and NO). Concentration of one of the lipid peroxidation end products, i.e., MDA, in liver tissue was estimated using a slightly modified version of previously reported procedure [87]. Briefly, 0.25 mL tissue homogenate in PBS was incubated at 37°C for 1 h in a water bath. Incubation was followed by addition of 0.25 mL of 5% trichloroacetic acid (TCA) and 0.5 mL of 0.67% thiobarbituric acid (TBA) to the homogenates. Absorbance was recorded at 535 nm.

The MPO activity was estimated using hexadecyltrimethylammonium bromide (HTAB) buffer and o-dianisidine method described in a previously published report [88]. HTAB in 50 mM PBS having pH 6 was used to release MPO from the cells. The tissue was then subjected to freeze thaw cycle for three times and later centrifuged. The supernatant was then mixed with a mixture of hydrogen

peroxide and o-dianisidine, and MPO activity level was recorded at 540 nm using a microplate reader.

The level of nitric oxide was assessed both in plasma and liver tissue homogenates. The Griess reagent method was followed and the absorbance was recorded at 540 nm using a microplate reader [89].

4.7.8. Histological Investigation (Hematoxylin-Eosin and Masson's Trichrome Staining). The evaluation of any changes in liver histology was carried out by employing paraffin-embedded staining protocols. Following dissection, liver tissue was fixed by using 10% buffered formaldehyde solution (pH 7.4) at room temperature for 12 h. The removal of traces of infiltrated wax and water was assured via numerous ethanol (50, 70, 90, and 100%) washings of the fixed tissue. Small pieces (3-5 μm thickness) of the embedded tissue were sectioned to prepare slides and later stained with eosin and hematoxylin (H and E) [16]. The trichrome staining was also performed to assess fibrosis in liver tissue [87]. Lastly, the slides were examined under microscope (Nikon, Eclipse 80i Japan).

4.7.9. Immunohistochemistry. The immunohistochemistry staining was performed to examine the effect of DSL-EA extract on nuclear factor erythroid 2 (Nrf2) and inducible nitric oxide synthase (iNOS) following liver injury caused by CCL_4 toxicity. Paraffin-embedded staining protocol was followed. The tissue was washed with xylene and ethanol followed by treatment with proteinase-k, normal goat serum (NGS), and primary and secondary antibodies (Nrf2 and iNOS) [90].

4.8. Statistical Analysis. The data presented in the study was procured from experiments run in triplicate, and the results are expressed as mean \pm SD. A one-way analysis of variance (ANOVA) was performed followed by Dunnett's test to determine the variability between test groups. Statistical significance was set at $P < 0.05$. The SPSS software (SPSS version 10.0, Chicago, IL) was used to analyze data.

5. Conclusion

Estimation of pharmacologically significant phytoconstituents and proficient results in the *in vitro* biological screening steered the comprehensive evaluation of anti-inflammatory potential of selected extract of *D. stramonium*. Noteworthy acute *in vivo* anti-inflammatory potential further supported the execution of subsequent chronic *in vivo* model. Findings of our study recommend that DSL-EA within a prudently calculated dosing window has the aptitude to restore liver functionality in the event of CCL_4 -induced damage. This claim is supported by results procured from a series of investigations including hematological, biochemical, liver enzymes level, oxidative stress markers, histological, and immunohistochemistry studies. The selected leaf extract of *D. stramonium* has effectively managed to curb the liver damage caused by CCL_4 intoxication. Robust anti-inflammatory action of *D. stramonium* has validated its traditional use in numerous inflammatory conditions. More advanced studies for further elaboration of the molecular

mechanism of its action will be the most logical extension of our preliminary research work.

Data Availability

The datasets presented in the current study are available from the corresponding author on reasonable request

Ethical Approval

The approved guidelines of ethical committee of Quaid-i-Azam University, Islamabad, Pakistan, for animal care and experiments (letter number # PHM-QAU/2018-70) were strictly followed. Guidelines provided by the National Institute of Health (NIH), Islamabad, Pakistan, were ensured. Minimal pain, distress, and discomfort to test animals was guaranteed during the study.

Consent

Written informed consent was obtained from the subjects involved in the study.

Disclosure

The study was independently designed by the authors and the funding body had no role in collection, analysis and interpretation of the data.

Conflicts of Interest

The authors declare no conflict of interest.

Authors' Contributions

IH conceptualized and supervised execution of experiments, critically revised the manuscript, and approved the final version of this manuscript. BN designed the study, performed experiments, analyzed and interpreted the data, and wrote and revised the manuscript. AUK and MWB contributed to the conduction of experiments, acquisition of the data, and critical review of the manuscript. YSA and MF critically reviewed the manuscript and assisted in data analysis. All authors have read and approved the final manuscript.

Acknowledgments

We acknowledge Prof. Dr. Rizwana Aleem Qureshi, Department of Plant sciences, Faculty of Biological sciences, Quaid-i-Azam University, Islamabad, Pakistan, for identifying the plant sample. The authors would also like to thank Prof. Dr. John J Walsh, School of Pharmacy and Pharmaceutical Sciences, Trinity College Dublin, Ireland, for critical review of the abstract, making necessary language corrections, and finalizing the title of our manuscript. The project was funded by the Quaid-i-Azam University, Islamabad, Pakistan, through university research fund (URF). Yusuf S. Althobaiti was supported by the Taif University Research, Taif, Saudi Arabia, Supporting Project Number TURSP-2020/78.

References

- [1] S. Di Meo, T. T. Reed, P. Venditti, and V. M. Victor, "Role of ROS and RNS sources in physiological and pathological conditions," *Oxidative Medicine and Cellular Longevity*, vol. 2016, 44 pages, 2016.
- [2] P. Dey, S. Dutta, A. Biswas-Raha, M. P. Sarkar, and T. K. Chaudhuri, "Haloalkane induced hepatic insult in murine model: amelioration by Oleander through antioxidant and anti-inflammatory activities, an in vitro and in vivo study," *BMC Complementary and Alternative Medicine*, vol. 16, no. 1, p. 280, 2016.
- [3] A. Barzegar and A. A. Moosavi-Movahedi, "Intracellular ROS protection efficiency and free radical-scavenging activity of curcumin," *PLoS One*, vol. 6, no. 10, article e26012, 2011.
- [4] G. N. De Iuliis, R. J. Newey, B. V. King, and R. J. Aitken, "Mobile phone radiation induces reactive oxygen species production and DNA damage in human spermatozoa in vitro," *PLoS One*, vol. 4, no. 7, article e6446, 2009.
- [5] N. Tirkey, S. Pilkhwai, A. Kuhad, and K. Chopra, "Hesperidin, a citrus bioflavonoid, decreases the oxidative stress produced by carbon tetrachloride in rat liver and kidney," *BMC Pharmacology*, vol. 5, no. 1, p. 2, 2005.
- [6] K. S. Kasprzak, "Oxidative DNA and protein damage in metal-induced toxicity and carcinogenesis," *Free Radical Biology and Medicine*, vol. 32, no. 10, pp. 958–967, 2002.
- [7] R. A. Jacob and G. Sotoudeh, "Vitamin C function and status in chronic disease," *Nutrition in Clinical Care*, vol. 5, no. 2, pp. 66–74, 2002.
- [8] S. C. Jeong, S. M. Kim, Y. T. Jeong, and C. H. Song, "Hepato-protective effect of water extract from Chrysanthemum indicum L. flower," *Chinese Medicine*, vol. 8, no. 1, p. 7, 2013.
- [9] H. Cichoż-Lach and A. Michalak, "Oxidative stress as a crucial factor in liver diseases," *World Journal of Gastroenterology: WJG*, vol. 20, no. 25, pp. 8082–8091, 2014.
- [10] M. M. Aydın and K. C. Akçalı, "Liver fibrosis," *The Turkish Journal of Gastroenterology*, vol. 29, no. 1, pp. 14–21, 2018.
- [11] R. Hernández-muñoz, M. Díaz-muñoz, J. Suárez, and V. C. de Sánchez, "Adenosine partially prevents cirrhosis induced by carbon tetrachloride in rats," *Hepatology*, vol. 12, no. 2, pp. 242–248, 1990.
- [12] P. Govind, "Medicinal plants against liver diseases," *IJPR*, vol. 2, pp. 115–121, 2011.
- [13] Z. Memariani, S. Q. Abbas, S. S. Ul Hassan, A. Ahmadi, and A. Chabra, "Naringin and naringenin as anticancer agents and adjuvants in cancer combination therapy: efficacy and molecular mechanisms of action, a comprehensive narrative review," *Pharmacological Research*, vol. 171, p. 105264, 2021.
- [14] R. Batoool, M. R. Khan, and M. Majid, "Euphorbia dracunculoides L. abrogates carbon tetrachloride induced liver and DNA damage in rats," *BMC Complementary and Alternative Medicine*, vol. 17, no. 1, p. 223, 2017.
- [15] X. Meng, Y. Li, S. Li, R. Y. Gan, and H. B. Li, "Natural products for prevention and treatment of chemical-induced liver injuries," *Comprehensive Reviews in Food Science and Food Safety*, vol. 17, no. 2, pp. 472–495, 2018.
- [16] B. Nasir, M. W. Baig, M. Majid et al., "Preclinical anticancer studies on the ethyl acetate leaf extracts of Datura stramonium and Datura inoxia," *BMC complementary medicine and therapies*, vol. 20, pp. 1–23, 2020.

- [17] K. Bonde, "The genus *Datura*: from research subject to powerful hallucinogen," *Ethnobotanical Leaflets*, vol. 1998, p. 10, 2001.
- [18] S. Berkov, R. Zayed, and T. Doncheva, "Alkaloid patterns in some varieties of *Datura stramonium*," *Fitoterapia*, vol. 77, no. 3, pp. 179–182, 2006.
- [19] B. P. Gaire and L. Subedi, "A review on the pharmacological and toxicological aspects of *Datura stramonium* L.," *J integr med*, vol. 11, no. 2, pp. 73–79, 2013.
- [20] G. Sonika, R. Manubala, and J. Deepak, "Comparative studies on anti-inflammatory activity of *Coriandrum sativum*, *Datura stramonium* and *Azadirachta indica*," *Asian Journal of Experimental Biological Sciences*, vol. 1, pp. 151–154, 2010.
- [21] O. I. Aruoma, "Methodological considerations for characterizing potential antioxidant actions of bioactive components in plant foods," *Mutation Research, Fundamental and Molecular Mechanisms of Mutagenesis*, vol. 523–524, pp. 9–20, 2003.
- [22] J. McRae, Q. Yang, R. Crawford, and E. Palombo, "Review of the methods used for isolating pharmaceutical lead compounds from traditional medicinal plants," *The Environmentalist*, vol. 27, no. 1, pp. 165–174, 2007.
- [23] S. O. Otimenyin, "Antiinflammatory medicinal plants: a remedy for most disease conditions?," in *Natural Products and Drug Discovery*, pp. 411–431, Elsevier, 2018.
- [24] B. P. Gaire, *Monograph on Datura stramonium*, 2008.
- [25] F. H. Afshar, A. Delazar, H. Nazemiyeh, S. Esnaashari, and S. B. Moghadam, "Comparison of the total phenol, flavonoid contents and antioxidant activity of methanolic extracts of *Artemisia spicigera* and *A. splendens* growing in Iran," *Pharmaceutical sciences*, vol. 18, pp. 165–170, 2019.
- [26] H. Fatima, K. Khan, M. Zia, T. Ur-Rehman, B. Mirza, and I. U. Haq, "Extraction optimization of medicinally important metabolites from *Datura innoxia* Mill.: an in vitro biological and phytochemical investigation," *BMC Complementary and Alternative Medicine*, vol. 15, no. 1, p. 376, 2015.
- [27] L. S. Chua, "A review on plant-based rutin extraction methods and its pharmacological activities," *Journal of Ethnopharmacology*, vol. 150, no. 3, pp. 805–817, 2013.
- [28] J. P. V. Singh, K. Selvendiran, S. M. Banu, R. Padmavathi, and D. Sakthisekaran, "Protective role of Apigenin on the status of lipid peroxidation and antioxidant defense against hepatocarcinogenesis in Wistar albino rats," *Phytomedicine*, vol. 11, no. 4, pp. 309–314, 2004.
- [29] S. Choubey, L. R. Varughese, V. Kumar, and V. Beniwal, "Medicinal importance of gallic acid and its ester derivatives: a patent review," *Pharmaceutical patent analyst*, vol. 4, no. 4, pp. 305–315, 2015.
- [30] T. Vuong, J.-F. Mallet, M. Ouzounova et al., "Role of a polyphenol-enriched preparation on chemoprevention of mammary carcinoma through cancer stem cells and inflammatory pathways modulation," *Journal of Translational Medicine*, vol. 14, no. 1, p. 13, 2016.
- [31] O. Karimi-Khouzani, E. Heidarian, and S. A. Amini, "Anti-inflammatory and ameliorative effects of gallic acid on fluoxetine-induced oxidative stress and liver damage in rats," *Pharmacological Reports*, vol. 69, no. 4, pp. 830–835, 2017.
- [32] H. Hosseinzadeh and M. Nassiri-Asl, "Review of the protective effects of rutin on the metabolic function as an important dietary flavonoid," *Journal of Endocrinological Investigation*, vol. 37, no. 9, pp. 783–788, 2014.
- [33] X.-B. Yang and Y. Huang, "Protective effects of apigenin, apigenin-8-sulfonate, and apigenin-3', 8-disulfonate on d-galactosamine-induced acute liver damage in mice," *Medicinal Chemistry Research*, vol. 29, no. 10, pp. 1867–1873, 2020.
- [34] A. Ganeshpurkar and A. Saluja, *The pharmacological potential of catechin*, 2020.
- [35] L. M. Coussens and Z. Werb, "Inflammation and cancer," *Nature*, vol. 420, no. 6917, pp. 860–867, 2002.
- [36] H. Bartsch and J. Nair, "Chronic inflammation and oxidative stress in the genesis and perpetuation of cancer: role of lipid peroxidation, DNA damage, and repair," *Langenbeck's Archives of Surgery*, vol. 391, no. 5, pp. 499–510, 2006.
- [37] D. B. Vendramini-Costa and J. E. carvalho, "Molecular link mechanisms between inflammation and cancer," *Current Pharmaceutical Design*, vol. 18, no. 26, pp. 3831–3852, 2012.
- [38] S. P. Hussain, L. J. Hofseth, and C. C. Harris, "Radical causes of cancer," *Nature Reviews Cancer*, vol. 3, no. 4, pp. 276–285, 2003.
- [39] C. Bogdan, M. Röllinghoff, and A. Diefenbach, "The role of nitric oxide in innate immunity," *Immunological Reviews*, vol. 173, no. 1, pp. 17–26, 2000.
- [40] U. H. Jin, S. G. Park, S. J. Suh et al., "Inhibitory effect of Panax notoginseng on nitric oxide synthase, cyclo-oxygenase-2 and neutrophil functions," *Phytotherapy Research: An International Journal Devoted to Pharmacological and Toxicological Evaluation of Natural Product Derivatives*, vol. 21, no. 2, pp. 142–148, 2007.
- [41] J. H. Yim, O.-H. Lee, U.-K. Choi, and Y. C. Kim, "Antinociceptive and anti-inflammatory effects of ethanolic extracts of *Glycine max* (L.) Merr and *Rhynchosia nulubilis* seeds," *International Journal of Molecular Sciences*, vol. 10, no. 11, pp. 4742–4753, 2009.
- [42] A. S. Aboluwodi, N. Avoseh, A. Lawal, I. Ogunwande, and A. Giwa, "Chemical constituents and anti-inflammatory activity of essential oils of *Datura stramonium* L.," *J Med Plants Stud*, vol. 5, pp. 21–25, 2017.
- [43] S. S. Sakat, K. Mani, Y. O. Demidchenko et al., "Release-active dilutions of diclofenac enhance anti-inflammatory effect of diclofenac in carrageenan-induced rat paw edema model," *Inflammation*, vol. 37, no. 1, pp. 1–9, 2014.
- [44] T. S. Rao, J. L. Currie, A. F. Shaffer, and P. C. Isakson, "Comparative evaluation of arachidonic acid (AA)- and tetradecanoylphorbol acetate (TPA)-induced dermal inflammation," *Inflammation*, vol. 17, no. 6, pp. 723–741, 1993.
- [45] E. Beurel, M. Toups, and C. B. Nemeroff, "The bidirectional relationship of depression and inflammation: double trouble," *Neuron*, vol. 107, no. 2, pp. 234–256, 2020.
- [46] S. Moylan, M. Maes, N. Wray, and M. Berk, "The neuroprogressive nature of major depressive disorder: pathways to disease evolution and resistance, and therapeutic implications," *Molecular Psychiatry*, vol. 18, no. 5, pp. 595–606, 2013.
- [47] M. Maes, M. Berk, L. Goehler et al., "Depression and sickness behavior are Janus-faced responses to shared inflammatory pathways," *BMC Medicine*, vol. 10, pp. 1–19, 2012.
- [48] N. Quan and W. A. Banks, "Brain-immune communication pathways," *Brain, Behavior, and Immunity*, vol. 21, no. 6, pp. 727–735, 2007.
- [49] A. H. Miller, E. Haroon, C. L. Raison, and J. C. Felger, "Cytokine targets in the brain: impact on neurotransmitters and neurocircuits," *Depression and Anxiety*, vol. 30, no. 4, pp. 297–306, 2013.

- [50] J. F. Cryan, C. Mombereau, and A. Vassout, "The tail suspension test as a model for assessing antidepressant activity: review of pharmacological and genetic studies in mice," *Neuroscience & Biobehavioral Reviews*, vol. 29, no. 4-5, pp. 571-625, 2005.
- [51] P. M. Guarrera, "Traditional antihelmintic, antiparasitic and repellent uses of plants in Central Italy," *Journal of Ethnopharmacology*, vol. 68, no. 1-3, pp. 183-192, 1999.
- [52] M. Barrot, "Tests and models of nociception and pain in rodents," *Neuroscience*, vol. 211, pp. 39-50, 2012.
- [53] G. Ibironke and K. Ajiboye, "Chenopodium Ambrosioides leaf extract in rats," *International Journal of Pharmacology*, vol. 3, pp. 111-115, 2006.
- [54] G. Njoroge, "Traditional medicinal plants in two urban areas in Kenya (Thika and Nairobi): diversity of traded species and conservation concerns," *Ethnobotany Research and Applications*, vol. 10, pp. 329-338, 2012.
- [55] P. Soni, A. A. Siddiqui, J. Dwivedi, and V. Soni, "Pharmacological properties of Datura stramonium L. as a potential medicinal tree: an overview," *Asian Pacific Journal of Tropical Biomedicine*, vol. 2, no. 12, pp. 1002-1008, 2012.
- [56] A. I. Cederbaum, Y. Lu, and D. Wu, "Role of oxidative stress in alcohol-induced liver injury," *Archives of Toxicology*, vol. 83, no. 6, pp. 519-548, 2009.
- [57] P. Dey, S. Dutta, M. P. Sarkar, and T. K. Chaudhuri, "Assessment of hepatoprotective potential of N. indicum leaf on haloalkane xenobiotic induced hepatic injury in Swiss albino mice," *Chemico-Biological Interactions*, vol. 235, pp. 37-46, 2015.
- [58] A. Bishayee, "The inflammation and liver cancer," *Inflammation and cancer*, pp. 401-435, 2014.
- [59] H. Ullah, A. Khan, M. W. Baig et al., "Poncirin attenuates CCL4-induced liver injury through inhibition of oxidative stress and inflammatory cytokines in mice," *BMC complementary medicine and therapies*, vol. 20, pp. 1-14, 2020.
- [60] A. I. Abuelgasim, H. Nuha, and A. Mohammed, "Hepatoprotective effect of Lepidium sativum against carbon tetrachloride induced damage in rats," *Research Journal of Animal and Veterinary Sciences*, vol. 3, pp. 20-23, 2008.
- [61] L. Pari and D. R. Amali, "Protective role of tetrahydrocurcumin (THC) an active principle of turmeric on chloroquine induced hepatotoxicity in rats," *Journal of Pharmacy & Pharmaceutical Sciences*, vol. 8, no. 1, pp. 115-123, 2005.
- [62] Z. K. Hassan, M. A. Elobeid, P. Virk et al., "Bisphenol A induces hepatotoxicity through oxidative stress in rat model," *Oxidative Medicine and Cellular Longevity*, vol. 2012, 6 pages, 2012.
- [63] U. Rashid, M. R. Khan, and M. Sajid, "Hepatoprotective potential of Fagonia olivieri DC. against acetaminophen induced toxicity in rat," *BMC Complementary and Alternative Medicine*, vol. 16, pp. 1-18, 2016.
- [64] C.-F. Tsai, Y.-W. Hsu, W.-K. Chen et al., "Hepatoprotective effect of electrolyzed reduced water against carbon tetrachloride-induced liver damage in mice," *Food and Chemical Toxicology*, vol. 47, no. 8, pp. 2031-2036, 2009.
- [65] J. Martensson, A. Meister, and J. Mrtensson, "Glutathione deficiency decreases tissue ascorbate levels in newborn rats: ascorbate spares glutathione and protects," *Proceedings of the National Academy of Sciences*, vol. 88, no. 11, pp. 4656-4660, 1991.
- [66] R. O. Silva, F. B. M. Sousa, S. R. Damasceno et al., "Phytol, a diterpene alcohol, inhibits the inflammatory response by reducing cytokine production and oxidative stress," *Fundamental & Clinical Pharmacology*, vol. 28, no. 4, pp. 455-464, 2014.
- [67] S. Sreenivasa, K. Vinay, and N. Mohan, "Phytochemical analysis, antibacterial and antioxidant activity of leaf extract of Datura stramonium," *International Journal of Science Research*, vol. 1, pp. 83-86, 2012.
- [68] G. Shobha, C. Soumya, K. Shashidhara, and V. Moses, "Phytochemical profile, antibacterial and antidiabetic effects of crude aqueous leaf extract of Datura stramonium," *Pharmacophore*, vol. 5, pp. 273-278, 2014.
- [69] R. K. Schindhelm, L. P. van der Zwan, T. Teerlink, and P. G. Scheffer, "Myeloperoxidase: a useful biomarker for cardiovascular disease risk stratification?," *Clinical Chemistry*, vol. 55, no. 8, pp. 1462-1470, 2009.
- [70] N. Kothari, R. S. Keshari, J. Bogra et al., "Increased myeloperoxidase enzyme activity in plasma is an indicator of inflammation and onset of sepsis," *Journal of Critical Care*, vol. 26, no. 4, pp. 435.e1-435.e7, 2011.
- [71] J. Sharma, A. Al-Omran, and S. Parvathy, "Role of nitric oxide in inflammatory diseases," *Inflammopharmacology*, vol. 15, no. 6, pp. 252-259, 2007.
- [72] G.-H. Lee, B. Bhandary, E.-M. Lee et al., "The roles of ER stress and P450 2E1 in CCL₄-induced steatosis," *The International Journal of Biochemistry & Cell Biology*, vol. 43, no. 10, pp. 1469-1482, 2011.
- [73] T. Slater, K. Cheeseman, and K. U. Ingold, "Carbon tetrachloride toxicity as a model for studying free-radical mediated liver injury," *Philosophical Transactions of the Royal Society of London. B, Biological Sciences*, vol. 311, no. 1152, pp. 633-645, 1985.
- [74] K. Ritesh, A. Suganya, H. Dileepkumar, Y. Rajashekar, and T. Shivanandappa, "A single acute hepatotoxic dose of CCL₄ causes oxidative stress in the rat brain," *Toxicology Reports*, vol. 2, pp. 891-895, 2015.
- [75] E. Altinoz, M. Erdemli, M. Gul et al., "Neuroprotection against CCL₄ induced brain damage with crocin in Wistar rats," *Biotechnic & Histochemistry*, vol. 93, no. 8, pp. 623-631, 2018.
- [76] M. Wang, X. Zhang, X. Xiong et al., "Bone marrow mesenchymal stem cells reverse liver damage in a carbon tetrachloride-induced mouse model of chronic liver injury," *In Vivo*, vol. 30, no. 3, pp. 187-193, 2016.
- [77] C. Mo, L. Wang, J. Zhang et al., "The crosstalk between Nrf2 and AMPK signal pathways is important for the anti-inflammatory effect of berberine in LPS-stimulated macrophages and endotoxin-shocked mice," *Antioxidants & Redox Signaling*, vol. 20, no. 4, pp. 574-588, 2014.
- [78] S. M. U. Ahmed, L. Luo, A. Namani, X. J. Wang, and X. Tang, "Nrf2 signaling pathway: pivotal roles in inflammation," *Biochimica et Biophysica Acta (BBA) - Molecular Basis of Disease*, vol. 1863, no. 2, pp. 585-597, 2017.
- [79] D. L. Diesen and P. C. Kuo, "Nitric oxide and redox regulation in the liver: part II. Redox biology in pathologic hepatocytes and implications for intervention," *Journal of Surgical Research*, vol. 167, no. 1, pp. 96-112, 2011.
- [80] S. Farooq, A. Mazhar, A. Ghouri, and N. Ullah, "One-pot multicomponent synthesis and bioevaluation of tetrahydroquinoline derivatives as potential antioxidants, α -amylase enzyme inhibitors, anti-cancerous and anti-inflammatory agents," *Molecules*, vol. 25, no. 11, p. 2710, 2020.
- [81] S. Khan, E. M. Shin, R. J. Choi et al., "Suppression of LPS-induced inflammatory and NF- κ B responses by anomalin in

- RAW 264.7 macrophages," *Journal of Cellular Biochemistry*, vol. 112, no. 8, pp. 2179–2188, 2011.
- [82] A. Saha, M. A. Masud, S. C. Bachar et al., "The analgesic and anti-inflammatory activities of the extracts of *Phyllanthus reticulatus*. In mice model," *Pharmaceutical Biology*, vol. 45, no. 5, pp. 355–359, 2007.
- [83] M. Majid, B. Nasir, S. S. Zahra, M. R. Khan, B. Mirza, and I.-U. Haq, "Ipomoea batatas L. Lam. ameliorates acute and chronic inflammations by suppressing inflammatory mediators, a comprehensive exploration using in vitro and in vivo models," *BMC Complementary and Alternative Medicine*, vol. 18, pp. 1–20, 2018.
- [84] W. K. Kayani, E. Dilshad, T. Ahmed, H. Ismail, and B. Mirza, "Evaluation of *Ajuga bracteosa* for antioxidant, anti-inflammatory, analgesic, antidepressant and anticoagulant activities," *BMC Complementary and Alternative Medicine*, vol. 16, pp. 1–13, 2016.
- [85] S. R. Dalton, S. M. Lee, R. N. King et al., "Carbon tetrachloride-induced liver damage in asialoglycoprotein receptor-deficient mice," *Biochemical Pharmacology*, vol. 77, no. 7, pp. 1283–1290, 2009.
- [86] A.-S. OA, T. M. El-Hadiyah, and A. A. Al-Majed, "Effect of prolonged vigabatrin treatment on hematological and biochemical parameters in plasma, liver and kidney of Swiss albino mice," *Scientia Pharmaceutica*, vol. 70, no. 2, pp. 135–145, 2002.
- [87] A. M. Khan, A. U. Khan, H. Ali, S. U. Islam, E. K. Seo, and S. Khan, "Continentalic acid exhibited nephroprotective activity against the LPS and *E. coli* -induced kidney injury through inhibition of the oxidative stress and inflammation," *International Immunopharmacology*, vol. 80, article 106209, 2020.
- [88] D. Palić, C. B. Andreasen, J. Ostojčić, R. M. Tell, and J. A. Roth, "Zebrafish (*Danio rerio*) whole kidney assays to measure neutrophil extracellular trap release and degranulation of primary granules," *Journal of Immunological Methods*, vol. 319, no. 1-2, pp. 87–97, 2007.
- [89] J. Ali, A. U. Khan, F. A. Shah et al., "Mucoprotective effects of Saikosaponin-A in 5-fluorouracil-induced intestinal mucositis in mice model," *Life Sciences*, vol. 239, p. 116888, 2019.
- [90] S. Ruiz, P. E. Pergola, R. A. Zager, and N. D. Vaziri, "Targeting the transcription factor Nrf2 to ameliorate oxidative stress and inflammation in chronic kidney disease," *Kidney International*, vol. 83, no. 6, pp. 1029–1041, 2013.

Research Article

Effects and Mechanism of *Ganoderma lucidum* Polysaccharides in the Treatment of Diabetic Nephropathy in Streptozotocin-Induced Diabetic Rats

Yu Hu,^{1,2} Shu-Xiang Wang ,¹ Fu-Yu Wu,² Ke-Jia Wu,² Rui-Ping Shi,² Li-Hong Qin,² Chun-Feng Lu,³ Shu-Qiu Wang,¹ Fang-Fang Wang,¹ and Shaobo Zhou ⁴

¹Basic Medical College, Jiamusi University, Jiamusi, Heilongjiang, China 154002

²School of Medicine, The First Affiliated Hospital of Jiamusi University, Jiamusi 154003, China

³School of Medicine, Huzhou University, Huzhou Central Hospital, Huzhou 313000, China

⁴School of Life Sciences, Institute of Biomedical and Environmental Science and Technology, University of Bedfordshire, Luton, UK LU1 3JU

Correspondence should be addressed to Shu-Xiang Wang; shuxiang_wsx@163.com and Shaobo Zhou; shaobo.zhou@beds.ac.uk

Received 5 November 2021; Accepted 7 January 2022; Published 8 March 2022

Academic Editor: Abdul Rehman Phull

Copyright © 2022 Yu Hu et al. This is an open access article distributed under the Creative Commons Attribution License, which permits unrestricted use, distribution, and reproduction in any medium, provided the original work is properly cited.

Ganoderma lucidum polysaccharides (GLP) have renal protection effect but there was no study on the diabetic nephropathy. This study was designed to investigate its effect and mechanism using a diabetic rat model induced by streptozotocin (50 mg/kg, i.p.). The diabetic rats were treated with GLP (300 mg/kg/day) for 10 weeks. The blood glucose, glycated hemoglobin, body weight, and the levels of blood creatinine, urea nitrogen, and urine protein were assessed. And renal pathologies were assessed by the tissue sections stained with hematoxylin-eosin, Masson's trichrome, and periodic acid-Schiff. The expression of phosphorylated phosphoinositide 3 kinase (p-PI3K), phosphorylated protein kinase B (p-Akt), and phosphorylated mammalian target of rapamycin (p-mTOR), the autophagy proteins beclin-1, LC3-II, LC3-I, and P62; the apoptosis-related proteins caspase-3 and caspase-9; and the inflammation markers IL-6, IL-1 β , and TNF- α were assessed. Results showed that GLP alleviated the impairment of renal function by reducing urinary protein excretion and the blood creatinine level and ameliorated diabetic nephropathy. The expression of p-PI3K, p-Akt, and p-mTOR in the diabetic kidney were significantly reduced in the GLP treatment group compared to the without treatment group. GLP treatment activated the autophagy indicators of beclin-1 and the ratio of LC3-II/LC3-I but reduced p62 and also inhibited the expression of caspase-3, caspase-9 and IL-6, IL-1 β , and TNF- α . In conclusion, the effect of GLP amelioration diabetic nephropathy may be via the PI3k/Akt/mTOR signaling pathway by inhibition of the apoptosis and inflammation and activation of the autophagy process.

1. Introduction

Diabetic nephropathy, a most common complication of glomerulosclerosis, is one of the important factors leading to renal failure in diabetic patients [1]. With the increase in newly diagnosed cases and a 5-year survival rate of approximately 20%, diabetic nephropathy has caused widespread concern [2]. Genetic, oxidative stress, hemodynamic abnormalities, and inflammatory responses are all related to the onset of diabetic nephropathy [3–5]. Presently, clinical treatment mainly aims to alleviate kidney injury by controlling

blood sugar, blood lipid, and blood pressure; however, this action can only slow down the process of renal failure and cannot prevent or reverse the development of the disease. Therefore, finding an efficacious medication for diabetes and its complications, e.g., diabetic nephropathy, is critical in clinical practice.

Ganoderma lucidum, an oriental porous fungus, contains a variety of active substances. *Ganoderma lucidum* polysaccharides (GLP), one of its active ingredients, have unique medicinal and healthcare value and have attracted various research interests [6]. GLP have important biological

activities, such as immunoregulation, anti-inflammatory, and antiaging effects, lowering blood glucose, and protecting the liver [6–9], but there is no research on its antinephropathic effect. Zhu et al. [9] isolated and purified a new polysaccharide (PSG-1) from *Ganoderma lucidum* and found that it significantly reduced fasting blood glucose levels, improved endothelium-dependent aorta relaxation, and increased phosphatidylinositol 3-kinase (PI3K), phosphorylated AKT (p-Akt), endothelial nitric oxide synthase (eNOS), and nitric oxide in the aorta of diabetic rats. After binding insulin to its receptor, PSG-1 can also activate the insulin receptor tyrosine kinase and phosphorylate it to produce PI3K [10]. One regulator of mesangial dysfunction in hyperglycaemia is mammalian target of rapamycin (mTOR) which plays a role in the occurrence and development of diabetic nephropathy. Its downstream effectors play a key role in cell growth and hypertrophy, while the inhibition of mTOR by rapamycin can prevent the development of diabetic nephropathy in animals with type 1 and type 2 diabetes [11].

Autophagy is a self-protection mechanism in cells. It can obtain energy by removing and degrading damaged organelles and recycling the biological macromolecules in the cell to maintain the metabolic balance and the stability of the internal environment [12]. Many studies have shown that autophagy is involved in the pathogenesis of diabetic nephropathy, and that it could serve as a new therapeutic target in the treatment of this condition [13]. Autophagy is an intracellular catabolic process, in which lysosomes are involved in the aging and degradation of damaged organelles and proteins, while LC3 and beclin-1 proteins are early marker proteins of autophagy. Apoptosis, also known as programmed cell death, is an important form of cell homeostasis.

Immune system activation and inflammatory response play important roles in the occurrence and development of diabetic nephropathy. Immune cells such as macrophages are involved in prediabetic nephropathy and renal function damage, and monocyte macrophages can also produce cytokines such as IL-6, IL-1 β , and TNF- α . Together with other inflammatory factors, they are involved in the development of diabetic microvascular disease. TNF- α is an important proinflammatory cytokine and is part of the acute phase response. It is mainly produced by macrophages and monocytes; however, increased expression of TNF- α has been observed in glomeruli and proximal tubular epithelial cells in a diabetic nephropathy model [14]. Through NF- κ B signaling, TNF- α can induce the transcription of cytokines, thereby, affecting the survival, proliferation, and adhesion of cells and promoting inflammatory responses and apoptosis. The occurrence of apoptosis is regulated by cysteine-specific protease (caspases). Caspase-9 is an important initiating factor in the process of apoptosis, while caspase-3 is the executive factor in the process of apoptosis.

This study intends to further explore the effect of GLP in protecting the kidney of diabetic rats with respect to its effect on the PI3K/Akt/mTOR signaling pathway as well as on autophagy, apoptosis, and inflammation, in order to further evaluate the application of GLP as a new agent in the prevention and treatment of diabetic nephropathy.

2. Materials and Methods

2.1. Animals and Research Protocols. This study was approved by the Research Ethics Committee of Jiamusi University (No. 216-JMSU). All steps were taken to reduce animal suffering by following the guideline of using laboratory animals by the Chinese Ministry of Science and Technology. Thirty 8-week-old male specific-pathogen-free (SPF) SD rats, weighing 180–220 g, animal license number: SCXK (Lu) 20140007, were purchased from the Animal Experiment Centre of Jiamusi University. All rats were kept in a laminar flow rack of the SPF Laboratory Animal Center of Jiamusi University. They were placed in an environment with sufficient air circulation and a humidity of 40–70% at a temperature of 22–25°C. They were exposed to 12 h of light, fed with ordinary chow, and provided free access to diet and drinking water for a week. Eight rats were used as a blank control, and the other remaining rats were injected with citric acid-sodium citrate buffer solution in the tail vein. After 12 h of fasting, each rat received a single intraperitoneal injection of streptozotocin 50 mg/kg (Sigma company, USA), and they were provided free access to food after injection. Three days later, fasting blood glucose levels were measured using a blood glucose test strip and a Sinocare ultrasimple blood glucose meter (GA-3); 16 rats with blood glucose values greater than 16.7 mmol/L were randomly divided into a diabetic group and diabetic+GLP group, with 8 animals in each group. The animals were provided normal chow.

The diabetic group was administered saline, the diabetic +GLP group was orally administered GLP (300 mg/kg body weight, per day), and the dosage was based on the previous studies used to efficient lower blood glucose [15, 16] as well as the hypolipidaemic effect [17] which also linked to the diabetic nephropathy. Body weight and fasting blood glucose levels were monitored weekly. After 10 weeks, the rats were placed in a metabolic cage individually to collect urine for 24 h. Subsequently, the rats were euthanized with isoflurane (3% for induction, 2% for maintenance), blood was collected from the eyeballs and centrifuged at 3000 \times g for 15 min at 20°C, the serum was separated from the cells, and the samples were stored at -80°C for further analysis. The left kidney was removed and placed in fixation solution for histological and immunohistochemical staining, and the right kidney was stored at -80°C for analysis including western blot detection.

2.2. Urine Protein, Serum Creatinine, and Blood Urea Nitrogen Measurement. Renal function was evaluated by measuring renal function indicators, including 24 h urine protein, serum creatinine, and blood urea nitrogen. All kits (Cat. C035-2, C011-2 and C013-2, respectively) were bought from Nanjing Jiancheng Bioengineering Institute (Nanjing, China), and the measurements were performed according to their instructions. The urine protein measurement is based on Microprotein Coomassie Brilliant Blue method. A urinary protein is introduced as a calibrator to improve the determination. Serum creatinine was measured based on colorimetric assay. Creatinine can be catalyzed by

sarcosamine hydrolases and generates creatine which can be hydrolyzed into sarcosine and urea by creatine amine hydrolase. The sarcosine is broken down by sarcosine oxidase to generate glycine, formaldehyde, and hydrogen peroxide. The reaction between hydrogen peroxide, 2,4-(6-tri-iodine-3-hydroxybenzoic acid) and 4-ampyrone can be catalyzed by peroxidase and form pink compound. Its optical density value at 515 nm can be used to calculate creatinine content. Blood urea nitrogen was measured by diacetyloxime colorimetry, and urea can react with diacetyl to form red diazine compound. The depth of color is proportional to the content of urea.

2.3. Hematoxylin-Eosin (H&E) Staining. Partial tissue of rat kidney was collected, fixed with 4% formaldehyde solution, and gradually dehydrated with a gradient of 75%, 80%, 95%, and 100% ethanol. Next, the tissue was embedded in paraffin, and sections with 3 μm thickness were cut using a microtome. After the xylene dewaxing treatment, the sections were washed with absolute ethanol, followed by washing with distilled water for 2 min. Next, the sections were stained with hematoxylin for 5 min, washed with tap water for 1 min, subjected to hydrochloric acid-ethanol differentiation for 15 sec, soaked in warm water at 50°C for 3 min, stained with eosin for 1 min, and dehydrated with gradient ethanol and xylene medium. They were sealed with dry gum when they were dried and, subsequently, observed under a $\times 400$ microscope (M165FC; Leica) to observe the pathological structure of rat kidneys. The cytoplasm was stained pink, and the nuclei were stained blue.

2.4. Masson Staining. Similar to the procedure described in the section of H&E staining, the paraffin section specimens were dewaxed using the conventional method with xylene, stained in hematoxylin solution for 5-10 min, washed with running water; subjected to 1% hydrochloric acid differentiation, rinsed with running water for a few minutes, immersed in Masson composite staining solution for 5-10 min, washed with distilled water slightly, treated with 5% molybdophosphoric acid solution for approximately 5 min, followed by direct counterstaining with aniline blue solution for 5 min, treated with 1% glacial acetic acid for 1 min, dehydrated with 95% alcohol and absolute ethanol separately, rendered transparent using xylene, and sealed with neutral gum. The sections were observed under an optical microscope; the procedure for image acquisition was the same as that in the section of H&E staining.

2.5. Periodic Acid-Schiff (PAS) Staining. The kidney tissues were fixed in Carnoy fixative solution at room temperature for 48 h. The paraffin-embedded tissues were cut into 4 μm sections, dewaxed, and washed with distilled water, oxidized with 1% periodic acid for 7 min, washed with distilled water, and immersed in Schiff's solution for 7 min in a dark environment at room temperature. Next, they were rinsed with running water for 10 min. The nucleus was lightly stained with alum hematoxylin staining solution for 2-3 minutes, slightly differentiated with 0.5% hydrochloric acid-alcohol solution after overstaining, rinsed with running water for

10 min, dehydrated with gradient ethanol, rendered transparent using xylene, and sealed with neutral gum. The sections were observed under an optical microscope; the procedure for image acquisition was same as that in Section of H&E staining.

2.6. Western Blotting (WB) and Immunohistochemical Staining (IHC). Western blotting was used to detect the expressions of proteins involved in the PI3K/Akt/mTOR signaling pathway and those associated with autophagy, inflammation, and apoptosis. Frozen kidney tissue was weighed and placed in a glass grinder. Next, 400 μL of RIPA was added for every 50 mg of kidney tissue to a lysis solution (containing 4 μL of phosphatase inhibitor and 4 μL of protease inhibitor); the supernatant was collected after centrifugation at 12000 $\times g$ for 30 min. Total protein was extracted using the BCA protein quantitative method according to the instructions provided for the protein extraction kit (Boster, Wuhan, China). The concentration of each protein sample was adjusted to the same, and then 10 μL of the sample was loaded into the gel for electrophoresis. The protein samples were separated by SDS-PAGE, and the proteins in the gel were electrically transferred to a polyvinylidene fluoride (PVDF) membrane. In 5% bovine serum, the nonspecific blots in the membrane were blocked. The PVDF membrane was incubated with the antibody at 4°C overnight and then treated with the corresponding horseradish peroxidase secondary antibody (goat anti-rabbit AB20718) (Goat anti-mouse AB67 898). The membrane was incubated at room temperature for 30 min and then placed in an incubator for 1 h. Next, images were recorded and analyzed after the membrane was washed (Tanon 5200). The main antibodies used were as follows: p-AKT (#4060, working solutions, for IHC, 1:1000), AKT (#4691, IHC, 1:300), p-mTOR (#5536, IHC, 1:50), mTOR (#2983, IHC, 1:100), and LC3 (#83506, WB, 1:1000; IHC, 1:800) from Cell Signaling Technology (Danvers, MA, USA) and p-PI3K (ab182651, IHC, 1:200), PI3K (ab191606, IHC, 1:500), beclin-1 (ab207612, IHC1:200), p62 (ab56416, IHC, 1:800), caspase-3 (ab13847, IHC1:500), caspase-9 (ab52298, IHC, 1:50), IL-6 (ab9324, IHC, 1:250), IL-1 β (ab9722, IHC, 1:100), TNF- α (ab6671, IHC, 1:100), and brain natriuretic peptide (BNP) (ab19645, IHC, 1:1000) from Abcam (Cambridge, UK). For western blot results of LC3, two bands of LC3I and LC3II generated according to protocol from Cell Signaling Technology.

Kidney tissue specimens were fixed with 4% formaldehyde, rinsed with tap water for 5 min, dehydrated with gradient ethanol, rendered transparent with xylene, and dipped and embedded in paraffin. The paraffin specimens were cut into 2 μm sections. After the paraffin sections were dewaxed and washed with water, they were incubated with 3% H₂O₂ and incubated at room temperature for 20 min to eliminate endogenous peroxidase activity. After washing them 3 times with distilled water, 50 μL of primary antibody working solution was added to cover the tissue section. Next, the box was covered with a lid to prevent evaporation and incubated at room temperature for 60 min. Subsequently, the sections were rinsed 3 times with PBS, treated with two

drops of secondary antibody solution, incubated at room temperature for 30 min, and rinsed thrice with PBS. They were stained using *Dolichos biflorus* agglutinin, incubated for 5 min at room temperature, and rinsed 3 times with PBS for 5 min each; 2 drops of hematoxylin solution were added into the tissue section. The sections were rinsed with running water after 5 min and then treated with 0.5% hydrochloric acid ethanol after approximately 10 sec, rinsed with tap water, dehydrated with gradient ethanol, rendered transparent with xylene, sealed with neutral gum, and observed under a light microscope. Six sliced section specimens were taken from each group; they were judged as positive by the appearance of clear light yellow/tan particles, and the dye signal in each selected glomerulus or tubulointerstitial region of the images was highlighted using Image Pro Plus quantitative software and quantified.

2.7. Data Analysis. Raw data was deposited in the reference [18]. Statistical analysis results were collected from three replicated independent experiments. Data are expressed as the mean \pm standard deviation (SD). For statistical comparison, a one-way analysis of variance (ANOVA) was performed on the parameter data. Statistical analysis was performed using GraphPad Prism 6 software (GraphPad, San Diego, California, USA). p value was calculated by one-way analysis of variance or multiple t -test. $p < 0.05$ was statistically significant.

3. Results

3.1. Effect of GLP Treatment on Blood Glucose and the Function of Kidney. Changes in the fasting blood glucose during the seventy-day experimental period were monitored weekly to assess the progress of diabetes. At end of experiment, serum glycosylated hemoglobin, 24 h urine protein, urea nitrogen, and serum creatinine were measured in order to assess the renal function. Rats with fasting blood glucose levels raised above 16.7 mmol/L after streptozotocin injection were used for the treatment with and without GLP. Compared to the diabetic group that was not administered treatment, the group administered GLP treatment showed significantly reduced fasting blood glucose at the ninth week till the end of experiment, even though it did not reach the normal level with GLP treatment alone (Table 1). At the end of the experiment, GLP treatment significantly decreased the level of glycosylated hemoglobin, 24 h urine protein, blood urea nitrogen, and serum creatinine, which were all significantly increased in the diabetic rats (Table 1). These changes indicate that GLP treatment could significantly improve the kidney function of the diabetic rats even though GLP could not reverse the increased biomarker levels back to normal.

3.2. Effect of GLP Treatment on the Histology of Diabetic Nephropathy. To further analyze the mechanism of GLP in the improvement of the renal function, pathological changes in the kidney specimens were examined by staining with H&E, Masson, or PAS stains (Figures 1(a)–1(c)). The kidney extra-

cellular matrix content via Masson staining (Figure 1(d)) and glycogen or mucin accumulation via PAS staining (Figure 1(e)) were analyzed. Compared to the control group, both were increased significantly in the diabetic group but were reduced significantly after GLP treatment.

The kidneys of the diabetic group that was not administered treatment showed hypertrophy through naked eye observation and felt harder in texture compared to those treated with GLP and the normal groups. In the micrograph of H&E-stained specimens, the glomeruli and kidney tubules of the control group were seen clearly with normal histological structures. However, in the diabetic group, thickened glomerular basement membranes were observed; furthermore, the glomerular cavities were enlarged with irregular outline, the cells in the bulb were unevenly distributed, more degenerated fat was presented, some kidney tubules showed atrophy and collapse, and the cell walls were arranged irregularly (arrows indicate typical changes) (Figure 1(a)). Masson staining shows tubulointerstitial fibrosis (collagen fibers, blue) in the diabetic group. However, after GLP intervention, kidney tubular injury was significantly reduced, and mesangial matrix proliferation was significantly reduced (Figures 1(b) and 1(d)). The specimens stained with PAS showed that the glomerular basement membranes of the control group were intact and significantly reduced extracellular matrix depositions that were observed (Figures 1(c) and 1(e)). A large amount of glycogen deposition was observed in the diabetic group. In the tubules and glomeruli, the glomerular mesangial area was enlarged, and the extracellular matrix was significantly increased (the arrows indicate the typical changes). The above pathological changes were significantly improved in the GLP treatment group, and normal appearance was restored in these tissues.

Body weight in the diabetic group increased slowly, and it was significantly lower compared to the GLP treatment group at week 5; body weight increased continuously and significantly in the GLP treatment group after week 5 (Figure 2(a)), while the body weight increase was the lowest in the diabetic group during the entire experimental period. At end of experiment, both the weight of the kidney (Figure 2(b)) and the ratio of kidney weight to body weight (Figure 2(c)) in the diabetic group were significantly higher than that in the control group; however, this effect was significantly reversed by GLP treatment.

3.3. Effect of GLP Treatment on the Level of α -SMA and BNP Expression. The level of α -SMA expression in the kidney tissue was assessed by western blotting (Figures 3(a) and 3(b)), while the level of BNP expression in the kidney tissues was assessed by immunohistochemical detection (Figures 3(d) and 3(c)). The results showed that the expression of both α -SMA and BNP in the kidney tissues of diabetic rats increased significantly compared with that in the control group ($p < 0.01$); however, after GLP intervention, the expression level of both α -SMA and BNP in the kidney tissues of diabetic rats decreased significantly, and the difference in these values between the diabetic+GLP group and the diabetic group was statistically significant ($p < 0.01$).

TABLE 1: The biochemical indices in different groups at end of experiment, day 70.

Group	Control	Diabetic	Diabetic+GLP	Improvement rate [^] (%)
Fasting blood glucose (mmol/L), day 0	4.56 ± 0.34	17.10 ± 1.34 ^{##}	17.77 ± 1.28 ^{##}	
Fasting blood glucose (mmol/L), day 70	4.87 ± 0.27	23.10 ± 1.59 ^{##}	19.98 ± 0.98 ^{##*}	13.51
Glycated hemoglobin (g/L)	1.65 ± 0.10	2.42 ± 0.08 [#]	2.03 ± 0.08 ^{##*}	16.12
24 h urine protein (mg/L)	184.6 ± 21.06	372.3 ± 34.57 ^{##}	244.5 ± 32.29 ^{##*}	34.33
Blood urea nitrogen (mmol/L)	4.40 ± 0.48	8.44 ± 0.68 ^{##}	6.70 ± 0.63 ^{##*}	20.62
Serum creatinine (μmol/L)	25.17 ± 1.72	38.00 ± 3.74 [#]	31.00 ± 1.41 ^{##*}	18.42

Note: data expressed as the mean ± standard deviation, $n = 6$ in each group. [^]Improvement rate was calculated by (diabetic – diabetic – GLP)/diabetic × 100%; [#] $p < 0.05$, ^{##} $p < 0.01$, compared with the control group; ^{*} $p < 0.05$, compared with the diabetic group using Tukey’s test. Control: 5 ml/kg saline (p.o.); diabetic: 50 mg/kg streptozotocin (intraperitoneal) and 5 ml/kg saline (p.o.); diabetic+GLP: 50 mg/kg streptozotocin (intraperitoneal) and 300 mg/kg *Ganoderma lucidum* polysaccharides (GLP) (p.o.).

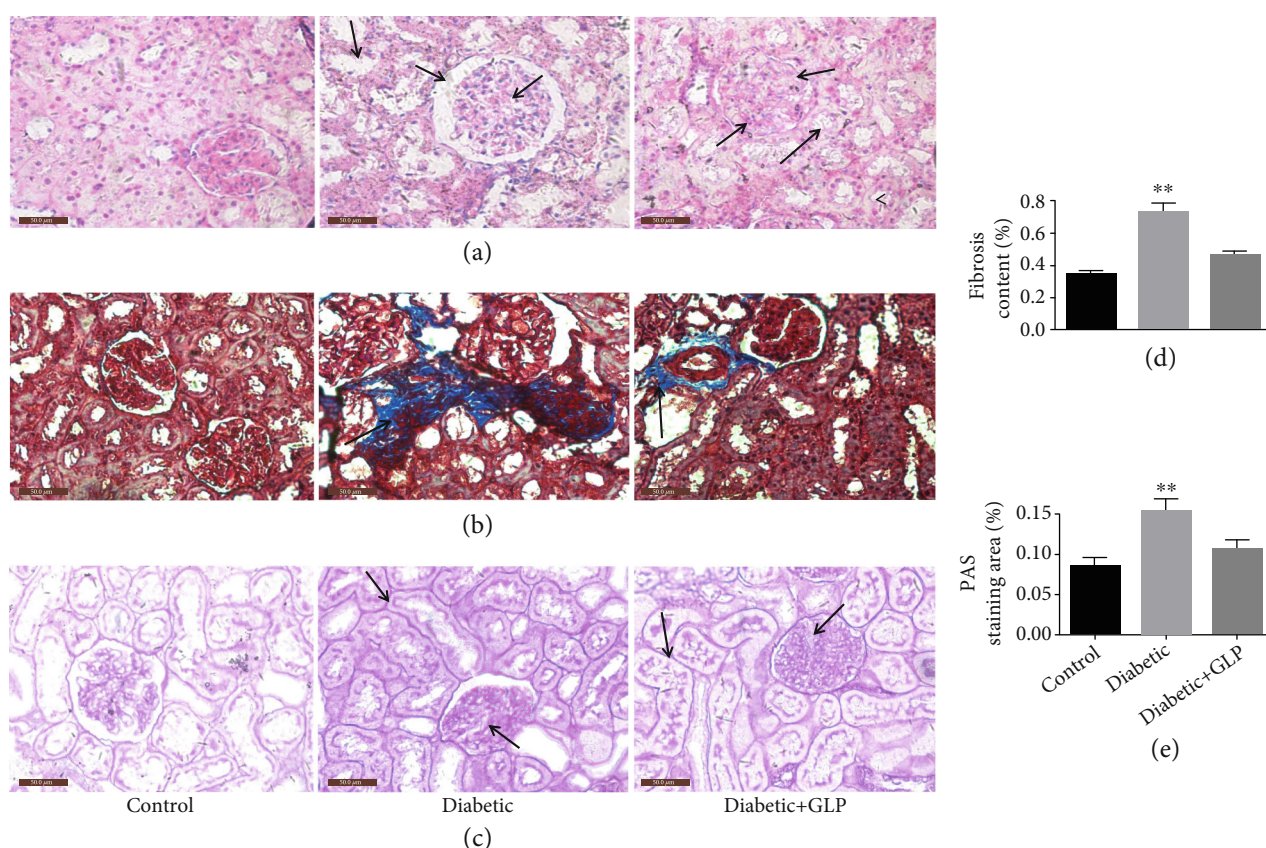


FIGURE 1: Pathological changes in the kidney tissue of diabetic rats. Representative images showing kidney tissue sections after (a) hematoxylin and eosin, (b) Masson’s trichrome, and (c) periodic acid–Schiff staining (PAS). Quantitative results for (d) collagen accumulation assessed using Masson’s trichrome staining and (e) extracellular matrix accumulation assessed using PAS staining for the different groups (original magnification ×400). The arrow in the kidney section in the diabetic group ((a), middle) indicates the irregularly arranged cell membranes, disturbed structures, disappeared nucleus, or unclear intercellular boundary. The arrow in the middle image of (b) indicates considerable deposition of collagen fibers, and the arrow in middle image of (c) indicates considerable deposition of reactive glycogen. Values are presented as the mean ± SE; $n = 4$ per group. ^{**} $p < 0.01$ versus either the control group or the diabetic+GLP group using Tukey’s test. Control: 5 ml/kg saline (p.o.); diabetic: 50 mg/kg streptozotocin (intraperitoneal) and 5 ml/kg saline (p.o.); diabetic+GLP: 50 mg/kg streptozotocin (intraperitoneal) and 300 mg/kg *Ganoderma lucidum* polysaccharides (GLP) (p.o.).

3.4. Effect of GLP Treatment on the PI3K/Akt/mTOR Signaling Pathway. The level of p-PI3K, p-Akt, and p-mTOR expression in the kidney tissue was assessed by immunohistochemical detection (Figures 4(a) and 4(b)), respectively. The expression of p-PI3K, p-Akt, and p-

mTOR in the kidney tissue of the diabetic group was significantly increased compared with that of the normal group ($p < 0.01$). The expressions of these proteins in the kidney tissues of diabetic rats were significantly reduced after GLP intervention ($p < 0.01$).

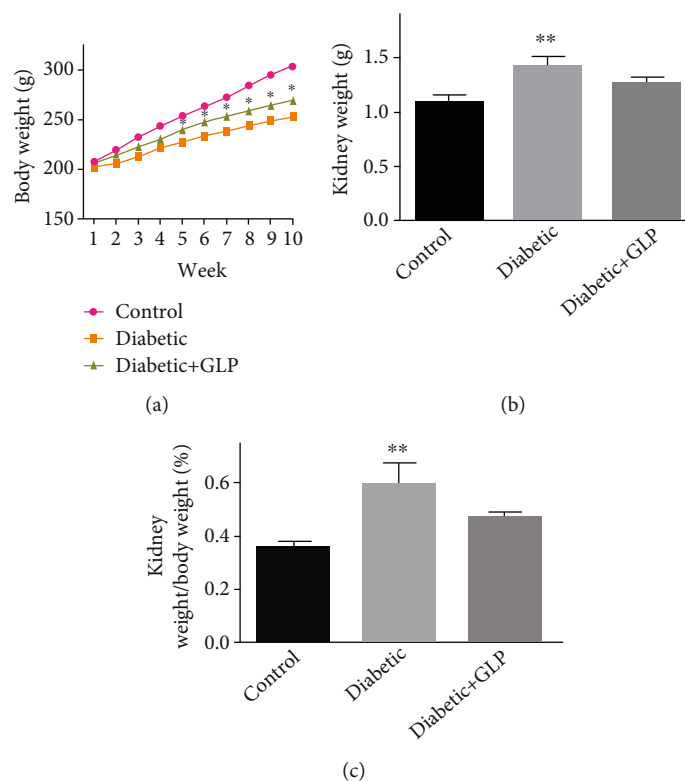


FIGURE 2: Body weight changes during the experimental period (a) and kidney weight (b) and kidney weight/body weight (%) (c) at the end of the experiment at day 70. Values are presented as the mean \pm SE; $n = 8$ per group. * compared to the control, both diabetic and diabetic +GLP shows $p < 0.05$ in (a). In (b) and (c), ** indicates $p < 0.01$ versus either the control group or the diabetic +GLP group using Tukey's test. Control: 5 ml/kg saline (p.o.); diabetic: 50 mg/kg streptozotocin (intraperitoneal) and 5 ml/kg saline (p.o.); diabetic+GLP: 50 mg/kg streptozotocin (intraperitoneal) and 300 mg/kg GLP (p.o.).

3.5. *Effect of GLP Treatment on the Expression LC3-II/LC3-I, Beclin-1, and P62.* The immunohistochemical results of beclin-1, LC3, and P62 were shown in Figure 5(a), and the LC3 was further analyzed by western blot to see the subtype of LC3-II and LC3-I expression, which were shown in Figure 5(c). Compared with the control group, the expression of both beclin-1 and LC3 as well as the ratio of LC3-II/LC3-I in the kidney tissue of the diabetic group was significantly decreased, and the expression of P62 was significantly increased ($p < 0.01$). However, after GLP intervention, beclin-1 and LC3 as well as the ratio of LC3-II/LC3-I were all significantly increased, and the expression of P62 was significantly reduced ($p < 0.01$).

3.6. *Effect of GLP Treatment on the Expression of Caspase-3 and Caspase-9.* The western blot and immunohistochemical results of caspase-3 and caspase-9 were shown in Figures 6(a) and 6(b). Results show that the expression of caspase-3 and caspase-9 in kidney tissues of the diabetic group was significantly increased compared with the control group ($p < 0.01$); however, after GLP intervention, their expressions in the kidney tissues were reduced significantly ($p < 0.01$).

3.7. *Effect of GLP Treatment on the Expression of TNF- α , IL-6, and IL-1 β .* The immunohistochemical results of the expression of IL-6, IL-1 β , and TNF- α were shown in

Figure 7. In the diabetic group, they were significantly increased compared with the control group ($p < 0.01$); however, after GLP intervention, their expressions were significantly reduced ($p < 0.01$).

4. Discussion

Diabetic nephropathy is the most common serious complication of diabetes. It occurs in diabetic patients with a long course, severe illness, and hypertension [19]. Once a large amount of proteinuria occurs, renal function will irreversibly decline progressively and eventually develop into end-stage renal disease. According to statistics, approximately 20-30% of diabetic patients clinically developed diabetic nephropathy [20], and diabetic nephropathy developed into end-stage renal disease, a critical disease, in 20-40% of patients. In China, some traditional Chinese medicines have been recommended to treat diabetic nephropathy [21, 22].

The main pathological features of diabetic nephropathy are glomerular hypertrophy, widened mesangial matrix, and development of fibrosis or sclerosis. The early symptom is the appearance of trace proteinuria, which can lead to kidney damage and failure upon further clinical progression of the disease [23]. Therefore, the production of proteinuria indicates impairment of the structure and function of the glomerular filtration membrane or damaged renal reabsorption. This study found that the 24h urinary protein, serum

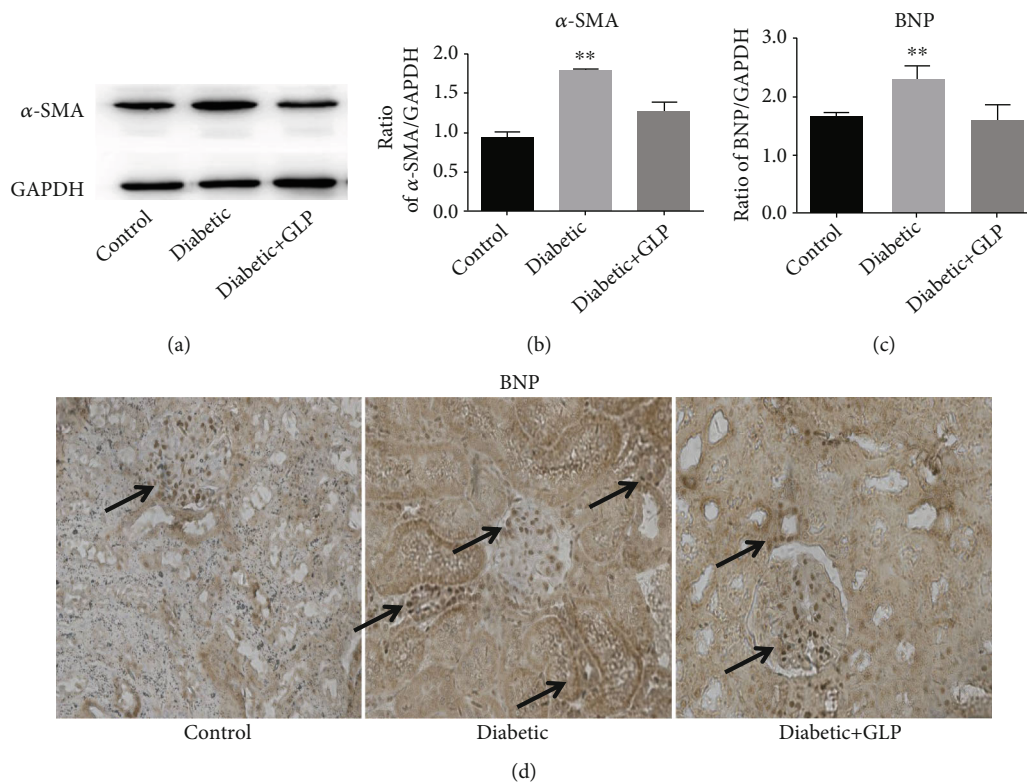


FIGURE 3: Effect of *Ganoderma lucidum* polysaccharide (GLP) on the protein expressions of α -SMA (molecular weight, 42 kDa) assessed by western blot and brain natriuretic peptide (BNP) for immunohistochemical analysis in the kidney tissues of rats from different groups. Micrographs, (d), original magnification $\times 400$; (c) statistic analysis. Representative western blot images (a) and quantitative analysis (b) for expression of α -SMA (d) Representative immunohistochemistry micrographs for BNP expression. Strong BNP immunostaining was observed in almost all kidney cells in the diabetic group, compared with the control and diabetic+GLP groups. (c) Statistical analysis of immunohistochemistry results for the renal BNP expression. The arrows in the kidney section in the diabetic group indicate BNP highly expressed areas. In control and treatment groups, BNPs are mainly expressed in the glomerular areas, but there are higher expression in the tubule area in the diabetic group. Values are expression rate represent the mean \pm SE; $n = 3$ in each group. ** $p < 0.01$ versus the control group and the diabetic+GLP group using Tukey's test. Control: 5 ml/kg saline (p.o.); diabetic: 50 mg/kg streptozotocin (i.p.) and 5 ml/kg saline (p.o.); diabetic+GLP: 50 mg/kg streptozotocin (i.p.) and 300 mg/kg GLP (p.o.).

creatinine and blood urea nitrogen in diabetic rats were significantly higher than that in the control group. Compared to the diabetic group, they were decreased by 35%, 18%, and 21%, respectively, after GLP treatment, which showed clearly improvement, even though these indices were unable to reach the normal level in the control group (Table 1). These improvements were partly caused by the decrease of fasting blood glucose and glycated hemoglobin by 14% and 16%, respectively. A human study showed an increased 1% of HbA1c which would increase 3 grams (95% CI: 1.5-4.6 grams) heart left ventricle mass which highly affects blood circulation and links to the kidney diseases [24]. In one study [15], GLP (250 mg/kg) could slow down the progression of streptozotocin-induced diabetic nephropathy in mice by decrease blood glucose and triglyceride levels, suggesting the metabolic modulation of GLP. This was also supported by our histological results which kidney tubular epithelial cells were shed, and vacuole degeneration was detected by kidney tissue staining. Inflammatory cells extensively infiltrated the kidney interstitium, kidney tubular hypertrophy and globules were significantly enlarged, the mesangial area was enlarged, and the extracellular matrix was significantly

increased. The results were the same as that of previous studies [25]. GLP treatment can maintain a relatively normal structure and the function of kidneys in diabetic rats. In addition, reversal of pathological changes, as observed through H&E, PAS, and Masson staining, suggests that GLP can ameliorate the damaged and pathologically altered kidney tissue. Li et al. [16] showed that GLP (100, 200, and 400 mg/kg) treatment improved streptozotocin-induced diabetic nephropathy and reversed the decreased matrix metalloproteinase-2/tissue inhibitor of metalloproteinase-2 in rats. This further decreased the accumulation of extracellular matrix, suggesting the renoprotective effect of GL-PS through rebalance matrix metalloproteinase-2/tissue inhibitor of metalloproteinase-2.

BNP is a substance composed of 32 amino acids, and it performs multiple functions. It can increase the excretion of sodium from the kidney by acting on the guanylate cyclase receptor, inhibit the sympathetic central nervous system activity and the renin-angiotensin aldosterone system, relax the vascular smooth muscle, and increase endothelial permeability. Recent studies [26] have shown that BNP can inhibit cardiac and vascular remodeling. Another finding

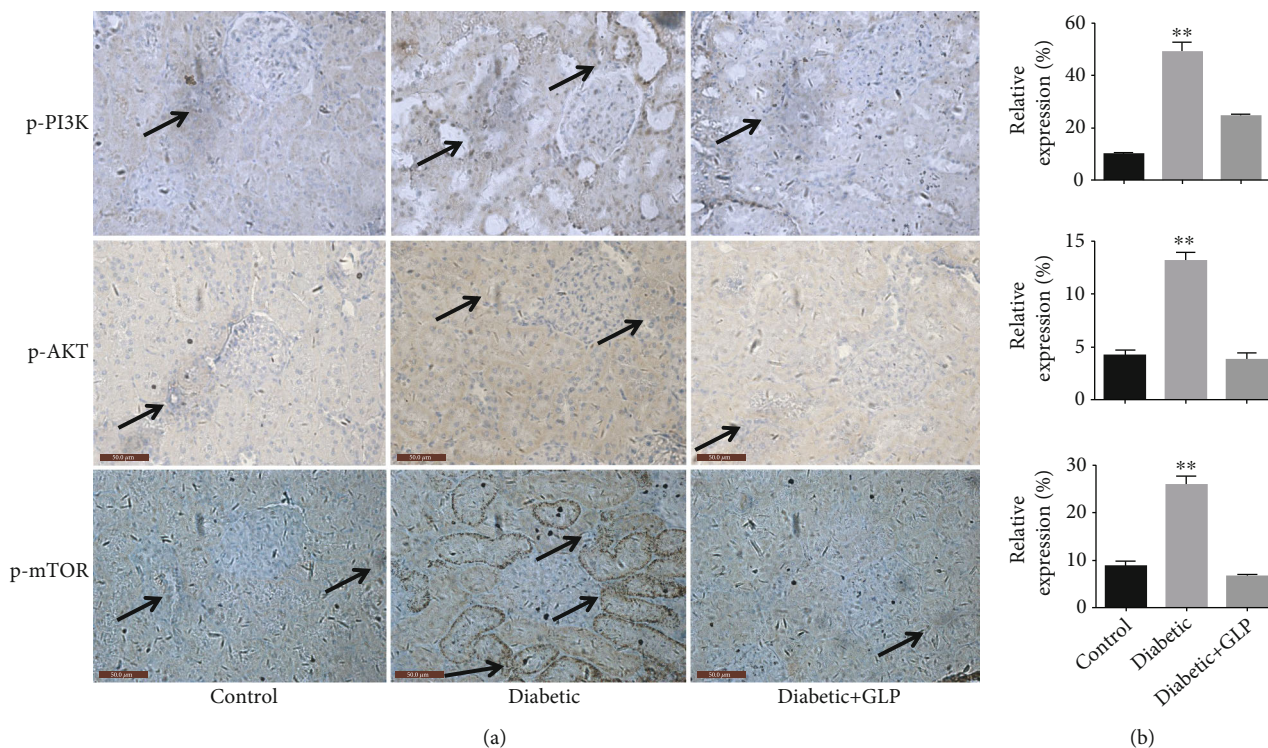


FIGURE 4: Effect of *Ganoderma lucidum* polysaccharide (GLP) on the protein expression of p-PI3K, p-Akt, and p-mTOR according to immunohistochemical results (a) and their statistical analysis (b) in renal tissues in different groups. (a) micrographs, magnification $\times 400$. Arrows indicate the changed areas. Values represent the mean \pm SE; $n = 3$ in each group. ** $p < 0.01$ versus the control group and the diabetic+GLP group using Tukey's test. Control: 5 ml/kg saline (p.o.); diabetic: 50 mg/kg streptozotocin (i.p.) and 5 ml/kg saline (p.o.); diabetic+GLP: 50 mg/kg streptozotocin (i.p.) and 300 mg/kg GLP (p.o.).

[27] showed that BNP increased the risk of renal function in patients with type 2 diabetes. Researches on patients with diabetic nephropathy [28, 29] showed that BNP increased, especially at the early stage of diabetic nephropathy. When fibroblasts transform into myofibroblasts, there is an increase in α -SMA expression, migration, and proinflammatory signals and the production of proteins that reshape the extracellular matrix [30]. Meroterpenoids from *Ganoderma* cochlear, cochlearols A and B and polycyclic meroterpenoids, exerted renoprotectivity by inhibiting the expression of renal fibrosis related markers such as collagen I, fibronectin, and α -SMA in a dose-dependent manner (5, 10, and 20 μ M) [31]. The decreased expression of BNP and α -SMA after GLP treatment indicates that GLP plays an important role in kidney protection. This observation was confirmed through the assessment of H&E staining, Masson staining, and PAS staining, which showed that pathological changes in the kidney and kidney fibrosis in diabetic rats were significantly reduced after the GLP treatment.

In terms of the mechanism, PI3K, Akt, and mTOR are considered to play key roles in the insulin signalling pathway, which regulates glucose uptake and glycogen synthesis [32]. In recent years, the role of the PI3k/Akt/mTOR signalling pathway in the development of diabetic nephropathy has received increasing attention. Lu et al. [33] reported that the activation of the PI3k/Akt/mTOR signalling pathway can accelerate the occurrence and deterioration of kidney fibrosis in diabetic rats. This study found that compared with

the control group, the expression of p-PI3K, p-Akt, and p-mTOR increased in the diabetic group had significantly decreased after GLP treatment, indicating that GLP may improve diabetic nephropathy by inhibiting the PI3k/Akt/mTOR signalling pathway. Fibrosis of diabetic nephropathy tissue is consistent with the results from previous studies. PI3k/Akt/mTOR is a very important signalling pathway that regulates cell autophagy. It plays an important role in the signal regulation and molecular mechanism of autophagy. This pathway is also key in other important cellular processes, such as cellular survival, appreciation, growth, and differentiation [34]. The PI3k/Akt/mTOR signalling pathway is currently known as the only inhibitory pathway for autophagy, and its activation can inhibit autophagy. Zhong et al. [35] found that ligustrazine can inhibit the expression of p-PI3K, p-Akt, and p-mTOR in the kidney tissues of diabetic rats, thereby, increasing the expression level of the autophagy marker protein LC3B and the ratio of LC3B-II/LC3B-I. The results of this experiment indicate that the PI3k/Akt/mTOR signalling pathway is activated, and autophagy is inhibited in diabetic nephropathy; however, the signalling pathway is inhibited, and autophagy is reactivated after GLP treatment, indicating that GLP plays a renal protective role. The mechanism may be related to its inhibition of the PI3k/Akt/mTOR signalling pathway, which in turn promotes kidney autophagy.

According to previous research, the apoptosis of kidney cells plays an important role in the occurrence and

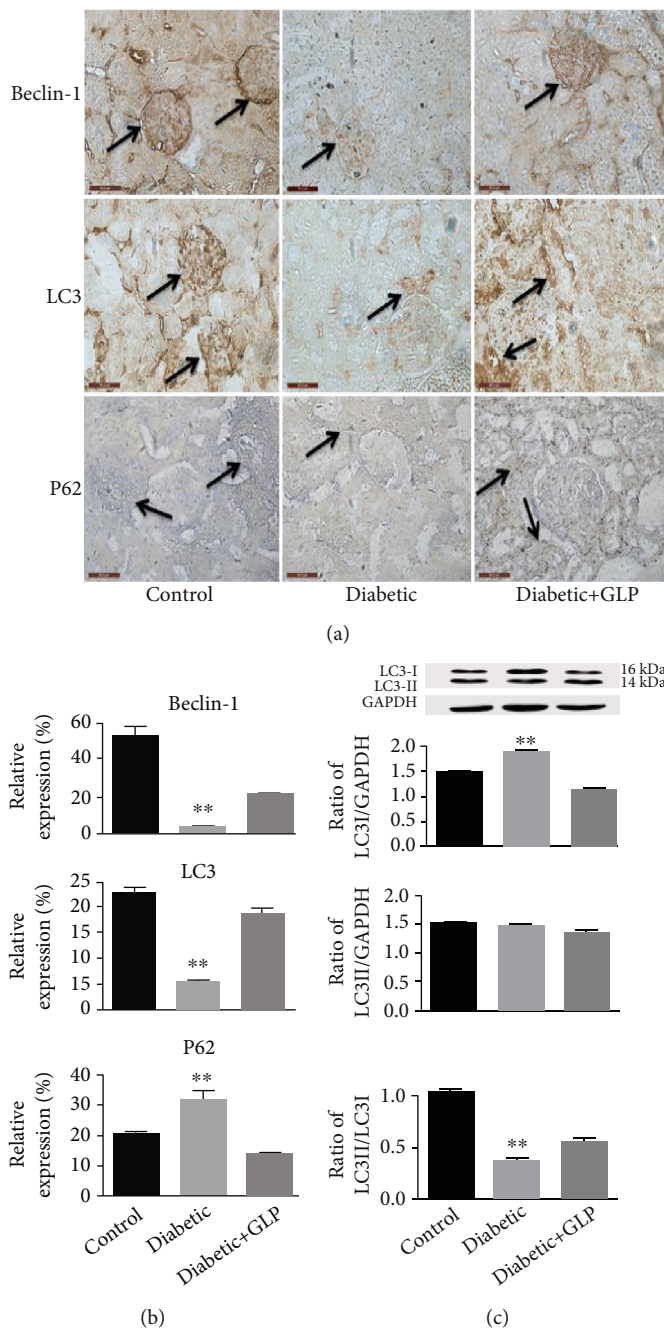


FIGURE 5: Effect of *Ganoderma lucidum* polysaccharide (GLP) on the expression of beclin-1, LC3, and P62 ((a) immunohistochemical micrographs and (b) their statistical analysis) as well as the LC3-I and II (western blot results, (c)). (a) micrographs, magnification $\times 400$. Arrows indicate the changed areas. Values in (b) and (c) represent the mean \pm SE; $n = 3$ in each group. ** $p < 0.01$ versus the control group and the diabetic+GLP group using Tukey's test. Control: 5 ml/kg saline (p.o.); diabetic: 50 mg/kg streptozotocin (i.p.) and 5 ml/kg saline (p.o.); diabetic+GLP: 50 mg/kg streptozotocin (i.p.) and 300 mg/kg GLP (p.o.).

development of diabetic nephropathy. In recent years, increasing evidence shows that there is an interactive effect between apoptosis and cell autophagy, and that the two are interrelated and mutually regulated. When diabetic nephropathy is stimulated by factors such as high glucose, podocytes can not only discard proteins and organelles through autophagy but also undergo apoptosis. The activities of autophagy and apoptosis may vary during different periods. A literature review to understand the relationship

between the two revealed the following two aspects: autophagy involves autophagy genes, e.g., ce, which is upstream of the apoptosis process; these genes initiate apoptosis, and their expression affects the degree of apoptosis [36]. Autophagy can maintain the stability of the cell environment and inhibit apoptosis through multiple pathways [37]. Studies have found that normal autophagy plays an important role in reducing the cerebral ischemia-reperfusion injury via inhibition of apoptosis, while an abnormally high level of

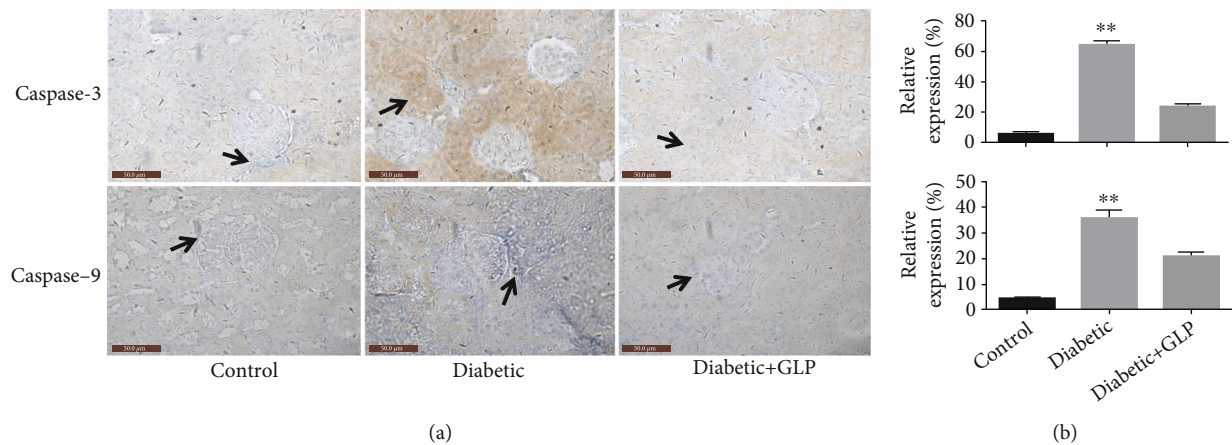


FIGURE 6: Effect of *Ganoderma lucidum* polysaccharide (GLP) on the protein expression of caspase-3 and -9 in renal tissues according to immunohistochemical micrographs ((a) magnification $\times 400$, arrows indicate the changed areas) and statistical analysis (b). Values represent the mean \pm SE; $n = 3$ in each group. ** $p < 0.01$ versus the control group and the diabetic+GLP group using Tukey's test. Control: 5 ml/kg saline (p.o.); diabetic: 50 mg/kg streptozotocin (i.p.) and 5 ml/kg saline (p.o.); diabetic+GLP: 50 mg/kg streptozotocin (i.p.) and 300 mg/kg GLP (p.o.).

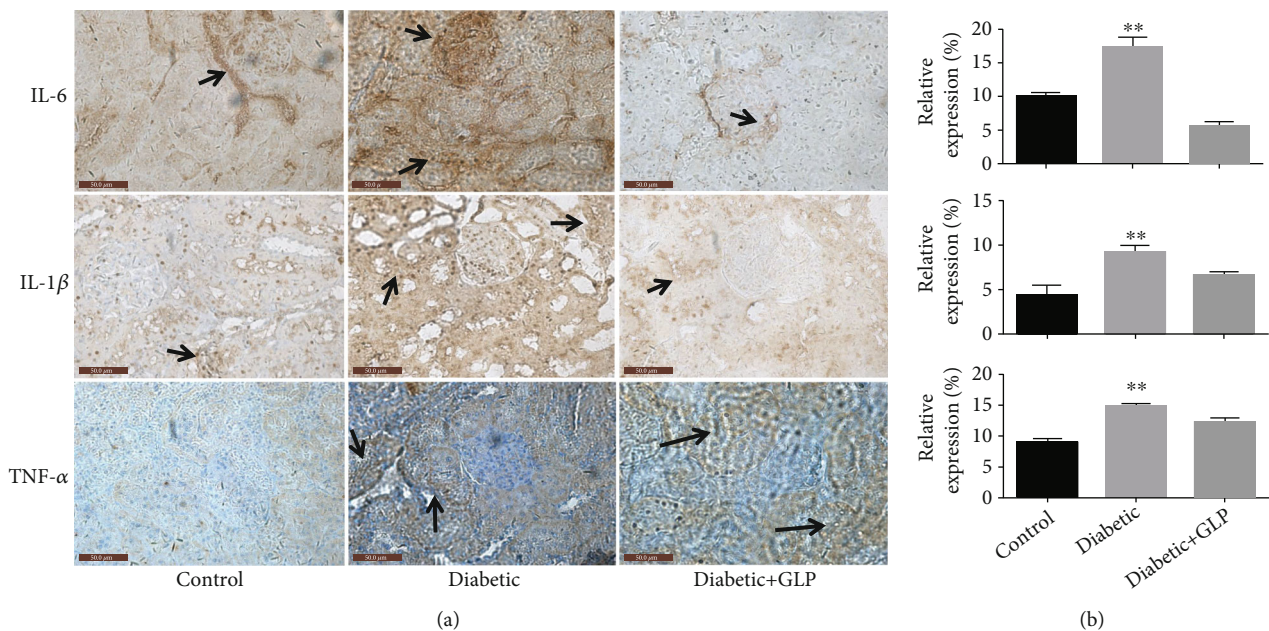


FIGURE 7: Effect of *Ganoderma lucidum* polysaccharide (GLP) on the protein expression of IL-6, IL-1 β , and TNF- α in renal tissues according to immunohistochemical micrographs ((a) magnification $\times 400$, arrows indicate the changed areas) and statistical analysis (b). Values are presented as the mean \pm SE, $n = 3$ in each group; ** $p < 0.01$, compared with either the control group or diabetic+GLP group using Tukey's test. Control: 5 ml/kg saline (p.o.); diabetic: 50 mg/kg streptozotocin (i.p.) and 5 ml/kg saline (p.o.); diabetic+GLP: 50 mg/kg streptozotocin (i.p.) and 300 mg/kg GLP (p.o.).

autophagy can aggravate this injury [38]. Another example of the protective effect of autophagy is demonstrated in intervertebral disc degeneration; activation of autophagy inhibits the degradation of the extracellular matrix of the endplate chondrocytes via inhibition of apoptosis [39]. In terms of apoptosis, autophagy is indispensable, but the typical apoptosis inhibitory proteins, e.g., Bcl-2, can affect this process [40]. The results of this experiment also showed that the expression of the apoptosis-related proteins caspase-3 and caspase-9 increased in the diabetic group and decreased after treatment with GLP, indicating that GLP can activate

autophagy, play an antiapoptotic effect, and improve damaged kidney tissue. Autophagy is an innate immune mechanism that can kill pathogens and control inflammation. Autophagy reduces pathogen burden and participates in the processing of antigens to activate adaptive immunity [41]. In recent years, increasing studies have shown that the inflammatory process may play an important role in the pathogenesis of diabetic nephropathy, and adhesion molecules, inflammatory chemokines, and inflammatory factors play specific roles in the development of diabetic nephropathy [42]. Autophagy can negatively regulate

inflammatory factors. Lipopolysaccharide (LPS) stimulates the expression levels of IL-1 β and IL-8 in mice in which the key autophagy gene Atg16L1 was knocked out [43]. In addition, autophagy can reduce the occurrence of inflammation by regulating the composition and activation of inflammatory bodies via regulating the secretion of proinflammatory factors such as IL-1 β and IL-18 [44]. Kimura et al. [45] showed that renal tubules are one of the most active areas of inflammatory response in chronic kidney injury. Autophagy can effectively reduce damaged and dysfunctional mitochondria by removing damage-related molecules and abnormal lysosomes. Subsequently, this process inhibits the inflammatory response and improves immunoregulation, resulting in protection of renal function. Ma et al. [46] reported that a specific dose of GLP induces a significant effect on diabetic nephropathy, and the mechanism underlying this effect may be through inhibiting the activation of NF- κ B/NLRP3 inflammatory bodies, reducing the inflammatory response, and improving renal function, thus restoring the biochemical indicators of diabetes in the blood and urine of mice with nephropathy. Patients with diabetic nephropathy have elevated IL-6, and patients with dominant proteinuria have higher serum albumin levels than patients with microalbuminuria or normal albuminuria [47]. Studies have found [48] that the expression of TNF- α is significantly increased in the kidneys of rats with type I diabetes. TNF- α , as a key factor that mediates the inflammatory response, can induce an adhesion effect in glomerular endothelial cells. Inflammatory substances cause an increase in the mesangial matrix and mesangial cell proliferation, destroying the glomerular structure [49]. Several extracts of *Ganoderma lucidum* showed amelioration in this progress in a review [50], e.g., one study [51] showed that proteoglycan isolated from *Ganoderma lucidum* fruiting bodies shows protection renal morphology in diabetic mice in a dose-dependently (75, 250, and 450 mg/kg) manner during a 8-week treatment. According to previous research, the mechanism appears also via directly elimination reactive oxygen species, suppresses lipid peroxidation, and indirectly scavenges the radicals via activating antioxidant enzyme systems and chelation with metal ion by forming crossbridge between carboxyl groups decreasing reactive oxygen species generation [52–60]. This study showed that the expressions of the inflammatory factors IL-6, IL-1 β , and TNF- α in the diabetic group were significantly increased, while they were reduced significantly after GLP treatment.

5. Conclusion

In summary, these results indicate that GLP produces a significant protective effect in diabetic nephropathy by reducing the renal pathological damage and decreasing blood glucose and glycated hemoglobin and improves the kidney function indicated by decreasing the levels of serum creatinine, blood urea nitrogen, and 24h urine protein as well as the renal α -SMA and BNP expressions and even more GLP increased body weight and kidney weight. GLP inhibited the PI3K/Akt/mTOR signaling pathway and inhibited apoptosis indicators of both caspase-3 and -9 expression.

These may be contributed by the activation of autophagy via stimulation beclin-1, LC3-II/LC-I, and reduction the expression of p62. These changes may be used partly to explain the molecular mechanism of GLP on alleviation kidney tissue fibrosis. These effects indicate the potential application of GLP for the treatment of diabetic nephropathy.

Abbreviations

GLP: *Ganoderma lucidum* polysaccharides
 mTOR: Mammalian target of rapamycin
 p-Akt: Phosphorylated protein kinase B
 PAS: Periodic acid–Schiff staining
 PI3K: Phosphoinositide 3 kinase
 LC3: Cytoplasmic light chain 3
 TNF- α : Tumor necrosis factor- α .

Data Availability

The data are available here: <https://data.mendeley.com/datasets/xf58rsgj94/1> doi:10.17632/xf58rsgj94.1.

Conflicts of Interest

The authors have declared no conflict of interest.

References




- [1] D. Sharma, P. Bhattacharya, K. Kalia, and V. Tiwari, “Diabetic nephropathy: new insights into established therapeutic paradigms and novel molecular targets,” *Diabetes Research and Clinical Practice*, vol. 128, pp. 91–108, 2017.
- [2] C. Magee, D. J. Grieve, C. J. Watson, and D. P. Brazil, “Diabetic nephropathy: a tangled web to unweave,” *Cardiovascular Drugs and Therapy*, vol. 31, pp. 579–592, 2017.
- [3] M. J. Yahya, P. B. Ismail, N. B. Nordin et al., “Association of CCL2, CCR5, ELMO1, and IL8 polymorphism with diabetic nephropathy in Malaysian type 2 diabetic patients,” *International journal of chronic diseases*, vol. 2019, Article ID 2053015, 13 pages, 2019.
- [4] N. B. Flemming, L. A. Gallo, and J. M. Forbes, “Mitochondrial dysfunction and signaling in diabetic kidney disease: oxidative stress and beyond,” *Seminars in Nephrology*, vol. 38, no. 2, pp. 101–110, 2018.
- [5] H. Yang, T. Xie, D. Li et al., “Tim-3 aggravates podocyte injury in diabetic nephropathy by promoting macrophage activation via the NF- κ B/TNF- α pathway,” *Molecular Metabolism*, vol. 23, pp. 24–36, 2019.
- [6] X. Cai, W. He, and G. Yang, “Research progress on the biological activity of *Ganoderma lucidum* polysaccharides,” *Edible Fungi*, vol. 40, no. 3, pp. 1–4, 2018.
- [7] X. Gong, M. Ji, J. Xu, C. Zhang, and M. Li, “Hypoglycemic effects of bioactive ingredients from medicine food homology and medicinal health food species used in China,” *Critical Reviews in Food Science and Nutrition*, vol. 60, no. 14, pp. 2303–2326, 2020.
- [8] B. Wei, R. Zhang, J. Zhai et al., “Suppression of Th17 Cell Response in the Alleviation of Dextran Sulfate Sodium-Induced Colitis by *Ganoderma lucidum* Polysaccharides,” *Journal of Immunology Research*, vol. 2018, Article ID 2906494, 10 pages, 2018.

- [9] K. X. Zhu, S. Nie, C. Li, D. Gong, and M. Y. Xie, "Ganoderma atrum polysaccharide improves aortic relaxation in diabetic rats via PI3K/Akt pathway," *Carbohydrate Polymers*, vol. 103, pp. 520–527, 2014.
- [10] Y. Ma, F. Chen, S. Yang, Y. Duan, Z. Sun, and J. Shi, "Silencing of TRB3 ameliorates diabetic tubule interstitial nephropathy via PI3K/Akt signaling in rats," *Medical Science Monitor*, vol. 23, pp. 2816–2824, 2017.
- [11] X. Shao, D. Lai, L. Zhang, and H. Xu, "Induction of Autophagy and Apoptosis via PI3K/AKT/TOR Pathways by Azadirachtin A in *Spodoptera litura* Cells," *Scientific Reports*, vol. 6, no. 1, article 35482, 2016.
- [12] M. Long and T. G. McWilliams, "Monitoring autophagy in cancer: from bench to bedside," *Seminars in cancer biology*, vol. 66, pp. 12–21, 2020.
- [13] W. Wei, X. R. An, S. J. Jin, X. X. Li, and M. Xu, "Inhibition of insulin resistance by PGE1 via autophagy dependent FGF21 pathway in diabetic nephropathy," *Scientific Reports*, vol. 8, p. 9, 2018.
- [14] Y. Moriwaki, T. Yamamoto, Y. Shibutani et al., "Elevated levels of interleukin-18 and tumor necrosis factor- α in serum of patients with type 2 diabetes mellitus: Relationship with diabetic nephropathy," *Metabolism*, vol. 52, no. 5, pp. 605–608, 2003.
- [15] C. Y. He, W. D. Li, S. X. Guo, S. Q. Lin, and Z. B. Lin, "Effect of polysaccharides from Ganoderma lucidum streptozotocin-induced diabetic nephropathy in mice," *Journal of Asian Natural Products Research*, vol. 8, no. 8, pp. 705–711, 2006.
- [16] W. Li, C. Mao, and Q. Yin, "Effects of Ganoderma lucidum polysaccharides on the expression of matrix metalloproteinase-2/tissue inhibitor of metalloproteinase-2 in diabetic rat kidney," *Chinese Journal of Gerontology*, vol. 3, pp. 226–229, 2008.
- [17] S. Wu, "Hypolipidaemic and anti-lipidperoxidant activities of Ganoderma lucidum polysaccharide," *International journal of biological macromolecules*, vol. 118, no. Part B, pp. 2001–2005, 2018.
- [18] <https://data.mendeley.com/datasets/xf58rsgj94/1>.
- [19] Y. Li, R. Miao, Y. Liu et al., "Efficacy and safety of tripterygium glycoside in the treatment of diabetic nephropathy: a systematic review and meta-analysis based on the duration of medication," *Front Endocrinol (Lausanne)*, vol. 12, article 656621, 2021.
- [20] H. Chen, *Study on the Protective Mechanism of Apelin Peptide on Pancreatic and Renal Injury*, [Ph.D Thesis], Huazhong University of Science and Technology, Hubei, 2014.
- [21] The microvascular complications Group of Diabetes Association of the Chinese Medical Association, "The expert consensus of diabetic kidney disease prevention and control," *Chin Journal Diabetes Mellitus*, vol. 6, no. 11, pp. 792–801, 2014.
- [22] G. D. Sun, C. Y. Li, W. P. Cui et al., "Review of herbal traditional chinese medicine for the treatment of diabetic nephropathy," *Journal Diabetes Research*, vol. 2016, article 5749857, 18 pages, 2016.
- [23] G. Scherthaner and G. H. Scherthaner, "Diabetic nephropathy: new approaches for improving glycemic control and reducing risk," *Journal of Nephrology*, vol. 26, no. 6, pp. 975–985, 2013.
- [24] H. Skali, A. Shah, D. K. Gupta et al., "Cardiac structure and function across the glycemic spectrum in elderly men and women free of prevalent heart disease: the Atherosclerosis Risk In the Community study," *Circulation. Heart Failure*, vol. 8, no. 3, pp. 448–454, 2015.
- [25] S. Hwang, J. Park, J. Kim et al., "Tissue expression of tubular injury markers is associated with renal function decline in diabetic nephropathy," *Journal of Diabetes and its Complications*, vol. 31, no. 12, pp. 1704–1709, 2017.
- [26] A. Porzionato, V. Macchi, M. Rucinski, L. K. Malendowicz, and R. De Caro, "Natriuretic peptides in the regulation of the hypothalamic-pituitary-adrenal axis," *International Review of Cell and Molecular Biology*, vol. 280, pp. 1–39, 2010.
- [27] P. J. Saulnier, E. Gand, G. Velho et al., "Association of circulating biomarkers (adrenomedullin, TNFR1, and NT-proBNP) with renal function decline in patients with type 2 Diabetes: A french prospective cohort," *Diabetes Care*, vol. 40, no. 3, pp. 367–374, 2017.
- [28] L. Yuan, "The significance of combined detection of brain natriuretic peptide, cystatin c and homocysteine in the diagnosis of early diabetic nephropathy," *Zhejiang Practical Medicine*, vol. 18, no. 4, pp. 240–241, 2013.
- [29] X. Wang and D. Zheng, "The significance of detecting type B brain natriuretic peptide in patients with diabetic nephropathy," *Chinese Journal of Gerontology*, vol. 33, no. 14, pp. 3450–3451, 2013.
- [30] H. Dai, L. Chen, D. Gao, and A. Fei, "Phosphocreatine attenuates isoproterenol-induced cardiac fibrosis and cardiomyocyte apoptosis," *BioMed Research International*, vol. 2019, Article ID 5408289, 7 pages, 2019.
- [31] M. Dou, L. Di, L. L. Zhou et al., "Cochlearols A and B, polycyclic meroterpenoids from the fungus Ganoderma cochlear that have renoprotective activities," *Organic Letters*, vol. 16, pp. 6064–6067, 2014.
- [32] S. Horita, M. Nakamura, M. Suzuki, N. Satoh, A. Suzuki, and G. Seki, "Selective insulin resistance in the kidney," *BioMed Research International*, vol. 2016, Article ID 5825170, 8 pages, 2016.
- [33] Q. Lu, W. Z. Zuo, X. J. Ji et al., "Ethanolic *Ginkgo biloba* leaf extract prevents renal fibrosis through Akt/mTOR signaling in diabetic nephropathy," *Phytomedicine*, vol. 22, no. 12, pp. 1071–1078, 2015.
- [34] Y. Li, Z. Zhao, and W. Liu, "Regulation of autophagy by PI3K / Akt / mTOR signaling pathway in hormonal ischemic necrosis of the femoral head," *China Tissue Engineering Research*, vol. 23, no. 12, pp. 1921–1929, 2019.
- [35] H. Yang and S. Wu, "Retracted Article: Ligustrazine attenuates renal damage by inhibiting endoplasmic reticulum stress in diabetic nephropathy by inactivating MAPK pathways," *RSC advances*, vol. 8, no. 39, pp. 21816–21822, 2018.
- [36] L. Espert, M. Denizot, M. Grimaldi et al., "Autophagy is involved in T cell death after binding of HIV-1 envelope proteins to CXCR4," *The Journal of Clinical Investigation*, vol. 116, no. 8, pp. 2161–2172, 2006.
- [37] S. Bernales, K. I. McDonald, and P. Walter, "Autophagy counterbalances endoplasmic reticulum expansion during the unfolded protein response," *PLoS Biology*, vol. 4, no. 12, article e423, 2006.
- [38] J. Puyal, V. Ginet, Y. Grishchuk, A. C. Truttmann, and P. G. H. Clarke, "Neuronal autophagy as a mediator of life and Death," *The Neuroscientist*, vol. 18, no. 3, pp. 224–236, 2012.
- [39] K. Chen, X. Lv, W. Li et al., "Autophagy is a protective response to the oxidative damage to endplate chondrocytes in intervertebral disc: implications for the treatment of

- degenerative lumbar disc,” *Oxidative Medicine and Cellular Longevity*, vol. 2017, Article ID 4041768, 9 pages, 2017.
- [40] M. C. Maiuri, G. le Toumelin, A. Criollo et al., “Functional and physical interaction between Bcl-XL and a BH3-like domain in Beclin-1,” *The EMBO Journal*, vol. 26, no. 10, pp. 2527–2539, 2007.
- [41] V. Deretic, T. Saitoh, and S. Akira, “Autophagy in infection, inflammation and immunity,” *Nature Reviews. Immunology*, vol. 13, no. 10, pp. 722–737, 2013.
- [42] J. F. Navarro-González, C. Mora-Fernández, M. M. de Fuentes, and J. García-Pérez, “Inflammatory molecules and pathways in the pathogenesis of diabetic nephropathy,” *Nature Reviews. Nephrology*, vol. 7, no. 6, pp. 327–340, 2011.
- [43] T. Saitoh, N. Fujita, M. H. Jang et al., “Loss of the autophagy protein Atg16L1 enhances endotoxin-induced IL-1 β production,” *Nature*, vol. 456, no. 7219, p. 264, 2008.
- [44] D. S. Arroyo, E. A. Gaviglio, J. M. Ramos, C. Bussi, M. C. Rodriguez-Galan, and P. Iribarren, “Autophagy in inflammation, infection, neurodegeneration and cancer,” *International Immunopharmacology*, vol. 18, no. 1, pp. 55–65, 2014.
- [45] T. Kimura, Y. Isaka, and T. Yoshimori, “Autophagy and kidney inflammation,” *Autophagy*, vol. 13, no. 6, pp. 997–1003, 2017.
- [46] J. Ma, H. Rui, Q. Chen, Z. H. Wang, and Y. Cheng, “Anti-inflammatory activity and therapeutic effect of *Ganoderma lucidum* polysaccharide on streptozotocin-induced diabetic nephropathy in mice,” *Journal of Nanjing Medical University (Natural Science Edition)*, vol. 39, no. 3, pp. 326–331, 2019.
- [47] Y. Aso, N. Yoshida, K. Okumura et al., “Coagulation and inflammation in overt diabetic nephropathy: association with hyperhomocysteinemia,” *Clinica Chimica Acta*, vol. 348, no. 1–2, pp. 139–145, 2004.
- [48] D. U. Nguyen, F. U. Ping, W. E. Mu, P. Hill, R. C. Atkins, and S. J. Chadban, “Macrophage accumulation in human progressive diabetic nephropathy,” *Nephrology (Carlton, Vic)*, vol. 11, no. 3, pp. 226–231, 2006.
- [49] F. Barutta, G. Bruno, S. Grimaldi, and G. Gruden, “Inflammation in diabetic nephropathy: moving toward clinical biomarkers and targets for treatment,” *Endocrine*, vol. 48, no. 3, pp. 730–742, 2015.
- [50] P. Geng, D. Zhong, L. Su, Z. Lin, and B. Yang, “Preventive and therapeutic effect of *Ganoderma lucidum* on kidney injuries and diseases,” *Advances in Pharmacology*, vol. 87, pp. 257–276, 2020.
- [51] D. Pan, D. Zhang, J. Wu et al., “A novel proteoglycan from *Ganoderma lucidum* fruiting bodies protects kidney function and ameliorates diabetic nephropathy via its antioxidant activity in C57BL/6 db/db mice,” *Food and Chemical Toxicology*, vol. 63, no. 111–118, pp. 111–118, 2014.
- [52] F. Shaher, S. Wang, H. Qiu et al., “Effect and mechanism of *Ganoderma lucidum* spores on alleviation of diabetic cardiomyopathy in a pilot in vivo Study,” *Diabetes, Metabolic Syndrome and Obesity: Targets and Therapy*, vol. Volume 13, pp. 4809–4822, 2020.
- [53] F. Shaher, H. Qiu, S. Wang et al., “Associated targets of the antioxidant cardioprotection of *Ganoderma lucidum* in diabetic cardiomyopathy by using open targets platform: a systematic review,” *BioMed Research International*, vol. 2020, Article ID 7136075, 20 pages, 2020.
- [54] H. N. Li, L. L. Zhao, and D. Q. Di Yi Zhou, “*Ganoderma lucidum* polysaccharides ameliorates hepatic steatosis and oxidative stress in db/db mice via targeting nuclear factor E2 (erythroid-derived 2)-related factor-2/heme oxygenase-1 (HO-1) pathway,” *Medical Science Monitor: international medical journal of experimental and clinical research*, vol. 26, article e921905, 2020.
- [55] H. Liang, Y. Pan, Y. Teng et al., “A proteoglycan extract from *Ganoderma lucidum* protects pancreatic beta-cells against STZ-induced apoptosis,” *Bioscience, Biotechnology, and Biochemistry*, vol. 84, no. 12, pp. 2491–2498, 2020.
- [56] K.-J. Wu, S.-Q. Wang, R.-P. Shi et al., “Neuroprotective effect of *Ganoderma lucidum* polysaccharides on epilepsy in a rat’s epileptic model,” *Current Topics in Nutraceutical Research*, vol. 20, no. 2, 2022.
- [57] Z. M. Jiang, H. B. Qiu, S. Q. Wang, J. Guo, Z. W. Yang, and S. Zhou, “Ganoderic acid A potentiates the antioxidant effect and protection of mitochondrial membranes and reduces the apoptosis rate in primary hippocampal neurons in magnesium free medium,” *Die Pharmazie-An International Journal of Pharmaceutical Sciences*, vol. 73, no. 2, pp. 87–91, 2018.
- [58] S. Zhou, S. Q. Wang, C. Y. Sun et al., “Investigation into anti-epileptic effect and mechanisms of *Ganoderma lucidum* polysaccharides in vivo and in vitro models,” *Proceedings of the Nutritional Society*, vol. 74, no. OCE1, p. E65, 2015.
- [59] S. Q. Wang, X. J. Li, H. B. Qiu et al., “Anti-epileptic effect of *Ganoderma lucidum* polysaccharides by inhibition of intracellular calcium accumulation and stimulation of expression of CaMKII α in epileptic hippocampal neurons,” *PLoS ONE*, vol. 9, no. 7, article e102161, 2014.
- [60] S. Q. Wang, X. J. Li, S. Zhou et al., “Intervention effects of *Ganoderma lucidum* spores on epileptiform discharge hippocampal neurons and expression of neurotrophin-4 and N-cadherin,” *PLoS One*, vol. 8, no. 4, article e61687, 2013.

Research Article

Preparation of Spice Extracts: Evaluation of Their Phytochemical, Antioxidant, Antityrosinase, and Anti- α -Glucosidase Properties Exploring Their Mechanism of Enzyme Inhibition with Antibrowning and Antidiabetic Studies *In Vivo*

Yahya S. Alqahtani,¹ Mater H. Mahnashi ,¹ Bandar A. Alyami,¹ Ali O. Alqarni,¹ Mohammed A. Huneif,² Mohammed H. Nahari ,³ Anser Ali,⁴ Qamar Javed,⁴ Hina Ilyas,⁴ and Muhammad Rafiq ⁵

¹Department of Pharmaceutical Chemistry, College of Pharmacy, Najran University, Najran, Saudi Arabia

²Pediatric Department, Medical College, Najran University, Najran, Saudi Arabia

³Department of Clinical Laboratory Sciences, Najran University Najran, Saudi Arabia

⁴Department of Zoology, Mirpur University of Science and Technology (MUST), Mirpur, 10250 AJK, Pakistan

⁵Department of Physiology & Biochemistry, Cholistan University of Veterinary and Animal Sciences, Bahawalpur 63100, Pakistan

Correspondence should be addressed to Mater H. Mahnashi; aleen9542@gmail.com

Received 14 November 2021; Revised 12 January 2022; Accepted 17 February 2022; Published 4 March 2022

Academic Editor: Syed Sameer Aga

Copyright © 2022 Yahya S. Alqahtani et al. This is an open access article distributed under the Creative Commons Attribution License, which permits unrestricted use, distribution, and reproduction in any medium, provided the original work is properly cited.

Tyrosinase and α -glucosidase enzymes are known as promising target candidates for inhibitors to control unwanted pigmentation and type II diabetics mellitus. Therefore, twenty extracts as enzyme inhibitors were prepared from edible spices: nutmeg, mace, star anise, fenugreek, and coriander aiming to explore their antioxidant, antibrowning, and antidiabetic potential. Results confirmed that all extracts showed potent antioxidant activity ranging from $IC_{50} = 0.14 \pm 0.03$ to $3.69 \pm 0.37 \mu\text{g/mL}$. In addition, all extracts exhibited excellent antityrosinase ($IC_{50} = 1.16 \pm 0.06$ to $71.32 \pm 4.63 \mu\text{g/mL}$) and anti- α -glucosidase ($IC_{50} 4.76 \pm 0.71$ to $42.57 \pm 2.13 \mu\text{g/mL}$) activities outperforming the corresponding standards, hydroquinone, and acarbose, respectively. Among all extracts, star anise ethyl acetate (Star anise ETAC) was found most potent inhibitor for both tyrosinase and α -glucosidase enzymes and was further studied to explore the mechanism of enzyme inhibition. Kinetic analysis revealed its irreversible but mixed-type tyrosinase inhibition with preferentially competitive mode of action. However, it binds reversibly with α -glucosidase through competitive mode of action. Further, star anise ETAC extract showed concentration dependent and posttreatment time-dependent antibrowning effect on potato slices and antidiabetic effect on diabetic rabbits *in vivo* proposing it promising candidate for tyrosinase-rooted antibrowning and α -glucosidase-associated diabetes management for future studies.

1. Introduction

Spices, a tropical herbal plant or its specific part, are not only valuable part of food but also used in fragrances, cosmetics, and medicines. Spices have been studied rigorously in recent times to understand their nature and chemical constituents. Many studies reported their important therapeutic uses, i.e., as appetizer, digestive, analgesic, carminative, hepatoprotective, blood purifier, hypolipidemic, antipyretic, antidiabetic,

anti-inflammatory, antimicrobial, and antioxidant agents [1–3]. Inspired by their medicinal values, five common species of daily use, i.e., nutmeg, mace, star anise, fenugreek, and coriander, were selected. They are reported to show medicinal properties, i.e., nutmeg: astringent, stimulant, aphrodisiac, carminative, and anti-inflammatory agent; fenugreek: tonic, carminative, aphrodisiac, coriander; tonic, refrigerant, stimulant, diuretic, carminative, stomachic, analgesic, aphrodisiac, and anti-inflammatory agent [3]. These

TABLE 1: Antioxidant activity of prepared extracts.

Extract	DDPH assay inhibition IC ₅₀ ± SEM (µg/mL)			
	MeOH	ETAC	n-Hex	CHLO
Nutmeg	3.39 ± 0.67	1.65 ± 0.36	1.38 ± 0.27	1.19 ± 0.09
Mace	1.33 ± 0.16	0.64 ± 0.09	0.26 ± 0.1	0.59 ± 0.07
Star anise	2.67 ± 0.65	0.68 ± 0.13	3.16 ± 0.16	1.67 ± 0.17
Fenugreek	1.83 ± 0.18	0.14 ± 0.03	0.22 ± 0.02	0.41 ± 0.04
Coriander	0.7 ± 0.11	0.31 ± 0.06	3.69 ± 0.37	0.79 ± 0.12
Ascorbic acid		1.16 ± 0.06		

spices are commonly available and consumed in Asia; they penetrate our lives from birth to death. Therefore, we selected them to prepare the extracts for present study. This study would be the first preparing twenty extracts from five common edible spices in the region, nutmeg, mace, star anise, fenugreek, and coriander, using four solvents, methanol, ethyl acetate, n-hexane, and chloroform, comparing their antioxidant, antityrosinase, and anti- α -glucosidase activities identifying most potent candidate for antibrowning and diabetic potential, and having real-life applications in food and medicines.

Oxidative stress, diabetes mellitus, skin abnormal pigmentation, and fruit browning are the burning issues of this era [4–7]. Free radicals are produced during normal metabolic activities. Nearly 1/4 of inhaled oxygen is converted into free radicals. However, their excess and over accumulation have deteriorating effects on biologically important molecules like proteins, enzymes, and DNA. Although human body has well equipped and efficient antioxidant defence system, it becomes compromised when free radicals are produced higher than scavenging capacity of the body, a condition developing due to human's overdependence on synthetically processed food which ultimately requires supplements to cope [5]. Thus, excessive reactive oxygen species adversely affect the antioxidant system resulting in multiple abnormalities, i.e., neurodegenerative diseases, arthritis, cancer, diabetes mellitus, and ageing [8]. Moreover, free radical association with pigmentation and conversion of tyrosinase to dopaquinone is critical. The increased activity of free radicals in living systems leads to an increased pigmentation [9, 10], which is undesirable. Browning of fruit is another major problem occurring during storage adversely effecting its quality and posing huge economic loss [4, 6].

Tyrosinase is a key enzyme in pigment synthesis. It is responsible for skin and hair color as well as for undesirable enzymatic browning in fresh-cut fruits or plant-derived foods limiting their shelf-life with the resultant economic loss [11]. Likewise, abnormal skin pigmentation causes authentic problems, i.e., freckles, age spots, and melanoma [12]. Compounds with antioxidant and pigment inhibitory properties are desirable for skin whitening cosmetic prod-

ucts and for the antibrowning to maintain food quality. Spices may acquire special attention for cosmetic product improvement and to control unwanted browning of fruits as they could have less toxicity than the synthetic compounds.

In addition to pigmentation, growing scientific evidences are connecting oxidative stress with the development of diabetes and its secondary complications [13]. Oxidative stress or outrageous ROS release from autoxidation of glucose, glycated proteins, and glycation of antioxidant enzymes limit the ability to detoxify the free radicals [14]. Ultimately, high ROS load interrupts the glucose level by destroying pancreatic β -cells; the cells shown to have high ROS sensitivity due to their poor natural enzymatic antioxidant defence system than other body tissues, i.e., liver [15, 16]. Thus, chemicals with antioxidant properties are suggested to help in diabetic management [17]. Moreover, to control postprandial rise in blood glucose, α -glucosidase inhibition is critical because it delays or inhibit the carbohydrate digestion or absorption ultimately dropping the postprandial glucose level in blood [18–21]. Therefore, α -glucosidase inhibition is the simplest approach, and α -glucosidase inhibitors are attractive candidate for diabetes management [22, 23].

Thus, search for safe and potent antioxidants with tyrosinase and α -glucosidase inhibitory properties preferably from natural sources is desirable which may help in enzyme-associated pigmentation and diabetic management.

2. Materials and Method

2.1. Chemicals. Mushroom tyrosinase, 3,4-dihydroxyphenylalanine (L-DOPA), α -glucosidase from *S. cerevisiae*, acarbose, sodium carbonate, p-nitrophenyl- α -d-glucopyranoside (pNPG), and sodium phosphate dibasic were obtained from Sigma Aldrich and stored according to manufacturer's instructions.

2.2. Extract Preparation. Spices, i.e., nutmeg (*Myristica fragrans*), mace (*Myristica fragrans*), star anise (*Illicium verum*), fenugreek (*Trigonella foenum-graecum*), and coriander (*Coriandrum sativum*), were purchased from the local market, Mirpur, AJK, Pakistan. They were ground. Spices in powder form were dipped (1:10 g/mL) in different solvents, i.e., methanol (MeOH), ethyl acetate (ETAC), n-hexane (n-Hex), and chloroform (CHLO) for 8 days. These solvents were used because of their easy availability, easy evaporation during rotary evaporation process at low temperature, and most importantly, because of their frequent use in scientific community, availability in literature, and partitioning based on chemical solubility. Dipped samples were shaken gently two times per day. After 8 days, samples were filtered, and filtrate was evaporated by using rotary evaporator (Heidolph, Germany) at 37°C. Finally, obtained extracts were air dried at room temperature and stored at 4°C until further use.

2.3. Antioxidant Bioassay. Antioxidant activity using 2,2-diphenylpicrylhydrazyl (DPPH) was determined following Sharma et al. [24], with slight modifications. Briefly, 50 µL

TABLE 2: Tyrosinase and α -glucosidase inhibitory activity of prepared extracts.

Extract	MeOH	ETAC	n-Hex	CHLO
		Tyrosinase inhibition IC ₅₀ \pm SEM (μ g/mL)		
Nutmeg	24.66 \pm 2.46	6.43 \pm 0.96	1.91 \pm 0.1	2.74 \pm 0.1
Mace	5.91 \pm 0.45	2.82 \pm 0.18	2.39 \pm 0.63	7.99 \pm 0.6
Star anise	9.86 \pm 0.84	1.16 \pm 0.06	3.9 \pm 0.58	2.09 \pm 0.14
Fenugreek	31.23 \pm 1.56	2.73 \pm 0.27	19.12 \pm 1	34.86 \pm 1.74
Coriander	71.32 \pm 4.63	10.5 \pm 0.53	3.02 \pm 0.3	9.65 \pm 0.63
Hydroquinone		131.34 \pm 9.82 (standard for tyrosinase)		
		α -Glucosidase inhibition IC ₅₀ \pm SEM (μ g/mL)		
Nutmeg	40.65 \pm 4.05	6.72 \pm 0.67	23.37 \pm 1.17	5.5 \pm 0.55
Mace	22.31 \pm 2.22	20.18 \pm 2.01	16.78 \pm 2.34	23.32 \pm 2.21
Star anise	42.57 \pm 2.13	4.76 \pm 0.71	16.52 \pm 1.65	9.21 \pm 1.82
Fenugreek	17.76 \pm 1.33	6.05 \pm 0.67	15.82 \pm 2.36	17.86 \pm 2.22
Coriander	19.13 \pm 1	25.82 \pm 1.29	30.52 \pm 1.92	42.57 \pm 2.13
Acarbose		201.34 \pm 20.07 (standard for α -glucosidase)		

DPPH and 50 μ L inhibitor mixture was incubated in dark for 10 min at room temperature, and then, absorbance was recorded at 490 nm wavelength. Ascorbic acid was used as standard. The experiment was performed in duplet, and IC₅₀ value was calculated by using excel to compare the results.

2.4. Tyrosinase Inhibitory Activity. Antityrosinase assay was performed following Zaman et al. [25]. Briefly, a reaction mixture, enzyme (20 μ L (30 U/mL) of mushroom tyrosinase, 140 μ L (20 mM, pH 6.8) phosphate buffer, and 20 μ L of test extract, was mixed, incubated for 10 min at 37°C. Later, 20 μ L (0.85 mM) L-DOPA as substrate was added, incubated again for 20 min at 37°C followed by tracking dopachrome formation as measure of tyrosinase inhibition at 490 nm was checked. Each concentration was analysed in two independent experiments run in duplicate. Kojic acid was used as standard. The extent of inhibition showed by the tested extract was calculated by % inhibition formula given below, and the IC₅₀ was determined by using the Microsoft Excel.

$$\text{Inhibition activity (\%)} = \frac{(\text{OD}_{\text{control}} - \text{OD}_{\text{sample}} \times 100)}{\text{OD}_{\text{control}}}, \quad (1)$$

where OD_{control} and OD_{sample} represent the optical densities in the absence and presence of sample, respectively.

2.5. α -Glucosidase Inhibitory Activity. α -Glucosidase assay was performed following Umamaheswari and Sangeetha [26]. Briefly, a reaction mixture, 25 μ L of 0.1 M (pH 6.9) sodium phosphate buffer, 12.5 μ L (0.5 mM) of pNPG as substrate, 10 μ L extract as inhibitor, and 12.5 μ L of α -glucosidase enzyme, was mixed and incubated for 30 min at 37°C. Later, 50 μ L (0.2 M) sodium carbonate solution was added to terminate the reaction, and inhibition was monitored at 405 nm using microplate reader. Acarbose was used as stan-

dard, and IC₅₀ value was calculated to compare with test extract results.

2.6. Kinetic Analysis of Tyrosinase and α -Glucosidase Enzyme Inhibition. To determine the mechanism of enzyme inhibition, a series of kinetic assays was performed following Zaman et al. [25] for tyrosinase and Rehman et al. [27] and Motoshima et al. [28] for α -glucosidase. To explore type of enzyme inhibition, Lineweaver-Burk plot (LBP) was plotted as inverse of velocities 1/V versus inverse of substrate concentration 1/[S] mM⁻¹. The inhibition constant (K_i) was determined by two methods, the second plots of the apparent slope versus the extract concentrations, and through Dixon plot. Dixon plot was obtained by plotting different extract concentrations (as indicated in plots) versus inverse of velocities (1/V) with changing substrate concentrations. To check enzyme behaviour, reversible or irreversible, complexes established between extracts and enzyme were explored.

2.7. Phytochemical Analysis. For phytochemical analysis, qualitative tests were performed by following Chelladurai and Chinnachamy [29]. Briefly, star anise ETAC extract stock 10 mg/mL was prepared in DMSO. For flavonoid test, 125 μ L extract was shaken with pet ether, then dissolved in 5 mL ethanol (80%), and filtered. The filtrate was mixed with 1% KOH (1:1 ratio), and appearance of dark yellow colour confirmed its presence. For saponins, 250 μ L extract was mixed in 1 mL boiling distilled water (DI). Later, sample was cooled, mixed thoroughly, and the appearance of foam indicated its presence. For alkaloids, 125 μ L extract and 2 mL HCl (1%) were mixed, warmed, and filtered. The filtrate was treated with Mayer's reagent, and turbidity was noticed indicating its presence. For tannins, 125 μ L extract was boiled in DI (5 mL) and filtered. Few drops of FeCl₃ (0.1%) were added, and brownish green appearance

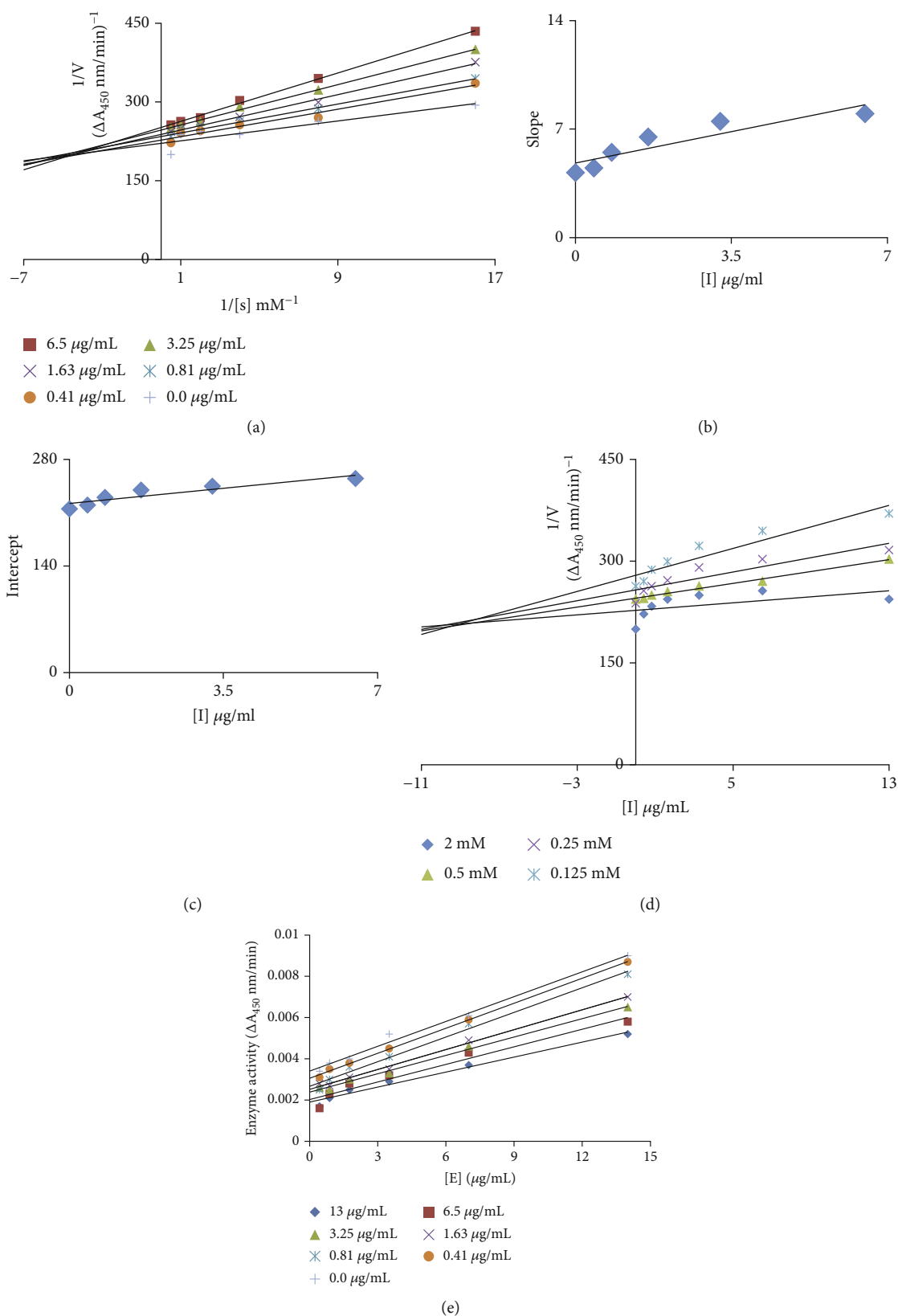


FIGURE 1: Mechanism of tyrosinase inhibition. (a) Lineweaver-Burk plot (LBP) for inhibition of tyrosinase enzyme in the presence of Star anise ETAC extract. The extract concentrations 0-13 $\mu\text{g/mL}$; however, L-DOPA concentrations ranging from 0.125 to 2 mM were used. (b) The insets represent the plot of the slope from LBP versus extract. (c) The secondary replot of the LBP, $1/V$ (y-intercept) of versus various concentrations of extract. (d) The Dixon plot of the reciprocal of the initial velocities versus various concentrations of extract as inhibitor. (e) Relationship between the catalytic activity of L-DOPA and various concentrations of extract.

TABLE 3: Inhibitory behaviour of most potent extract on tyrosinase and α -glucosidase enzymes.

Extract	Enzyme	K_i ($\mu\text{g/mL}$)	K_i' ($\mu\text{g/mL}$)	Type of inhibitor	Catalytic activity
Star anise ETAC	Tyrosinase	8.2	37	Mix type	Irreversible
	α -Glucosidase	34	34	Competitive	Reversible

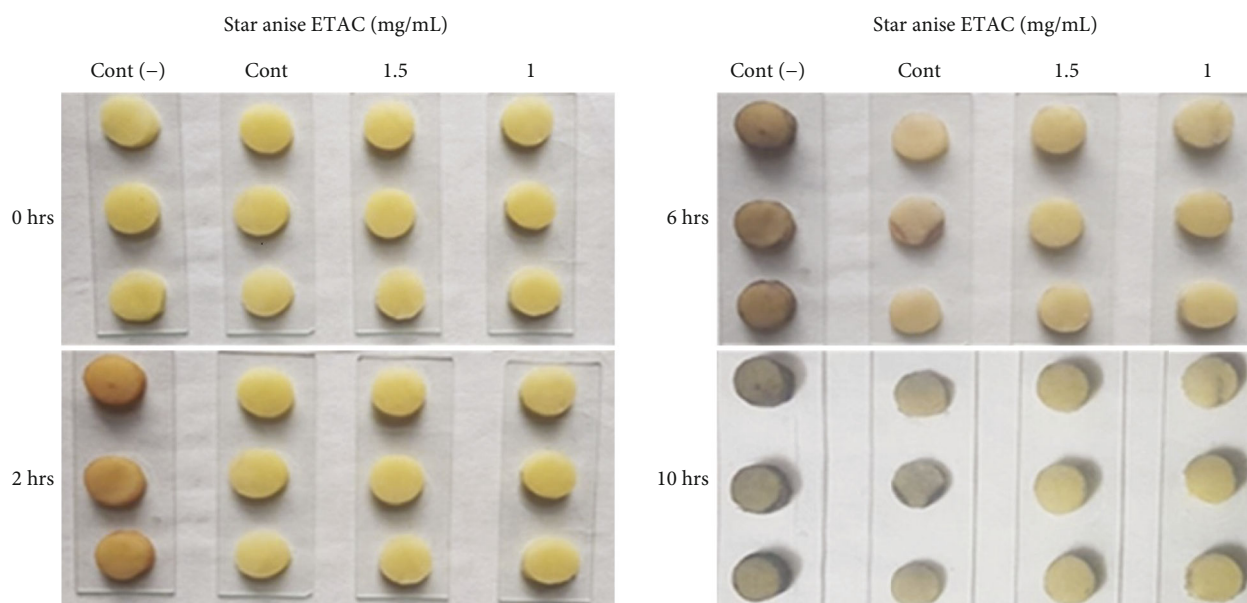


FIGURE 2: Antibrowning effect of star anise ETAC extract on potato slices. Cont (-): slices without any treatment; Cont: water; star anise ETAC extract = 1 and 1.5 mg/mL.

confirmed its presence. To test coumarins, 250 μL extract in small tube was covered with 1N NaOH-moistened filter paper, placed in boiling DI and examined under UV light for yellow fluorescence indicating its presence. To test anthocyanin and betacyanin, 1 mL extract with 2N sodium hydroxide (500 μL) was heated (3 min, 100°C), and formation of yellow colour was confirmed. For glycosides, 1 mL extract, 1.5 mL chloroform, and few drops of ammonium solution (10%) were mixed. Formation of pink colour indicated glycoside presence. For cardiac glycosides, 250 μL extract, glacial acetic acid (1 mL), and few drops of ferric chloride (5%) were mixed. Later, conc. sulphuric acid (0.5 mL) was added, and the formation of brown ring at interface confirmed its presence. To test terpenoids, 0.5 mL extract, 2 mL chloroform, and conc. sulphuric acid were mixed. The formation of red brown colour confirmed its presence. For phenols, 0.5 mL extract, 1 mL DI, and few drops of ferric chloride (10%) were mixed, and the appearance of blue colour was observed. To test quinones, 0.5 mL extract and 0.5 mL conc. sulphuric acid were mixed, and the appearance of red colour confirmed its presence. To test steroids, 125 μL extract, 1 mL chloroform, and 0.5 mL sulphuric acid were mixed, and the appearance of reddish brown ring confirmed steroid's presence.

2.8. In Vivo Diabetes Analysis in Rabbits. To induce diabetes and to analyse antidiabetic potential of test extract, standard

method reported previously was followed [30, 31] with slight modifications. Briefly, healthy rabbits (*Oryctolagus cuniculus*) ($n = 18$) were kept in controlled area and fed on mixed vegetables, and tap water was available *ad libitum*. After habituation, diabetes was induced in 12 hr fasting rabbits ($n = 12$) by intraperitoneal administration of alloxan monohydrate (150 mg/kg of body weight) dissolved in sodium citrate buffer (4.5 pH). After 50 hrs of alloxan injection, diabetic animals ($n = 12$) were divided into 2 groups (B and C) by injecting sodium citrate (pH 4.5) in group B ($n = 6$) and by injecting test extract star anise ETAC (250 mg/kg of body weight) in group C ($n = 6$) to compare with control (untreated) group A ($n = 6$).

Group A: untreated animals

Group B: alloxan treated animals

Group C: alloxan + extract treated animals

Finally, their weight in grams (g) and blood glucose level in mg/dL were measured by blood glucose meter On Call® Plus (Acon, USA), and results were compared.

2.9. Antibrowning Analysis on Potato Slices. Antibrowning potential of test extract was determined following Wu et al. [32] with slight modifications. Briefly, potato slices were washed and cut into small identical slices using a slicer. They were dipped in deionized water (DI) as control and were dipped in extract star anise ETAC (1 and 1.5 mg/mL prepared in DI). Samples without any treatment were kept as

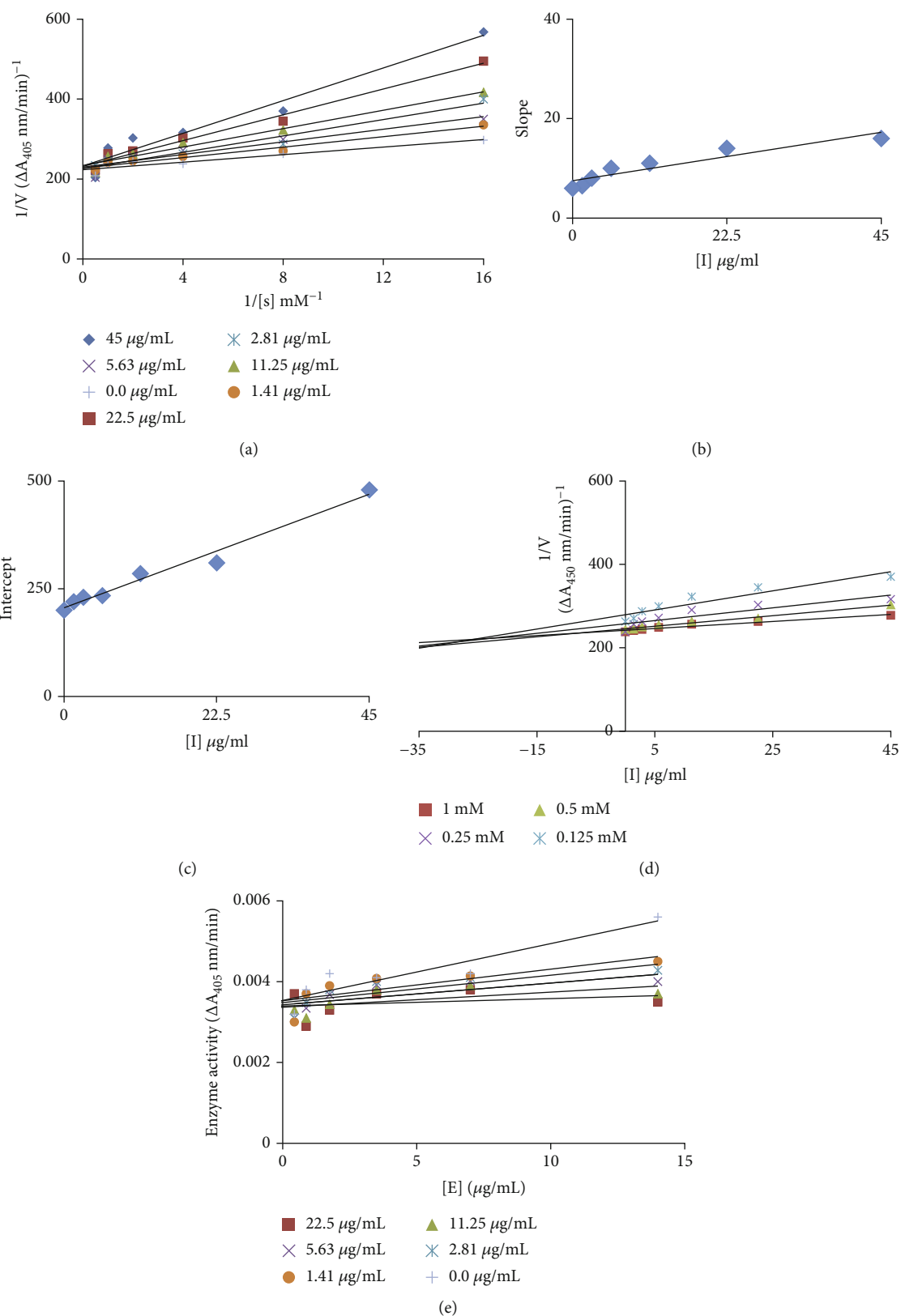


FIGURE 3: Mechanism of α -glucosidase inhibition. (a) Lineweaver-Burk plot (LBP) for the inhibition of α -glucosidase in the presence of Star anise ETAC extract. The extract concentrations 0-45 μ g/mL; however, pNPG concentrations (0.125 to 1 mM) were used. (b) The insets represent the plot of the slope from LBP versus inhibitor. (c) The secondary replot of the LBP, $1/V$ (y-intercept) of versus various concentrations of inhibitor. (d) The Dixon plot of the reciprocal of the initial velocities versus various concentrations of extract as inhibitor. (e) Relationship between the catalytic activity of pNPG and various concentrations of extract.

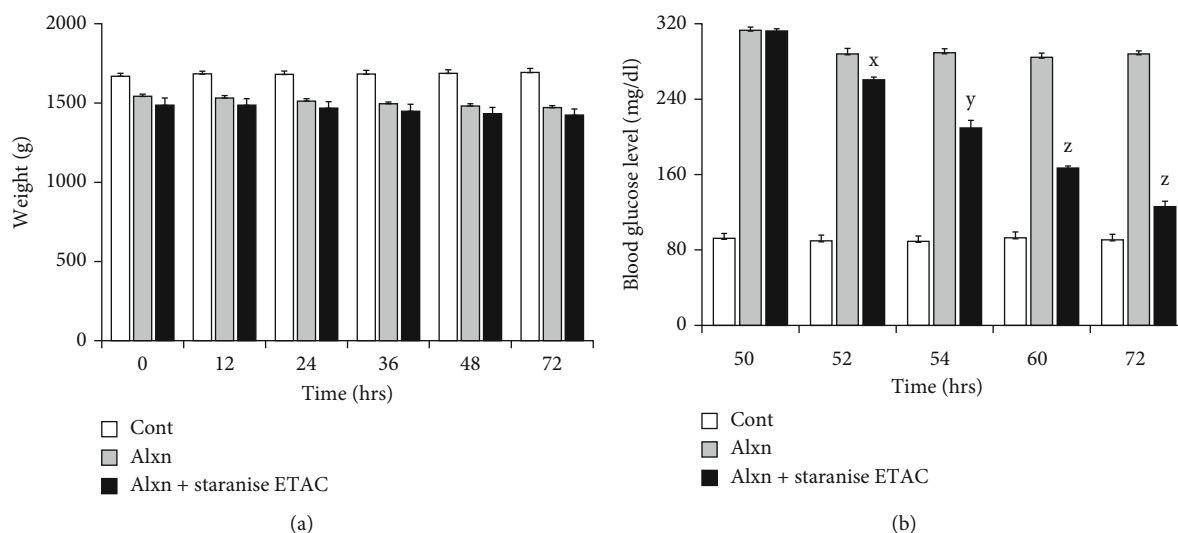


FIGURE 4: Diabetes analysis in rabbits. (a) Body weight of rabbits. (b) Measurement of blood glucose level. Experiments were performed thrice, and significance between alloxan (alxn) and alxn+Star anise ETAC was determined by Student's *t*-test as $x < 0.00001$, $y < 0.0000001$, and $z < 0.000000001$.

negative control. All samples were placed on absorbent paper, at room temperature and photographed at 0, 2, 6, and 10 hrs to track change in colour.

2.10. Statistical Analysis. All experiments were performed thrice in triplicate or more. The data was organised in Microsoft Excel. To find the significance, Student's *t*-test was applied, and level of significance was expressed as $x < 0.0001$, $y < 0.0000001$, and $z < 0.000000001$.

3. Result and Discussion

In the present study, twenty extracts were prepared using five common spices, nutmeg, mace, star anise, fenugreek, and coriander, and four solvents, MeOH, ETAC, n-Hex, and CHLO, aiming to explore their antioxidant, antibrowning, and antidiabetic potential.

Results confirmed that all extracts possess significant antioxidant activity with IC_{50} values ranging from 0.14 ± 0.03 to $3.69 \pm 0.37 \mu\text{g/mL}$ (Table 1). Interestingly, 50% of total test extracts outperform the ascorbic acid, used as positive control ($IC_{50} = 1.16 \mu\text{g/mL}$). Previous studies also reported the antioxidant activity of star anise extracts [33, 34]. Gupta et al. [35] reported antioxidant activity of nutmeg methanolic extract as $IC_{50} = 1.04 \text{ mg/mL}$. Another study used methanolic extract of three coriander varieties, i.e., *Coriandrum sativum* L., Tunisian, Syrian, and Egyptian, and reported antioxidant activity as 27, 36, and $32 \mu\text{g/mL}$, respectively [36]. Antioxidants are shown to have close association with antibrowning [37, 38]. Browning of fruits remained a challenge in the food industry. This physiological disorder results mainly from the oxidation process leading to the formation of brown pigments which are shown to be controlled by the application of antioxidants or by reducing/inhibiting the activities of associated enzymes [37]. Thus, along antioxidant activity, we tested

potential of prepared extracts to inhibit tyrosinase, key enzyme in pigmentation [39].

Analysis revealed that all extracts exhibit excellent tyrosinase inhibitory activity, IC_{50} ranging from 1.16 ± 0.06 to $71.32 \pm 4.63 \mu\text{g/mL}$ where all extracts outperformed the standard hydroquinone ($IC_{50} = 131.34 \pm 9.82 \mu\text{g/mL}$) (Table 2). Among all extracts, star anise ETAC extract was found most active tyrosinase inhibitor with lowest IC_{50} value ($1.16 \pm 0.06 \mu\text{g/mL}$); thus, it was selected for kinetic studies to further explore the mechanism of its enzyme inhibition and antibrowning activity. The Lineweaver-Burk plot for tyrosinase produced family of straight slopes where V_{max} reduces with increasing K_m value and by increasing concentrations of extract expressing its mixed type mode of inhibition (Figure 1(a)). In other words, star anise ETAC extract bound with free enzyme (E) as well as with enzyme-substrate (ES) complex [40]. The dissociation constant (K_i) and ESI dissociation constant (K_i') were shown by secondary replots of slope versus extract concentration and intercept versus extract concentration, respectively (Figures 1(b) and 1(c)). The $K_i = 8.2 \mu\text{g/mL}$ and $K_i' = 37 \mu\text{g/mL}$ for star anise ETAC indicate stronger binding with enzyme [41] that justifies its preferred competitive mode of inhibition (Table 3). Plot between catalytic activity of L-DOPA and various concentrations of Star anise ETAC extract showed irreversible mode of enzyme action (Figure 1(e)). A range of important biological activities of star anise includes antimicrobial, carminative, diuretic, and stomachic and is used in digestive disturbances, cough mixtures, and colic pain [42]. However, the present study confirms its antityrosinase activity with mechanism of enzyme inhibition. To further recapitulate tyrosinase inhibition results, further antibrowning test for star anise ETAC was performed. The visual results confirmed dose and posttreatment time-dependent antibrowning effect of star anise ETAC extract on potato slices (Figure 2). The extract-treated samples showed

TABLE 4: Phytochemical analysis of star anise ETAC extract.

Phytochemicals tested	Star anise ETAC	Phytochemicals tested	Star anise ETAC
Flavonoids	+	Glycosides	+
Saponins	+	Cardiac glycosides	+
Alkaloids	+	Terpenoids	+
Tannins	+	Phenols	+
Coumarins	+	Quinones	+
Anthocyanin and betacyanin	+	Steroids	+

+: present.

less browning than untreated negative control and H₂O-treated control indicating useful application of star anise ETAC for antibrowning increasing the fruit shelf life. Thus, use of antioxidants including spices, i.e., star anise ETAC extract, can therefore be regarded as a natural antibrowning approach which helps to mitigate browning of fruits important for food and beverage industry.

Likewise, α -glucosidase inhibitory activity of all test extracts was evaluated with potential application in diabetes management. The result confirmed the α -glucosidase inhibition with range of IC₅₀ from $4.76 \pm 0.71 \mu\text{g/mL}$ to $42.57 \pm 2.13 \mu\text{g/mL}$. All extracts outperformed the acarbose (IC₅₀ = $201.34 \pm 20.07 \mu\text{g/mL}$), used as standard (Table 2). Our results are in accordance to the report who found *Illicium verum* seed aqueous extract with α -glucosidase inhibitory activity as IC₅₀ = $392.13 \mu\text{g/mL}$ [43]. Star anise ETAC extract, like best antityrosinase activity, was found best α -glucosidase inhibitor with lowest IC₅₀ value ($4.76 \pm 0.71 \mu\text{g/mL}$), thus was further explored for kinetic analysis and diabetic activity *in vivo*. The Lineweaver-Burk plot produced family of straight slopes joining at y-axis with fixed V_{max} indicating competitive mode of enzyme inhibition (Figure 3(a)). The K_i value = $34 \mu\text{g/mL}$ was obtained by secondary replot and Dixon plot (Figures 3(b) and 3(d)). Furthermore, analysis revealed reversible mode of α -glucosidase inhibition by star anise ETAC extract (Figure 3(e)). To recapitulate α -glucosidase inhibition *in vitro* results to *in vivo*, antidiabetic experiments on rabbits were performed. To induce diabetes, alloxan (alxn) was injected. The results showed no significant change in body weight among untreated, alloxan-injected, and alloxan+star anise ETAC extract-injected animals till 72 hrs (Figure 4(a)). However, star anise ETAC injection in diabetic rabbits (group C) decreases the blood glucose level significantly in time-dependent manners as compared to alloxan-induced diabetic animals (group B) (Figure 4(b)). The untreated animals (group A) showed no significant change in glucose level throughout the experiment period. The blood glucose level in group B was 313, 288, 289, 285, and 288 mg/dL, and group C was 312, 260, 209, 166, and 126 mg/dL at 50, 52, 54, 60, and 72 hrs, respectively (Figure 4(b)), indicating star anise ETAC extract as promising candidate for diabetic management.

Previous studies have shown evidences connecting oxidative stress with the development of diabetes and its secondary

complications [13]. Oxidative stress or excessive ROS compromises the free radical detoxification ability of body and also interrupts the glucose level by destroying pancreatic β -cells [14–16]. Thus, antioxidants such as star anise ethyl acetate extract can therefore be regarded as a natural antidiabetic approach which helps improve health and blood glucose level without the use of prescription medicine.

Moreover, the phytochemical analysis of the most potent extract Star anise ETAC confirmed the presence of flavonoids, saponin, alkaloid, tannin, coumarin, anthocyanin/bethyl acetateyanin, glycoside, cardiac glycoside, terpenoid, phenol, quinone, and steroids (Table 4). Many studies have shown their tyrosinase inhibitory [44–46] and α -glucosidase inhibitory [47–49] effects, important for antibrowning [50] and diabetic management [22].

Thus, it is established that all extracts exhibited efficient antioxidant, antityrosinase, and anti- α -glucosidase activities; however, star anise ETAC extract among all was found the most potent extract. It further showed potential for tyrosinase-rooted antibrowning and α -glucosidase-rooted diabetic management important for food and health improvement in future.

4. Conclusion

The present study concluded that all twenty extracts obtained from edible spices exhibited potent antioxidant activity, important to achieve antibrowning and antidiabetic activities. In addition, all extracts exhibited excellent antityrosinase and anti- α -glucosidase activities outperforming their respective standards. Among all, star anise ETAC extract was found most potent inhibitor for both tyrosinase and α -glucosidase enzymes. Interestingly, its kinetic analysis revealed irreversible but mixed-type tyrosinase inhibition with preferentially competitive mode of action. However, it binds reversibly with α -glucosidase through competitive mode of action. Further, star anise ETAC extract showed concentration-dependent and posttreatment time-dependent antibrowning effect on potato slices and antidiabetic effect on diabetic rabbits *in vivo* proposing it promising candidate for tyrosinase-rooted antibrowning and α -glucosidase-associated diabetes management for future studies. For the future, characterization of star anise ETAC extract is suggested, and determination of key extract agent responsible for observed activities is recommended.

Data Availability

All data are included in the manuscript.

Conflicts of Interest

The authors show no conflict of interest.

Acknowledgments

The authors would like to acknowledge the support from the Ministry of Education, Saudi Arabia and the Deanship of Scientific Research at Najran University for funding this

research through a grant number NU/MRC/10/369. We also thankfully acknowledge Mirpur University of Science and Technology (MUST), AJK, Pakistan, for providing support to complete the current study.

References

- [1] A. K. Sachan, S. Kumar, K. Kumari, and D. Singh, "Medicinal uses of spices used in our traditional culture: worldwide," *Journal of Medicinal Plants Studies*, vol. 6, pp. 116–122, 2018.
- [2] M. Gupta, "Pharmacological properties and traditional therapeutic uses of important Indian spices: a review," *International Journal of Food Properties*, vol. 13, no. 5, pp. 1092–1116, 2010.
- [3] K. V. Peter and M. R. Shylaja, "Introduction to herbs and spices: definitions, trade and applications," in *Handbook of Herbs and Spices*, pp. 1–24, Woodhead Publishing, 2012.
- [4] G. Sahu, V. Paradkar, and R. Kumar, "Effect of anti-browning solutions on quality of fresh-cut apple slice," *International Journal of Current Research*, vol. 7, pp. 602–607, 2019.
- [5] S. Naz, M. Zahoor, M. N. Umar et al., "Enzyme inhibitory, antioxidant and antibacterial potentials of synthetic symmetrical and unsymmetrical thioureas," *Drug Design, Development and Therapy*, vol. 13, p. 3485, 2019.
- [6] Y. Jiang, X. Duan, H. Qu, and S. Zheng, "Browning: enzymatic browning," in *Encyclopedia of Food and Health*, pp. 508–514, Elsevier, 2016.
- [7] A. G. Pandya and I. L. Guevara, "Disorders of hyperpigmentation," *Dermatologic Clinics*, vol. 18, no. 1, pp. 91–98, 2000.
- [8] V. R. Patel, P. R. Patel, and S. S. Kajal, "Antioxidant activity of some selected medicinal plants in western region of India," *Advances in Biological Research*, vol. 4, pp. 23–26, 2010.
- [9] N. Alam, K. N. Yoon, J. S. Lee, H. J. Cho, and T. S. Lee, "Consequence of the antioxidant activities and tyrosinase inhibitory effects of various extracts from the fruiting bodies of *Pleurotus ferulae*," *Saudi Journal of Biological Sciences*, vol. 19, no. 1, pp. 111–118, 2012.
- [10] L. H. Peng, S. Liu, S. Y. Xu et al., "Inhibitory effects of salidroside and paeonol on tyrosinase activity and melanin synthesis in mouse B16F10 melanoma cells and ultraviolet B-induced pigmentation in Guinea pig skin," *Phytomedicine*, vol. 20, no. 12, pp. 1082–1087, 2013.
- [11] L. Saghaie, M. Pourfarzam, A. Fassihi, and B. Sartippour, "Synthesis and tyrosinase inhibitory properties of some novel derivatives of kojic acid," *Research in Pharmaceutical Sciences*, vol. 8, no. 4, pp. 233–242, 2013.
- [12] A. Lee, J. Y. Kim, J. Heo et al., "The inhibition of melanogenesis via the PKA and ERK signaling pathways by *Chlamydomonas reinhardtii* extract in B16F10 melanoma cells and artificial human skin equivalents," *Journal of Microbiology and Biotechnology*, vol. 28, no. 12, pp. 2121–2132, 2018.
- [13] U. Asmat, K. Abad, and K. Ismail, "Diabetes mellitus and oxidative stress—a concise review," *Saudi Pharmaceutical Journal*, vol. 24, no. 5, pp. 547–553, 2016.
- [14] P. Martín-Gallán, A. Carrascosa, M. Gussinyé, and C. Domínguez, "Biomarkers of diabetes-associated oxidative stress and antioxidant status in young diabetic patients with or without subclinical complications," *Free Radical Biology and Medicine*, vol. 34, no. 12, pp. 1563–1574, 2003.
- [15] J. Wang and H. Wang, "Oxidative Stress in Pancreatic Beta Cell Regeneration," *Oxidative Medicine and Cellular Longevity*, vol. 2017, Article ID 1930261, 9 pages, 2017.
- [16] M. Tiedge, S. Lortz, J. Drinkgern, and S. Lenzen, "Relation between antioxidant enzyme gene expression and antioxidative defense status of insulin-producing cells," *Diabetes*, vol. 46, no. 11, pp. 1733–1742, 1997.
- [17] S. Bhattacharya and P. C. Sil, "Role of plant-derived polyphenols in reducing oxidative stress-mediated diabetic complications," *Reactive Oxygen Species*, vol. 5, pp. 15–34, 2018.
- [18] D. S. H. Bell, "Type 2 diabetes mellitus: what is the optimal treatment regimen?," *The American Journal of Medicine*, vol. 116, no. 5, pp. 23–29, 2004.
- [19] T. Matsui, T. Tanaka, S. Tamura et al., "α-Glucosidase inhibitory profile of catechins and theaflavins," *Journal of Agricultural and Food Chemistry*, vol. 55, no. 1, pp. 99–105, 2007.
- [20] Y. M. Kim, Y. K. Jeong, M. H. Wang, W. Y. Lee, and H. I. Rhee, "Inhibitory effect of pine extract on α-glucosidase activity and postprandial hyperglycemia," *Nutrition*, vol. 21, no. 6, pp. 756–761, 2005.
- [21] T. Chipiti, M. A. Ibrahim, M. Singh, and M. S. Islam, "In vitro α-amylase and α-glucosidase inhibitory and cytotoxic activities of extracts from *Cissus cornifolia* plant parts," *Pharmacognosy Magazine*, vol. 13, no. 50, p. 329, 2017.
- [22] S. Kumar, V. K. Narwal, and O. Prakash, "α-Glucosidase inhibitors from plants: a natural approach to treat diabetes," *Pharmacognosy Reviews*, vol. 5, no. 9, pp. 19–29, 2011.
- [23] S. S. Nair, V. Kavrekar, and A. Mishra, "In vitro studies on alpha amylase and alpha glucosidase inhibitory activities of selected plant extracts," *European Journal of Experimental Biology*, vol. 3, pp. 128–132, 2013.
- [24] O. P. Sharma and T. K. Bhat, "DPPH antioxidant assay revisited," *Food Chemistry*, vol. 113, no. 4, pp. 1202–1205, 2009.
- [25] Z. Ashraf, M. Rafiq, H. Nadeem et al., "Carvacrol derivatives as mushroom tyrosinase inhibitors; synthesis, kinetics mechanism and molecular docking studies," *PLoS One*, vol. 12, no. 5, article e0178069, 2017.
- [26] S. Umamaheswari and K. S. Sangeetha, "Inhibitory action against alpha glucosidase by selected dihydroxy flavones," *International Journal of Current Research*, vol. 11, no. 7, pp. 5–8, 2019.
- [27] N. U. Rehman, S. A. Halim, M. Al-Azri et al., "Triterpenic acids as non-competitive α-glucosidase inhibitors from *Boswellia elongata* with structure-activity relationship: in vitro and in silico studies," *Biomolecules*, vol. 10, no. 5, p. 751, 2020.
- [28] K. Motoshima, T. Noguchi-Yachide, K. Sugita, Y. Hashimoto, and M. Ishikawa, "Separation of α-glucosidase-inhibitory and liver X receptor-antagonistic activities of phenethylphenyl phthalimide analogs and generation of LXRA-selective antagonists," *Bioorganic and Medicinal Chemistry*, vol. 17, no. 14, pp. 5001–5014, 2009.
- [29] G. R. M. Chelladurai and C. Chinnachamy, "Alpha amylase and alpha glucosidase inhibitory effects of aqueous stem extract of *Salacia oblonga* and its GC-MS analysis," *Brazilian Journal of Pharmaceutical Sciences*, vol. 54, no. 1, 2018.
- [30] C. V. Rynjah, N. N. Devi, N. Khongthaw, D. Syiem, and S. Majaw, "Evaluation of the antidiabetic property of aqueous leaves extract of *Zanthoxylum armatum* DC. using in vivo and in vitro approaches," *Journal of Traditional and Complementary Medicine*, vol. 8, no. 1, pp. 134–140, 2018.
- [31] P. Yin, Y. Wang, L. Yang, J. Sui, and Y. Liu, "Hypoglycemic effects in alloxan-induced diabetic rats of the phenolic extract from Mongolian oak cups enriched in ellagic acid, kaempferol and their derivatives," *Molecules*, vol. 23, no. 5, p. 1046, 2018.

- [32] J. J. Wu, K. W. Cheng, E. T. S. Li, M. Wang, and W. C. Ye, "Antibrowning activity of MRPs in enzyme and fresh-cut apple slice models," *Food Chemistry*, vol. 109, no. 2, pp. 379–385, 2008.
- [33] S. E. Aly, B. Sabry, M. S. Shaheen, and A. S. Hathout, "Assessment of antimycotoxigenic and antioxidant activity of star anise (*Illicium verum*) in vitro," *Journal of the Saudi Society of Agricultural Sciences*, vol. 15, no. 1, pp. 20–27, 2016.
- [34] C. H. Yang, F. R. Chang, H. W. Chang, S. M. Wang, M. C. Hsieh, and L. Y. Chuang, "Investigation of the antioxidant activity of *Illicium verum* extracts," *Journal of Medicinal Plants Research*, vol. 6, no. 2, pp. 314–324, 2012.
- [35] A. D. Gupta, V. K. Bansal, V. Babu, and N. Maithil, "Chemistry, antioxidant and antimicrobial potential of nutmeg (*Myristica fragrans* Houtt)," *Journal of Genetic engineering and Biotechnology*, vol. 11, no. 1, pp. 25–31, 2013.
- [36] K. Msaada, M. B. Jemia, N. Salem et al., "Antioxidant activity of methanolic extracts from three coriander (*Coriandrum sativum* L.) fruit varieties," *Arabian Journal of Chemistry*, vol. 10, pp. S3176–S3183, 2017.
- [37] C. Dias, A. Fonseca, A. L. Amaro et al., "Natural-based antioxidant extracts as potential mitigators of fruit browning," *Antioxidants*, vol. 9, no. 8, p. 715, 2020.
- [38] X. Duan, G. Wu, Y. Jiang, G. Wu, and Y. Jiang, "Evaluation of the antioxidant properties of litchi fruit phenolics in relation to pericarp browning prevention," *Molecules*, vol. 12, no. 4, pp. 759–771, 2007.
- [39] M. V. Del and F. Beermann, "Tyrosinase and related proteins in mammalian pigmentation," *FEBS Letters*, vol. 381, no. 3, pp. 165–168, 1996.
- [40] W. Yi, X. Wu, R. Cao, H. Song, and L. Ma, "Biological evaluations of novel vitamin C esters as mushroom tyrosinase inhibitors and antioxidants," *Food Chemistry*, vol. 117, no. 3, pp. 381–386, 2009.
- [41] E. Rattanangkool, P. Kittikhunnatham, T. Damsud, S. Wacharasindhu, and P. Phuwapraisirisan, "Quercitylcinnamates, a new series of antidiabetic bioconjugates possessing α -glucosidase inhibition and antioxidant," *European Journal of Medicinal Chemistry*, vol. 66, pp. 296–304, 2013.
- [42] K. V. Peter and K. N. Babu, "Introduction to herbs and spices: medicinal uses and sustainable production," in *Handbook of Herbs and Spices*, pp. 1–16, Elsevier, 2012.
- [43] P. E. S. Anise, "Antioxidant and anti-diabetic activities of polyphenol-enriched star anise (*Illicium verum*) seeds extract," *International Journal of Biotechnology and Biochemistry*, vol. 14, pp. 77–84, 2018.
- [44] A. R. Zuo, H. H. Dong, Y. Y. Yu et al., "The antityrosinase and antioxidant activities of flavonoids dominated by the number and location of phenolic hydroxyl groups," *Chinese Medicine*, vol. 13, no. 1, pp. 1–12, 2018.
- [45] W. M. Chai, Q. Huang, M. Z. Lin et al., "Condensed tannins from longan bark as inhibitor of tyrosinase: structure, activity, and mechanism," *Journal of Agricultural and Food Chemistry*, vol. 66, no. 4, pp. 908–917, 2018.
- [46] F. Shaheen, M. Ahmad, M. T. H. Khan et al., "Alkaloids of *Aconitum laeve* and their anti-inflammatory, antioxidant and tyrosinase inhibition activities," *Phytochemistry*, vol. 66, no. 8, pp. 935–940, 2005.
- [47] Q. Huang, W. M. Chai, Z. Y. Ma et al., "Inhibition of α -glucosidase activity and non-enzymatic glycation by tannic acid: inhibitory activity and molecular mechanism," *International Journal of Biological Macromolecules*, vol. 141, pp. 358–368, 2019.
- [48] C. Proença, M. Freitas, D. Ribeiro et al., " α -Glucosidase inhibition by flavonoids: an in vitro and in silico structure–activity relationship study," *Journal of Enzyme Inhibition and Medicinal Chemistry*, vol. 32, no. 1, pp. 1216–1228, 2017.
- [49] J. Zhen, Y. Dai, T. Villani, D. Giurleo, J. E. Simon, and Q. Wu, "Synthesis of novel flavonoid alkaloids as α -glucosidase inhibitors," *Bioorganic and Medicinal Chemistry*, vol. 25, no. 20, pp. 5355–5364, 2017.
- [50] T. H. M. Khan, "Novel tyrosinase inhibitors from natural resources—their computational studies," *Current Medicinal Chemistry*, vol. 19, no. 14, pp. 2262–2272, 2012.